

# Calcined Clayey Soils as a Potential Replacement for Cement in Developing Countries

THÈSE N° 4302 (2009)

PRÉSENTÉE LE 6 FÉVRIER 2009

À LA FACULTÉ SCIENCES ET TECHNIQUES DE L'INGÉNIEUR  
LABORATOIRE DES MATÉRIAUX DE CONSTRUCTION  
PROGRAMME DOCTORAL EN SCIENCE ET GÉNIE DES MATÉRIAUX

ÉCOLE POLYTECHNIQUE FÉDÉRALE DE LAUSANNE

POUR L'OBTENTION DU GRADE DE DOCTEUR ÈS SCIENCES

PAR

Rodrigo FERNANDEZ LOPEZ

acceptée sur proposition du jury:

Prof. L. Zuppiroli, président du jury  
Prof. K. Scrivener, directrice de thèse  
Prof. K. Folliard, rapporteur  
Prof. F. Glasser, rapporteur  
Prof. H. Hofmann, rapporteur



ÉCOLE POLYTECHNIQUE  
FÉDÉRALE DE LAUSANNE

Suisse  
2009



## Abstract

Concrete is the building material with the greatest potential for meeting the increasing housing demand in developing countries. Locally available materials should be considered as cement replacement in order to lower the costs and the environmental impact associated with the production of cement. Hence, this study investigated the potential use of calcined clayey soils to be used as reactive mineral admixtures in concrete, with special emphasis on a Cuban clayey soil. The study of the thermal behaviour of common clay types such as kaolinite, illite and montmorillonite was of key importance for the understanding of more complex locally available soils generally composed of a mixture of clays with companion minerals and impurities.

Clays were calcined at temperatures ranging from 500°C to 1000°C. The characterization of the raw and calcined clays included XRD, TGA, DTA, NMR, PSD, BET and SEM. The study of the pozzolanic activity was done in cement pastes by replacing 30% of cement by calcined clays at a water/binder ratio of 0.4. Curing was done in water at 30°C to simulate the Cuban climate. CH depletion was monitored using XRD and TGA up to 90 days. The degree of hydration of the clinker component was assessed by BSE-image analysis. The identification of the hydrated phases in pastes was done by XRD, NMR and SEM. Long-term Isothermal Calorimetry as well as chemical shrinkage allowed the chemical contribution of the pozzolans to be identified independently of the filler effect and the hydration of cement.. To see how did the different reactivities of calcined clays translate into mechanical properties, standard mortar bars (w/b 0.5) were prepared and cured under the same conditions as the pastes for testing in compressive strength at 1, 7, 28 and 90 days. Sorptivity measurements were also performed to assess the durability properties.

Kaolinite was found to have the highest potential for activation when calcined in the range of 600°C to 800°C. Locally available clays with only around 40% of kaolinite showed good pozzolanic properties in pastes. The time at which the pozzolanic activity starts to be significant varied between 1 and 7 days. Calcined clays in cement tend to favour the formation of AFm phases such as hemicarboaluminate or monocarboaluminate. Strätlingite was also detected by <sup>27</sup>Al NMR. The Compressive strength of mortars incorporating kaolinite-based calcined clays was systematically similar or higher than the 100% OPC mortar from around 7 days and the sorptivity of the blended systems was reduced. These studies indicate that locally available calcined clayey soils have significant potential for replacing cement in concrete.

Keywords: Calcined clays, Pozzolans, Metakaolin, Thermal activation





## Résumé

En réponse à la demande croissante de logements dans les pays en voie de développement l'utilisation adéquate des matériaux de construction valorisant les ressources locales est un choix incontournable. Afin de diminuer le coût économique et environnemental associé à la production du ciment, ce projet a évalué le potentiel d'activation thermique de sols argileux pour la production de pouzzolanes réactives substituant le ciment dans les ouvrages en béton. Une attention particulière a été portée à un sol argileux d'origine cubaine. L'étude d'argiles standards du type kaolinite, illite et montmorillonite s'est avéré d'une importance capitale pour la compréhension de systèmes plus complexes tels que les sols argileux qui sont généralement composés de mélanges d'argiles ainsi que d'autres minéraux et impuretés.

Les argiles ont été calcinées entre 500°C et 1000°C. La caractérisation des argiles avant et après calcination s'est faite par DX, ATG, ATD, RMN, granulométrie laser, BET ainsi que par MEB. L'étude de leur caractère pouzzolanique s'est effectuée sur des pâtes de ciment. Le taux de substitution du ciment par les argiles calcinées a été de 30%, le ratio eau/liant a été fixé à 0.4. La cure s'est effectuée dans l'eau à 30°C afin de simuler les conditions climatiques cubaines. Le contenu en hydroxyde de calcium a été suivi sur 90 jours par DX ainsi que par ATG. Des mesures de calorimétrie isotherme sur 28 jours ont permis d'isoler la contribution chimique des pouzzolanes de la réaction d'hydratation du ciment. Le degré d'hydratation de ce dernier a été mesuré par analyse d'images au MEB. Les hydrates formés ont été identifiés par DX, RMN et MEB. Afin de mesurer l'influence des réactivités pouzzolaniques sur les propriétés mécaniques ainsi que sur les propriétés de perméabilité, des mortiers ont été fabriqués avec le même degré de substitution et un ratio eau/liant de 0.5. Les conditions de cure ont été similaires aux pâtes de ciment.

Parmi les types d'argiles étudiés, la kaolinite a le plus fort potentiel d'activation, qui est entre 600°C et 800°C. L'argile cubaine, avec seulement 40% de kaolinite, a révélé une excellente réactivité pouzzolanique. Le temps requis pour que cette réaction devienne significative semble dépendre du contenu en kaolinite de l'argile et se trouve systématiquement entre 1 et 7 jours. Les argiles calcinées substituant le ciment favorisent la formation de phase AFm. La strätlingite a été détectée par RMN en  $^{27}\text{Al}$ . Les résistances en compression des mortiers incorporant des argiles calcinées à base de kaolinite ont été similaires ou supérieures à la référence (100%CPO) dès environ 7 jours et ont montré une perméabilité réduite. Ces résultats suggèrent que les sols argileux calcinés ont un grand potentiel de substitution dans les ouvrages en béton afin de leur donner un caractère toujours plus durable.

Mots-clés : Argiles calcinées, Pouzzolanes, Métakaolin, Activation thermique



## Zusammenfassung

Beton ist ein Baumaterial mit dem grössten Potential, die steigende Nachfrage für Bebauungen in den Entwicklungsländern gerecht zu werden. Lokal erhältliche Materialien sollten als Ersatz für Zement berücksichtigt werden, um die Kosten und die Umwelteinflüsse während der Zementherstellung zu reduzieren. Deshalb beschäftigt sich diese Arbeit mit dem potentiellen Gebrauch von kalzinierten Tonerden, die als reaktive Mineralzusätze im Beton genutzt werden, mit Schwerpunkt auf kubanische Tonerden. Die Untersuchungen des thermischen Verhaltens der gebräuchlichen Tontypen wie z.B. Kaolinit, Illit und Montmorillonit waren die Voraussetzung für das Verstehen der sehr komplexen, lokal verfügbaren Erden, die generell aus einer Mischung von Tonen, Mineralien und Verunreinigungen bestehen.

Die Tone wurden bei einer Temperatur von 500 bis 1000 °C kalziniert. Die Charakterisierung der Roh- und kalzinierten Tone erfolgte mittels XRD, TGA, DTA, NMR, BET und REM. Die Untersuchungen der puzzolanischen Aktivität wurde am Zementleim durchgeführt in dem 30% des Zementes durch kalzinierte Tone bei einem Wasser/Binder Verhältnis von 0.4 ersetzt wurden. Die Nachbehandlung erfolgte in Wasser bei 30 °C, um das kubanische Klima zu simulieren. Die Abreicherung von CH wurde mit Hilfe der XRD und TGA für die Nachbehandlungszeiten 1, 7, 14, 28 und 90 Tage untersucht. Die Langzeit Isothermalkalorimetrie als auch das chemische Schwinden, ermöglichten die chemische Beteiligung der Puzzolane zu identifizieren, unabhängig vom Füllereffekt und der Hydratation des Zements. Der Hydratationsgrad des Klinkers wurde mit Hilfe der BSE-Bild Analyse bestimmt. Die Bestimmung der Hydratphasen im Zementstein wurde mittels XRD, NMR und REM durchgeführt. Um festzustellen, wie sich die Reaktivitäten der verschiedenen kalzinierten Tone auf die mechanischen Eigenschaften auswirkt, wurden Standardmörtelprismen ( $w/b = 0.5$ ) hergestellt und unter den gleichen Bedingungen wie der Zementstein nachbehandelt und die Druckfestigkeiten nach 1, 7, 28 und 90 Tagen bestimmt.

Es zeigte sich, dass das Kaolinit das höchste Aktivierungspotential hat, wenn es in einem Bereich von 600 bis 800 °C gebrannt wird. Die lokal vorhandenen Tone mit nur rund 40% Kaolinit zeigten gute puzzolanische Eigenschaften am Zementstein. Der Zeitraum indem die puzzolanische Aktivität signifikant started, kann zwischen 1 und 7 Tagen schwanken und scheint vom Kaolinitgehalt abzuhängen. Kalzinierte Tone im Zement tendieren zur AFmphasenbildung, wie z.B. Hemikarboaluminat oder Monocarboaluminat. Strätlingit wurde teilweise mittels <sup>27</sup>ALNMR bestimmt. Die Druckfestigkeiten der Mörtel mit kaolinithaltigen, kalzinierten Tonen waren nach ungefähr 7 Tagen systematisch gleich, oder teilweise höher als die der OPC Mörtel und die Sorption der Mischsysteme war reduziert, was ein grosses Potential der lokal verfügbaren, kalzinierten Tonerden bezüglich des Zementersatz im Beton zeigt.



## Resumen

El hormigón es el material de construcción con el mayor potencial para atender la creciente demanda de vivienda en los países en desarrollo. No obstante ello, los materiales disponibles a nivel local deben ser considerados como posible reemplazo, con miras a abaratar los costos y el impacto ambiental asociados a la producción del cemento. En consecuencia, este proyecto evalúa el potencial de activación térmica de los suelos arcillosos para ser utilizados como adición mineral activa en el cemento, con especial énfasis en un suelo arcilloso cubano. El estudio de las descomposiciones térmicas de los tipos comunes de arcilla, como la kaolinita, illita y montmorillonita, fue de importancia capital para el entendimiento de los suelos disponibles localmente, que presentan mayor complejidad, compuestos generalmente de una mezcla de arcillas acompañadas de minerales e impurezas. Las arcillas fueron calcinadas a temperaturas entre 500° C y 1000° C.

La caracterización de las arcillas antes y después de su calcinado se realizó por DRX, TG, ATD, RMN, granulometría láser, BET como también por MEB. El estudio de la actividad puzolánica se hizo en pastas de cemento, reemplazando el 30% del cemento por arcillas calcinadas y una relación (agua/aglomerante) de 0.4. El tratamiento se llevó a cabo en agua a 30°C para simular el clima cubano. El contenido en hidróxido de calcio fue monitoreado mediante DRX y también TG por períodos de 1, 7, 14, 28 y 90 días. Medidas de calorimetría isotérmica a lo largo de 28 días permitieron aislar y separar la contribución química de las puzolánas de la reacción de hidratación del cemento. El grado de hidratación de este último fue calculado mediante análisis de imagen BSE. Los hidratos formados fueron identificados mediante DRX, RMN y MEB. Con el fin de medir la influencia de las diferentes reactividades de las arcillas calcinadas sobre las propiedades mecánicas y de permeabilidad, se fabricaron morteros standard con el mismo grado de sustitución y una relación agua/aglomerante de 0.5.

Entre los tipos de arcillas estudiadas, la kaolinita mostró el mayor potencial de activación, cuando estuvo calcinada entre 600°C y 800°C. La arcilla cubana, con sólo un 40% de kaolinita, mostró una excelente reactividad puzolánica. El tiempo requerido para que la reacción puzolánica comience a ser significativa parece depender del contenido de kaolinita de la arcilla y puede variar entre 1 y 7 días. Las arcillas calcinadas en sustitución del cemento favorecen la formación de fases AFm, tales como hemicarboaluminato o monocarboaluminato. La strätlingita fue también detectada mediante RMN del <sup>27</sup>Al. La resistencia en compresión de los morteros, incorporando las arcillas calcinadas a base de kaolinita, fue sistemáticamente similar o superior a la referencia (100%CPO) a partir de 7 días aproximadamente, mientras que la permeabilidad fue reducida. Estos resultados indican que los suelos arcillosos calcinados tienen un gran potencial para reemplazar al cemento en los trabajos con hormigón, otorgándole un carácter siempre más duradero.



## Acknowledgements

I would like to thank Prof. Karen Scrivener for giving me the opportunity to do my PhD in the Laboratory of Construction Materials at EPFL and for her supervision of this work. I would also like to thank the Swiss National Science Foundation for financial support; Prof. Fernando Martirena of the Central University of Las Villas, Cuba, for bringing all his scientific background in the field of low-cost housing materials and for coordinating all the field trips; Dr. Kurt Rhyner and his team of Grupo Sofonías for giving me the opportunity to visit their building materials workshops in Nicaragua and Ecuador and identify the needs of rural and suburban communities; all my colleagues from the Laboratory of Construction Materials for their help and support and in particular Dr. Emmanuel Gallucci for his advises and supervision of the work with Scanning Electron Microscopy and Dr. Gwen Le Saoût for carrying out Nuclear Magnetic Resonance; Dr. Paul Bowen and Carlos Morais for the advises and assistance in the use of the facilities of the Laboratory of Powders Technology; Jacques Castano for the assistance with the furnace in the Laboratory of Ceramics; Dr. Steve Feldman for the enlightening discussions on clay mineralogy and X-Ray Diffraction; Dr. Bénédicte Rousset and Dr. Jessica Chiaverini for the discussions on characterization of clays and pozzolanic reaction.

I wouldn't like to forget my Cuban partners in this joint research project, with whom I have shared so many experiences and thoughts: Juan José Dopico, Adrián Alujas Díaz and Rances Castillo Lara. My acknowledgements go also to all the people in Cuba that have helped and encouraged me during my stays: María Teresa, Eulalia, Yolanda, Cachita, Niury, Alfredo y Juan Antonio.

Finally I would like to express all my gratitude to my parents, Mrs. Maria Emilia Fernandez Lopez and Mr. Carlos Fernandez Ballesteros, to my sisters, Emilia and Jimena, to my brother, Guzmán, to the rest of my family, Vanessa, Max, Robert, Fernando, Isabela, Andrés, Diego and Leopold, for their love and encouragement, and in particular to my beloved Sonia, for her patience and her support.





# Table of Contents

<b>Abstract</b> .....	<b>I</b>
<b>Résumé</b> .....	<b>III</b>
<b>Zusammenfassung</b> .....	<b>V</b>
<b>Resumen</b> .....	<b>VII</b>
<b>Acknowledgements</b> .....	<b>IX</b>
<b>Table of Contents</b> .....	<b>XI</b>
<b>List of Tables</b> .....	<b>XIII</b>
<b>List of Figures</b> .....	<b>XV</b>
<b>Glossary</b> .....	<b>XXI</b>
<b>1 Introduction</b> .....	<b>1</b>
1.1 Context .....	1
1.2 Need for new supplementary cementitious materials .....	2
1.3 Objectives of the study .....	3
1.4 Experimental approach.....	5
<b>2 Clay activation</b> .....	<b>7</b>
2.1 Structure and composition of clayey materials .....	7
2.2 State of the art in clay activation.....	11
2.2.1 <i>Nature of the clay and activation temperature</i> .....	12
2.2.2 <i>Understanding decomposition mechanisms for optimizing the metakaolin product</i> .....	14
2.3 Experimental studies of clay activation .....	19
2.3.1 <i>Raw materials selection</i> .....	19
2.3.2 <i>Characterization methods</i> .....	20
2.3.3 <i>Activation process (thermal treatment)</i> .....	22
2.4 Activation of standard clays.....	23
2.4.1 <i>Raw materials</i> .....	23
2.4.2 <i>Characterization of calcined clays</i> .....	27
2.5 Activation of a clay mixture: the Cuban clay.....	36
2.5.1 <i>Raw materials and pre-treatments</i> .....	36
2.5.2 <i>Characterisation of calcined clays</i> .....	41
<b>3 Pozzolanic reaction in cement-calcined clays pastes</b> .....	<b>51</b>
3.1 Theoretical background.....	51
3.1.1 <i>Cement hydration</i> .....	51

3.1.2	<i>Pozzolans and pozzolanic reaction.....</i>	52
3.2	State of the art on cement substitution by calcined clays.....	53
3.2.1	<i>Calorimetry.....</i>	54
3.2.2	<i>Calcium hydroxide quantification by thermogravimetric analysis .....</i>	54
3.2.3	<i>Changes in the microstructure &amp; phases formed (XRD, SEM).....</i>	55
3.2.4	<i>Nature of C-S-H using NMR.....</i>	55
3.2.5	<i>Improvement of mechanical and durability properties .....</i>	55
3.3	Experimental approach for the study of cement-calcined clays pastes.....	60
3.3.1	<i>Characterization methods.....</i>	61
3.3.2	<i>Starting materials and mix designs .....</i>	63
3.4	Results and discussions .....	69
3.4.1	<i>Pozzolanic activity of standard clays .....</i>	69
3.4.2	<i>Pozzolanic activity of Cuban clay .....</i>	76
3.4.3	<i>Comparing reactivity of the Cuban clay with other kaolinite-rich activated clays.....</i>	83
3.4.4	<i>Scanning electron microscopy.....</i>	94
<b>4</b>	<b>Mechanical properties and sorptivity of cement-calcined clays mortars.....</b>	<b>111</b>
4.1	Starting materials and mix designs.....	111
4.2	Assessment of mechanical performances and degree of hydration.....	113
4.3	Capillary sorption.....	120
<b>5</b>	<b>Towards practical use of activated clays.....</b>	<b>123</b>
<b>6</b>	<b>Conclusions and perspectives.....</b>	<b>127</b>
6.1	Conclusions .....	127
6.1.1	<i>Activation of standard and locally available clays .....</i>	127
6.1.2	<i>The calcined clay-cement interaction.....</i>	127
6.2	Perspectives.....	129
6.2.1	<i>Minimum kaolinite content of a clay .....</i>	129
6.2.2	<i>Moving to concrete applications and addressing the workability issues .....</i>	129
6.2.3	<i>Durability.....</i>	130
6.2.4	<i>Moving towards a more efficient calcination process.....</i>	130
	<b>Bibliography .....</b>	<b>133</b>
	<b>Appendices .....</b>	<b>139</b>

## List of Tables

Table 1-1: Mismatch of housing demand and supply in selected developing countries, from Landaeta[1].....	1
Table 1-2: Objectives of the joint research programme distributed in 4 sub-projects .....	4
Table 2-1 : Characteristics of clay minerals of most abundance.....	11
Table 2-2: Activation temperatures and times for different types of clays .....	13
Table 2-3: Optimization of the metakaolin product .....	16
Table 2-4: Chemical composition of kaolinite, illite and montmorillonite.....	23
Table 2-5 : Summary chart on the effect of calcination on standard clays .....	35
Table 2-6 : Chemical analysis for cuban soil and its clayey extract after deflocculation .....	36
Table 2-7 : Percentage of kaolinite in cuban clay and standard kaolinite.....	40
Table 2-8 : Summary chart on the effect of calcination on mixed cuban clay.....	49
Table 3-1 : Summary of studies undertaken on lime-calcined clays systems .....	58
Table 3-2 : Summary of studies undertaken on cement-calcined clays systems .....	59
Table 3-3 : Chemical analysis of uncalcined and calcined clays .....	63
Table 3-4 : Characteristics of the clays retained for the study on pastes .....	64
Table 3-5 : Chemical composition of cements and filler .....	64
Table 3-6 : Phase quantification by XRD Rietveld analysis on anhydrous cements .....	65
Table 3-7 : Formulations of cement-calcined clays pastes for XRD, TGA, BSE-IA and NMR .....	67
Table 3-8 : Formulation of cement-calcined clays pastes for Isothermal Calorimetry and Chemical Shrinkage .....	67
Table 3-9 : Summary of the performed measurements on different series .....	68

Table 3-10 : Assignment of $^{27}\text{Al}$ peaks for pastes of series 3 .....	80
Table 3-11 : Characteristics of kaolinite-rich clays .....	83
Table 4-1 : Formulation of cement-calcined clays mortars.....	112
Table 4-2 : Assessed mortar properties .....	112
Table 5-1: % mass losses of the set of clays for each temperature zone, determined experimentally with a laboratory furnace and a balance.....	124

## List of Figures

Figure 1-1: Structure of the investigation .....	5
Figure 2-1: (a): Silicon in tetrahedral position, (b): Silica sheet, (Grim [7]) .....	8
Figure 2-2: (a): Aluminium in Octahedral position, (b): Alumina sheet, (Grim [7]).....	8
Figure 2-3: Synthesis pattern for the clay minerals (Mitchell [8]).....	9
Figure 2-4 : Structures of kaolinite (a), illite (b) and montmorillonite (c) (adapted from Grim[7]) .....	9
Figure 2-5 : Models for Metakaolin based on NMR measurments. left : Mackenzie [33], right: Rocha [34].....	15
Figure 2-6: Experimental approach for clay activation.....	19
Figure 2-7: Temperature profile in the laboratory furnace for a thermal treatment at 600°C for 60min.....	22
Figure 2-8 : XRD patterns of kaolinite, as received and with centrifugation process (M: muscovite).....	24
Figure 2-9 : XRD patterns of Illite, as received and with centrifugation process (c: clinochlore).....	24
Figure 2-10 : XRD patterns of Montmorillonite, as received and after centrifugation (cr.:cristobalite, f.: feldspath) .....	25
Figure 2-11: DTG of standard clays (as received) .....	25
Figure 2-12 : XRD patterns for untreated and calcined kaolinite (m: muscovite).....	31
Figure 2-13 : $^{27}\text{Al}$ NMR spectras (left) and DTG curves (right) for untreated and calcined kaolinite.....	31
Figure 2-14 : XRD patterns for untreated and calcined illite (c: clinochlore) .....	32
Figure 2-15 : $^{27}\text{Al}$ NMR spectras (left) and DTG curves (right) for untreated and calcined illite .....	32

Figure 2-16 : XRD pattern for untreated and calcined montmorillonite (a: albite, cr: cristobalite, m: muscovite) .....	33
Figure 2-17 : <sup>27</sup> Al NMR spectras (left) and DTG curves (right) for untreated and calcined montmorillonite .....	33
Figure 2-18 : Particle size distributions for standard clays before and after calcination .....	34
Figure 2-19 : Effect of temperature on specific surface of standard clays .....	34
Figure 2-20 : Effect of deflocculation and centrifugation on diffraction pattern of cuban clay (m: montmorillonite, i: illite, k: kaolinite, a: albite, Q: quartz) .....	38
Figure 2-21 : DTG analysis on cuban clay (and standards) .....	38
Figure 2-22 : TGA curves of cuban clay after different treatments vs kaolinite .....	40
Figure 2-23 : DTG and DTA curves of cuban clay and standard kaolinite .....	40
Figure 2-24 : XRD patterns of cuban clay in the 500 - 1000°C range .....	43
Figure 2-25 : XRD patterns of cuban clay in the 825 - 1000°C range .....	43
Figure 2-26 : DTG measurments on raw cuban clay and its calcined products .....	44
Figure 2-27 : DTG measurments on calcined products .....	44
Figure 2-28 : NMR spectra of untreated and calcined Cuban clay and standard kaolinite .....	46
Figure 2-29: Comparison of NMR spectra (Cuban clay vs standard clays) .....	46
Figure 2-30 : Particle size distribution for raw and calcined Cuban clay .....	47
Figure 2-31 : BET and He-Picnometer measurments for raw and calcined Cuban clay .....	47
Figure 2-32 : BSE images of the cuban clay: untreated(a), at 600°C (b), 800°C (c), 925°C (d) .....	48
Figure 3-1 : Experimental approach for pastes and mortars .....	61
Figure 3-2 : PSD of the cements and filler .....	66

Figure 3-3 : 28 days XRD patterns of cement-calcined clays pastes, series 1 (30°C).....	70
Figure 3-4 : Calcium hydroxide content and degree of hydration at 28 days, series 1 (30°C)	72
Figure 3-5 : Chemically bound water, series 1 (30°C).....	72
Figure 3-6 : <sup>27</sup> Al NMR spectra of anhydrous cement and blends .....	74
Figure 3-7 : <sup>27</sup> Al NMR spectra of hydrated pastes at 28 days, series 1 (30°C).....	74
Figure 3-8 : Detection of strätlingite by low-angle XRD, series 1 (30°C).....	75
Figure 3-9 : DTG curves of cu800_2 .....	76
Figure 3-10 : CH content relative to cement, series 2 (20°C).....	78
Figure 3-11 : CH content relative to cement vs degree of hydration at 28 days, series 3 (20°C) .....	78
Figure 3-12 : CH content based on CH content of opc, series 2 and 3 (20°C) .....	79
Figure 3-13 : Chemical shrinkage, series 3 (20°C).....	79
Figure 3-14 : <sup>27</sup> Al NMR spectra of hydrated pastes at 28 days, series 3 (20°C).....	81
Figure 3-15 : <sup>29</sup> Si NMR spectra of anhydrous and hydrated pastes (opc and cu600), series 3 (20°C).....	81
Figure 3-16 : Isothermal calorimetry, series 5 (20°C) .....	85
Figure 3-17 : Isothermal calorimetry, series 5 (30°C) .....	85
Figure 3-18 : Cumulated heat relative to cement and chemical shrinkage, series 5 (20°C) ....	87
Figure 3-19 : Cumulated heat relative to anhydrous content and filler-substracted curves, series 5 (20°C).....	88
Figure 3-20 : Cumulated heat relative to cement, series 5 (30°C).....	88
Figure 3-21 : Cumulated heat relative to anhydrous content and filler-substracted curves, series 5 (30°C).....	88

Figure 3-22 : 28 days XRD patterns of cement-calcined clays pastes, series 4 (30°C).....	90
Figure 3-23 : Detection of Strätlingite by low-angle XRD, series 4 (30°C).....	90
Figure 3-24 : CH content relative to cement, series 4, (30°C).....	91
Figure 3-25 : 28 days XRD pattern of cu600, k600 and k800, series 1 (30°C).....	92
Figure 3-26 : CH content of cu600, k600 and k800 and degree of hydration at 28 days, series1 (30°C).....	92
Figure 3-27 : CH content based on CH content of opc, series 1 and 4, (30°C).....	93
Figure 3-28 : Representative BSE image of a 28 days calcined clay-cement paste.....	95
Figure 3-29 : 28 days microstructure of opcB_1, series 1 (30°C).....	98
Figure 3-30 : 28 days microstructure of k600_1, series 1 (30°C).....	98
Figure 3-31 : k600_1 paste at 28 days with EDS spectrum for s: strätlingite, k: calcined kaolinite.....	99
Figure 3-32: 28 days microstructure of i600_1, series 1 (30°C).....	100
Figure 3-33: 28 days microstructure of m600_1, series 1 (30°C).....	100
Figure 3-34 : 28 days microstructure of opcA_4, series 4 (30°C).....	101
Figure 3-35: 28 days microstructure of cu600_4, series 4 (30°C).....	101
Figure 3-36 : 28 days microstructure of cu800_4, series 4 (30°C).....	102
Figure 3-37: 28 days microstructure of cu925_4, series 4 (30°C).....	102
Figure 3-38 : 28 days microstructure of MK_4, series 4 (30°C).....	103
Figure 3-39 : MK_4 paste at 28 days with EDS spectrum for strätlingite (s).....	103
Figure 3-40: cu800_4 paste at 28 days with EDS spectrum for calcium monosulfoaluminate (ms).....	104



Figure 3-41: Example for the choice of points for EDX analysis on inner C-S-H, (sample cu800_3, 14 days) .....	106
Figure 3-42: Example for the choice of points for EDX analysis on outer C-S-H, (sample cu600_3, 14 days) .....	106
Figure 3-43 : EDS analysis in inner CSH of cu600_3 and control paste at 14 days (20°C)..	107
Figure 3-44 : EDS analysis in outer CSH of cu600_3 and control paste at 14 days (20°C)..	107
Figure 3-45 : EDS analysis in inner CSH of cu800_3 and control paste at 14 days (20°C)..	108
Figure 3-46 : EDS analysis in outer CSH of cu800_3 and control paste at 14 days (20°C)..	108
Figure 3-47 : Average Ca/(Si+Al) and Al/Ca ratios for inner and outer C-S-H, series 3, (20°C) .....	108
Figure 3-48: Mapping of calcined clay grain in cu800_3 system at 28 days (20°C).....	109
Figure 3-49: Typical calcined clays grains in a 28days microstructure, serie 3 (20°C) .....	109
Figure 4-1 : Compressive strength and degree of hydration for standard calcined clays, series 1 (30°C).....	114
Figure 4-2 : Compressive strength and degree of hydration for kaolin-based calcined clays, series 1 (30°C).....	115
Figure 4-3 : Compressive strength and degree of hydration for series 2 (30°C) .....	115
Figure 4-4 : Strength relative to control mortar for series 1 and 2.....	118
Figure 4-5 : Strength relative to filler system for series 1 and 2.....	118
Figure 4-6: Comparison of strength profiles with heat of pozzolanic reaction by isothermal calorimetry .....	119
Figure 4-7: Correlation between strength increase and CH consumed in the pozzolanic systems .....	119
Figure 4-8 : Capillary porosity for series 1 (30°C) .....	121

Figure 4-9 : Water absorption for the first 8 hours, series 1 (30°C) .....	122
Figure 4-10: Sorptivity of cement-calcined clays mortars, serie 1 (30°C).....	122
Figure 5-1: DTG curves of a set of clays .....	124
Figure 5-2 : XRD pattern of 3 south american clays and one swiss clay.....	125
Figure 6-1: Influence of calcination time on specific surface of Cuban clays.....	131

## Glossary

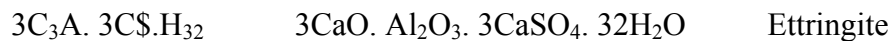
A simplified notation is used when describing cement compounds:

A: $\text{Al}_2\text{O}_3$	S: $\text{SiO}_2$	C: $\text{CaO}$	M: $\text{MgO}$
F: $\text{Fe}_2\text{O}_3$	\$: $\text{SO}_3$	H: $\text{H}_2\text{O}$	N: $\text{Na}_2\text{O}$
K: $\text{K}_2\text{O}$			

This leads to the following abbreviations for anhydrous and hydrates phases:

$\text{C}_3\text{S}$	$3\text{CaO} \cdot \text{SiO}_2$	Tricalcium silicate
$\text{C}_2\text{S}$	$2\text{CaO} \cdot \text{SiO}_2$	Dicalcium silicate
$\text{C}_4\text{AF}$	$4\text{CaO} \cdot \text{Al}_2\text{O}_3 \cdot \text{Fe}_2\text{O}_3$	Ferrite
$\text{C}_3\text{A}$	$3\text{CaO} \cdot \text{Al}_2\text{O}_3$	Tricalcium aluminate
$\text{C}\$\text{H}_2$	$\text{CaSO}_4 \cdot 2 \text{H}_2\text{O}$	Gypsum
$\text{C}\underline{\text{C}}$	$\text{CaCO}_3$	Calcium carbonate
$\text{CH}$	$\text{Ca}(\text{OH})_2$	Calcium hydroxide
$\text{C-S-H}$	$\text{CaO} \cdot \text{SiO}_2 \cdot \text{H}_2\text{O}$	Calcium silicate hydrate
$\text{C-A-S-H}$	$\text{CaO} \cdot \text{Al}_2\text{O}_3 \cdot \text{SiO}_2 \cdot \text{H}_2\text{O}$	Calcium silicate aluminate hydrate

AFt phase:



AFm phases:

$3\text{C}_3\text{A} \cdot \text{C}\$. \text{H}_{12}$	$3\text{CaO} \cdot \text{Al}_2\text{O}_3 \cdot \text{CaSO}_4 \cdot 12\text{H}_2\text{O}$	Tricalcium monosulfo aluminate
	$3\text{CaO} \cdot \text{Al}_2\text{O}_3 \cdot 0.5\text{Ca}(\text{OH})_2 \cdot 0.5 \text{CaCO}_3 \cdot 11.5\text{H}_2\text{O}$	Hemicarboaluminate
$3\text{C}_3\text{A} \cdot \underline{\text{C}} \cdot \text{H}_{11}$	$3\text{CaO} \cdot \text{Al}_2\text{O}_3 \cdot \text{CaCO}_3 \cdot 11\text{H}_2\text{O}$	Monocarboaluminate
$\text{C}_2\text{ASH}_8$	$2\text{CaO} \cdot \text{Al}_2\text{O}_3 \cdot \text{SiO}_2 \cdot 8\text{H}_2\text{O}$	Strätlingite (or gehlenite)

OPC:	Ordinary Portland Cement
SFB:	Solid Fuel Block
XRD:	X-Ray Diffraction
TGA:	Thermogravimetric Analysis
DTG:	Derivative Thermogravimetry
DTA:	Differential Thermal Analysis
DSC:	Differential Scanning Calorimetry
SEM-IA:	Scanning Electron Microscopy – Image Analysis
EDX analysis:	Energy Dispersive X-Ray analysis (or EDS)
EDS:	Energy Dispersive Spectroscopy
NMR:	Nuclear Magnetic Resonance
BSE:	Backscattered Electron
PSD:	Particle Size Distribution
BET:	Brunauer Emmet Teller (theory for specific surface measurements)
MIP	Mercury Intrusion Porosimetry
EPMA:	Electron Probe Micro Analyser

# 1 Introduction

## 1.1 Context

Housing shortage in developing countries is a serious issue. Due to the lack of facilities or investment to exploit local natural resources, the supply channels for most of the building materials (steel, glass, wood) is based on predominantly imported sources, increasing the cost and reducing the availability of the products. Although it is difficult to find data on the housing situation in developing countries, Table 1-1 shows figures from a study in 1994 reporting on a typical situation where most countries faced increased housing shortage. Due to the fast growing population in Africa, Asia and Latin America this situation is not likely to have improved in the last 15 years.

Country	Estimated Accumulated Housing Shortages	Increase in Housing Demand (units/year)	Housing by Formal Sector (units/year)	Estimated Housing - Informal Sector
Nicaragua	520,000 (1979)	20,000 (1979)	1,100 (1958-1978)	80%
Mexico	8,000,000 (1989)	700,000 (1989)	360,000 (1989)	65%
Guatemala	840,000 (1991)	56,500 (1991)	13,000 (1988)	65%
Cuba	813,000 (1990)	49,000 (1993)	17,300 (1990-1993)	35%
Panama	240,000 (1990)	20,000 (1990)	6,500 (1986-1988)	65%
Costa Rica	256,510 (1993)	25,000 (1992)	34,500 (1993)	-
El Salvador	573,676 (1983)	15,000 (1983)	21,800 (1983)	63%

**Table 1-1: Mismatch of housing demand and supply in selected developing countries, from Landaeta[1]**

What is important to retain from this table in the context of this study is the necessity from the informal sector of meeting their own housing needs. Unfortunately, About 50% of the total cost of all construction can be accounted for by building materials alone, and, in low-income shelter, the value of building materials can be as high as 80% of the total cost because of the relatively low requirements for other inputs such as equipment, installations and specialized skills [2]. For these reasons, the solutions adopted so far by local communities for their housing are rudimentary and not durable. Accessibility to basic building materials in sufficient quantities and at affordable costs is of key importance to meet the need of constantly growing urban and rural settlements. This implies organization at the community level and the revalorisation of locally available materials.

## **1.2 Need for new supplementary cementitious materials**

In spite of its often negative image based on misconceptions, concrete is the building material best suited to meet the housing demand – it is flexible, gives good performance in use, the basic raw materials are widely available and it has a relatively low energy and environmental impact compared to alternatives. Nevertheless, cement, the central ingredient is often disproportionately expensive in developing countries due partly to the significant energy consumption associated with its manufacture.

The most promising option to lower costs (and environmental impact) is to blend conventional Portland cement with pozzolanic materials. Pozzolans occur in natural deposits or can be obtained as by products in agri-industrial applications. They have drawn the attention of cement manufacturers for their good performance as cement replacement materials. Fly ash and slag, derived from the coal fired power stations and steel industry respectively, are good examples of industrial by-products that are being extensively used to substitute cement.

However, it is important to realise that in the long term, the existing by-products cannot fulfil the growing demand for supplementary cementitious materials (SCM's). Moreover, the availability of these by-products in developing countries is scarce. Thus, there is growing concern to find new alternative SCM's from local sources that are affordable and yet contribute to providing durable housing solutions.

With these considerations in mind, there was growing interest in this project to focus on calcined clayey soils. First, because it is as a widely accessible material, and second because it was already shown that under specific calcination conditions, this materials could reveal excellent pozzolanic properties. However, as they are the result of complex process of weathering of rocks with different mineralogies, these materials are found on the earth crust with a great variety of crystallographic structures and chemical compositions and clayey sediments are generally composed of a combination of clay types, clay purities and companion minerals. This emphasised the need for a scientific approach to the problem in order to understand the influence of the type of clay and the amount of companion minerals on the activation potential of these materials by thermal treatment.

### **1.3 Objectives of the study**

This project is part of a joint research programme with the University of Santa Clara in Cuba. It was funded by the Swiss National Science Foundation (SNSF) with the intention of promoting research in cooperation with developing countries.

The original idea that was considered by the Cuban partners was to take advantage of the considerable amounts of agricultural waste from the sugar industry available in Cuba [3, 4]. The sugar can straw and bagasse represent large volumes of waste that could be used for their calorific value in order to calcine the clay. The technology consisted of producing a form of pellet, called solid fuel block (SFB), which is a densified mixture of waste biomass and clay in a given proportion. The clay had to be soaked in water in order to form a slurry that would facilitate the binding of the shredded particles of biomass. Once dried, the SFB would be burnt and the heat used for different purposes, while the resulting ash could be used as a pozzolan. This technology was promising for the idea that it could provide renewable energy for many applications and simultaneously produce low-cost ecological building materials in the form of a reactive ash (pozzolan). An experimental kiln was built to burn solid fuel blocks and follow temperature changes as well as cooling regimes. Unfortunately, too many parameters were influencing the quality of the ash such as size of the block, density, clay/biomass ratio. Due also to uncontrolled burning conditions in the experimental kiln, the amount of unburnt material and carbon residues was too high and the reactivity of the produced pozzolan was seriously compromised.

It was soon realised that the complexity of the thermal activation of clays had to be understood in more details in order to address the issue of co-calcination with organic wastes. Therefore, it was decided to put the idea of the Solid Fuel Block aside and perhaps reconsider it in future projects once the thermal activation of the clayey materials was understood.

4 PhD projects were initiated (3 in Santa Clara and 1 in EPFL), each of them with a specific task related to the scientific background of the participants, as can be seen in Table 1-2. Care has been taken to try and tackle the issue of pozzolanic activity of calcined clays from the pure chemical aspects of the thermal activation up to the incorporation of these materials in concrete.

	Location	Scientific background of the PhD candidate	Objective
Sub-project 1	Santa Clara	Inorganic chemistry	Determine the calcination parameters for optimizing pozzolanic potential of a cuban clayey soil
Sub-project 2	Lausanne	Material science	Understand the influence of cristallinity and kaolinite content of calcined clays on the interaction with cement
Sub-project 3	Santa Clara	Civil engineering	Study the effect of grinding and deflocculation on the pozzolanic activity of a cuban clayey soil
Sub-project 4	Santa Clara	Civil engineering	Optimise mix designs for high levels of substitution of cement by pozzolans in concrete

**Table 1-2: Objectives of the joint research programme distributed in 4 sub-projects**

The present work reports on the research activities undertaken in the second sub-project. The objective is detailed in the subsequent paragraph.

*Main objectives:*

- Study the decomposition mechanisms leading to clay activation

Although many works report on phase changes of clays with temperature, the decomposition sequence of these materials is still unknown and the structure of metastable phases is still unresolved (see section 2.2).

- Identify parameters controlling the pozzolanic reactivity of a calcined clay

These parameters are chemical or physical and will depend on the raw material and the thermal treatment.

- Understand the effect of calcined clays on the microstructure of cementitious materials

Little work has been done to explain the mechanical properties of cement-calcined clays blends based on the interaction of these materials at the microstructural level.

*Secondary objectives:*

- Predict the pozzolanic activity of any clay according to its mineralogy
- Provide local communities with simple techniques derived from fundamental studies to evaluate the activation potential of any given clay
- Identify new or already existing technologies where the activation process could be performed



## 1.4 Experimental approach

As observed in Figure 1-1, this work is a multi-step approach that first focused on characterizing the raw and calcined materials and then assessed their pozzolanic properties and changes in the microstructure of cement pastes. 3 Standard clays were first studied: kaolinite, illite and montmorillonite. They were investigated as a means to understand the thermal behaviour of different clay types. Then, a more complex clay consisting in a natural mixture of clay types was studied to evaluate to which extent it could be used as reactive mineral admixture. A highly reactive metakaolin was also used for comparative reasons. Cement-calcined clays mortars were prepared to see how the microstructural changes translated into mechanical properties. It also brought a practical dimension to the research. Final perspectives including ideas on simple methodologies for the identification of potentially reactive clayey soils in developing countries are presented.

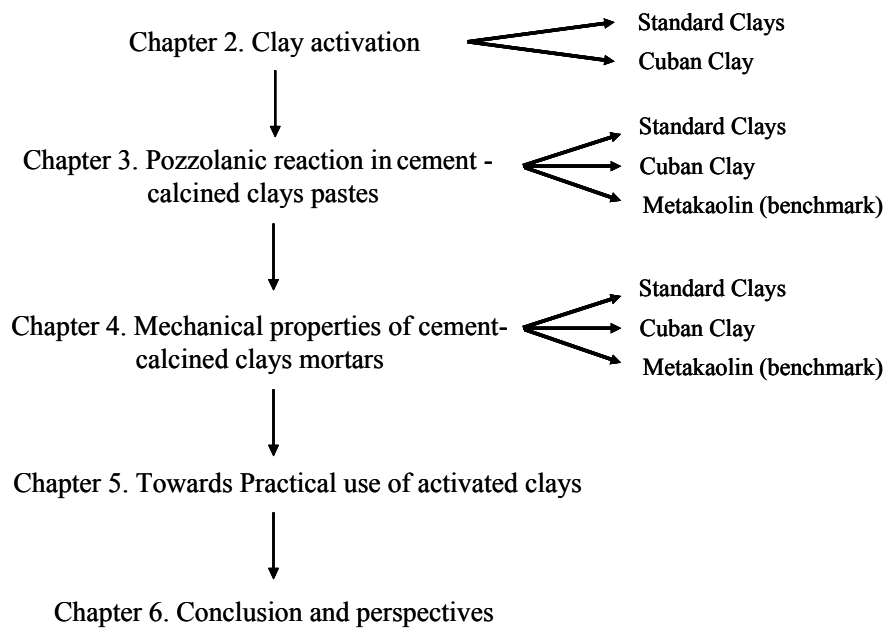


Figure 1-1: Structure of the investigation



## 2 Clay activation

### 2.1 Structure and composition of clayey materials

Clay minerals are formed by weathering of silicate minerals in rocks, such as feldspar, micas, amphiboles and piroxenes. They are considered as being phyllosilicates<sup>1</sup> that usually occur in particle sizes of 2µm or less[5]. However, many examples of these minerals are also of larger particle size and many non-clay minerals may occur in particles considerably less than 2mm in diameter[6]. Crystal structure and chemical composition are thus what really differentiates clays from non-clay minerals as they define their characteristic physical properties such as plasticity.

Each clay particle or micelle is made up of several tens or even hundreds of layers, whose structure is a combination of silicon and aluminium sheets. As can be seen in Figure 2-1, a silica sheet is composed of silicon atoms in tetrahedral coordination, where three of the four oxygens in each tetrahedron are shared to form a hexagonal net. Alumina sheets, as represented in Figure 2-2, are composed of aluminium atoms in octahedral coordination with oxygens or hydroxyls.

Isomorphous substitutions are very common in this type of sheet.  $Mg^{2+}$ ,  $Fe^{2+}$ ,  $Fe^{3+}$ ,  $Mn^{2+}$  cations typically substitute for  $Al^{3+}$ . If the cation is trivalent, then normally only two-thirds of the possible cationic spaces are filled, and the structure is termed *dioctahedral*, as it is the case for *gibbsite*  $Al_2(OH)_6$ . If the cation is divalent, then all possible cation sites are occupied and the structure is *trioctahedral*, as it is the case for *brucite*  $Mg_3(OH)_6$ . Substitutions of silicon by aluminium in the tetrahedron are also possible but less common.

---

<sup>1</sup> Clay particles are made up of thin sheets or leaves, which is why argillaceous minerals are referred to as phyllite (“Phylon” means leaf in Greek). Thus, like micas, they form part of the phyllosilicates group.

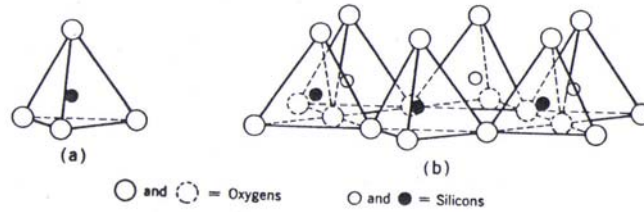


**Figure 2-1: (a): Silicon in tetrahedral position, (b): Silica sheet, (Grim [7])**

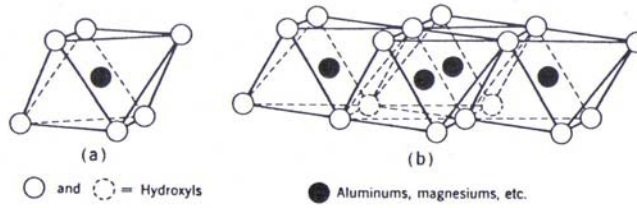


**Figure 2-2: (a): Aluminium in Octahedral position, (b): Alumina sheet, (Grim [7])**

It should be mentioned that other types of clay exist, based on oxides other than silica and alumina but silica and magnesia or silica and iron oxide. Nevertheless, the alumino-silicates minerals represent 74% of the earth's crust [5] and this why clays based on alumino-silicates structures will be considered exclusively in this study.

Different clay mineral groups are characterized by the stacking arrangements of sheets and the manner in which two, successive two or three-sheet layers are held together [8]. Figure 2-3 gives the synthesis pattern for the clay minerals.

From this schematic representation, three groups can be identified:

- The **1:1** layer group (Kaolinite, Halloysite)
- The **2:1** layer group ( Pyrophyllite, Smectite (Montmorillonite), Vermiculite, Illite)
- The **2:1:1** layer group (Chlorite)

Note that more than one type of clay mineral is usually found in most soils. Also, irregular or random interstratification of two or more layer types often occurs within a single particle. Montmorillonite-illite is most common, and chlorite-vermiculite and chlorite-montmorillonite are often found.

Our interest will focus on the three clay types of major abundance, which are kaolinite, illite and montmorillonite (smectite). The structure of these clays are shown in Figure 2-4.

Chapter 2: Clay activation

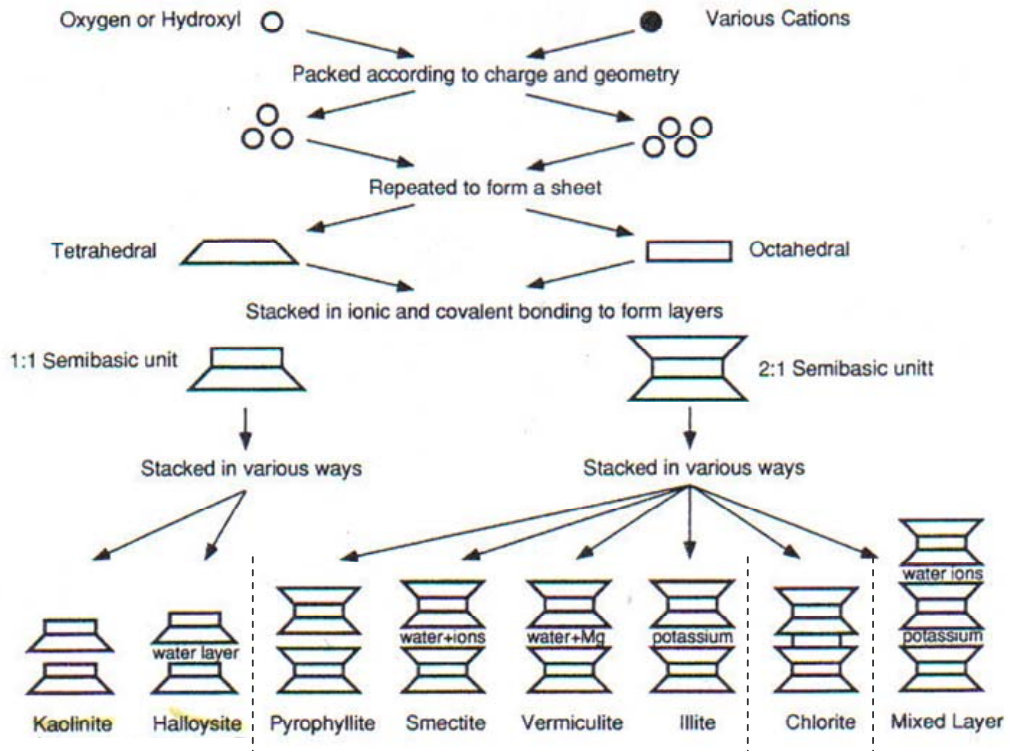


Figure 2-3: Synthesis pattern for the clay minerals (Mitchell [8])

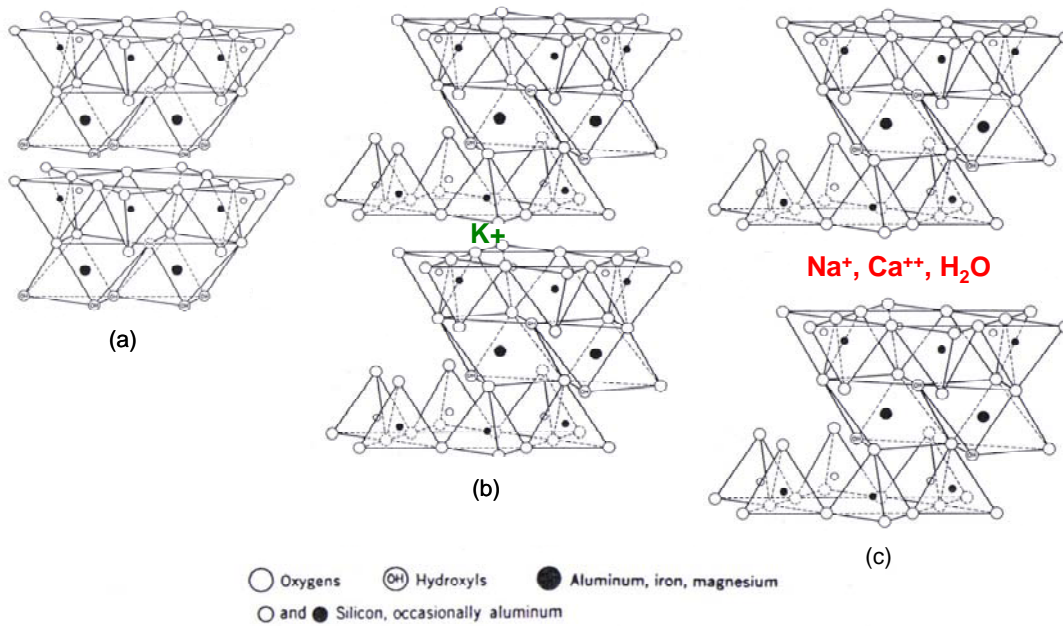


Figure 2-4 : Structures of kaolinite (a), illite (b) and montmorillonite (c) (adapted from Grim[7])

Kaolinite minerals are composed of alternating silica and octahedral sheets [8]. In the plane of atoms common to both sheets, two-thirds of the atoms are oxygen, one third are hydroxyls. Because of slight differences in the oxygen-to-oxygen distances in the tetrahedral and octahedral layers, there is some distortion of the ideal tetrahedral network. As a result, kaolinite is triclinic instead of monoclinic. Mineral particles of the kaolinite subgroup consist of the basic unit stacked in the *c* direction (see Figure 2-4 (a)). The bonding between successive layers is both by Van der Waals forces and hydrogen bonds. The bonding is sufficiently strong that there is no interlayer swelling in the presence of water. The basal spacing in the *c* direction  $d_{(001)}$  is 7.2 Å. Well-crystallised particles of kaolinite generally occur in the form of hexagonal plates, whose lateral dimensions are in the range 0.1 to 4 µm and thickness from 0.05 to 2 µm.

Illite usually occurs as very small, flaky particles mixed with other clay and non-clay minerals [8]. High-purity deposits of illite are uncommon. The flaky particles may have a hexagonal outline if well crystallized, with lateral dimensions in the order of those of Kaolinite, but with plate thicknesses as small as 30 Å. As for its structure, it is a three-layer silica-gibbsite-silica sandwich with the tips of all the tetrahedra pointing towards the centre and common with octahedral sheet ions (see Figure 2-4 (b)). Two types of isomorphous substitutions occur in this mineral. First, about one fourth of the silicon positions are filled by aluminium, and the resulting charge deficiency of 1.3 to 1.5 per unit cell is balanced by potassium between the layers. Interlayer bonding by potassium is so strong that the basal spacing of illite remains fixed at 10 Å in the presence of polar liquids. Second, some magnesium or iron can substitute aluminium in the octahedral sheets.

Crystal structure of Montmorillonite is very similar to that of Illite, as can be seen in Figure 2-4 (c), except that the bonding between successive layers and the balance charge is made by different cations, such as  $\text{Na}^+$  or  $\text{Ca}^{++}$ . These bonds are weak and easily separated by cleavage or adsorption of water or other polar liquids. Thus, the basal spacing in the *c* direction,  $d_{(001)}$ , is variable, ranging from about 9.6 Å to complete separation, which explains the swelling capacity of this type of mineral. In the octahedral sheet, every sixth aluminium is usually replaced by magnesium, which generates a charge deficiency of 0.66 per unit cell. Again these charge deficiencies are counterbalanced by exchangeable cations located between the unit cell layers and on the surfaces of particles. Montmorillonite may occur as equidimensional flakes that are so thin as to appear more like films. Particles range in

thickness from 1nm unit layers up to about 20nm. The long axis of the particle is usually less than 1 or 2  $\mu\text{m}$  [8]. Table 2-1 summarises principal characteristics of the three most common clay minerals.

Name	Group	Crystal system	Ideal Formula <sup>2</sup>	Isomorphous substitution	Interlayer Bond	Basal spacing
Kaolinite	1:1	Triclinic	$\text{Al}_2\text{Si}_2\text{O}_5(\text{OH})_4$	Very little	O-OH, strong	7.2 Å
Illite	2:1	Monoclinic	$(\text{Si}_4)(\text{Al},\text{Mg},\text{Fe})_{2,3}\text{O}_{10}(\text{OH})_2 \cdot (\text{K},\text{H}_2\text{O})$	Some Si by Al, balanced by K between layers	K ions, strong	10 Å
Montmorillonite	2:1	Monoclinic	$\text{Na}_{0.33}(\text{Al}_{1.67}\text{Mg}_{0.33})\text{Si}_4\text{O}_{10}(\text{OH})_2 \cdot n(\text{H}_2\text{O})$	Mg for Al	O-O, very weak, expanding lattice	> 9.6 Å

**Table 2-1 : Characteristics of clay minerals of most abundance**

## 2.2 State of the art in clay activation

Activation of a clayey material refers to the process of modifying its original crystalline structure by means of mechanical, chemical or thermal action in order to make it chemically more reactive to its environment. Extrusion or attrition milling [9, 10] are examples of mechanical activation as it delaminates the clay to give a more open structure. Alkali activation is reported as being an effective chemical technique that improves solubility of silica and alumina in the system [11-14].

As for thermal activation, it consists of heating the clay to a given temperature in order to remove its structural water [15]. This process is known as dehydroxilation. As OH groups form part of the octahedral layer and link it to the tetrahedral layer, removal of these groups leads to a state of more structural disorder that is a metastable state. Therefore, the term metakaolin refers to the mineral kaolin that has been heated to disorder the structure through

<sup>2</sup> All formulas are reduced to the smallest unit formula; they do not reflect unit cell composition. Many variations can occur, particularly in the interlayer positions of the montmorillonite. Cations such as  $\text{Ca}^{++}$  and  $\text{Na}^+$  are often present.

the removal of water from the clayey sheets (see Figure 2-5 (right)). As opposed to the original mineral that has high levels of crystallinity, a metastable clayey phase has a lower degree of crystalline order and is often referred as a semi-crystalline phase[16]. The benefits of a thermally activated clay, over its untreated precursor, have been widely studied for use in cementitious materials [17, 18]. Thus, thermal processing is probably the most common technique to activate clays and several studies can be found in the literature in this topic, as discussed in the following two sections.

### *2.2.1 Nature of the clay and activation temperature*

Among the different parameters influencing pozzolanic reactivity, researchers have mainly looked at the nature of the clay and the temperature of activation.

For example, He [17, 19-23] evaluated the optimum activation temperature of different standard clayey materials and assessed the reactivity of the calcined clays when mixed with lime or cement. The optimum temperatures of activation were 650°C for kaolinite, 830°C for Ca-montmorillonite, Na-montmorillonite and sepiolite, 930°C for illite and 960°C for a mixed-layer mica/smectite. He concluded that kaolin and Ca-Montmorillonite had the highest pozzolanic activity, the rest of the materials could be considered of low-pozzolanic activity even when calcined at their optimum activation temperature. It should be mentioned that different water to binder ratio were used depending on the water demand of the clay, and that values of compressive strength had to be adjusted according to Feret's law [24]. Comparison between the different samples is thus difficult.

Ambroise [25, 26] worked with an activation temperature of 750°C based on previous studies by Murat [27] and found best results for kaolinites from France as compared to Montmorillonite and Illite, which did not give satisfying results at this temperature when mixed with lime in different proportions. His work also assessed the pozzolanic properties of 3 lateritic soils from Mali and 1 from Cameroun. The four soils contained different percentages of kaolinite ranging between 33 and 55%. They were calcined at 750°C for 5h and mixed with calcium hydroxide in various proportions to form pastes. Results showed that these materials behave reasonably well and that there is a relationship between the 28 days compressive strength and proportion of kaolin in the soil.

Chakchouk [28] also found that Tunisian clays with highest kaolinite content had high pozzolanic activity when compared with clays containing illite or montmorillonite as main



*Chapter 2: Clay activation*

constituents. 700°C-800°C was found to be the optimum activation range for clays containing kaolin.

Authors	Year	Type of studied clay / soil	Treatment Temperatures (°C)	Calcination times	Optimum activation Temperature (and time)	Pozzolanic activity
Ambroise	1984	Kaolinite	750	5h	750°C	high
		Montmorillonite				low
		Illite				low
		Lateritic soils				medium
Martin-Calle	1989	Kaolinites	600, 650, 700, 750, 800, 850	2h, 5h, 24h	700°C, 24h	high
		Brick clays (Illite/Kaolinite)	700, 750, 800	2h, 5h, 24h	700°C, 24h	medium
C.He	1995	Kaolinite	550, 650, 800, 950	100 min	650°C	high
		Na-Montmorillonite	740, 830, 920		830°C	low
		Ca-Montmorillonite	730, 830, 920		830°C	medium
		Illite	650, 790, 930		930°C	low
		Sepiolite	370, 570, 830		830°C	low
		Mixed layer Mica-Smectite	560, 760, 960		960°C	low
Chakchouk	2006	Kaolinite	500, 600, 700	5h	700°C-800°C	high
		Illite/Montmorillonite clays	500, 700, 800	5h	-	low

**Table 2-2: Activation temperatures and times for different types of clays**

It appears that, among the studied clays, kaolin has the highest potential for pozzolanic activity, its activation temperature being in the 650 – 800 °C range depending on its purity and companion minerals (see summary in Table 2-2).

As a result, several studies used thermoanalytical techniques to try and optimize the calcination process of kaolinite and improve its reactivity. Other studies have also attempted to understand the decomposition mechanisms of kaolin clays from a structural point of view,

mainly with the help of X-Ray Diffraction and NMR techniques. A selection of papers treating these subjects is presented in the following section.

### 2.2.2 *Understanding decomposition mechanisms for optimizing the metakaolin product*

In 2001, Sabir [29] wrote an interesting review including many of the studies cited below. It looked at the product metakaolin from many perspectives: starting with its production optimization, on to its positive influence on mechanical properties and durability of cementitious materials.

Brindley's survey back in 1959 [30] compared the work of various scientists who investigated the phase transformations of kaolin, from its dehydroxylation to the recrystallisation phenomena. Based on these findings, he proposed a semicrystalline structure for metakaolin [31] satisfying a gradual transition from the kaolin mineral to the mullite phase obtained at higher temperatures (925°C) [32]. He recognised however that the structure suggested a stable phase and provided no obvious explanation why metakaolin has a disordered structure in the c direction.

MAS NMR (Magic Angle Spinning Nuclear magnetic resonance) has been shown to be an interesting technique to determine the chemical environment of the aluminium or silicon atoms, distinguishing between the microcrystalline and amorphous phases in calcined clays. Using this technique, other authors have investigated on the structure of metakaolin and presented, based on their findings, a revised structure from that of Brindley. It is the case of Mackenzie [33], who explained the distortion in the c-direction by observing a chemical shift and a broadening of the peak corresponding to Q<sup>3</sup> environment of Si in thermally treated kaolins. The proposed model for metakaolinite including only 4 and 6-coordinated Al is presented in Figure 2-5 (left). He was followed by Rocha & Klinowski [34] who based in previous works on aluminosilicates by Lippmaa [35] and Gilson [36], showed the occurrence of 5-coordinated aluminium. They monitored thermal transformations of kaolinite by <sup>27</sup>Al MAS NMR and showed that the amounts of the three existing populations of aluminium change with temperature. Below 800°C, 4- and 5- coordinated Al appears at the expense of 6-coordinated Al, but above 800°C the amount of 6-coordinated Al increases again, associated with the formation of new Al species such as mullite or  $\gamma$ -alumina. As for <sup>29</sup>Si NMR, an important broadening of the original single resonance assigned to a Q<sup>3</sup> Si environment was observed. This indicates the presence of amorphous material, but the 4 additional signals resulting from deconvolution of the parent resonance could not be assigned to particular

silicon environments although Q<sup>4</sup> environments were suggested. They also explained how a 5-coordination aluminium could be obtained from 6-coordinated Aluminium by elimination of water by neighbouring hydroxyl groups, as can be seen in Figure 2-5 (right).

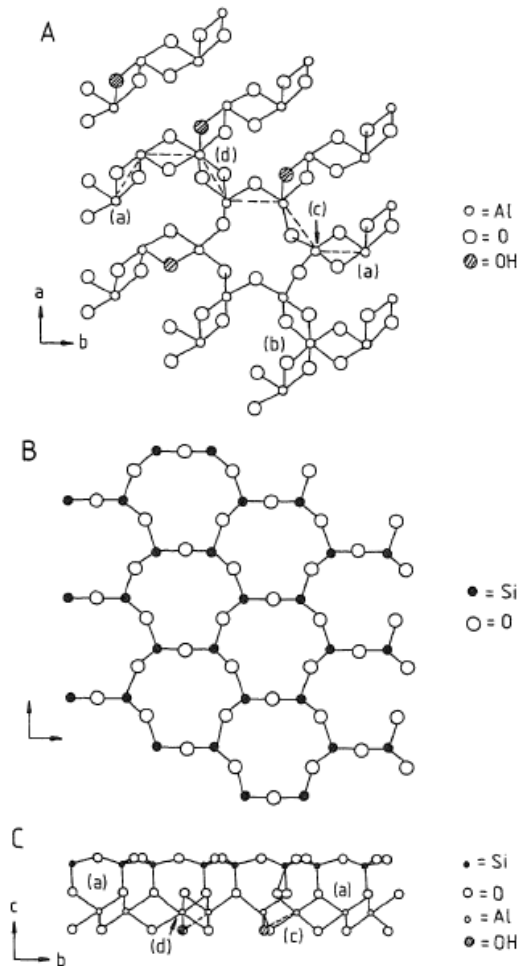


Fig. 6. Computer-generated view of typical regions of the proposed metakaolinite structure;  $a = 0.5396$  nm,  $b = 0.9379$  nm,  $c = 0.737$  nm,  $\alpha = 91.6^\circ$ ,  $\beta = 104.8^\circ$ , and  $\gamma = 89.9^\circ$ . (A) Al-O (OH) layer, projection on (001) plane showing (a) typical distorted 4-coordinated anhydrous Al, (b) regular 6-coordinated anhydrous Al, (c) regular 4-coordinated Al, which can either be anhydrous or contain an isolated residual hydroxyl, and (d) regular 6-coordinated Al containing isolated residual hydroxyl; site (d) can also occur in anhydrous form. (B) Si-O layer, projection on (001) plane. (C) View along  $a$  axis, including only Al atoms joined by dashed line in (A); bonds shown by dashed lines connect to aluminums out of plane of paper.

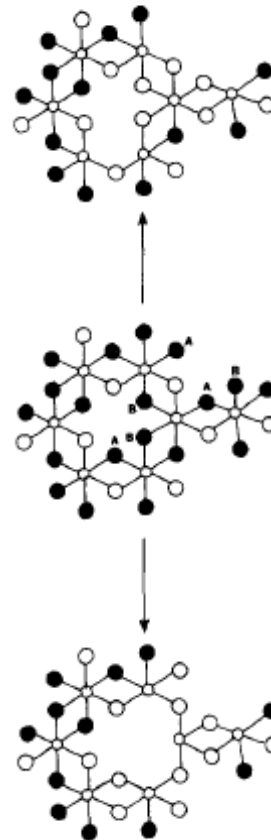


Fig. 9. Possible dehydroxylation sequences leading to different coordination of aluminium via reactions between neighbouring hydroxyl groups (A and B). The Si sheet is not shown for clarity. Small and large open circles denote Al and O atoms, respectively; solid circles denotes OH groups

**Figure 2-5 : Models for Metakaolin based on NMR measurements. left : Mackenzie [33], right: Rocha [34]**

Similarly, Macedo [37] showed the occurrence of three resolved peaks for metakaolin in Al MAS NMR and Massiot [38] described the metakaolinite product as an amorphous material based on a disordered polymerized silicon/aluminium network in which aluminium preferably occupies four- and five-fold structural positions in the ratio 60% Al<sup>[IV]</sup>, 30% Al<sup>[V]</sup>, and 10% Al<sup>[VI]</sup>. Liu [39], however, did not observe 5-coordinated Al in his thermally treated samples of kaolinite, but only 4- and 6-coordinated Al.

Most of the interest with NMR has been focused on kaolinite transformations, but some papers also report on thermal behaviour of illite [40] and montmorillonite [41].

With a more practical approach targeting the construction industry, Murat [27] looked at the calcination conditions for obtaining the most reactive pozzolan from kaolinite. He compared a fixed bed calcination process to a rotary kiln process and found that the first option gave better results in terms of strength of a lime-calcined clay paste, almost independently of the calcination temperature and time.

Authors	Year	Type of studied clay / soil	Treatment Temperatures (°C)	Calcination times	Optimum activation Temperature (and time)	optimization
Brindley	1959	Kaolinite	490 – 1400	48h	-	Proposed metakaolin structure
Murat	1983	French Kaolinites	600°C-850	t<3h, t<6h	750°C	Fixed bed vs rotary kiln
Salvador	1995	French Kaolinites	550-950	0.54s, 2s, 6s, 12s, 5h		Fixed Bed vs Flash calcination
Shvarzman	2003	Israeli kaolinite	400, 450, 500, 570, 700	5h	700°C	Quenching, amorphous phase content
Badogiannis	2005	Kaolinites	550, 650, 750, 850, 950	1h, 2h, 3h, 4h, 6h, 8h	650°C-750°C, 3h	
Cara	2006	Sardinian Kaolinites	530, 630, 800	100 min	630	Temperature

**Table 2-3: Optimization of the metakaolin product**

Martin-Calle [42] looked at the influence of mineralogy and calcination conditions on the pozzolanic activity of various kaolinites and two clayey soils used in brick manufacturing. For the most ordered kaolinitic clays, the temperature at which most of the material is in an amorphous state was found to be 800°C. But he showed that this material was not necessarily the most reactive and that there is a compromise between degree of crystallinity, particle size distribution and surface properties in order to define the optimum activation temperature.

## *Chapter 2: Clay activation*

The effect of flash calcination on pozzolanic reactivity was investigated by Salvador [43], who showed that reactivity can be slightly increased by reducing the residence time from hours (soak-calcination) to a few seconds in a pilot flash calcining plant. However, little information on the difference in morphology or crystalline state of the calcined materials were given.

Shvarzman et al. [44] found a linear relationship between the weight loss from TGA analysis and the amorphous phase content. They assume that the clay has reached its highest degree of dehydroxylation /amorphisation when the weight loss becomes negligible upon heating. By comparing TGA curves of untreated kaolin doped with different amounts of totally dehydroxylated clay with those of kaolin calcined at different temperatures, they estimated an amorphous content for each treatment temperature. They concluded that their local kaolin clay calcined at 700°C is transformed into 75% amorphous material and 25% of inert material that could not be further activated as the additional weight loss was negligible above that temperature. The problem of this approach is that compressive strength results for different kaolins with same amorphous content did not give similar results. Indeed, the author identified other important parameters affecting reactivity such as morphology and surface features that could possibly explain these important differences, but no further investigation was carried out in that area.

The work of Badogiannis [45] looked at the influence of kaolin content of different Greek clays on their pozzolanic activity. The optimum activation temperature and time were 650°C and 3 hours respectively. For 2 out of the 4 clays studied, he managed to get slightly higher mechanical resistance than the control paste with a 20% cement substitution. Unlike Ambrose [25], no clear correlation could be made between kaolinite content and mechanical performance, probably due to unknown particle size distribution or lack of accuracy in the determination of mineralogical composition of the materials.

Cara [46] looked at three different activation temperatures for the activation of Sardinian kaolin clays. The reactivity was assessed by determining the residual lime content in calcined-clays lime pastes measured by DTA. He concluded that reactivity was similar for activation temperatures of 630°C and 800°C and therefore the lowest one should be kept for economical reasons. However, no mechanical test was undertaken.

To summarize, studies undertaken so far have shown that among the clayey structures studied, kaolinite can be systematically and rather easily activated. The optimum temperature of activation seems to depend on the purity of the material and the companion minerals. This activation temperature is located in the range 630-800°C. Montmorillonite seems to give some signs of reactivity when calcined at its optimum calcination temperature of 830°C, but again there is no general agreement about this. Other clay types such as illite have been found to show very little to almost no reactivity even after complete dehydroxylation.

It should also be mentioned that previous studies have not sufficiently characterized their material before and after thermal treatment and have concentrated on the results given by the lime-pozzolan mixtures (a more detailed literature survey on the assessment of pozzolanic activity on cement-pozzolan pastes is presented in chapter 3). Also, little effort has been made to pre-process materials before calcination. Thus, it is believed that a complete characterization of the calcined material combining a variety of techniques such as XRD TGA, NMR, BET, PSD, and SEM could help to further understanding the decomposition processes and above all will serve as basis for the interpretation of its microstructural behaviour in a cementitious matrix.

Having these background considerations in mind, it is reasonable to continue the investigation of clay activation for its use as cement replacement material for the following reasons:

On the one hand, gain more knowledge on the decomposition process of clayey materials, which has not yet been perfectly understood due to the complexity of the crystal structures we are dealing with and the variability of these materials in terms of chemical composition.

On the other hand, reach general agreement on the type of clays that can be easily activated. In the context of developing countries and more specifically low-cost housing, simple tools to rapidly identify the activation potential of any clay locally available together with simple field methods for improving quality of the raw material have not yet been developed.

Also, studies on calcined clays so far have been separated in two parts: those that studied the thermal activation and have invested little time on the assessment of the reactivity (generally one technique). The other, that did not study the activation parameters but concentrated in the interaction of these pozzolans with lime and cement. The idea of this work is to link the two areas of research by going from a study of activation to a complete characterization of a cementitious system incorporating calcined clays.

### 2.3 Experimental studies of clay activation

This part of the work focused on the understanding of the thermal behaviour of the three clayey structures most commonly found on the earth crust, which are as already mentioned kaolinites, montmorillonites (smectites) and illite (micas) structures. Based on the behaviour of these so-called standard clays, a more detailed study on a Cuban clay was made, the aim being to look at a locally available material in order to reach its maximum pozzolanic potential by optimizing activation parameters and see if it can be used in a low-cost building material.

After studying the behaviour of the untreated material, clays were subjected to a calcination process in the range of 500 to 1000°C. These materials were then characterized by several different techniques. Figure 2-6 summarises the experimental approach and the techniques used.

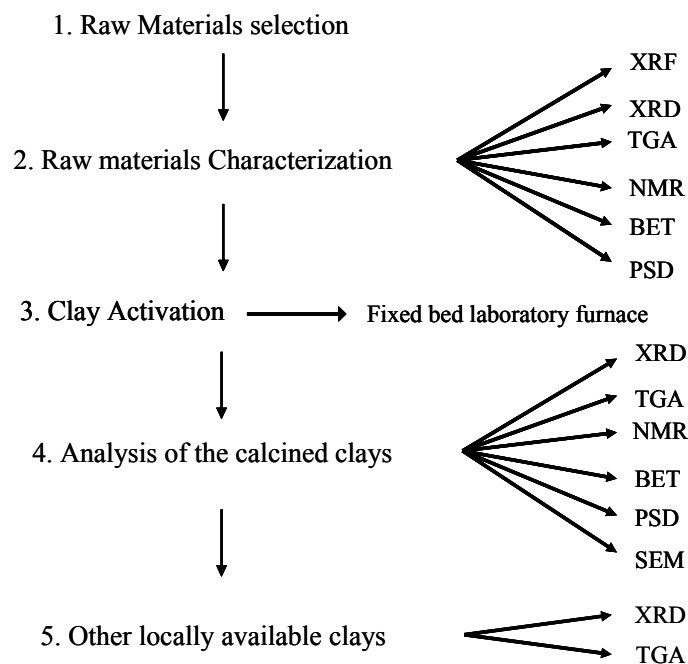


Figure 2-6: Experimental approach for clay activation

#### 2.3.1 Raw materials selection

The standard clays (kaolinite, montmorillonite illite) were purchased from Ward's natural science (<http://wardsci.com>). Technical data on standard clays is presented in appendix I. The first two were in the form of powder and used as received for characterization and thermal treatment, whereas illite was received in the form of shale and had to be crushed for 1min in a ring crusher in order to get a homogeneous powder.

The Cuban clay was taken from a quarry in the town of Manicaragua, in Villa Clara Province. This clayey soil is commonly used by local brick manufacturers. First in the form of dry lumps, the material was put in a 400mm-diameter water barrel to separate the clayey particles from quartz sand, which was present in considerable proportions in the quarry. Sodium hexametaphosphate (SHMP) was used as a deflocculating agent. For each batch, 10kg of soil was put into 40 litres of water and 3 litres of a 50 g/L SHMP solution were added. A 5cm-diameter propeller was fixed to a drilling machine and used to deagglomerate the lumps by constantly mixing for 15min. Separation of the clayey fraction was thus done by sedimentation. After 5h, the clayey suspension was siphoned out of the barrel and let to dry for 1 week at 80°C. Dry flakes of clayey material were crushed in the ring crusher for 1min to get a homogeneous powder. One sedimentation batch produced on average 3 kg of clay.

For more detailed study of the crystal structure and thermal behaviour, the clayey samples were also further treated by a centrifugation process [47] in order to collect particles under 2µm in size. The protocol for centrifugation is presented in appendix II. The resulting refined clayey pastes were used by XRD and thermogravimetric analysis.

### 2.3.2 Characterization methods

The characterisation of the untreated material and calcined materials included X-Ray Diffraction (XRD) with a Panalytical X'Pert Pro MPD diffractometer in a  $\theta$ - $\theta$  configuration employing the CuK $\alpha$  radiation ( $\lambda=1.54 \text{ \AA}$ ) with a fixed divergence slit size 0.5° and a rotating sample stage. The samples were scanned between 4 and 70 ( $^{\circ}2\theta$ ) with the X'Celerator detector. Step size and time per step were set to 0.017 ( $^{\circ}2\theta$ ) and 80 s respectively.

A Mettler-Toledo TGA/SDTA 851 instrument was used for thermogravimetric measurements. 10°C/min was systematically used as temperature ramp and experiments were carried out from 30°C up to 900°C. A 30 ml/min nitrogen flux was used in the heating chamber in order to avoid carbonation of the samples during the experiment. Water loss from dehydroxylation of the clays was measured by the tangent method.

Differential scanning calorimetry measurements were performed with a Netzsch DSC/DTA Model 404 C *Pegasus*®, using a 10°C/min heating rate. The samples in the form of powders were weighed ( $20 \pm 4 \text{ mg}$ ) and placed in an alumina crucible pan, an empty alumina crucible being used as reference. A nitrogen flux was maintained in the heating chamber to avoid



carbonation of the samples during the experiment. Heat flow data was recorded using a computer-driven data acquisition system.

The  $^{29}\text{Si}$  NMR spectra were carried out on a Bruker ASX 300 spectrometer (7.05 T magnetic field) at 59.6 MHz. Spectra were recorded at 7 kHz spinning rate in 4 mm  $\text{ZrO}_2$  rotors. Single pulse experiments without  $^1\text{H}$  decoupling were carried out by applying  $90^\circ$  pulses with recycle delay of 8 s in order to respect the relaxation times of the species present in the samples. The  $^{27}\text{Al}$  NMR experiments were performed on a Bruker ASX 500 spectrometer, in a 11.7 Tesla field, operating at 129.80 MHz for  $^{27}\text{Al}$ . Spectra were recorded at 10 kHz spinning rate in 4 mm  $\text{ZrO}_2$  rotors. All experiments employed single pulse ( $\pi/12$ ) excitation width pulse of time pulse 0.5 ms without  $^1\text{H}$  decoupling and a 1s relaxation delay.

X-Ray Fluorescence (XRF) measurements were performed by an external company (APC Solutions SA, CH-1021 Denges) using a Bruker AXS S4 Explorer spectrophotometer operating at a power of 1 kW and equipped with a Rh X-ray source. Crystals used were OVO55FC for Na, F, Cl with  $0.46^\circ$  divergence collimator, PET for Al, Si, P et Mn with  $0,23^\circ$  divergence collimator and LiF220, with  $0,23^\circ$  divergence collimator for all other elements.

Particle size distribution was measured with a Malvern Mastersizer type S laser beam granulometer allowing measurements of particles sizes ranging from 0.05 to 900  $\mu\text{m}$  in dispersion. Cements were dispersed in isopropanol, whereas clays were dispersed in a 0.01% PAA solution (poly acrylic acid).

A Micromeritics Accupyc 1330 V2 instrument was used for bulk density measurements, and a Micromeritics Gemini 2375 V4 instrument allowed the determination of specific surface (BET).

Backscattered electron (BSE) images were taken with a FEI machine type quanta 200, equipped with a tungsten filament. The accelerating voltage was set to 15 keV. In order to get flat surfaces, powders as well as hardened cement pastes had to be impregnated with epoxy resin and polished using a Struers Rotopol machine. Abrasive agent were sprays with different diamond particle sizes ranging from 9  $\mu\text{m}$  to  $\frac{1}{4}$   $\mu\text{m}$  (9, 3, 1,  $\frac{1}{4}$   $\mu\text{m}$ ). They are provided by the same manufacturer. For good surface finishing, 90 minutes polishing per diamond size together with constant lubrication using laboratory petrol were required.

### 2.3.3 Activation process (thermal treatment)

For the thermal treatment of the clays, a Nabertherm laboratory furnace was used. 50 g of clay were put into 50 ml cylindrical alumina crucibles, which were introduced in the furnace prior to heating. 4 crucibles were introduced per thermal treatment. The heating rate was set to 300°C/h and soak time at desired temperature was 60 min. Calcination temperatures ranging between 500 and 1000°C were studied in order to follow with precision the decomposition steps of the clays.

Figure 2-7 shows a typical temperature profile in the laboratory furnace given by a thermocouple placed in the upper part of the chamber.

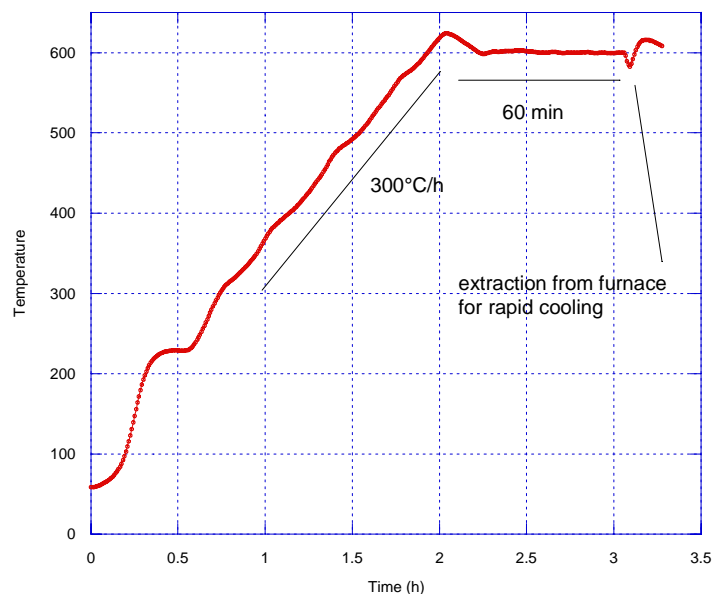


**Figure 2-7: Temperature profile in the laboratory furnace for a thermal treatment at 600°C for 60min**

When reaching the desired temperature, an overshoot can be observed due to the thermal inertia of the furnace. This overshoot was considered as being part of 60 minutes thermal treatment. Cooling was done rapidly by removing the crucibles from the hot furnace with the help of long tweezers and spreading the material on a metal plate. The material is left to cool down for a few minutes on the plate and then it is collected with a paintbrush.

## 2.4 Activation of standard clays

Based on the thermogravimetric measurements that will be presented below, calcination temperatures for standard clays were set to 600°C and 800°C. Raw materials as well as calcined products were characterized in order to evaluate the changes in properties brought by the thermal treatment.

### 2.4.1 Raw materials

Chemical composition of the three standard clays is given in Table 2-4. Note that aluminium content is highest in kaolinite, potassium content is highest in illite and sodium content is highest in montmorillonite. These results confirm theoretical aspects of clay structures presented in section 2.1.

% weight	SiO <sub>2</sub>	Al <sub>2</sub> O <sub>3</sub>	Fe <sub>2</sub> O <sub>3</sub>	CaO	MgO	SO <sub>3</sub>	K <sub>2</sub> O	MnO	Na <sub>2</sub> O	Others	LOI	total	Alkalis % (Na <sub>2</sub> Oeq)
Kaolin.	48.00	36.40	0.85	0.14	0.11	0.03	0.48	0.01	0.02	0.55	13.41	100.00	0.33
Illite	58.68	19.25	5.04	1.29	2.50	0.17	6.12	0.05	0.19	1.00	5.71	100.00	4.22
Montm.	63.15	20.09	3.96	1.15	2.27	0.51	0.54	0.02	2.22	0.20	5.90	100.01	2.57

**Table 2-4: Chemical composition of kaolinite, illite and montmorillonite**

The diffraction patterns for the standard clays are reported in Figure 2-8 to Figure 2-10. The red patterns refer to the materials as received (except for illite that had to be crushed). The blue ones are the materials after a centrifugation/sedimentation process, as described in appendix II.

X-Ray diffraction patterns on the centrifuged samples (< 2 µm particles) reveal the presence of companion minerals, indicating that the clays are not pure. For kaolinite, there seems to be some traces of muscovite, which is a 2:1 dioctahedral layer structure resembling that of illite. A 2:1:1 structure (chlinochlore) could also be detected in the illite sample, while traces of cristobalite were found in the montmorillonite sample. It should be mentioned that the so called < 2µm particle samples were in the form of a paste as it was the result of a centrifugation process to collect the smaller particles. Therefore, stacking of the clayey particles induces preferential orientations for diffraction and the signal of the basal planes is increased. This can be a very useful technique for the identification of clayey minerals as randomly distributed particles may not allow peaks coming from different clayey phases to be distinguished. Another interesting feature can be seen in Figure 2-10 with the shift of

the 001 plane. This corresponds to an increase of the basal spacing from  $d = 12.3 \text{ \AA}$  to  $d = 15.0 \text{ \AA}$ , due to water molecules adsorbed in the interlayer space of the montmorillonite. This phenomenon was only observed for montmorillonite, as the interlayer bonds in kaolinite and illite are too strong. Note that aluminium peaks detected in the centrifuged sample of montmorillonite are due to the sample holder and should not be taken into account for the interpretation.

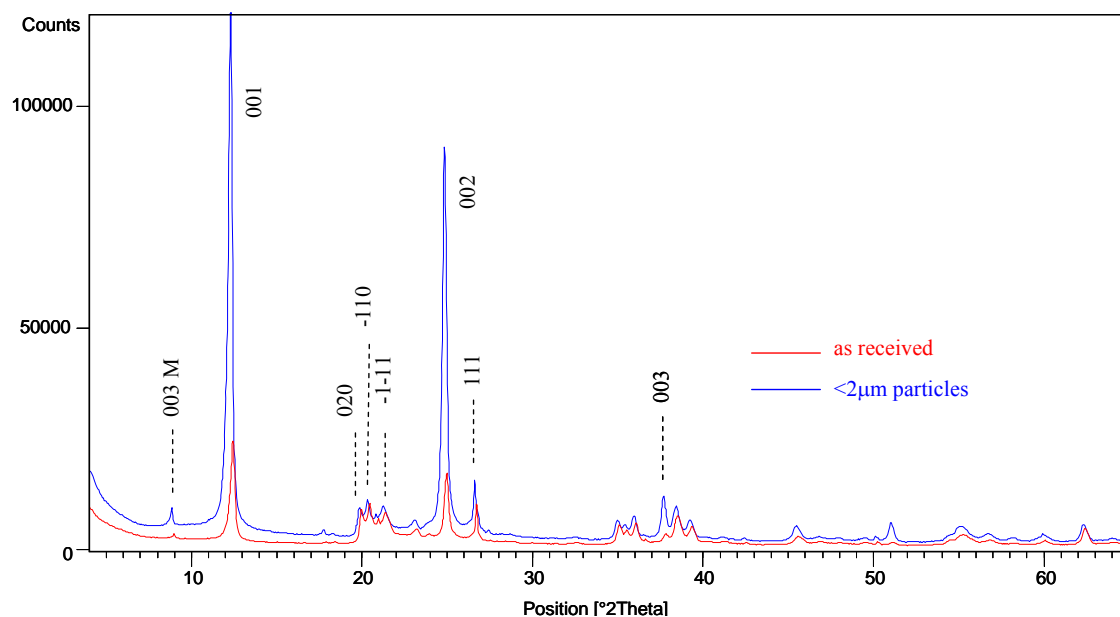


Figure 2-8 : XRD patterns of kaolinite, as received and with centrifugation process (M: muscovite)

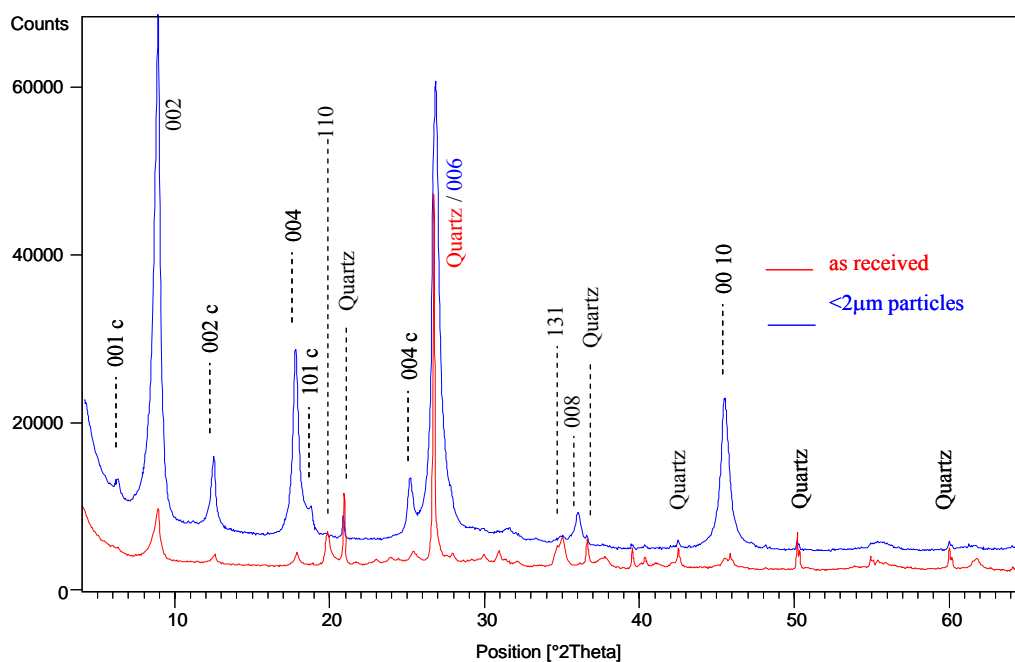
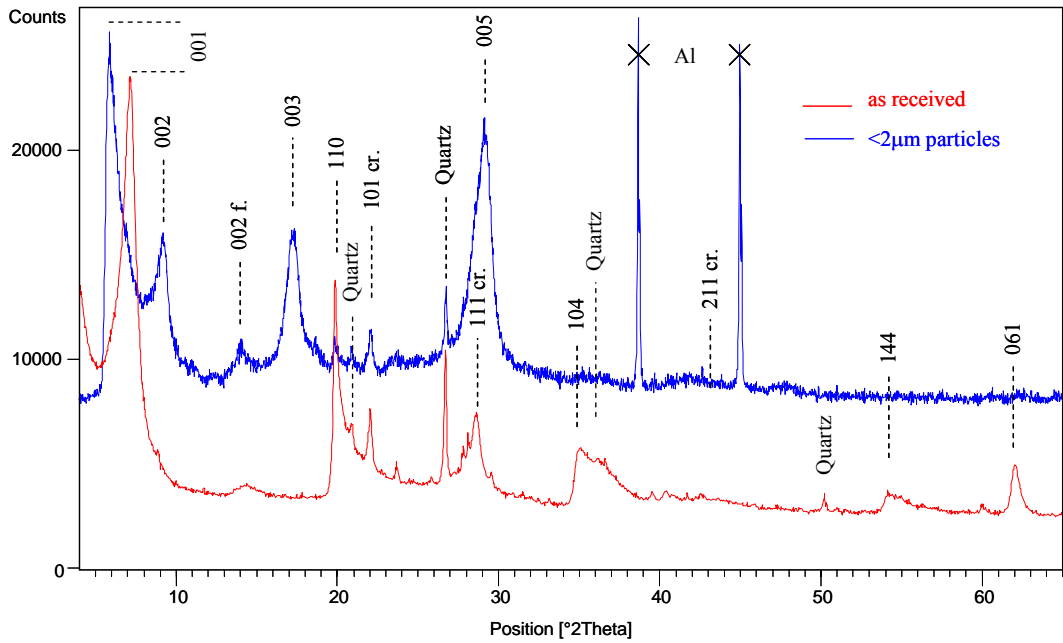
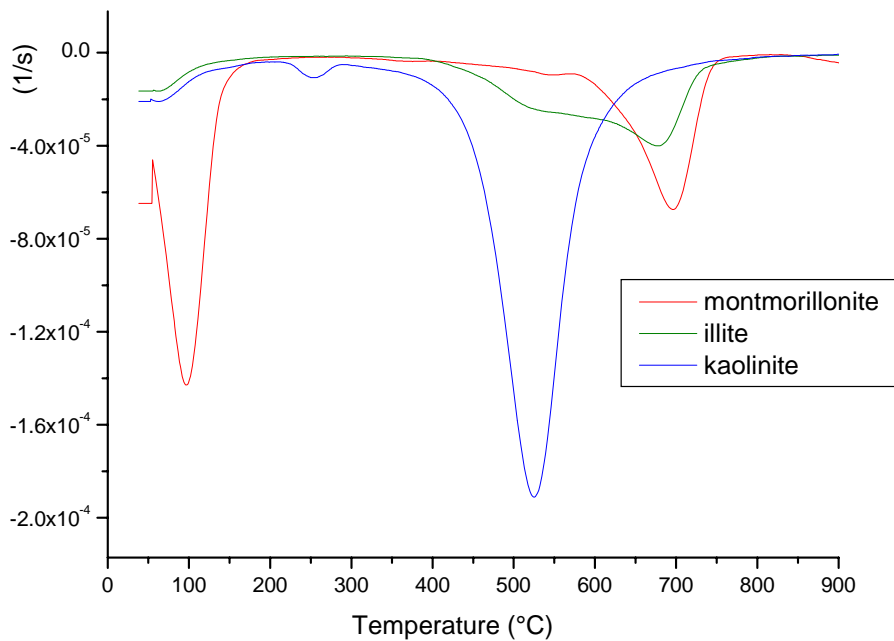


Figure 2-9 : XRD patterns of Illite, as received and with centrifugation process (c: clinocllore)



**Figure 2-10 : XRD patterns of Montmorillonite, as received and after centrifugation (cr.:cristobalite, f.: feldspath)**



**Figure 2-11: DTG of standard clays (as received)**

The differential thermogravimetric analyses in Figure 2-11 reveal the decomposition phenomena that are characteristic of the clay type [15]. Small mass loss in the range of 30 to 250°C for kaolinite and illite can be assigned to drying of the absorbed water. Montmorillonite exhibits a more important release of water from between the layers. Following Todor [48] and Grim [7], the property of retaining different amounts of water

depends on the absorbed cation. The hydration energy of this exchanged cation affects the form of the thermal effect. According to Barshad [49], a single thermal effect (as observed in this type of montmorillonite) indicates that the exchanged cations is monovalent (e.g.  $\text{Na}^+$ ,  $\text{K}^+$ ). Although the samples were dried at  $60^\circ\text{C}$  before the analysis, water was retained in the interlayer space of montmorillonite or reabsorbed between the drying stage and the thermal analysis, indicating the reversibility of the process.

Dehydroxylation refers to the removal of the structural water molecules and can be observed in our case in the  $400^\circ\text{C}$  to  $800^\circ\text{C}$  range. Note that the kaolinite peak between  $400^\circ\text{C}$  and  $650^\circ\text{C}$  is characteristic of the kaolinite structure and is often used to quantify the purity of this type of clay (see. section 2.5.1). Indeed, these peaks are indicative of the amount of hydroxyls originally present in the structure. As one could expect, based on the theoretical chemical formulas of the clays presented in Table 2-1, kaolinite has more OH groups incorporated in its structure compared to the 2:1 structures. The position of the dehydroxylation peak depends mainly on the type of structure and how the hydroxyls are bound to it, whereas its shape or range depend more on the crystallinity or particle size distribution; the more crystalline the material, the sharper the dehydroxylation peak for a given structural hydroxyl. The small mass loss clearly identified on the kaolinite sample around  $275^\circ\text{C}$  could be due to the dehydration of halloysite, a clay mineral of the kaolinite subgroup.

Dehydroxylation of illite is more gradual and occurs over a wide temperature range ( $400$ - $750^\circ\text{C}$ ). It seems that two peaks overlap each other, attributable to two phenomena. As supplied by XRD studies described below, dehydroxylation of the companion mineral (chlinochlore) could possibly explain this thermal behaviour. For montmorillonite, removal of the hydroxyls from the structure occurs at higher temperatures ( $600$ - $800^\circ\text{C}$ ).

Bulk density measurements together with specific gravity were performed using the Helium pycnometer and BET analyser respectively. Results are given in the following section (Table 2-5).

### 2.4.2 Characterization of calcined clays

According to their thermal behaviour that was presented in Figure 2-11, the clays were calcined at 600°C and 800°C. This was the best compromise to investigate the effect of partial to complete dehydroxylation on the physical properties of the clays.

Figure 2-12 and Figure 2-13 present the XRD patterns, <sup>27</sup>Al NMR spectra and DTG curves of the raw and calcined kaolinite. At 600°C, practically all peaks corresponding to the 1:1 structure have disappeared, indicating an important destructure. A treatment at 800°C does not bring many more changes to the decomposed structure, apart perhaps from the shape of the “hump” between  $2\theta = 15^\circ$  and  $35^\circ$ . This shape is a typical sign of amorphous material. Traces of muscovite and some quartz could be identified whose structures have not been altered by temperature.

DTG shows how effective a given thermal treatment has been on the clay dehydroxylation. For kaolinite, dehydroxylation can be considered to be complete at 600°C, as the amount of hydroxyls remaining in the sample after such thermal treatment is negligible. As mentioned in section 2.2, dehydroxylation is, in this case, the process which causes the loss of crystallinity. Indeed, in a 1:1 layer group, most of the hydroxyls are located at the lower surface of the layer. They link layers together by forming hydrogen bonds in the interlayer spacing. Therefore, hydroxyls in this conformation have higher free energy than if they were trapped in between sheets, as it is the case for 2:1 layer groups.

The effect of dehydroxylation on the structure of kaolinite was observed by single-pulse <sup>27</sup>Al MAS NMR, where Al in different coordination sites could be distinguished. The sharp peak that can be observed around 1ppm for the reference kaolinite has been previously observed (e.g. [33, 39]) and attributed to Al<sup>[VI]</sup>. In this case the sharpness of this peak indicates a well ordered octahedral structure. After calcination at 600°C, two peaks appear, at 28ppm and 56ppm, attributed to Al<sup>[V]</sup> and Al<sup>[IV]</sup> respectively. These peaks were also observed in previous studies presented in section 2.2.2 (Lippmaa [35], Gilson [36] and Rocha [34]). It is interesting to note that the Al<sup>[V]</sup> peak increases with increasing temperature to be the dominant coordination at 800°C. This clearly indicates a disordering of the original crystalline structure. Surprisingly, small changes in the XRD and DTG patterns from 600 to 800°C do not reflect the structural changes occurring in the surroundings of the aluminium in that range of temperature. This suggests that the mechanism of dehydroxylation alone can not explain the observed disordered state for metakaolinite and there must be another mechanism that

increases the number of 5-coordinated Al when going from 600°C to 800°C. Following Rocha, this could be the modification of the short-range order of Si in metakaolinite observed by  $^{29}\text{Si}$  NMR, indicating that a range of  $\text{Q}^m(\text{nAl})$  environments could be formed with Al in all three coordinations. This hypothesis could also explain the persistence of the 6-coordinated Al that was rather unexpected due to the complete dehydroxylation at 800°C observed by DTG.

Figure 2-14 and Figure 2-15 present the XRD patterns,  $^{27}\text{Al}$  NMR spectra and DTG curves of the raw and calcined illite. Little change from the original material could be observed in the XRD patterns. Traces of chlinochlore were diminished at 600°C and disappeared at 800°C, suggesting that its structure has broken down in this range of temperatures. The basal planes (002, 004, 006, 0010) seem to resist well thermal treatment as only a small drop in intensity was observed for those peaks. Surprisingly, the 110 plane, which is a perpendicular plane to the basal ones, has a more intense reflexion after thermal treatment. One interpretation could be that the thermal treatment can lead to a re-ordering of the planes rather than a loss in crystallinity, but problems of preferential orientation could also explain these intensity variations and should not be neglected. DTG curves for illite show that not all hydroxyls have been removed at 600°C, suggesting that the structure is not completely decomposed. It is interesting to note that dehydroxylation has no effect on crystallinity as observed by XRD.

The  $^{27}\text{Al}$  NMR spectra for Illite exhibit 2 peaks with maxima at 1 ppm and 56 ppm, that could be assigned to  $\text{Al}^{\text{[VI]}}$  and  $\text{Al}^{\text{[IV]}}$  respectively. The shape and position of the peaks corresponds well with previous published studies on this type of clay [40]. The presence of the 4-coordinated peak indicates that Al is substituting Si in tetrahedral positions and is very common in clays belonging to the 2:1 layer groups (this applies also to montmorillonite presented below). The sample undergoes a clear transition from  $\text{Al}^{\text{[VI]}}$  to  $\text{Al}^{\text{[IV]}}$  with a thermal treatment at 600°C. The results for illite could well correspond with DTG and XRD observations. Indeed, a gradual shift of the aluminium coordination from VI to IV with increasing temperature is a clear sign of dehydroxylation as OH groups in a clayey structure are originally bound to aluminium. The loss of hydroxyls would be such that in XRD little change in the 001 spacing of the crystal could be detected (small decrease of the 002, 004, 0010 peak height), whereas a reordering in the 110 directions could be observed (increase of 110 peak).

Figure 2-16 shows the changes in montmorillonite by XRD. The collapse of the basal planes with temperature is apparent. The main basal spacing (001 plane) goes from 12.3 Å for the



raw material to 9.6 Å at 600°C. This is actually due to the removal of the interlayer water originally contained in the sample, as seen by DTG in Figure 2-17. It should therefore not be considered as an activation process. The value of 9.6 Å as lowest possible basal spacing confirms the mineral as montmorillonite (see Table 2-1). The presence of rather inert companion minerals such as albite (a feldspar) and muscovite, are useful indicators of montmorillonite decomposition. Indeed, their signal increases with temperature, indicating that their contribution to the total amount of crystalline material increases. For this to happen, one crystalline material has to be altered so that its signal decreases. It is the case for montmorillonite and most of its reflexions (001, 002, 104, 114, 061). However, this decomposition cannot be compared to the kaolinite decomposition as some peaks remain at 800°C and no sign of an amorphous material (“hump”) could be detected. After a treatment at 800°C, the mass loss from dehydroxylation is not detectable with thermogravimetric analysis and the signal is flat. Thus the amount of remaining hydroxyls after such thermal treatment can be considered as negligible.

<sup>27</sup>Al NMR spectra for montmorillonite presented in Figure 2-17 exhibit the 2 same peaks as the illite spectra (1 ppm and 56 ppm assigned to Al<sup>[VI]</sup> and Al<sup>[IV]</sup> respectively). Previous works found the same shape and position of peaks for this type of clay [41]. However, compared with illite, the sample undergoes a more gradual transition from Al<sup>[VI]</sup> to Al<sup>[IV]</sup> with thermal treatment at 600°C. DTG curves explain this phenomenon, as most of the dehydroxylation occurs between 600 and 800°C. No clear sign of Al<sup>[IV]</sup> could be detected in montmorillonite, although broadening of the Al<sup>[IV]</sup> peaks to the right at 800°C could suggest the presence of this type of coordination. Al<sup>[VI]</sup> peak disappeared at 800°C, coinciding with total dehydroxylation observed by DTG.

The fact that the amount of hydroxyls present in the illite and montmorillonite structures is less than for kaolinite (see Table 2-1) could explain the little effect of dehydroxylation on the loss of crystallinity.

These correlations between the techniques lead to the conclusion that the decomposition phenomenon of Illite and Montmorillonite is clearly different from that of kaolinite. Their dehydroxylation is more likely to induce a reorganisation of the crystal than a proper disordering. For kaolinite, dehydroxylation does result in loss of crystallinity, as can be observed in XRD. The NMR spectra do not show a shift in the coordination state of aluminium, but rather an appearance of new coordination states in addition to Al<sup>[VI]</sup>. This

tends to indicate a more advanced state of disorder rather than a structural reorganisation. One possible explanation could be that kaolinite, among the clays studied here, is the only one to have an octahedral layer in direct contact with the interlayer space, the other clays having the octahedral layer located in between two tetrahedral layers (see section 2.1). Therefore, the loss of OH groups to form a water molecule may be facilitated and would leave Al linked to one oxygen atom instead two OH groups, diminishing its coordination number to 5. The presence of aluminium in tetrahedral coordination would result from further removal of oxygen atoms from the structure and could form a transitional structure between metakaolin and the mullite phase appearing above 850°C, as described by Brindley [31, 32].

To gain more knowledge on the changes of physical properties due to thermal treatment, particle size distribution and specific surface were measured. Figure 2-18 shows the effect of temperature on particle size distribution of the standard clays. As it was expected, thermal treatment tends to agglomerate particles together. This effect is more or less pronounced depending on the nature of the clay. Agglomeration was found to be highest for montmorillonite, followed by kaolin and illite.

The evolution of median particle size is also reported in Figure 2-18 and gives a good indication of the tendency of particles to agglomerate. The particle size distribution will have an effect on pozzolanic reactivity as well as on mechanical properties. Therefore, this parameter should be taken into account when interpreting results on cement-pozzolan pastes and mortars.

The changes in specific surface with temperature are reported in Figure 2-19. Again, most detrimental effects are seen for montmorillonite, whereas specific surface of illite and kaolinite particles seems to be less affected by temperature.

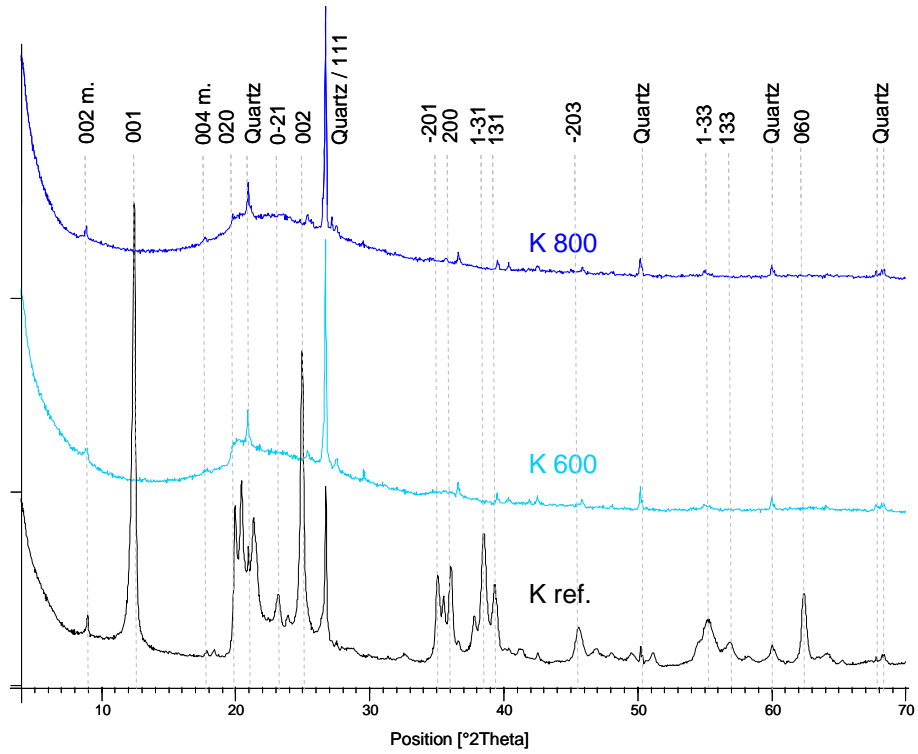


Figure 2-12 : XRD patterns for untreated and calcined kaolinite (m: muscovite)

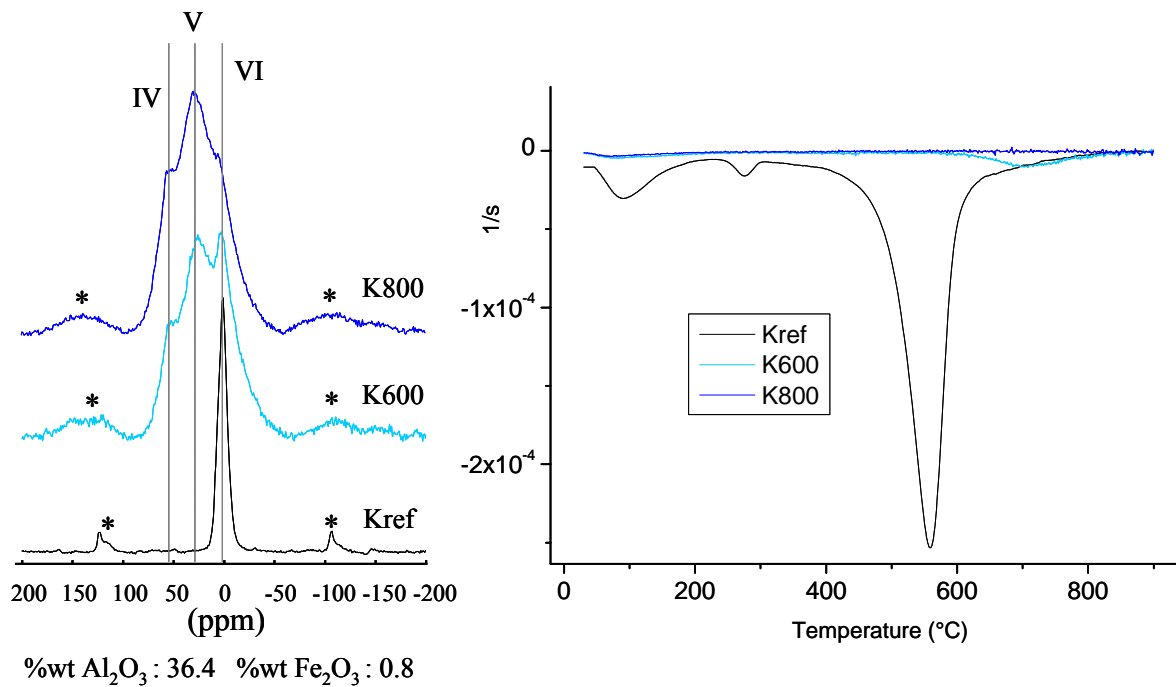


Figure 2-13 : <sup>27</sup>Al NMR spectras (left) and DTG curves (right) for untreated and calcined kaolinite

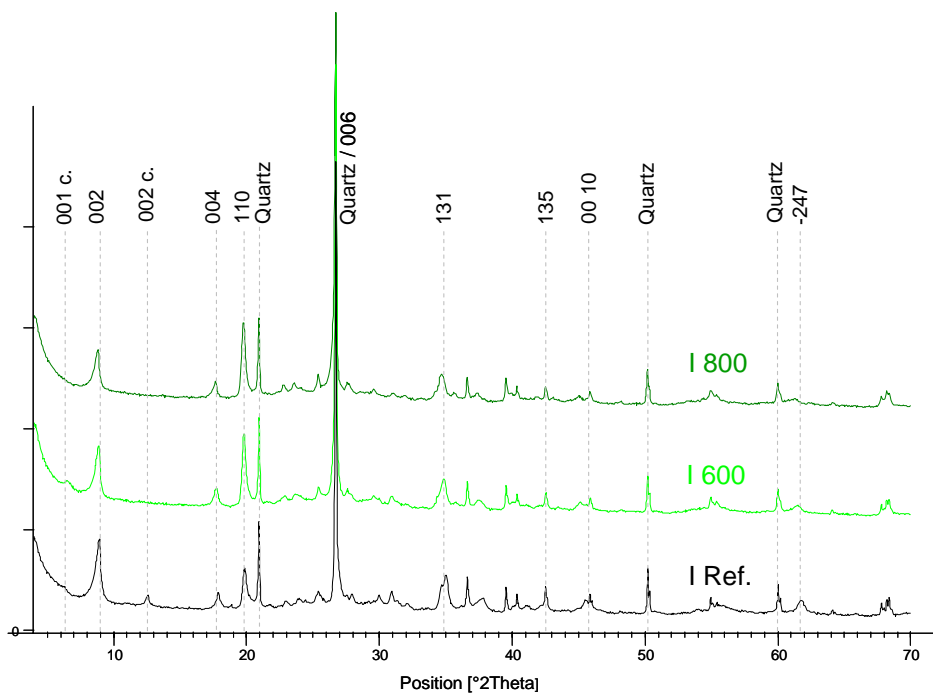


Figure 2-14 : XRD patterns for untreated and calcined illite (c: clinocllore)

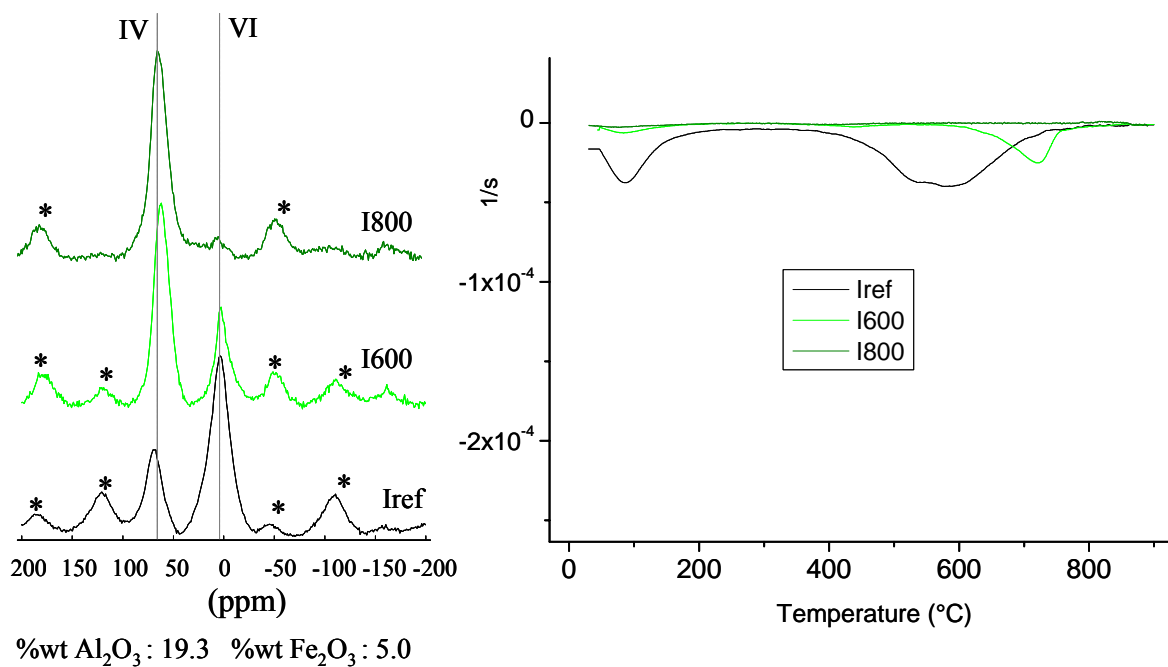


Figure 2-15 : <sup>27</sup>Al NMR spectras (left) and DTG curves (right) for untreated and calcined illite

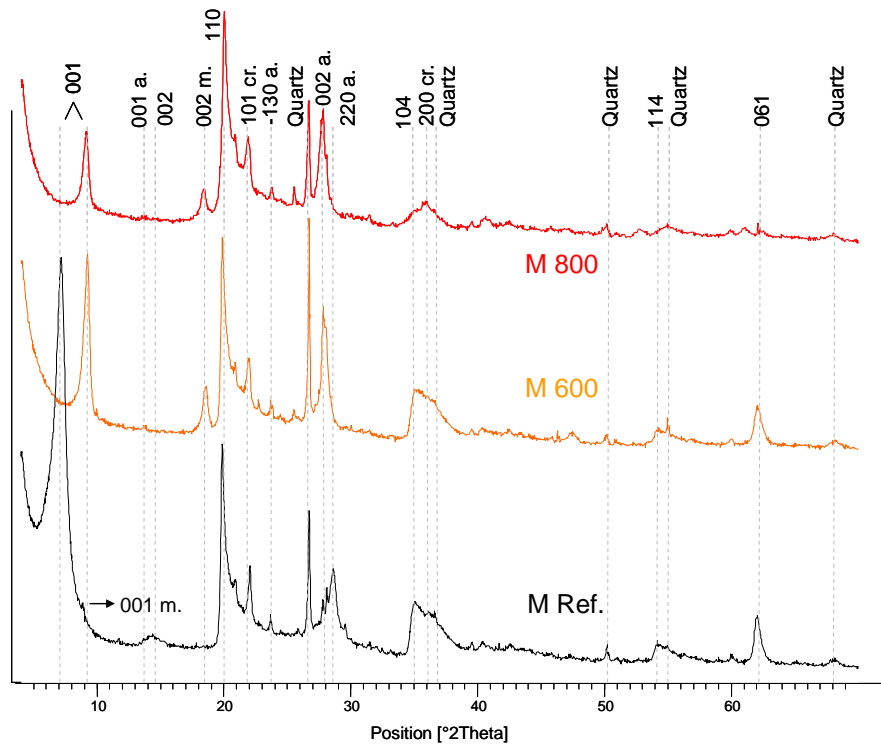


Figure 2-16 : XRD pattern for untreated and calcined montmorillonite (a: albite, cr: cristobalite, m: muscovite)

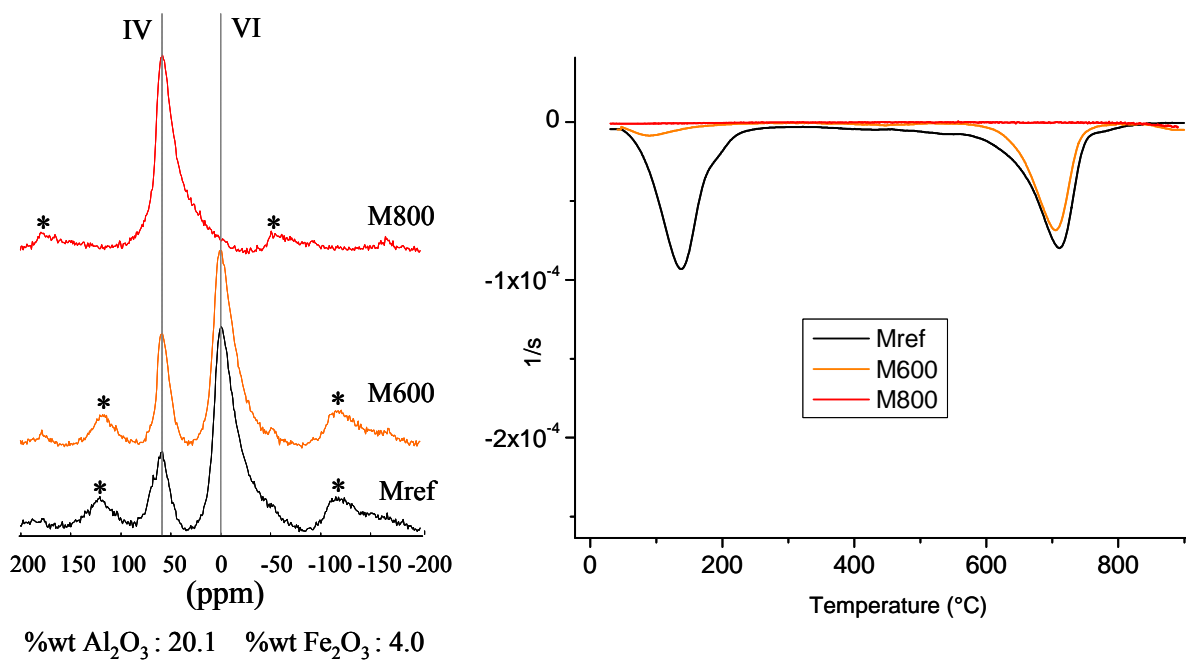


Figure 2-17 :  $^{27}\text{Al}$  NMR spectras (left) and DTG curves (right) for untreated and calcined montmorillonite

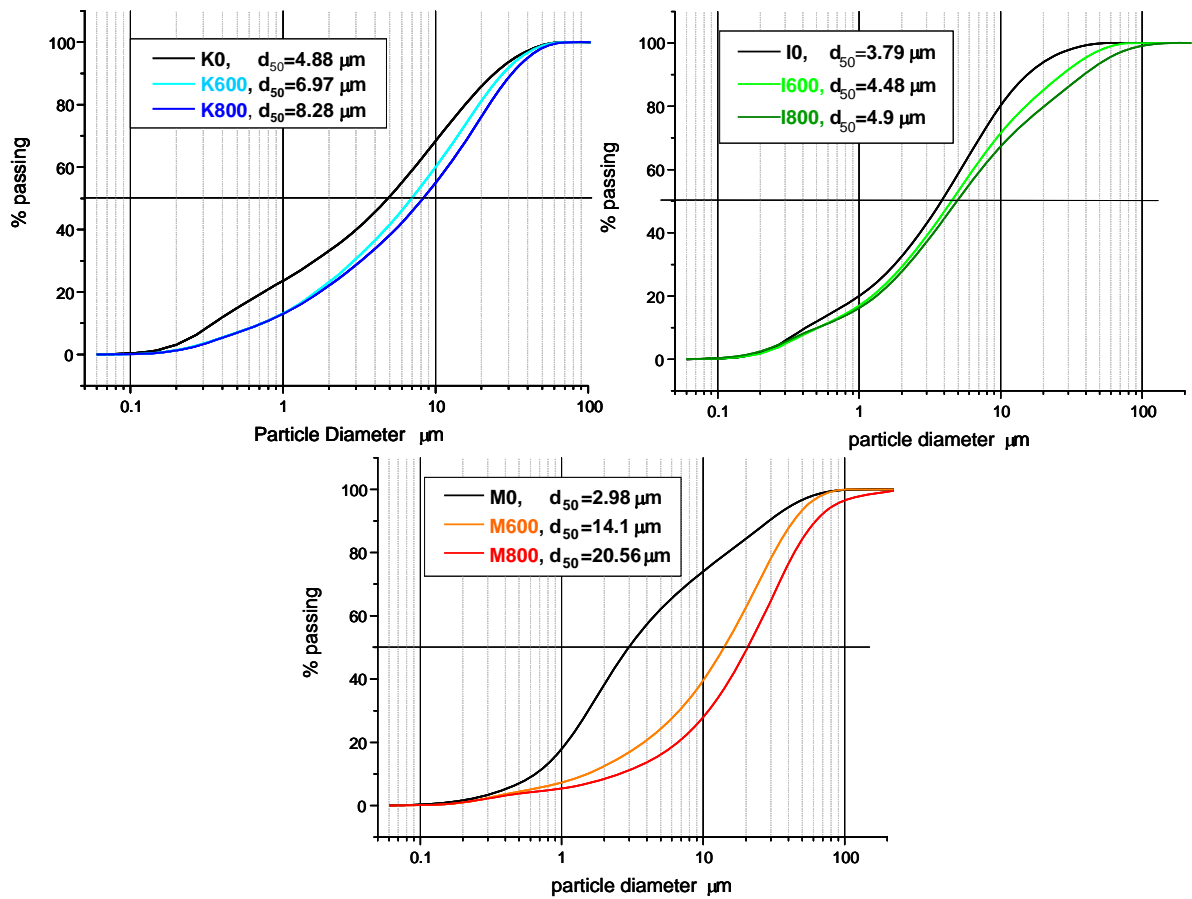


Figure 2-18 : Particle size distributions for standard clays before and after calcination

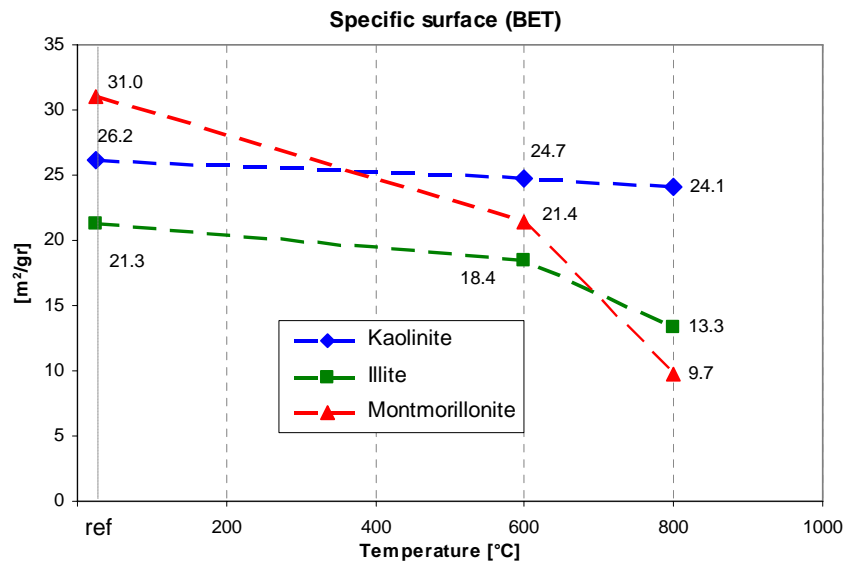


Figure 2-19 : Effect of temperature on specific surface of standard clays

Table 2-5 summarises main physical parameters of standard clays and their calcined products.

- Kaolinite seems to transform into a totally amorphous material, as shown by XRD. NMR results on the calcined products showed that Al in coordination 5 could be observed, indicating a short range disorder of this structure. Temperature has little effect on specific surface with moderate effect on particle size distribution.
- Illite gave almost no sign of destructureation by XRD and NMR results showed a direct transition from Al<sup>[VI]</sup> to Al<sup>[IV]</sup>. The effects of temperature on specific surface and particle size distribution are respectively moderate and very low.
- Montmorillonite particles are heavily affected by temperature, as PSD and BET results showed. Recrystallisations could have explained this phenomenon but as no new peaks were identified by XRD, this hypothesis was excluded. The little reduction of intensity of the main peaks of montmorillonite and the increase of the peaks corresponding to companion minerals suggests that some loss in crystallinity could be observed by XRD (particularly at 800°C).

Hence, kaolinite exhibits a totally different decomposition process that leads to the disordering of the crystal structure, whereas illite and montmorillonite seem to loose their hydroxyls without changing their crystalline state. Based on these results, kaolinite is expected to have the highest pozzolanic activity, followed by montmorillonite and illite.

Method:	BET	PSD	He-Picnometer	NMR	XRD
Parameter:	specific surface [m <sup>2</sup> /gr]	median diameter d50 [μm]	bulk density [gr/cm <sup>3</sup> ]	Al coordination	clay decomposition
Kaolinite ref.	26.15	4.88	2.67	Al <sup>[VI]</sup>	-
Kaolinite 600°C	24.7	6.97	2.55	Al <sup>[IV]</sup> , Al <sup>[V]</sup> , Al <sup>[VI]</sup>	high
Kaolinite 800°C	24.13	8.28	2.65	Al <sup>[IV]</sup> , Al <sup>[V]</sup> , Al <sup>[VI]</sup>	high
Illite ref.	21.33	3.79	2.80	Al <sup>[IV]</sup> , Al <sup>[VI]</sup>	-
Illite 600°C	18.43	4.48	2.69	Al <sup>[IV]</sup> , Al <sup>[VI]</sup>	low
Illite 800°C	13.32	4.9	2.71	Al <sup>[IV]</sup>	low
Montm. Ref.	31.03	2.98	2.42	Al <sup>[IV]</sup> , Al <sup>[VI]</sup>	-
Montm. 600°C	21.39	14.1	2.70	Al <sup>[IV]</sup> , Al <sup>[VI]</sup>	low
Montm. 800°C	9.72	20.56	2.58	Al <sup>[IV]</sup>	medium

Table 2-5 : Summary chart on the effect of calcination on standard clays

## 2.5 Activation of a clay mixture: the Cuban clay

### 2.5.1 Raw materials and pre-treatments

A locally available clay-rich soil from Cuba was investigated in order to see if its thermal behaviour resembles somehow that of the standard clays. The work included a preliminary study on the role of a deflocculating agent in separating the clayey particles from the quartz sand contained in the raw material. Little information is found on pre-treatment of clay rich soils for optimizing the final properties of the calcined products. It is believed that considerable improvements could be achieved by concentrating the clayey material prior to thermal treatment. Indeed, clay particles found on the surface of land generally forms part of what is called the soil. Soil is made of particles having different composition and particle sizes. Most commonly found particles are gravel, sand, silt, organic matter and clay. In many cases and except for the organic matter, the non-clay particles may be treated as relatively inert with respect to cement, with interaction that are predominantly physical in nature[8]. The aim of this study is to try and separate the clay from the non-clay particles in order to increase the chance for obtaining a reactive pozzolan during the calcination process. Hexametaphosphate  $(\text{Na}_2\text{PO}_6)_x$  was used as a deflocculating agent in the sedimentation process as described in section 2.3.1. XRF analysis of the Cuban soil and its clayey extract is presented in Table 2-6 below.

compound		SiO <sub>2</sub>	Al <sub>2</sub> O <sub>3</sub>	Fe <sub>2</sub> O <sub>3</sub>	CaO	MgO	SO <sub>3</sub>	K <sub>2</sub> O	MnO	Na <sub>2</sub> O	Others	LOI	total	Alkalies % (Na <sub>2</sub> Oeq)
weight fraction %	soil	57.74	18.71	7.07	1.85	1.80	0.02	0.65	0.12	2.68	0.76	8.57	99.97	3.11
	clay	43.89	24.73	11.13	1.38	2.63	0.08	1.10	0.14	1.99	3.11	9.81	99.99	2.70

**Table 2-6 : Chemical analysis for cuban soil and its clayey extract after deflocculation**

It is not surprising to see the silica content drop for the clay sample, as most of the quartz could be removed by sedimentation. Note that for the clay, level of potassium is higher than for kaolinite or montmorillonite, suggesting that illite is present. Also, level of sodium is higher than for kaolinite or illite, suggesting that montmorillonite is present.

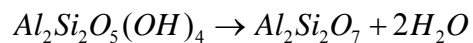
The effect of deflocculation on phase composition is presented in Figure 2-20. It is very interesting to see how the nature of the clay is hidden by the presence of companion minerals such as quartz and albite (felspar), which are present in high amounts in the soil as it was collected from the Manicaragua site. The use of deflocculating agent helped to reduce drastically the amounts of non-clayey minerals. This resulted in increased intensity of the



peaks corresponding to clayey phases. It clearly shows the effectiveness of hexametaphosphate in concentrating the clay as it allowed the separation of the particles according to their size. The diffraction pattern for the centrifuged sample (< 2 µm particles) confirmed the presence of montmorillonite and allowed the indexation of the peaks with more precision. Indeed, as explained in section 2.4.1, samples coming out of the centrifugation process are in the form of a paste that induces preferential orientation during sample preparation. This is why all basal planes independently of the nature of the crystal are more intense in this sample. From this XRD analysis, it is evident that the Cuban clay is mainly composed of a mixture of kaolinite, illite and montmorillonite.

The DTG curve of the Cuban clay presented in Figure 2-21 has features that resemble those of the standard clays. Interlayer water loss in the 50 to 200°C range could indicate the presence of montmorillonite, whereas dehydroxylation in the range of 400 to 650°C is characteristic of kaolinite. These results correlate well with the identification of crystals by XRD. DTG did not indicate the presence of illite in the Cuban clay, but this is probably due to the fact that its content is rather low and its signal adds to the kaolinite signal to form one broad peak.

It is not possible to measure the proportions of different clay types from XRD due to preferential orientation. However, thermogravimetric can be used to estimate the kaolinite content of the clay mixture. Figure 2-22 gives the TG curves for the Cuban clay with the different treatments mentioned earlier, together with that of kaolinite for comparative purposes. Dehydroxylation in the range of 400 to 650°C originates from the kaolinite structure and water loss can be directly related to the percentage of kaolin in the analysed sample.



Considering that 2 water molecules account for 13.9% in mass of a kaolinite unit formula, water losses (determined graphically using the tangent method) together with the corresponding kaolin percentages are presented in Table 2-7. Again, the effectiveness of hexametaphosphate as deflocculating agent is clearly seen as the percentage of kaolinite is more than two times that of the originally collected material (39% vs 17%). Note also that the amount of kaolinite in the centrifuged sample (<2µm particles) and the sedimented sample (deflocculating agent) are similar. The amount of kaolinite in the standard kaolin from Wards Natural Science is estimated as 76%.

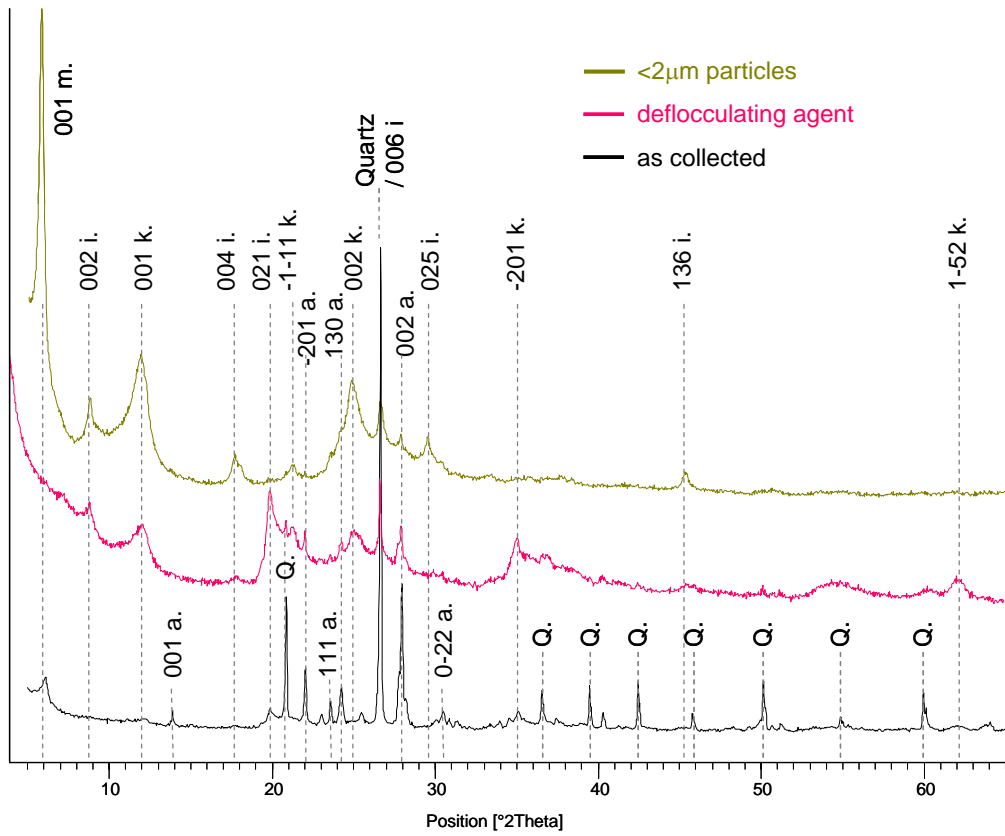


Figure 2-20 : Effect of deflocculation and centrifugation on diffraction pattern of cuban clay (m: montmorillonite, i: illite, k: kaolinite, a: albite, Q: quartz)

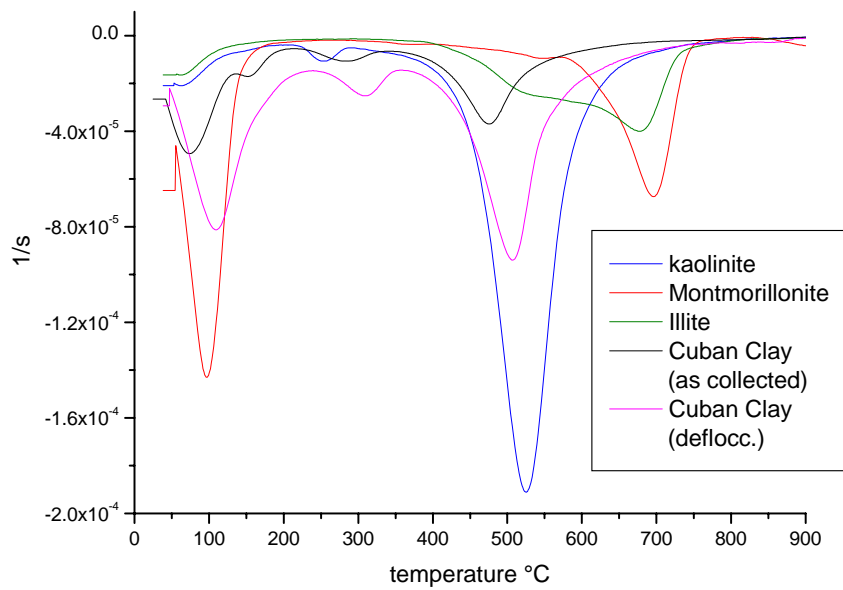
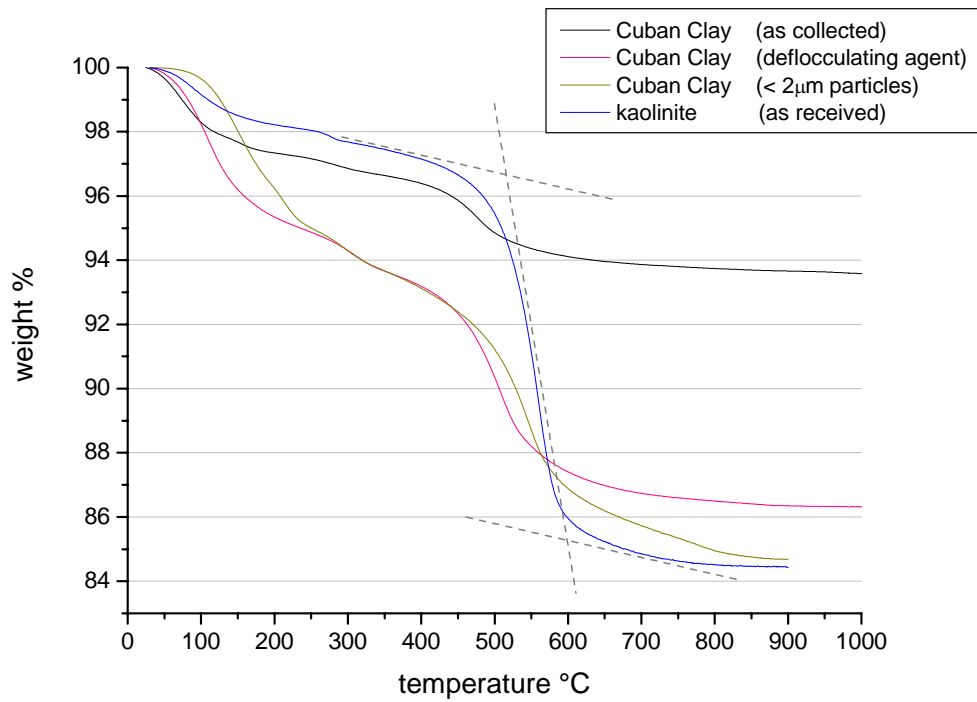


Figure 2-21 : DTG analysis on cuban clay (and standards)

Another interesting characteristic feature of thermally-treated kaolin-rich clays is the exothermic effect that appears between 900 and 1000°C, corresponding to a structural reorganisation [15]. DSC analysis presented in Figure 2-23 allowed identifying with precision for the Cuban clay and the standard kaolinite the temperature at which this type of reorganisation occurs (Note that DTG curves are related the mass loss only and do not inform on the exothermic or endothermic character of the reactions). The size, shape and location of the exothermic reaction give information on the degree of crystallisation of kaolinite. Poorly-crystallized kaolinites will give a less intense exothermic effect taking place in a broader temperature range[48]. It is clearly the case for the Cuban clay, as opposed to the standard kaolinite, which exhibits a sharp and intense peak.

The crystals formed in this range of temperature as a result of the reorganisation have been identified as  $\gamma$ -alumina, although other authors have concluded on the formation of primary mullite [48]. According to Parmelee [50], the presence of considerable amounts of iron in the Cuban clay could explain the lower onset temperature of this exothermic effect (~900°C) compared to the reference kaolinite (~1000°C). The temperature of recrystallisation sets the limit in temperature for the thermal activation of the clays, as reorganisation of the structure leads to more stable and crystalline phases that are not likely to dissolve or to show pozzolanic activity.

Hence, results confirm that the Cuban clay is made of a mixture of standard clay types. The kaolinite fraction of this clay is considerably less crystalline than standard kaolinite.



**Figure 2-22 : TGA curves of cuban clay after different treatments vs kaolinite**

	Cuban Clay (<2µm) (centrifugation)	Cuban Clay (deflocc. agent)	Cuban Clay (as collected)	Kaolinite (Wards) (as received)
% H <sub>2</sub> O loss (tangent method)	6.2	5.5	2.4	10.7
% kaolinite	44.6	39.4	17.4	76.3

**Table 2-7 : Percentage of kaolinite in cuban clay and standard kaolinite**

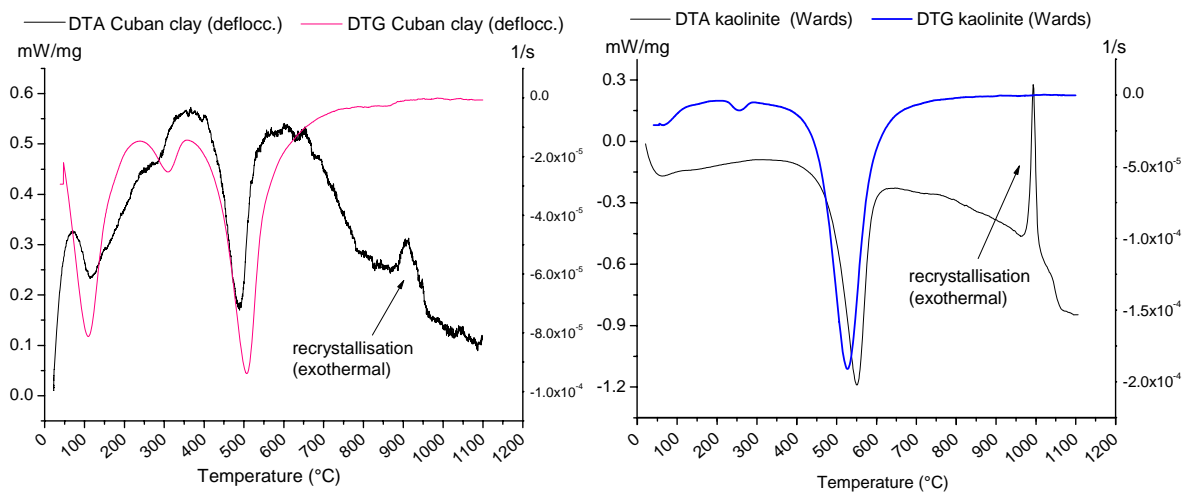


**Figure 2-23 : DTG and DTA curves of cuban clay and standard kaolinite**

### 2.5.2 Characterisation of calcined clays

The same calcination process and characterization techniques used for the standard clays were used to investigate on the Cuban clay. It was subject to a more detailed study not only to understand the influence of a mixture of clays on reactivity but also to follow with precision the changes in morphology occurring with temperature and see how these would affect the behaviour of clays in a cementitious matrix. Therefore, more firing temperatures were tested and the most relevant samples were observed in the electron microscope.

Figure 2-24 shows diffraction patterns of the Cuban clay after deflocculation (Ref.) and after calcination in the 500-1000°C range. The evolution of the patterns with temperature indicates several structural changes:

- At 500°C already, collapse of the basal planes of Kaolinite ( $2\theta = 12^\circ$  and  $2\theta = 25^\circ$ ) and Montmorillonite ( $2\theta = 12^\circ$ ). For kaolinite only, non-basal planes are also affected ( $2\theta = 20^\circ$ ,  $2\theta = 35^\circ$ ,  $2\theta = 62^\circ$ ). Note that peaks at  $20^\circ$  and  $35^\circ$  did not totally disappear as they overlap with unaffected non-basal planes of montmorillonite and illite. These interpretations are also based on the XRD results on standard clay types presented in section 2.4.2.
- Formation of Hematite ( $\text{Fe}_2\text{O}_3$ ) can be detected around 700°C
- Collapse of the illite structure occurs around 900°C
- New crystals such as spinel, tridymite and cristobalite form around 1000°C

As the purpose of the thermal treatment is to transform as much as possible the crystalline material into an amorphous state, recrystallisations need to be avoided. The iron content in the Cuban clay is considerably high. Although some could be found in substitution for aluminium in the octahedral sheets of illite or montmorillonite, it is believed that small non-clay particles rich in iron or iron in solution were extracted from the soil through the sedimentation process. The formation of hematite around 700°C will be difficult to avoid if no other pre-treatment to get rid of iron has been done prior to calcination. However, the formation of this phase does not originate from the transformation of amorphous phases that were stabilized by thermal treatment, as would the recrystallisation of spinelle or cristobalite do. Hence, it is assumed that the influence of this phase on the pozzolanic potential of the clay should be low.

In order to define with more precision the temperature at which illite and montmorillonite structures are decomposed, calcination of the Cuban clay was done at temperatures ranging from 800 to 1000°C with a 25°C interval. The results are presented in Figure 2-25. The peaks of the illite structure ( $2\theta=8.5^\circ$  and  $2\theta=20^\circ$ ) and peak of montmorillonite structure ( $2\theta=20^\circ$ ) could be detected up to 900°C. At 925°C, the decomposition of the Cuban clay can be assumed to be total. Note also that the main peak of spinel ( $2\theta = 37^\circ$ ), that in our case can be attributed to mullite as their crystal structure is identical, appears between 900 and 925°C. This is in accordance with DTA analysis in Figure 2-23 that showed an exothermal peak typical of recrystallisations in that same range of temperatures. Two transformations are thus observed simultaneously in the 900 to 925 °C range, the final decomposition of illite and recrystallisation of cristobalite and mullite. These would be supposed to have antagonist effects on pozzolanic reactivity. 925°C is a key temperature for the Cuban clay and it will be interesting to study the differences in reactivity with a clay burned at lower temperature , such as 600°C or 800°C, where no sign of recrystallisation can yet be seen but clay dehydroxylation is not complete.

The calcined clays were also characterised using thermogravimetric techniques, allowing the identification of the remaining hydroxyl structures for each firing temperature. DTG curves in Figure 2-26 are in agreement with X-Ray patterns as the typical hydroxyl peak corresponding with the decomposition of kaolinite between 400 and 600°C is disappearing for the clay calcined at 500°C. As the clay is calcined at increasingly higher temperatures, dehydroxylation of the kaolinite progresses, resulting in the apparent shift of the dehydroxylation peak to higher temperatures. This shift is simply due to the change in sample composition: decreasing with respect to kaolinite content and increasing with respect to illite and montmorillonite, which dehydroxylate at higher temperatures. Thus remaining hydroxyls are probably those from the illite structure or further decomposition of montmorillonite in other crystal directions than 001. It is interesting to interpret this superposition of DTG measurements as a sort of deconvolution of the original signal given by the raw material that allows the distinction between different types of dehydroxylation. Also, by looking at Figure 2-27, the curves seem to follow 2 distinct small peaks at around 780°C and 880°C, suggesting that these are hydroxyls that were either not from the same clay structure or not in the same structural conformation. Note that thermograms 700 and 800 do not show the first peak, meaning that this hydroxyl must have been altered at 700°C already.

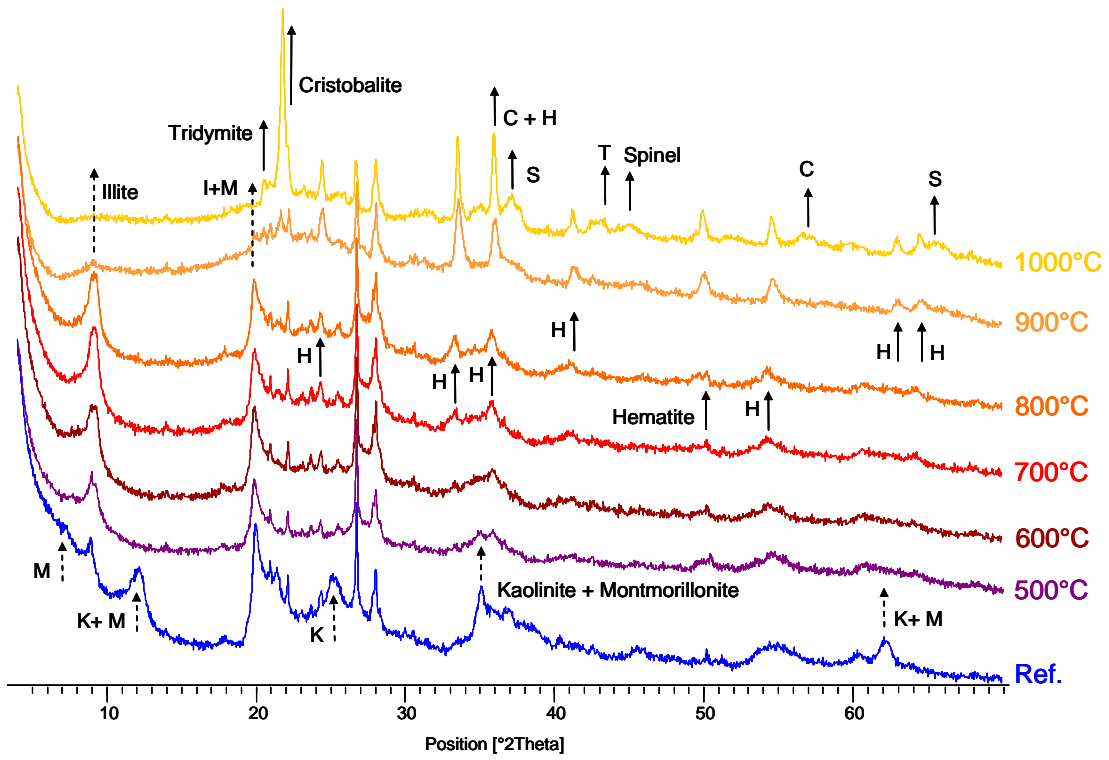


Figure 2-24 : XRD patterns of cuban clay in the 500 - 1000°C range

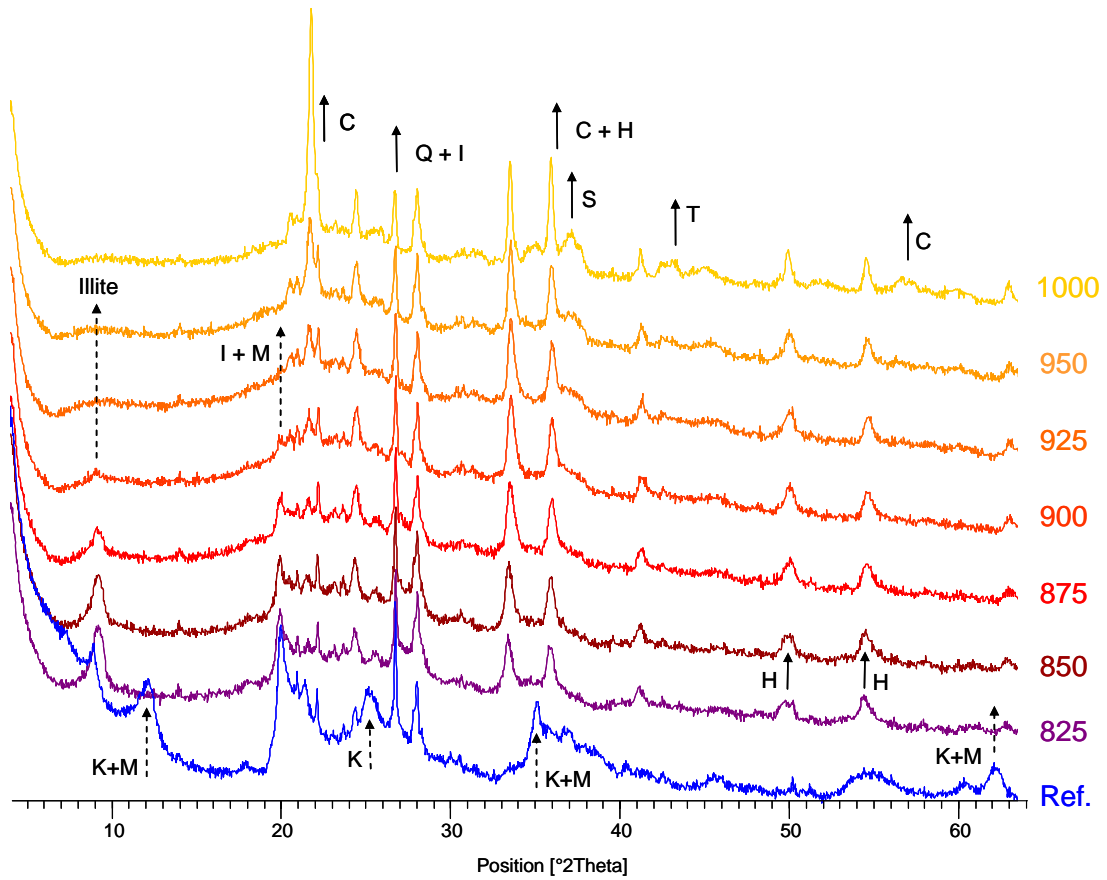
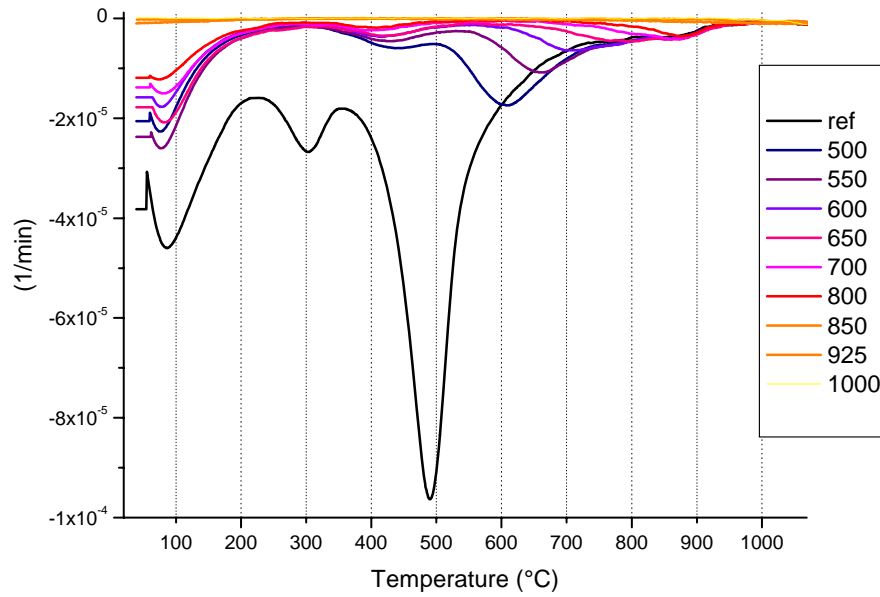
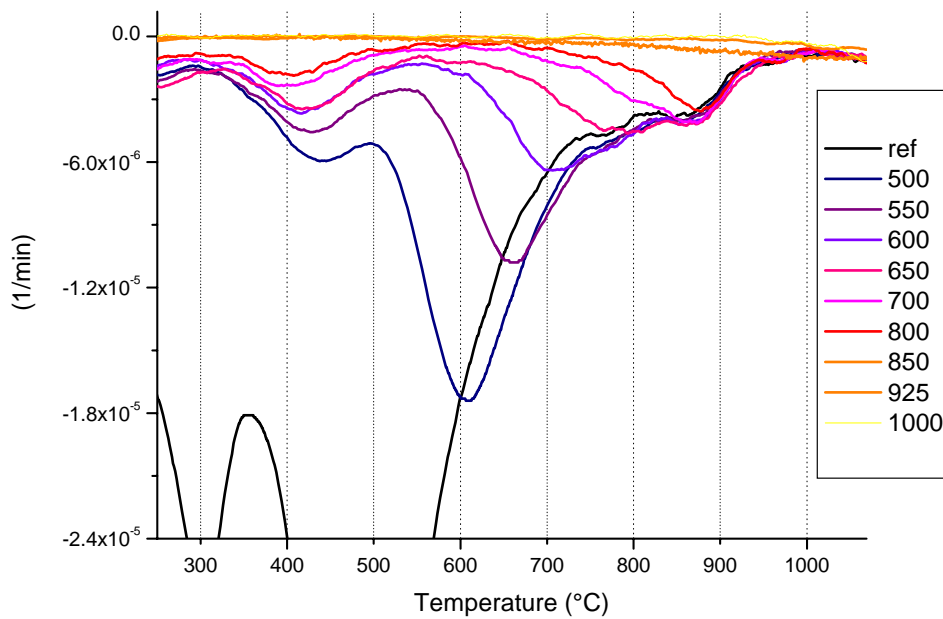


Figure 2-25 : XRD patterns of cuban clay in the 825 - 1000°C range



**Figure 2-26 : DTG measurements on raw cuban clay and its calcined products**



**Figure 2-27 : DTG measurements on calcined products**

Nevertheless, we should keep in mind that in terms of mass, decompositions identified above 700°C are very small compared to those at lower temperatures and will probably have a negligible contribution to final amorphous content. What we can be certain of from this technique, is that dehydroxylation can be considered as complete at 850°C, as weight loss for this sample and above are clearly negligible.



The NMR spectra of untreated and calcined Cuban clay are presented in Figure 2-28, together with spectra corresponding to standard kaolinite. Similarities between the Cuban clay and standard spectra can be seen in Figure 2-29. The two main peaks that can be found in the untreated material at 1 and 56 ppm correspond to  $\text{Al}^{\text{VI}}$  and  $\text{Al}^{\text{IV}}$  respectively. They correlate well with results on standard clays presented earlier, suggesting that this clay is made of a combination of kaolinite, montmorillonite and illite. The 56 ppm shift corresponding to  $\text{Al}^{\text{IV}}$  in illite and montmorillonite is actually slightly different and explains the shape of the 56 ppm peak in the reference Cuban clay spectrum (see Figure 2-29 left). NMR studies reflected that the coordination of aluminium in the Cuban mixed clay seems to follow the trend of illite and montmorillonite, the least dominating clay types in terms of mass, with a shift from 6-coordinated to 4-coordinated species with increasing temperature between 20 and 800°C.

However, a small peak at 35 ppm appears with calcination at 600°C, that cannot be attributed to either  $\text{Al}^{\text{VI}}$  or  $\text{Al}^{\text{IV}}$ . Although the position of the maxima does not coincide with that of the standard kaolinite (28 ppm), we have reasons to believe, due to the important kaolinite content of the Cuban clay, that it corresponds to  $\text{Al}^{\text{VI}}$ . At 800°C, an increase in the  $\text{Al}^{\text{IV}}$  signal is very clear, while little signal from  $\text{Al}^{\text{VI}}$  could be detected. More intensity was expected from the  $\text{Al}^{\text{VI}}$  peak, similarly to the decomposition pattern of kaolinite, but it was not the case. Thus, the decomposition steps of this mixed clay cannot be interpreted as independent contributions of thermal behaviours. Interactions between the calcined products or impurities at high temperature have probably occurred that favoured the transition from  $\text{Al}^{\text{VI}}$  of the kaolinite to  $\text{Al}^{\text{VI}}$  and  $\text{Al}^{\text{IV}}$ .

The effect of calcination on the particle size distribution can be seen in Figure 2-30. Coarsening of the particles is due to the combined effects of agglomeration and sintering phenomenon. Up to 850°C approximately, coarsening can be attributed to agglomeration, exclusively, while sintering is likely to dominate above 850°C.

More information on particle morphologies can be collected from the BET measurements and SEM images presented in Figure 2-31 and Figure 2-32 respectively. Note that the scale for the density in Figure 2-31 is very small and the little variation could be attributed to agglomeration phenomenon or phases changes during thermal treatment. As for the specific surface, an important drop can be observed between 800 and 850°C. This could be explained by the agglomeration or sintering of the particles with temperature. When compared to the results of specific surface obtained for the standard clays up to 800°C, values of specific

surface are higher for the Cuban clay. One of the possible reasons for this difference is that the Cuban clay was refined by sedimentation, while the standard were used as received. PSD results confirm these assumptions as the median diameter is smaller for the Cuban clay. Specific surface is an important criteria for reactivity of a pozzolan and its influence will have to be considered when monitoring pozzolanic reaction in pastes.

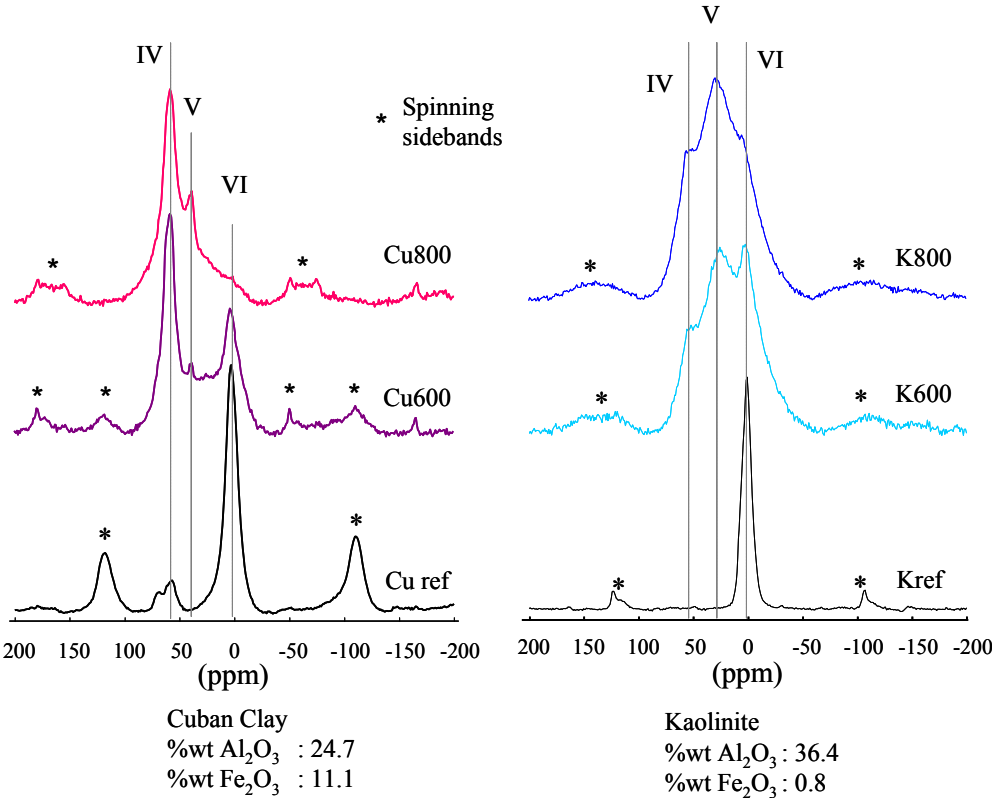


Figure 2-28 : NMR spectra of untreated and calcined Cuban clay and standard kaolinite

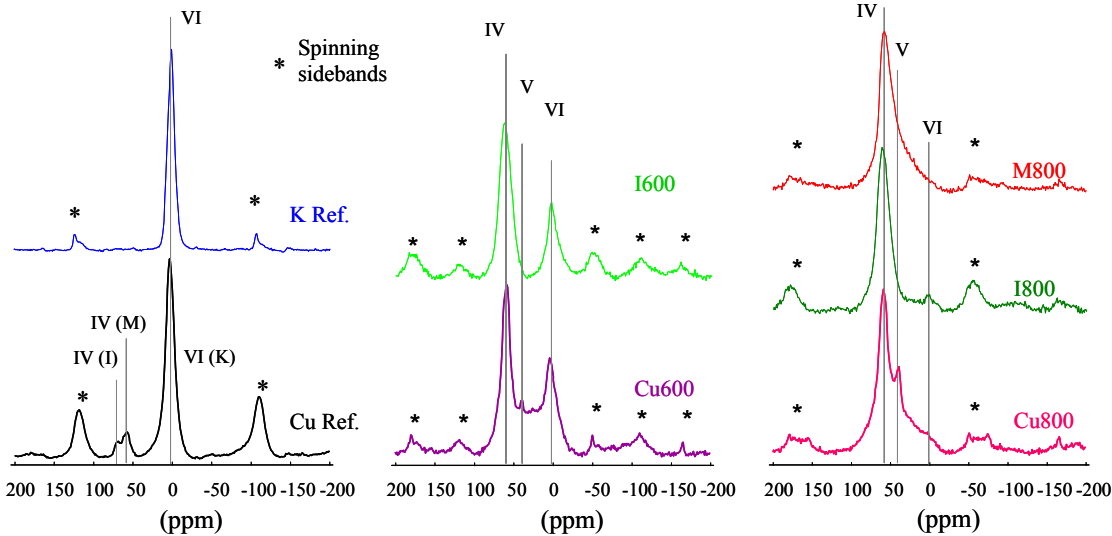


Figure 2-29: Comparison of NMR spectra (Cuban clay vs standard clays)

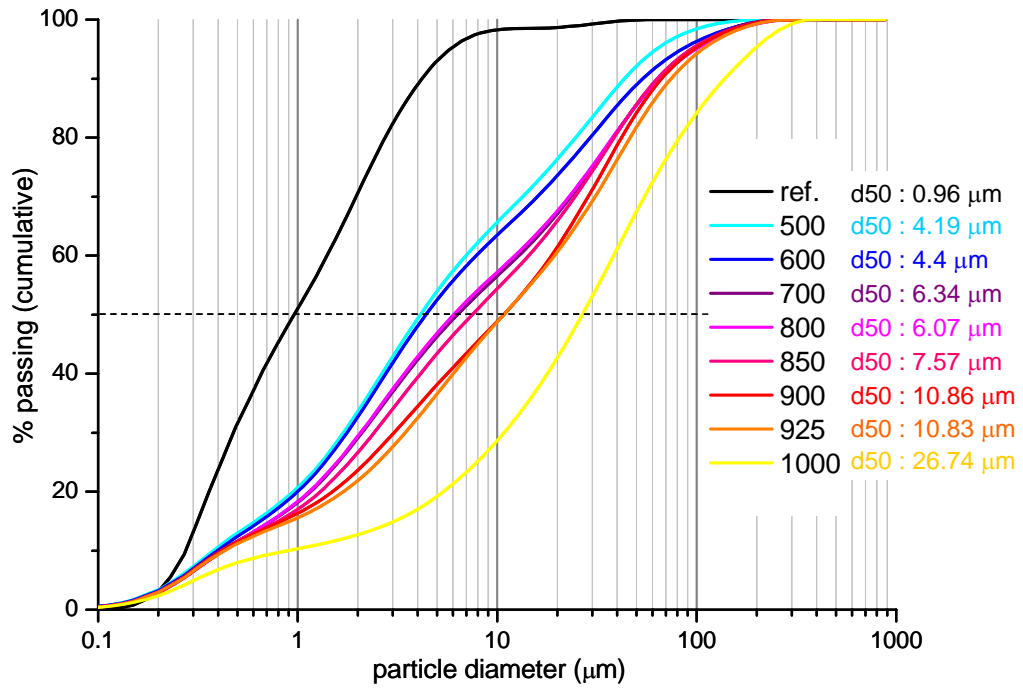


Figure 2-30 : Particle size distribution for raw and calcined Cuban clay

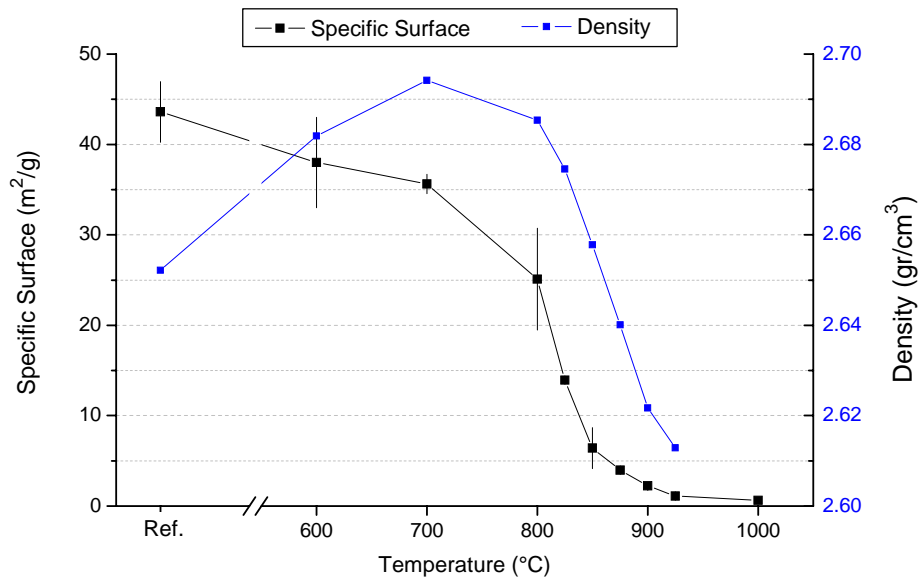
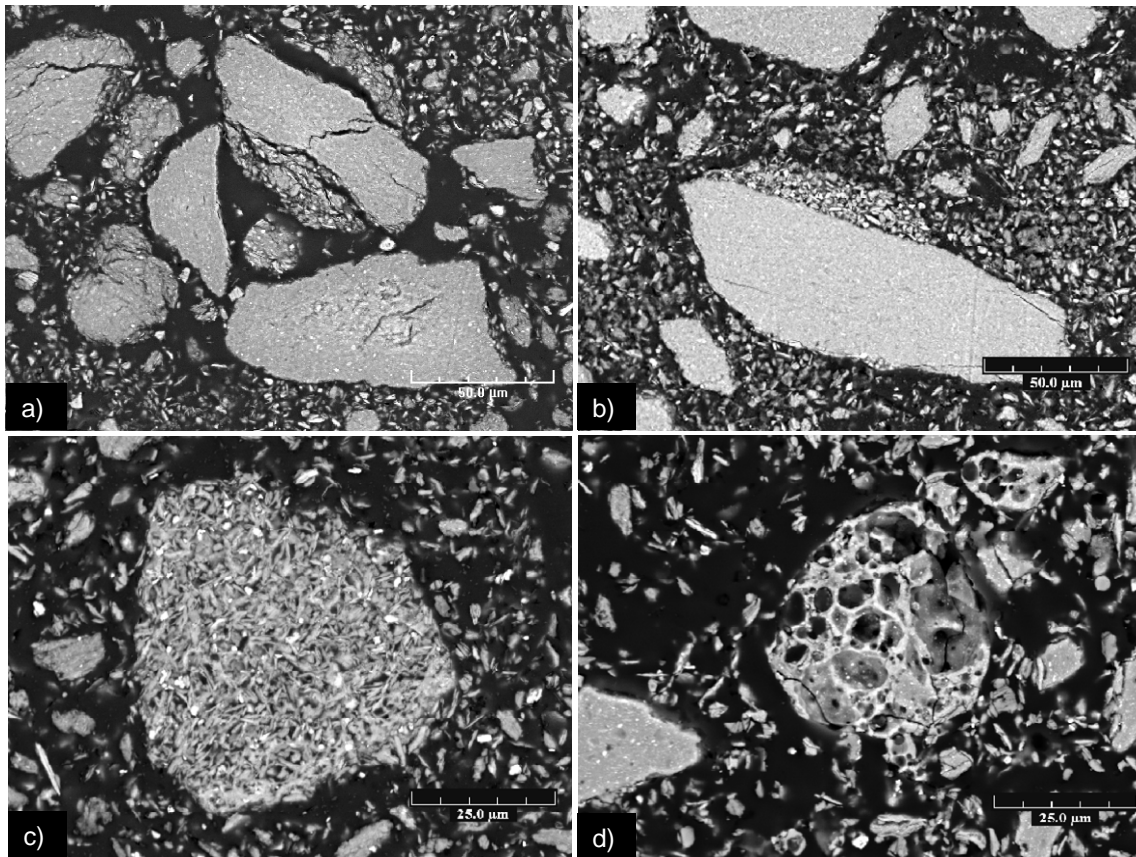


Figure 2-31 : BET and He-Picnometer measurements for raw and calcined Cuban clay



**Figure 2-32 : BSE images of the Cuban clay: untreated(a), at 600°C (b), 800°C (c), 925°C (d)**

Untreated and calcined clays were impregnated and polished for examination under the SEM. Figure 2-32 presents 4 images in the BSE mode showing the typical types of grain found depending on the firing temperature. There seems to be no significant change in morphology from the raw material to the material fired at 600°C. At 800°C, grains seem to be formed from an agglomeration of smaller particles. At 925°C, many grains show a porous structure that could almost not be detected in the 600°C and 800°C samples. Obviously, these images are not fully representative and some grains of the b) and c) type could also be found in the samples fired at higher temperatures. Also, grains of the c) type could also be found in the clay fired at 600°C. Thus, this sequence is meant to give an idea of the effect of temperature on the morphology of the calcined clays to try and explain differences in physical properties detected earlier. For example, the assumptions that coarsening could be due to particle agglomeration is confirmed by image c).

However, the most interesting phenomena to denote and that could explain the sudden drop in specific surface is the formation of these so-called porous grains. Actually, referring to the literature [51], the morphology observed in image d) is typical of a liquid phase sintering phenomenon. This means that one phase undergoes a liquid transition to allow the

Chapter 2: Clay activation

crystallisation of a new phase. If this is the case with the studied here, then these assumptions could well explain the drop in specific surface observed from 850°C. Indeed, the transition to a liquid phase induces the complete loss of the original morphology and leave space for the formation of bigger grains with characteristic closed porosity. This may actually partly explain the drop in specific weight. As a result, it is believed that bigger recrystallised particles with smaller specific surface will have very little to almost no pozzolanic activity.

Method:	BET	PSD	He-Picnometer	NMR	PSD / SEM	SEM	XRD
Parameter:	specific surface [m <sup>2</sup> /gr]	median diameter d50 [mm]	bulk density [gr/cm <sup>3</sup> ]	Al coordination	agglomeration	liquid phase sintering	clay decomposition
Cuban ref.	43.61	0.96	2.6522	Al <sup>[VI]</sup> , Al <sup>[IV]</sup>	-	-	-
Cuban 500°C	-	4.19	-	-	low	-	K
Cuban 600°C	38.00	4.40	2.6819	Al <sup>[VI]</sup> , Al <sup>[V]</sup> , Al <sup>[IV]</sup>	low	-	K
Cuban 700°C	35.63	6.34	2.6942	-	low	-	K
Cuban 800°C	25.11	6.07	2.6854	Al <sup>[VI]</sup> , Al <sup>[V]</sup> , Al <sup>[IV]</sup>	medium	-	K
Cuban 850°C	6.40	7.57	2.6578	-	medium	low	K
Cuban 925°C	1.11	10.83	2.6129	-	high	medium	K + M + I
Cuban 1000°C	0.51	26.74	-	-	high	high	K + M + I

Table 2-8 : Summary chart on the effect of calcination on mixed cuban clay

The important findings from the characterization stage of the Cuban calcined clay are summarised in Table 2-8.

From XRD analysis, kaolinite is already decomposed at 500°C, whereas complete structural decomposition of illite and montmorillonite are observed at 925°C. This was also observed in the patterns of standard clays. DTG results showed that dehydroxylation was complete at 850°C for the Cuban clay and 800°C for the standard clays. However, 5-coordinated species were also found, which could well originate from dehydroxylation of kaolinite. Particle size distribution and specific surface of all clays seem to be affected by thermal treatment due to the sintering effect. Presence of minor amounts of other minerals together with the formation of new phases at relatively low temperatures (hematite) could explain the increased tendency for agglomeration that was observed for montmorillonite and the Cuban clay. SEM analysis helped identifying different types of particles morphology depending on the treatment temperature, with particular emphasis on the effect of liquid phase sintering on specific surface and amorphous content.

Inevitably, a trade-off exists in the thermal activation process between parameters favouring pozzolanic activity such as high specific surface and high amorphous content and parameters that will tend to reduce it, such as sintering and recrystallisations. Moreover, the structure of the clay plays a major role as it defines the sensitivity to these different parameters and thus the potential for thermal activation. That being said, a lot of information was obtained from the characterization that is coherent with previous published work in the field of clay activation (see section 2.2) which identifies the activation window of most clays is in the range 500 °C to 900°C. The interesting additional output of this work is that it actually shows that many differences in properties can be found within this range that will certainly influence pozzolanic activity. As an example, the drop of specific surface observed in the Cuban clay from 800°C to 850°C is surprising and not yet fully understood, but indicates that reactivity could well be improved by keeping the calcining temperature under 850°C. On the other hand, it was shown by XRD that total destructureation of Cuban clay was reached at only 925°C, that would tend to indicate that more amorphous material is obtained at this temperature despite the appearance of sintered grains. For all these reasons, the key temperatures that were retained for the study on pastes were 600°C ( high specific surface, low destructureation), 800°C (lower specific surface, higher destructureation) and 925°C (lowest specific surface, highest destructureation, sintering).

Thus, the objectives of the following chapter dedicated to cement-calcined clay pastes were the following:

- Determine which type of standard clay has major pozzolanic activity
- Determine the optimal activation temperature of a mixed Cuban clay and compare its pozzolanic activity with standard clays
- Go further in the understanding of the calcined clays-cement interaction

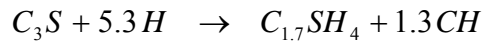
### 3 Pozzolanic reaction in cement-calcined clays pastes

#### 3.1 Theoretical background

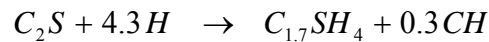
##### 3.1.1 Cement hydration

When Portland cement is mixed with water, its constituent compounds undergo a series of chemical reactions that are responsible for the hardening of cement pastes. Reactions with water are designated as hydration and the new solids formed on hydration are collectively referred as hydration products or hydrates.

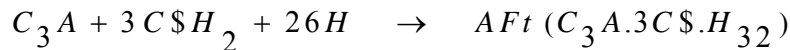
The reaction of impure tricalcium silicate ( $C_3S$ ), also called alite, with water leads to the formation of calcium hydroxide (CH) and a calcium silicate hydrate, which variable composition resulted in the use of the notation C-S-H.



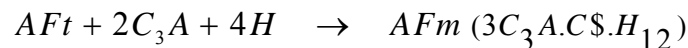
Dicalcium silicate ( $C_2S$ ), or belite, hydrates in a similar way to  $C_3S$  to form both C-S-H and CH phases.



In the presence of water and gypsum, the aluminate phase ( $C_3A$ ) reacts to form ettringite, the most important AFt phase:



When the sulphate is depleted, the reaction between  $C_3A$  and AFt gives calcium monosulfoaluminate (AFm) in the presence of water:



Ferrite ( $C_4AF$ ) phase exhibits low reaction rates to form hydrates similar to those formed by  $C_3A$  but with  $Fe^{3+}$  partly substituted for  $Al^{3+}$  [52].

AFm phases are among the hydration products of Portland cement[53]. Numerous types can occur when the ions they contain are brought together in aqueous systems at room temperature. They are classified in groups depending on the anions they contain ( $C_4AH_x$ ,  $C_4AC_{0.5}H_x$ ,  $C_4ACH_x$ ,  $C_4ASH_x$  and  $C_4ASH_x$ ).

### 3.1.2 *Pozzolans and pozzolanic reaction*

Pozzolans, whose name is derived from Pozzuoli, a town in the bay of Naples that was the source of a highly prized deposit of weathered ash from Vesuvius, were used by the Romans mixed with lime in building materials. Today, this name is applied to any reactive aluminosilicate material of natural or industrial origin that reacts with calcium hydroxide in the presence of water to form compounds that have cementitious properties.

According to ASTM Standard specification C 618-03 for coal fly ash and raw or calcined natural pozzolans for use in concrete, their chemical composition must be such that the sum of silica alumina and iron oxide exceeds 70% by mass. This requirement is followed by other specifications as for the physical and mechanical properties of mortars where cement has been partially substituted by pozzolans.

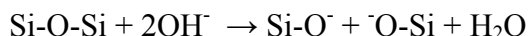
However, pozzolans should also be distinguished by their formation process, be it natural or artificial. The first type refers to a material that is the result of alteration of a parent rock by the effect of time or an episodic natural phenomenon (e.g. volcanic eruption), independently of human action. The most common natural pozzolans are volcanic ashes, weathered consolidated sediments such as tuffs and zeolites, diatomaceous earths and unburnt clays.

Artificial pozzolans, on the other hand, are materials that undergo controlled chemical or physical processes. Artificial pozzolans are usually an industrial by-product, as it is the case for fly ash (FA) or silica fume (SF) that come from coal fired power stations and the silicon industry respectively. Rice husks, or coffee husks, are other examples of industrial by-products that require a specific burning process after collection in order to get rid of the organic matter and obtain a pozzolan with high contents of amorphous silica. However, some pozzolans are specifically produced, the best example being that of metakaolin (MK). What these artificial pozzolans have in common is that they all result from a thermal process that either disrupts the long range order of the original material (SF, calcined clays), or removes the organic matter forming most of the original product (FA, RHA). The result is a material rich in silica or alumina with high content of amorphous or glassy phases.

The basis of the use of pozzolanic material in partial substitutions for clinker in Portland cement is the ability of the alkaline medium produced by the hydrating cement to break down the silica or the alumina-silica networks [52]. It is supposed that the  $\text{OH}^-$  ions provided by calcium hydroxide dissolution attach themselves to the  $\text{Al}_2\text{O}_3\text{-SiO}_2$  framework resulting in the



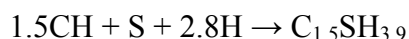
breaking of the bonds between the oxygen and the framework and the release of oxy-anions into the solution.



Since a cement pore solution is essentially one of alkali hydroxide, the immediate product is likely to be an amorphous material with  $\text{K}^+$  and  $\text{Na}^+$  as the dominant cations, but the more abundant supply of  $\text{Ca}^{2+}$  and the lower solubility of C-S-H and hydrated calcium aluminate or silicoaluminate phases will ensure that this is only an intermediate product [53].

The composition of this C-S-H is similar to that formed in cement hydration, although the C/S ratio is generally lower. However, with very reactive pozzolans of high silica content substituting for cement, as silica fume and rice husk ash, the C/S ratio can be significantly different depending on the level of substitution, being close to 1.5, and the H/S ratio is slightly lower.

A general formula for pozzolanic reaction can be written as follows:



When a pozzolan has appreciable quantities of reactive alumina, such as with natural pozzolans or calcined clays, it tends not only to favour the formation of calcium aluminate phases, but also to substitute for silica in the structure of C-S-H, thus increasing the Al/Ca ratio of the C-S-H. In this case, the hydrated phase is often referred as C-A-S-H.

### 3.2 State of the art on cement substitution by calcined clays

Many of the studies on clay activation reported in the previous chapter did actually pursue their investigation by mixing their calcined materials with cement or lime, either for determining the type of hydrates formed or to assess mechanical properties of the blends. Murat [27], Chakchouk [28], Salvador [43], Cara [46] and Ambroise [54] evaluated the pozzolanic activity using lime, while He [17] Shvarzman [44] and Badogianis[45] blended their calcined clays with cement. More studies on lime-pozzolans are summarized in Table 3-1.

Subsequently, additional papers that focused exclusively on the interaction of calcined clays with cement will be discussed, with special emphasis on those that used similar techniques to

the ones presented in this chapter as well as in next chapter on mechanical properties in mortars. Works presented below are also summarized in Table 3-2.

### 3.2.1 *Calorimetry*

Frias Rojas [55] used a Langavant calorimeter (semi-adiabatic calorimetry) to monitor the heat released from hydration of cement-pozzolan blends. Compared to the control, they found more heat for the systems blended with MK in the first 20 hours. This increment was explained by the reaction of the amorphous silica of MK around 6 hours and the reaction of the amorphous alumina of MK between 13 and 20 hours. These assumptions were based on previous works of the same authors who investigated the mechanism of pozzolanic reaction in a lime-MK system by DTA [56, 57]. Mostafa [58] worked with dealuminated kaolins. By substituting between 10 and 30% of cement in a paste, they observed a slight increase in the cumulated heat in the first 9 hours compared to the control. They attributed this increase to the pozzolanic reaction of dealuminated kaolin. The main reaction peak of the silicates around 10 hours was reduced due to a dilution effect. However, it should be said that pozzolanic reaction can have non negligible contributions to the heat output over longer periods of time and the study of the system over 45h is not sufficient to understand all chemical interactions between cement and reactive pozzolans.

### 3.2.2 *Calcium hydroxide quantification by thermogravimetric analysis*

Monitoring of calcium hydroxide has proved to be a reliable approach for the assessment of pozzolanic activity in cement pastes. Accurate measurements of CH content can be done by TGA or DTA. Wild [59] did an interesting study on the CH consumption of a cement-metakaolin system, comparing pastes and equivalent mortars with varying cement to MK ratios and therefore assessing the influence of aggregates in the cement-pozzolan interaction. He found systematically less CH in the mortars than in the equivalent pastes, attributing this effect to lower bulk w/c ratios and loss of water due to bleeding in the mortars. Nevertheless, relative to the control, he observed a decrease in the amount of CH for the blended pastes and mortars that reached 50% of the CH content of the control at one year. Determination of CH content followed the method suggested by Marsh [60], who worked with fly ash as a cement replacement material.

### 3.2.3 Changes in the microstructure & phases formed (XRD, SEM)

It has been reported that the substitution of cement by various mineral additions, including metakaolin, tends to favour the formation of AFm phases over AFt. Morsy [61] and Singh [62] have investigated the hydrated phases of cement-calcined kaolin paste by TGA up to 28 days. They have respectively associated the water loss around 175°C and 220°C to  $C_4AH_{13}$ . However, no coupled technique giving more information on the chemical or phase composition was used to confirm that. Sánchez de Rojas [63] blended cement with ceramic wastes and by curing the pastes at 40°C he identified little amounts of calcium aluminate phases by XRD (probably monocarboaluminate) that could not be seen in the control.

### 3.2.4 Nature of C-S-H using NMR

$^{29}\text{Si}$  and  $^{27}\text{Al}$  NMR has been used to study the structure of hydrates formed in a calcined clay-cement paste. Richardson [64] has clearly shown that in these types of systems Al substitutes for Si only in the bridging tetrahedrons forming C-S-H chains (Appearance of  $Q_2(1Al)$  peak in  $^{29}\text{Si}$  NMR). He also observed that the length of the alumino-silicates chains are very long compared to neat cement pastes. Supported by Faucon et al. [65] and Andersen [66, 67] et al., Love [68] suggested that Al was substituting for Ca in the interlayer of C-S-H. He also showed that after 4 weeks in a cement paste blended with metakaolin strätlingite could form, as the chemical shifts he observed in the cement-metakaolin blends are in accordance with those observed by Kwan [69] on two types of synthesised strätlingite. Jones and Macphee [70], using  $^{27}\text{Al}$  NMR, detected more calcium monosulfoaluminate than the control in a 6-months paste by substituting 15 percent of cement by metakaolin.

### 3.2.5 Improvement of mechanical and durability properties

S.Kelham [71] developed a simple water absorption test for concrete. Values of sorptivity are derived from the slope of a plot of mass vs square root of time if the porosity is known. The latter can be determined from the difference between the dry and the saturated weights. Sorptivity values for concretes incorporating ground granulated blast furnace slag or fly ash were compared to the reference concrete. Although calcined clays were not investigated in this work, some aspects of the methodology were applied to the sorptivity measurements presented in Chapter 4. Singh [62] showed the benefits of substituting 10% of cement by metakaolin for the production of mortars. The mechanical properties were considerably increased, together with a decrease of the porosity measured by MIP. Zhang [72] conducted an extensive research at the macroscopic level on the durability properties of concrete where

10% of the cement was replaced by MK. It included compressive, tensile and flexural strength, Young's modulus of elasticity, drying shrinkage, resistance to chloride-ion penetration freezing and thawing and salt scaling resistance. Results showed that the blended concrete performed better than the control in all the above mentioned tests, except for the salt scaling test, where it was marginally inferior to the reference. These results are encouraging and showed that MK could be used as highly pozzolanic cement replacement material for the production of high-performance concrete. He also concluded on the need for investigating higher replacement levels. Ambroise [73] used several techniques to identify the hydration characteristics of MK-blended cements and determine the optimal quantity of MK for ensuring good mechanical and durability properties of mortars. Up to 30% replacement, he found that the pore size distribution is displaced towards lower values, the CH content is reduced and the compressive strength are not affected. He also studied the interaction of  $C_3S$  with MK by isothermal calorimetry for the first 20h after mixing. He found higher values of cumulated heat output relative to the amount of cement for the mix containing 30% of MK that lead him to the conclusion that MK had an accelerating effect on the hydration of  $C_3S$ . However, the contribution of the pozzolanic reaction to the heat output over this period has been totally neglected, the induction period before the main reaction of  $C_3S$  was not shortened with the addition of MK and the slope of the  $C_3S$  reaction was lowered with the substitution. These observations tend to indicate that the addition of MK to cement had a retarding effect rather than an accelerating effect on  $C_3S$  hydration.

It is interesting to note that the identified phases are similar in a lime-based system than in a cement-based system. That was to be expected as the pozzolanic reaction does not change from one system to another as long as CH is available. However, the kinetics of the reaction are different due to fact that in cement the hydration reaction occurs simultaneously and the presence of alkalis is known to influence considerably the dissolution process of the pozzolans. This topic has not been sufficiently addressed by the previous authors and there is clearly a lack of understanding of the early and long term interaction of the cement with calcined clays. Calorimetric studies undertaken so far have not been convincing in explaining the early age behaviour of the blended pastes and long term studies are mainly limited to the assessment of compressive strength and identification of the hydrates formed.

That being said, the following chapter will try to study the influence of various characteristics of the clay on the interaction with cement:

- Influence of the **nature of the clay** on pozzolanic reaction and cement hydration (comparing reactivity of calcined kaolinite with illite and montmorillonite)
- Influence of the **activation temperature** on pozzolanic reaction and cement hydration (comparing reactivity of Cuban clay calcined at different temperatures)
- Influence of **kaolinite content of a clay** on pozzolanic reaction and cement hydration (comparing reactivity of calcined Cuban clay, calcined kaolinite and a very reactive metakaolin)

The objective is to identify the contribution of the pozzolans to the formation of hydrated products and consequently the development of the microstructure. The study of the latter will help explaining the mechanical properties of the mortars presented in Chapter 4.

Lime-based systems						
Authors	Year	Type of blend	Size of sample	Type of curing	Techniques to assess pozzolanic activity	Observed phases
Murat [27]	1983	Lime-metakaolin pastes MK/CH : 0.5 to 5 w/s : 0.75	20mm-diameter minicylinders	20°C, air-tight plastic boxes	Comp. Strength, DTA	C-S-H, C <sub>2</sub> ASH <sub>8</sub> , C <sub>4</sub> AH <sub>13</sub>
Ambroise [54]	1985	Lime-metakaolin pastes MK/CH : 0.66 to 10 w/s : 0.55 to 0.75	20mm-diameter minicylinders	20°C, in water	Comp. Strength, DTA	C-S-H, C <sub>2</sub> ASH <sub>8</sub>
P.S.de Silva [74]	1993	MK/CH : 0.17 to 2.5 w/s : 0.8	42-mm diameter minicylinders	20°C, 55°C, 85°C	XRD, DTA, EDX	C-S-H, CH, C <sub>4</sub> AH <sub>13</sub> , C <sub>2</sub> ASH <sub>8</sub> , C <sub>3</sub> AH <sub>6</sub>
Salvador [43]	1995	Lime-calcined kaolinites pastes CC/CH: 1.5 w/s : NFP 15-402	20mm-diameter minicylinders	French norm NFP 15-402	Compressive Strength	-
Alonso [13]	2001	Lime-metakaolin mixes MK/CH : 1 Na(OH) activated	Aqueous medium	45°C	Isothermal Calorimetry, XRD, FTIR, NMR	C-S-H, alkaline alumino-silicate
Mostafa [75]	2001	Lime-dealuminated CH/DK: 0.25, 0.5 w/s: 1	-	25°C	Isothermal Calorimetry	-
Frias Rojas and Cabrera [56, 57, 76]	2001 2002	Lime-metakaolin pastes MK/CH : 1 w/s : 2.37	-	20°C and 60°C	TGA/DTA/ XRD	C-S-H, CH, C <sub>4</sub> AH <sub>13</sub> , C <sub>2</sub> ASH <sub>8</sub> , C <sub>3</sub> AH <sub>6</sub> (60°C)
Chakchouk [28]	2006	Lime-Calcined Clays pastes CC/CH: 1 and 3 w/s : 0.75	20mm-diameter minicylinders	20°C	Comp. Strength	-
Cara [46]	2006	Lime-Calcined Clays pastes KC/CH: 1 w/s : 0.5	-	Sealed container	XRD, DTA	Following Murat: C-S-H, C <sub>2</sub> ASH <sub>8</sub> , C <sub>4</sub> AH <sub>13</sub>
Papayianni [77]	2006	Lime-Pozzolan mortars cem : pozz : sand : 50 : 50 : 300 w/s: 0.63-0.81	40x40x160 and 40x40x80 mm	20°C	Comp. Strength, MIP	-

**Table 3-1 : Summary of studies undertaken on lime-calcined clays systems**

Cement-based systems						
Authors	Year	Type of blend	Size of sample	Type of curing	Techniques to assess pozz. activity	Observed phases
Ambroise [73]	1994	C <sub>3</sub> S-MK and cement-MK pastes subst. level : 0 - 50% w/s : 0.25 to 0.54	20mm diameter minicylinders	20°C, 98%RH	Isoth. Calo., FTIR, XRD, DTA, Comp.S.	C-S-H, CH, AFt, C <sub>4</sub> AH <sub>13</sub> , C <sub>2</sub> ASH <sub>8</sub>
		Cement-MK mortars subst. level : 0 to 30% binder : sand : 1:3 w/s : 0.25 to 0.54	40x40x160 mm	20°C, lime-saturated water	Comp. Strength	-
He [17]	1995	Lime-calcined clays pastes CH/CC : 1 w/s : 1	-	40°C, in water	XRD, EPMA	C-S-H, CH, C <sub>4</sub> AH <sub>13</sub> , C <sub>2</sub> ASH <sub>8</sub> , C <sub>3</sub> AH <sub>6</sub>
		Cement-Calcined clays mortars cem : cc : sand : 70: 30: 300 w/s: 0.52-0.6	Mini-RILEM 20x20x150 mm	40°C, in water	Comp. Strength	-
Zhang [72]	1995	Cement-MK mortars cem : mk : sand : 90: 10: 300 w/s: 0.5	102x76x406mm	20°C, 100%RH	Comp. Strength Drying Shrinkage Cl- penetration freeze-thaw salt-scaling	
Wild [59]	1996	Cement-MK pastes cement substitution level : 5, 10, 15% w/s : 0.55	-	20°C, sealed specimens	TGA	C-S-H, CH
		Cement-MK mortars subst. level : 5, 10, 15% binder : sand : 100:250 w/s : 0.55	100x100x100 mm	20°C, sealed specimens	Comp. Strength	-
Khelam [71]	1988	Cement-Pozzolan mortars cem : pozz : sand : 80: 20: 300 w/s: 0.5	150mm-diameter cylinders	air cured, water cured	Sorptivity	-
Kaloumenou [78]	1999	Cement-MK mortars cem : mk : sand : 80: 20: 300 w/s: 0.5	40x40x160mm	25°C, in water	Comp. Strength	-
Richardson [64]	1999	Cement-MK pastes cement substitution level : 20% w/s : 0.55	-	25°C, sealed in bags	<sup>29</sup> Si NMR	C-S-H, C-A-S-H
Shvarzman [44]	2003	Cement-MK mortars cem : mk : sand : 80: 20: 300 w/s: 0.48	50mm cubes	20°C, in lime-water	Comp. Strength	-
Badogianis [45]	2005	Cement-MK mortars cem : mk : sand : 80: 20: 300 w/s: 0.5	40x40x160 mm	20°C, in water	Comp. Strength	-
Mostafa [58]	2005	Cement –dealuminated kaolin pastes: substitution level : 10, 20, 30% w/s: 1	-	25°C	Isothermal Calorimetry	-
M.I. Sánchez de Rojas [63]	2006	Cement-ceramic wastes pastes cem: pozz : 80:20 w/s : 0.5	-	40°C, closed beaker	SEM, XRD	C-S-H, MC
		Cement-ceramic wastes mortars, cem: pozz : sand: 85:15:300 w/s : 0.5	40x40x160 mm	20°C, in water	Comp. Strength	-
Singh [62]	2006	Cement-MK mortars subst. level : 5 - 25% binder: sand : 1:3 w/s: 0.5	50x50x50mm cubes	25°C, in water	Comp. Strength, MIP, DTA	C-S-H, CH, C <sub>4</sub> AH <sub>13</sub>
Love & Richardson [68]	2007	Cement-MK pastes cement substitution level : 20%, w/s : 0.55	5ml polypropylene vials	25°C, sealed in bags	NMR	C-(A)-S-H, Aft, AFm C <sub>2</sub> ASH <sub>8</sub>

Table 3-2 : Summary of studies undertaken on cement-calcined clays systems

### 3.3 Experimental approach for the study of cement-calcined clays pastes

The choice to investigate the pozzolanic reaction in a cement-pozzolan system rather than a lime-pozzolan system was based on the following criteria:

- Lime-pozzolan systems are often used as models for the study of pozzolanic reaction. However, they do not take into account the action of the alkalis in the dissolution process of the mineral admixtures, limiting the level of understanding of the real phenomena. Despite greater complexity of the cement-pozzolan interaction, characterization methods available nowadays allow the study of such cement-based materials.
- Because lowering cement content is also a concern for cement manufacturers due to environmental and economical constraints, results presented in this work could contribute to the development of solutions towards more sustainable industrial processes.
- This project is oriented towards practical applications in low-cost housing. The use of lime-pozzolan binders is limited to mortars or renderings. The increase in resistance at early age brought by the presence of cement allows a wider range of applications to be considered from renderings to hollow concrete blocks and other load-bearing structures. This would contribute to lowering the cement content of a construction to a greater extent.

The level of substitution chosen was 30% by weight of cement. This study was not designed for finding maximum substitution levels so 30% was taken as a typical substitution level. One way of achieving higher levels of substitution was suggested by Martirena [79] and consisted of adding a certain percentage of lime to the cement-pozzolan mixture (determined by stoichiometric calculations). This topic was addressed in sub-project 3 of the joint research programme.

Figure 3-1 gives a general view on how the cement-calcined clay interaction was investigated. The selection of materials included the Cuban clay calcined at 600, 800, 925 and 1000°C, together with the standards clays calcined at 600°C and 800°C.



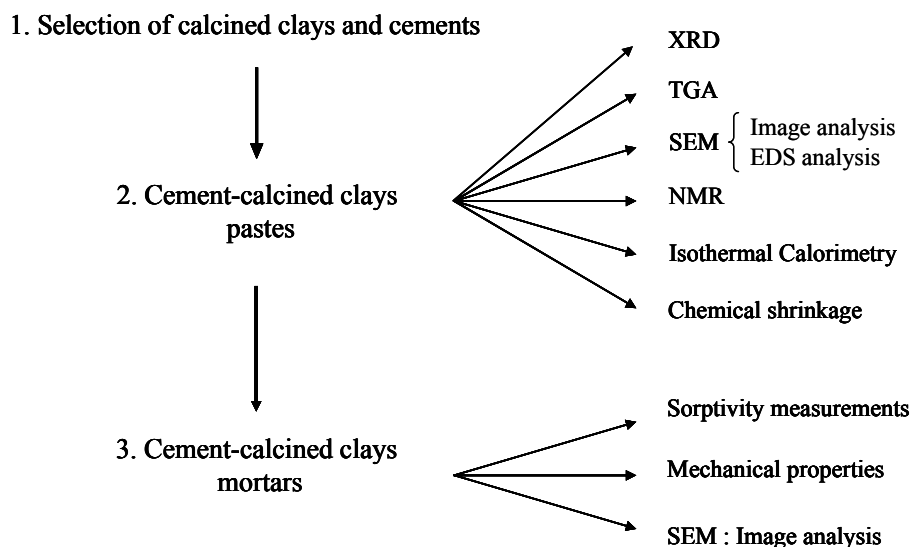


Figure 3-1 : Experimental approach for pastes and mortars

Results of the standard clays will be systematically presented before those of the Cuban clay.

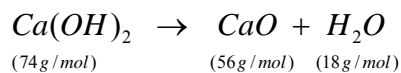
### 3.3.1 Characterization methods

Most of the techniques used during at this stage of research have already been presented in section 2.3.2. Therefore, only new techniques or new methodologies associated to a technique are presented below.

The Isothermal calorimeter was a TAM AIR from Thermometric with 8 channels available for simultaneous comparisons in the -600 to 600mV range. Water was used as reference.

The chemical shrinkage setup was designed at the Laboratory of Construction Materials and consists of pipettes mounted on plastic flasks into which the cement paste is poured. Water is filled on top of the cement paste until it fills also the pipettes. The system is sealed at the interface between the pipette and the flask with rubber lids and on top of the pipette with an oil drop. As the overall chemical reactions occurring during hydration lead to a reduction in volume, the level of water in the pipette decreases with degree of hydration. This level is recorded by a webcam that allows automated acquisition and processing of the data. The flasks are maintained in a thermostatic bath at 20°C to avoid effects of heat release on volumetric changes of the paste. Each curve presented is the average of a minimum of 2, but mostly 3, replicas of a cement-calcined clay system.

The determination of calcium hydroxide content from TGA analysis is based on the assumption that mass loss between 400 and 600°C in a calcined clay-cement pastes is mostly due to the loss of water from portlandite:



In this case the percentage of water released multiplied by a factor of (74/18) would be equivalent to the amount of calcium hydroxide originally present in a system. Mass losses were determined on the TG curves using the tangent method, as described by Marsh [60]. It should be noted that the values obtained can be an underestimate due to carbonation of the sample. Indeed, as data acquisition is an automated process, dry pastes are crushed to powders and loaded all at the same time in the device. Thus, samples can stay several hours exposed to air waiting for their turn to be analysed. Although alumina lids are provided to try and minimise this carbonation effect, it is difficult to avoid. Therefore, a correction to the CH content was done by quantifying the amount of carbonated CH, which can be detected in the decarbonation process between 600 and 900°C. An example of the calculation is presented in appendix III. Another possible source of error could be the leaching of Ca ions during the curing process, but this is not likely to have occurred as the same curing water was used over the period of study and the first slice of the paste cylinders exposed to water was systematically discarded.

To be able to compare blended systems with the control, values of calcium hydroxide are expressed as a percent of anhydrous cement present in the sample. According to Marsh [60], expressing results per weight of ignited cement, and not per total ignited weight, allows a better estimate of when the pozzolanic reaction starts to deplete calcium hydroxide to a significant degree. The value of chemically bound water was obtained by measuring the mass loss up to 600°C, temperature at which it was assumed that almost all water was removed from the sample.

Scanning electron microscopy was used in the BSE mode on polished sections for automated image analysis. It allowed the determination of the degree of hydration of the clinker component. By acquiring automatically around 120 images from a same polished section, the computer programme developed at the Laboratory of Construction Materials recognises the phases present in the microstructure by grey level differentiation. By knowing the density of each constituent and the initial cement content, it is thus possible to translate this volumetric

*Chapter 3: Pozzolanic reaction in cement-calcined clays pastes*

information into percentage weight of anhydrous cement remaining for a given time of curing and consequently determine the degree of hydration. EDX analysis was also used to determine atomic ratios in the inner C-S-H and outer C-S-H in order to compare the chemical composition of similar hydrates in different cementitious systems and thus evaluate the influence of calcined clays on cement hydration at the microstructural level. Around 100 analyses were made for each component.

*3.3.2 Starting materials and mix designs*

Following the study described in the previous chapter, the three standard clays (kaolinite, illite and montmorillonite), calcined at 600 and 800°C, were retained for the study in pastes with the objective of determining their pozzolanic activity. For the Cuban clay, three activation temperatures were investigated: 600, 800 and 925°C, with the objectives of determining the optimal activation temperature and comparing the pozzolanic activity with those of the standards clays.

The chemical composition of the clays and their characteristics after thermal activation are summarised in Table 3-3 and Table 3-4 respectively.

% weight	SiO <sub>2</sub>	Al <sub>2</sub> O <sub>3</sub>	Fe <sub>2</sub> O <sub>3</sub>	CaO	MgO	SO <sub>3</sub>	K <sub>2</sub> O	MnO	Na <sub>2</sub> O	Others	LOI	total	Alkalies % (Na <sub>2</sub> Oeq)
Uncalcined materials													
Kaolinite	48.00	36.40	0.85	0.14	0.11	0.03	0.48	0.01	0.02	0.55	13.41	100.00	0.33
Illite	58.68	19.25	5.04	1.29	2.50	0.17	6.12	0.05	0.19	1.00	5.71	100.00	4.22
Montm.	63.15	20.09	3.96	1.15	2.27	0.51	0.54	0.02	2.22	0.20	5.90	100.01	2.57
Cuba	43.89	24.73	11.13	1.38	2.63	0.08	1.10	0.14	1.99	3.11	9.81	99.99	2.70
Calcined materials													
Cu6	46.68	25.71	11.20	1.49	2.82	0.08	1.17	0.15	2.20	3.53	4.96	100.00	2.97
Cu8	48.33	26.63	11.31	1.48	0.90	0.06	1.20	0.15	2.22	3.51	2.20	98.0	3.01
MK	51.61	40.44	1.52	0.32	0.10	0.06	0.82	0.01	-	2.23	2.89	100.00	0.82

**Table 3-3 : Chemical analysis of uncalcined and calcined clays**

Type of clay	Kaolinite content (TGA)	Al <sub>2</sub> O <sub>3</sub> content before calcination (XRF)	activation temperature	calcination time	Al <sub>2</sub> O <sub>3</sub> content (XRF)	d <sub>50</sub> [μ]	Specific Surface [m <sup>2</sup> /g] (BET)	density [gr/cm <sup>3</sup> ]		
Kaolinite	85%	36.4 %	600°C	60min	-	6.97	24.7	2.55		
			800°C			8.28	24.13	2.65		
Illite	0%	19.3 %	600°C			4.48	18.43	2.69		
			800°C			4.90	13.32	2.71		
Montm.	0%	20.1 %	600°C			14.10	21.39	2.70		
			800°C			20.56	9.72	2.58		
Cuban	40%	24.7 %	600°C			60min	25.7 %	4.40	38	2.68
			800°C				26.6 %	6.07	25.11	2.69
			850°C	-	7.57		6.4	2.66		
			925°C		10.83		1.1	2.61		
			1000°C		26.74		0.51	-		
MK	~95%	~40%	~800°C	-	40.4 %	10.30	35.2	2.61		

**Table 3-4 : Characteristics of the clays retained for the study on pastes**

A very reactive metakaolin (MK) was included in the study to compare pozzolanic activities. This product was obtained by calcining a kaolin-rich clay for very short times and proved to be more reactive than conventional metakaolins available in the market.

2 different types of cements due to materials available were used, whose chemical compositions are given in Table 3-5. Cement A was a Cem I 42.5, whereas cement B was a Cem I 52.5R. A filler, consisting of microcrystalline quartz, was compared to the pozzolans by assuming it would behave as an inert material that would not react with calcium hydroxide. It was used to substitute cement at the same level of the calcined clays. Its chemical composition is also presented in Table 3-5.

XRD Rietveld analysis on the unreacted cements allowed the quantification of the anhydrous phases. Phase compositions are presented in Table 3-6 .

% weight	SiO <sub>2</sub>	Al <sub>2</sub> O <sub>3</sub>	Fe <sub>2</sub> O <sub>3</sub>	CaO	MgO	SO <sub>3</sub>	K <sub>2</sub> O	MnO	Na <sub>2</sub> O	Others	LOI	total	Alkalies % (Na <sub>2</sub> Oeq)
Cem A	19.30	5.10	2.97	61.93	2.47	2.69	0.85	0.04	0.31	0.53	3.81	100.00	0.87
Cem B	21.03	5.01	2.54	63.45	2.05	3.01	1.02	0.04	0.26	0.24	1.34	100.00	0.93
Filler	99.54	-	-	0.02	0.02	0.002	0.007	0.002	-	0.00	-	99.59	0.007

**Table 3-5 : Chemical composition of cements and filler**

Phases	Formula	Weight fractions (%)		
		Cem A	Cem B	SD
Alite	C <sub>3</sub> S	60.4	66.24	2.2
Belite	C <sub>2</sub> S	12.1	14.08	1.4
Ferrite	C <sub>4</sub> AF	11.5	10.6	1.0
Aluminate	C <sub>3</sub> A	6	3.67	0.7
Lime	C	0.4	0	0.4
Gypsum	CaSO <sub>4</sub> -2H <sub>2</sub> O	3.5	2.19	0.6
Hemihydrate	CaSO <sub>4</sub> -0.5H <sub>2</sub> O	0	0.64	0.8
Quartz	S	0.5	0	0.4
Calcite	CaCO <sub>3</sub>	4.1	0	0.5
Dolomite	CaMg(CO <sub>3</sub> ) <sub>2</sub>	1.6	0	0.5
Arcanite	K <sub>2</sub> (SO <sub>4</sub> )	0	1.86	0.4
Periclase	MgO	0	0.71	0.3

**Table 3-6 : Phase quantification by XRD Rietveld analysis on anhydrous cements**

The particle size distribution and the corresponding median diameter (d<sub>50</sub>) are presented in Figure 3-2. The particle size distribution of the filler was modified by attrition milling to get closer to the range of the calcined clays used. However, the calcined clays were not ground after thermal treatment and the various in particle size distributions observed are the same as presented in chapter 2. (Median particle diameters are given in Table 3-4. For more details see Figure 2-18 and Table 2-5 for standard clays and Figure 2-30 and Table 2-8 for the Cuban clay). The reason for not grinding the materials before introducing them in the cement paste is due to the fact that most of the calcined clays were already finer than the cement. Decreasing even more the particles sizes to reach the same distributions for all the calcined clays investigated would have taken too much time, considering the amounts of material necessary for the production of mortars. Besides, considering small-scale applications in developing countries, any additional treatment increases the cost of production and decreases productivity.

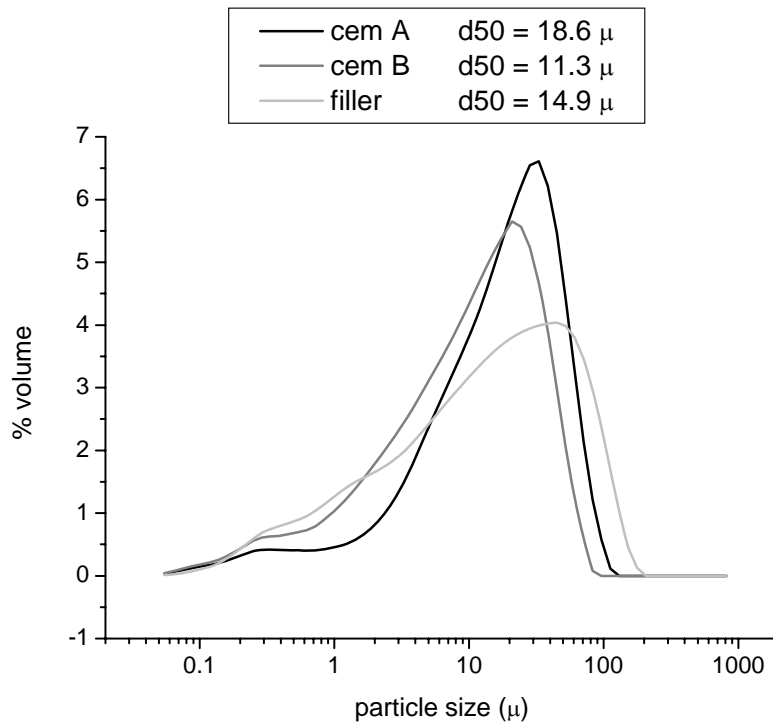


**Figure 3-2 : PSD of the cements and filler**

The curing temperatures were 20°C and 30°C. The first temperature was chosen as a reference working temperature and would facilitate the comparison with previous or future work on this topic. The second temperature was chosen to better simulate the field conditions in Cuba.

Different series of pastes were prepared, whose formulations are shown in Table 3-7. Note that pure cement paste (100% Cem A and Cem B) were prepared to serve as references. These pastes were studied by XRD, TGA, BSE-IA and NMR. Later, another series of essentially similar pastes to series 1 was made for chemical shrinkage and isothermal calorimetric measurements, as can be seen in Table 3-8. The main difference in this series is that illite and montmorillonite systems were replaced by cu800 and MK. This was done to restrict the study to a selection of kaolinite-based materials. Two runs were recorded in the isothermal calorimeter, one at 20°C and the other at 30°C. Chemical shrinkage measurements were made for series 3 and series 5 at 20°C. A summary of the measurements performed for each series is presented in Table 3-9.

Chapter 3: Pozzolanic reaction in cement-calcined clays pastes

series n°	type of clay	activation temperature	calcination time	cement used	substitution level	w/b	paste curing temperature	label	
1	kaolinite	600°C	60min	Cem B	30%	0.4	30°C	k600_1	
		800°C						k800_1	
	illite	600°C						i600_1	
		800°C						i800_1	
	montmorillonite	600°C						m600_1	
		800°C						m800_1	
	Cuban	600°C						cu600_1	
	filler							filler_1	
opc (reference paste)			opcB_1						
2	Cuban	800°C	60min	Cem A	30%	0.4	20°C	cu800_2	
		850°C						cu850_2	
		925°C						cu925_2	
		1000°C						cu1000_2	
	opc (reference paste)							opcA_2	
3	Cuban	600°C	60min	Cem A	30%	0.4	20°C	cu600_3	
		800°C						cu800_3	
		925°C						cu925_3	
	opc (reference paste)							opcA_3	
4	Cuban	600°C	60min	Cem A	30%	0.4	30°C	cu600_4	
		800°C						cu800_4	
		925°C						cu925_4	
	MK	-						-	MK_4
	opc (reference paste)							opcA_4	

Table 3-7 : Formulations of cement-calcined clays pastes for XRD, TGA, BSE-IA and NMR

series n°	type of clay	activation temperature	calcination time	cement used	substitution level	w/b	paste curing temperature	label
5	kaolinite	600°C	60min	Cem B	30%	0.4	20°C / 30°C	k600_5
	Cuban	600°C						cu600_5
	Cuban	800°C						cu800_5
	MK	-	-					MK_5
	filler							filler_5
	opc (reference paste)							opcB_5

Table 3-8 : Formulation of cement-calcined clays pastes for Isothermal Calorimetry and Chemical Shrinkage

80 g of paste was the typical amount produced for each mix (40 g of cement, 17.14 g of calcined clay, 22.86 g of water). Cement and calcined clays were first mixed in the dry state by hand for 1 minute. Once water was added, mixing was done with a high shear blender at 500 rpm for 2min. Pastes were poured into polypropylene cylindrical tubes that were tapped 50 times on the table to remove air bubbles. At 1day, the tubes were broken to unmold the hardened paste. Two 4mm slices were cut from these for analysis at 1 day, always discarding the first slice. The remainder of the sample was submerged under water in polyethylene flasks and kept at the right curing temperature with new slices cut at 7, 14, 28 and 90 days. Water in

the flasks was kept unchanged throughout the curing period. Hydration of the specimens was stopped by solvent exchange using isopropanol. After a week, samples were taken out of the solvent and stored in a desiccator for another week prior to testing (XRD, TGA, SEM, NMR). For Isothermal calorimetry as well as chemical shrinkage, the same procedure for paste preparation was followed, except that the pastes in the fresh state were poured in different flasks adapted to the experimental setups.

series n°	type of OPC	samples	XRD	TGA	SEM-IA	SEM-EDS Analysis	<sup>27</sup> Al NMR	<sup>29</sup> Si NMR	Isothermal Calorimetry	Chemical Shrinkage
			CH depletion	CH content	degree of hydration	phase assemblage	coord. of Al	conform. of Si	Heat evolution	Chemical activity
1	Cem B	k600, k800, i600, i800, m600, m800, cu600, filler	x	x	x	-	k600, i600, m600	-	-	-
2	Cem A	cu800, cu850, cu925, cu1000	x	x	-	-	-	-	-	-
3	Cem A	cu600, cu800, cu925	x	x	x	cu600, cu800	x	cu600	-	20°C
4	Cem A	cu600, cu800, cu925, MK	x	x	x	-	-	-	-	-
5	Cem B	k600, cu600, cu800, MK, filler	-	-	-	-	-	-	20°C, 30°C	20°C

x performed - not performed

**Table 3-9 : Summary of the performed measurements on different series**



### 3.4 Results and discussions

#### 3.4.1 Pozzolanic activity of standard clays

X-Ray diffraction coupled with Rietveld analysis has proved to be a powerful technique for the identification and quantification of anhydrous and hydrated phases of cement [80]. However, new hydrated phases of low crystallinity in the blended systems are not systematically detected by X-rays. Due to numerous crystalline phases from the clays with imprecise crystal structures, the quantification by Rietveld analysis could not be performed. Moreover, calcium hydroxide peaks, which should indicate the progress of the pozzolanic reaction over time, suffer quite severely from preferential orientation. As a result, monitoring of calcium hydroxide by XRD could be done on a qualitative basis only. It was thus decided to present most of the results in the appendix V and keep only some relevant figures for this section.

Thermogravimetric analysis has proven to be a much more suitable technique as it allowed the quantification of calcium hydroxide and chemically bound water in the different systems over time. Calcium hydroxide content was thus chosen to be the main indicator of pozzolanic activity.

XRD patterns of 28 day old pastes at 30°C produced in series 1 are shown in Figure 3-3 with the two main reflection of calcium hydroxide ( $2\theta = 18$  and  $2\theta = 34$ ) indicated. The intensity of the control (opc\_1) was scaled down by 70% to be able to compare the patterns at the same clinker content as blended systems. It is clear that systems incorporating calcined kaolin (k600, k800) seem to react with calcium hydroxide, whose peaks are notably reduced compared to the control. Systems i600, i800, m600 and m800 do not show a clear decrease in CH, suggesting that calcined illite and montmorillonite have little pozzolanic effect. These interpretations assume that the clinker component in the blended systems hydrates in the same way and forms equivalent amounts of calcium hydroxide. The paste containing the filler was not shown in this figure due to the dominant reflexion of quartz. The results for the Cuban clay are presented in sections 3.4.2 and 3.4.3.

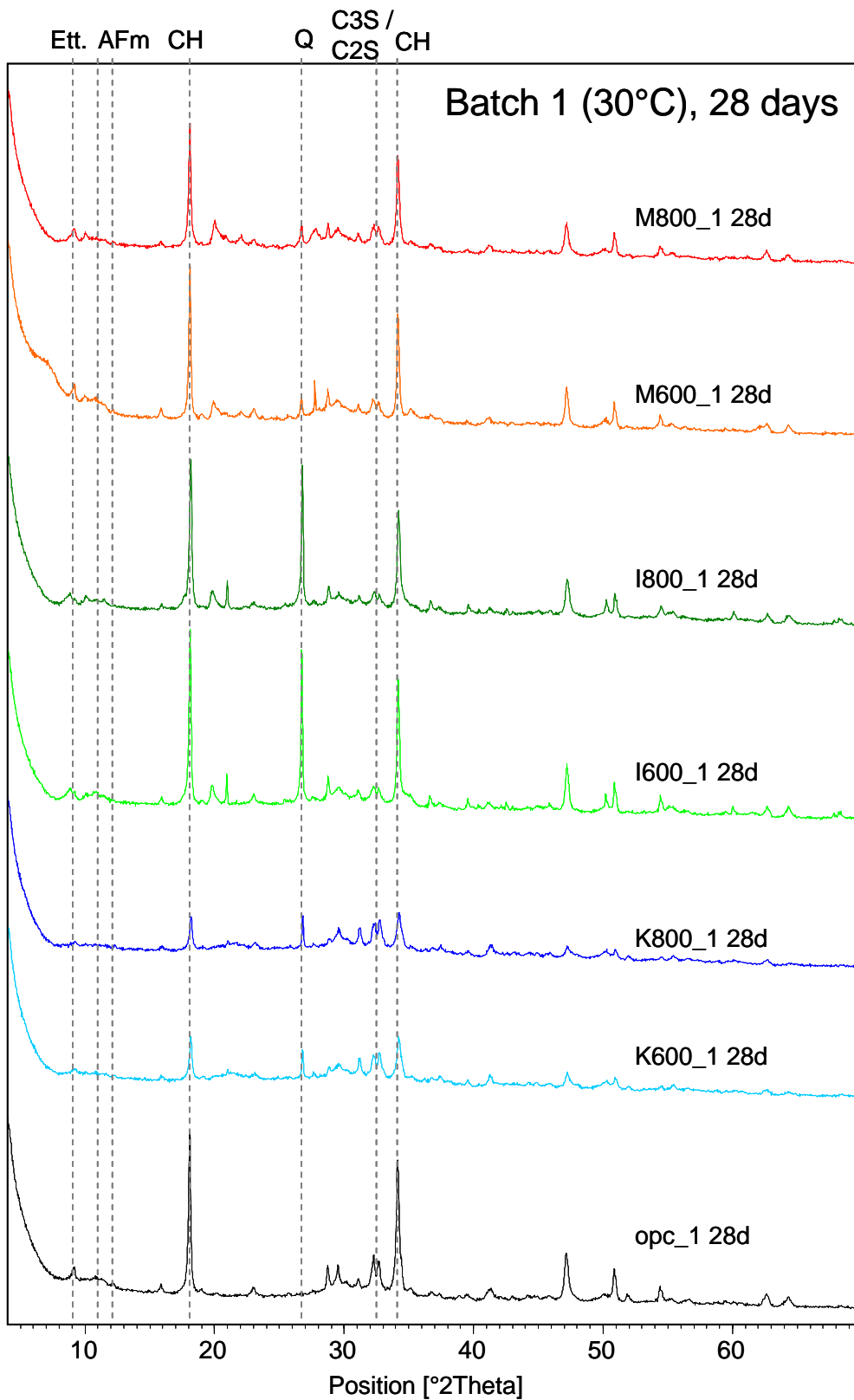


Figure 3-3 : 28 days XRD patterns of cement-calcined clays pastes, series 1 (30°C)

Figure 3-4 shows the TGA results of calcium hydroxide content relative to the cement clinker content with degree of hydration of the pastes at 28 days. The degree of hydration was obtained by backscattered electron image analysis. It is interesting to note that all mineral admixtures including the filler seem to enhance the hydration of the cement, as values of degree of hydration are centred around 85% compared to 80% for the control.

Quantification of portlandite confirms XRD results by showing that only calcined kaolinite and to a lesser extent calcined montmorillonite (600°C) are effective in consuming calcium hydroxide. The other systems, with calcium hydroxide content being at all times superior to the reference, tend to behave like the inert fillers. These results clearly show the reactivity potential of kaolinites over other standard clays commonly found in the earth's crust. The difference between the m600\_1 and the m800\_1 system indicates that reactivity of calcined montmorillonite is more sensitive to the activation temperature than the other clay types.

It should also be said that the change in activation temperature from 600°C to 800°C seems only to influence the pozzolanic activity of montmorillonite. This could be explained by the important sintering effect observed for this particular type of clay (see drop in specific surface and d50 in Table 3-4).

The chemically bound water results are shown in Figure 3-5. A renormalisation by the amount of clinker component makes no sense in this case because this measurement does not quantify a phase that was produced by the hydration of clinker alone, as it is the case for CH. Higher levels of bound water were expected for the control as more cement was initially present in this system. Based on theoretical assumptions (see section 3.1), the amount of water involved in the process of hydration of one mole of cement is almost double that of the pozzolanic reaction (5.3H for 1mol of C<sub>3</sub>S, 2.8H for 1mol of S or A). As for the standard clay systems, it is interesting to compare them to the filler as they have the same amount of cement and the same degree of hydration. Hence, bound water above that of the filler could be interpreted as water that was consumed by the pozzolanic reaction alone. There again, over 90 days, the calcined kaolinites and the calcined montmorillonite m600 bind slightly more water than other calcined clays, which seem to behave like inert fillers. Note that pozzolanic activity seems to kick off between 7 and 14 days, as at this age values of bound water in the reactive systems cross that of the filler.

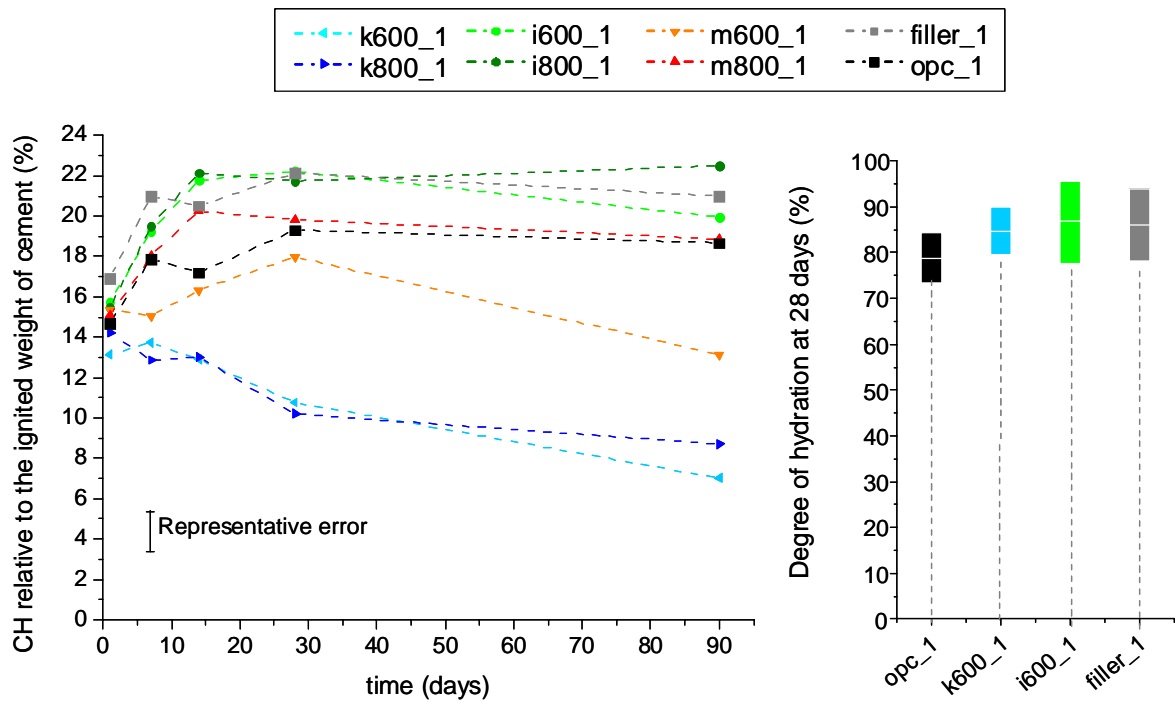


Figure 3-4 : Calcium hydroxide content and degree of hydration at 28 days, series 1 (30°C)

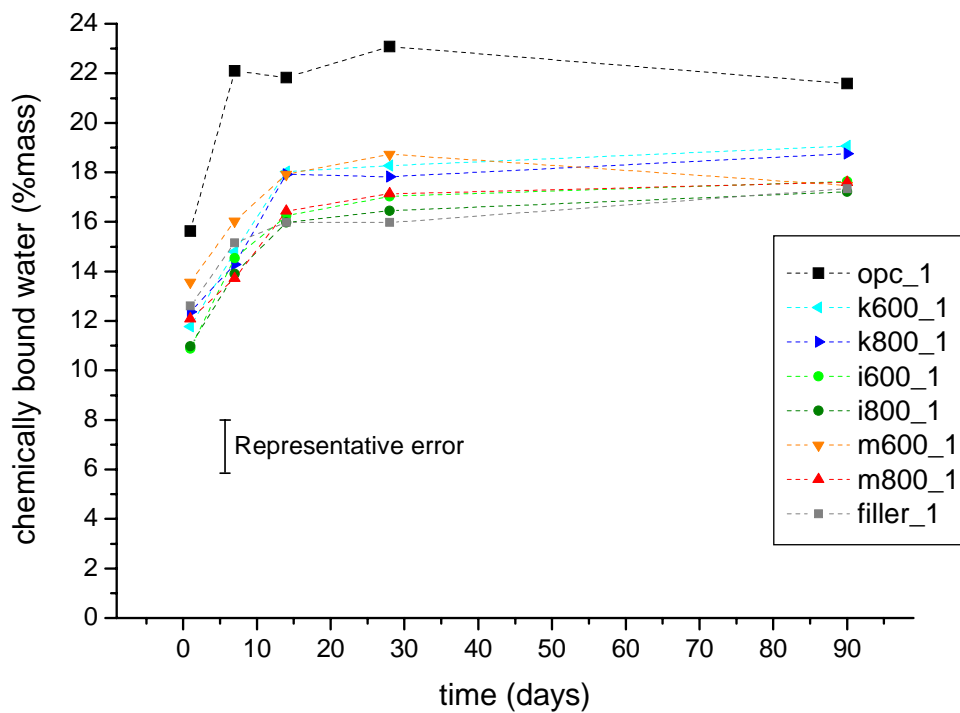


Figure 3-5 : Chemically bound water, series 1 (30°C)

The results of  $^{27}\text{Al}$  NMR for the anhydrous mixes and hydrated pastes at 28 days are presented in Figure 3-6 and Figure 3-7 respectively. In the first figure, contributions of the raw materials to the overall signal can be clearly identified. For the anhydrous cement, 6-coordinated aluminium could be detected, probably due to some pre-hydration. Spectra of hydrated pastes at 28 days reveal the presence of 4 main peaks around 9, 11, 60 and 70 ppm. The first two are assigned to  $\text{Al}^{[6]}$  in an AFm-type and  $\text{Al}^{[6]}$  AFt-type phase respectively. Note that the signal for these two phases is weaker for k600\_1, suggesting that they are present in lower amounts than in the other systems. Following Love et al. [68], while the peak at 70 ppm is assigned to  $\text{Al}^{[4]}$  in C-S-H, the overlapping peak at 60ppm is assigned to tetrahedral Al in an aluminosilicate anion in the interlayer of strätlingite, an AFm-type phase. This peak was not detected in the control paste, showing that it is a phase that developed due to the presence of calcined clays in the system. The strong indication of strätlingite in paste k600\_1 could explain the reduced intensity of AFt phases (11ppm), as one probably develops at the expense of the other. Also, according to Faucon et al.[65] and Andersen et al. [66], a minor peak at around 30 ppm can be assigned to  $\text{Al}^{[5]}$  substituting for Ca in the interlayer of C-S-H. The signal could be seen for k600 and m600, but neither for i600 nor the control.

The presence of strätlingite was confirmed by XRD. In order to detect its main diffraction peak at  $2\theta = 7.066$  corresponding to the 003 plane of the phase, the divergence slit size was lowered to  $0.25^\circ$  and the anti-scatter slit to  $0.5^\circ$  to bring better low-angle resolution. As observed in Figure 3-8, only samples k600\_1 and k800\_1 cured for 90 days revealed a low-intensity peak at this angle, showing the limitations of this technique to detect poorly crystallised phases. Patterns of pastes cured for 28 days did not reveal the strätlingite peak.

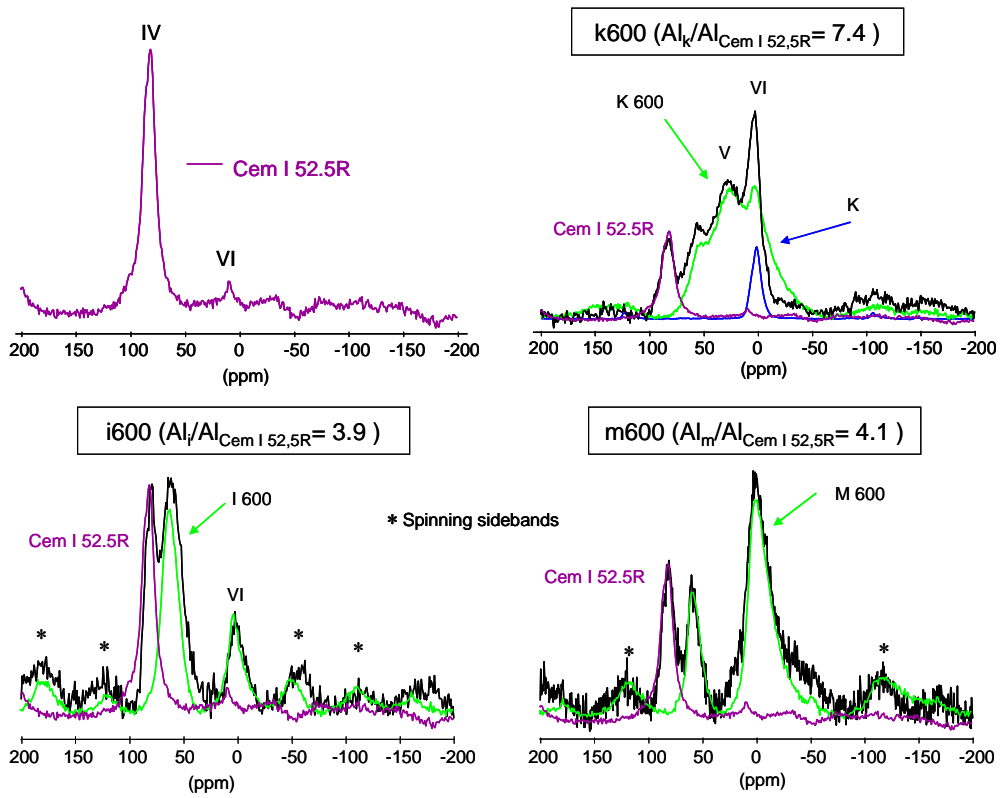


Figure 3-6 :  $^{27}\text{Al}$  NMR spectra of anhydrous cement and blends

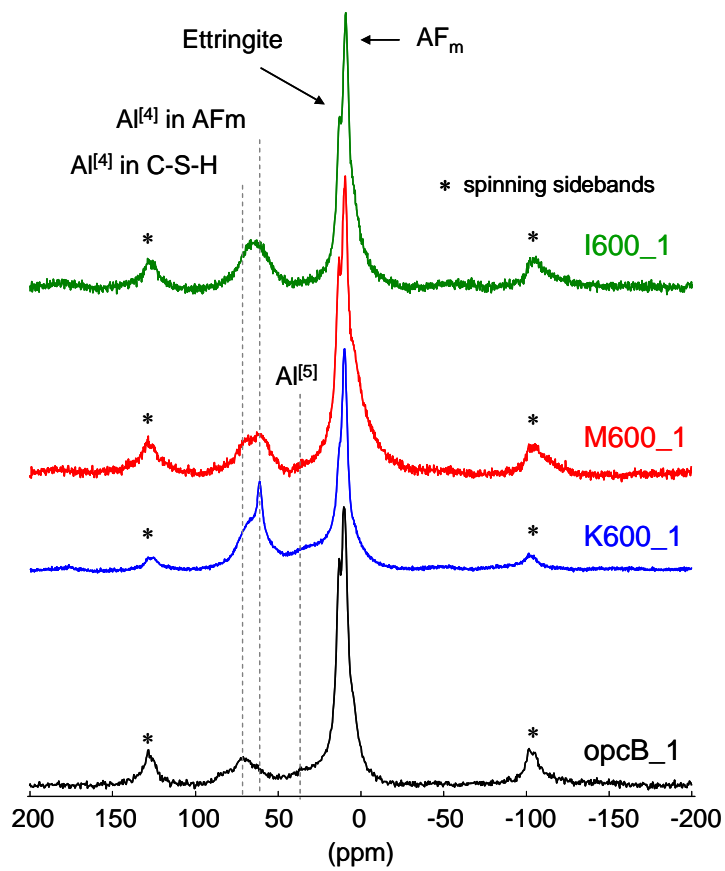


Figure 3-7 :  $^{27}\text{Al}$  NMR spectra of hydrated pastes at 28 days, series 1 (30°C)

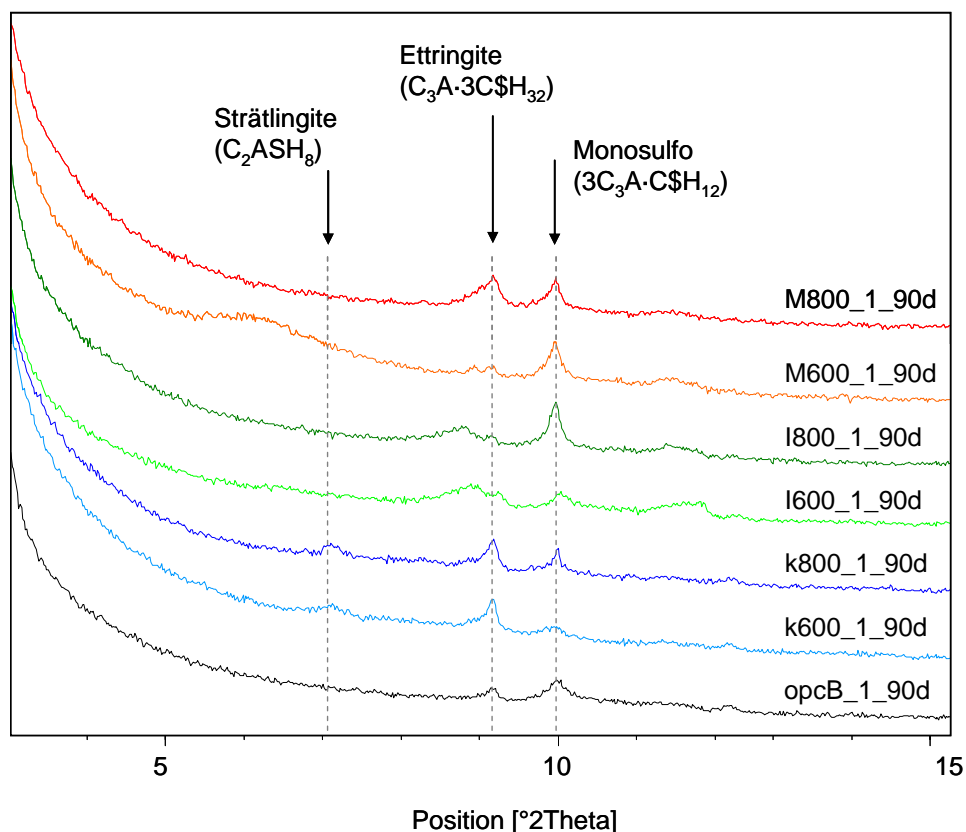


Figure 3-8 : Detection of strätlingite by low-angle XRD, series 1 (30°C)

The results of this section clearly show that kaolinite has the highest pozzolanic activity independently of the activation temperature. Illite seems to behave like a filler as no sign of reaction with calcium hydroxide could be observed. As for montmorillonite, some activity could be detected for the clay calcined at 600°C. In parallel to that, results of  $^{27}\text{Al}$  NMR showed that reactive systems tend to favour the formation of AFm-type phases such as strätlingite. This could be due to the fact that more aluminium is provided to the system when calcined clays dissolve in the alkaline environment of the cement paste. In other words, the pozzolanic potential of kaolinite over the other structures could be explained by the fact that its structure that has a higher content of hydroxyl groups. Located at the edge of the structural layer, these groups increase the potential for disruption by dehydroxylation with thermal treatment causing important losses of crystallinity. As a consequence, the aluminium conformation is more likely to become disordered (see Figure 2-13), favouring dissolution and reaction with Ca ions provided by the cement.

The effect of the pozzolans on mechanical properties in mortars is presented in Chapter 4 and the link with chemical changes discussed.

### 3.4.2 Pozzolanic activity of Cuban clay

This section focused on the pastes of series 2 and 3 (both cured at 20°C) with the objective of studying with more detail the influence of calcination temperature on the pozzolanic activity of the Cuban clay. No inert filler was included in these series.

The evolution of hydrated phases with time was followed by TGA/DTG, as can be seen in Figure 3-9 (DTG curves for all paste series are presented in appendix IV). Due to the overlapping of the decomposition of hydrated phases in the range of 30 to 300°C (C-S-H, AFm and AFt), quantification of these phases with time was not possible. Nevertheless it is interesting to observe qualitatively the increase of hydrates with time, with a particular emphasis on C-S-H and AFm phases, centred around 100°C and 160°C respectively. The sharp and precise location for the decomposition of calcium hydroxide in the range of 400 to 550°C allowed quantitative analysis, as described in section 3.3.1. Results of this quantification are presented in Figure 3-10 and Figure 3-11.

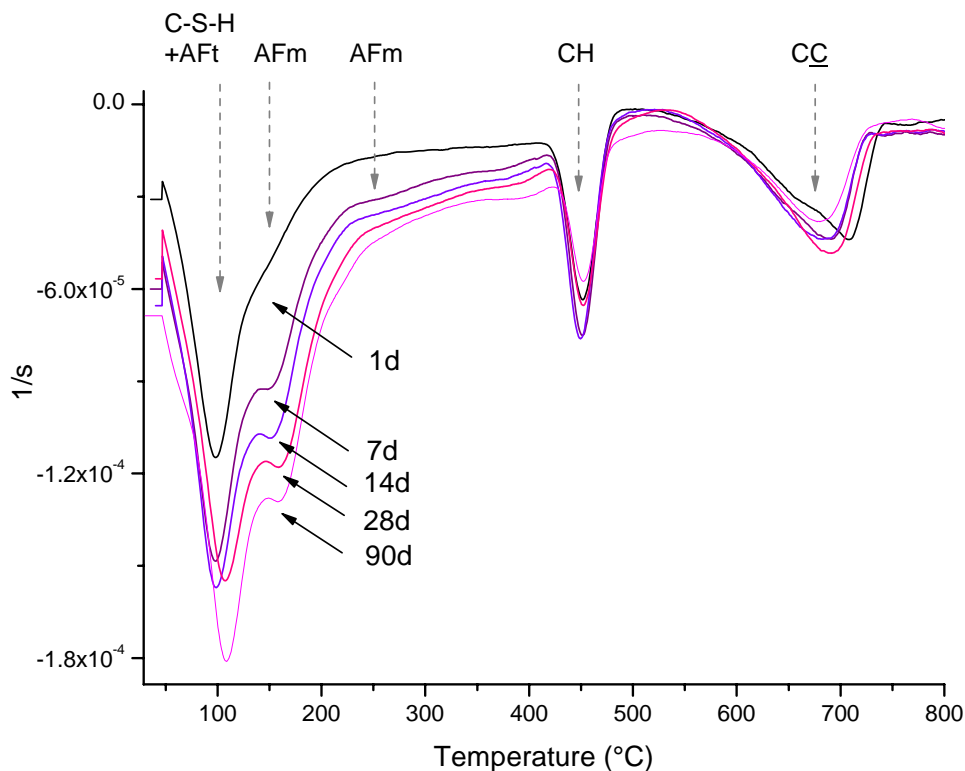


Figure 3-9 : DTG curves of cu800\_2

It is interesting to note that for all systems there is a first increase in the amount of CH due to the hydration of cement. This does not mean that there is no pozzolanic activity in the blended systems, but rather that the amount of calcium hydroxide produced by hydration is more than that which can be consumed by the pozzolanic reaction. The decrease in calcium hydroxide is



generally observed between 7 and 14 days, corresponding to a slow down in the rate of reaction of the clinker component and possibly indicating an increased reaction of the pozzolan. However, this decrease in CH content is present in the control sample too and is slightly bigger than the representative error on the measurement. No reasonable explanation could be found for this result. Another way of looking at these is to compare the levels of calcium hydroxide relative to that of the control. In this way systems having levels of calcium hydroxide above that of the control are systems where the mineral admixture acts only as filler, which enhances cement hydration. Alternatively, when CH contents are lower than the reference, calcined clays contained in the system react with calcium hydroxide to form more C-S-H. The fact that they also act as fillers is confirmed by the measurement of the degree of hydration presented in Figure 3-11, where values at 28 days are higher than the control for any system incorporating calcined clays. Measurement of degree of hydration for series 2 could not be performed.

A good way of presenting the results for minimizing the effect of storing conditions is to plot the values of CH as a percentage of CH content in the control which is equal to 100%. The effects of this renormalisation on the shape of the curves can be seen in Figure 3-12. One of the advantages of this renormalization is that it allows the results of different series to be combined in the same graph to get a clear picture of the trends.

Having these considerations in mind, the influence of activation temperature on the reactivity of the Cuban clay is clearly revealed. Clays calcined above 900°C show little to no sign of pozzolanic reaction, probably due to a combination of physical and chemical parameters such as specific surface, particles size and crystalline state (see characteristics of the clays in table Table 3-4). The latter is probably the most important parameter in defining reactivity. Among the reactive clays, the ones calcined at 600°C and 800°C seem to be the most reactive, followed by clays treated at 850°C.

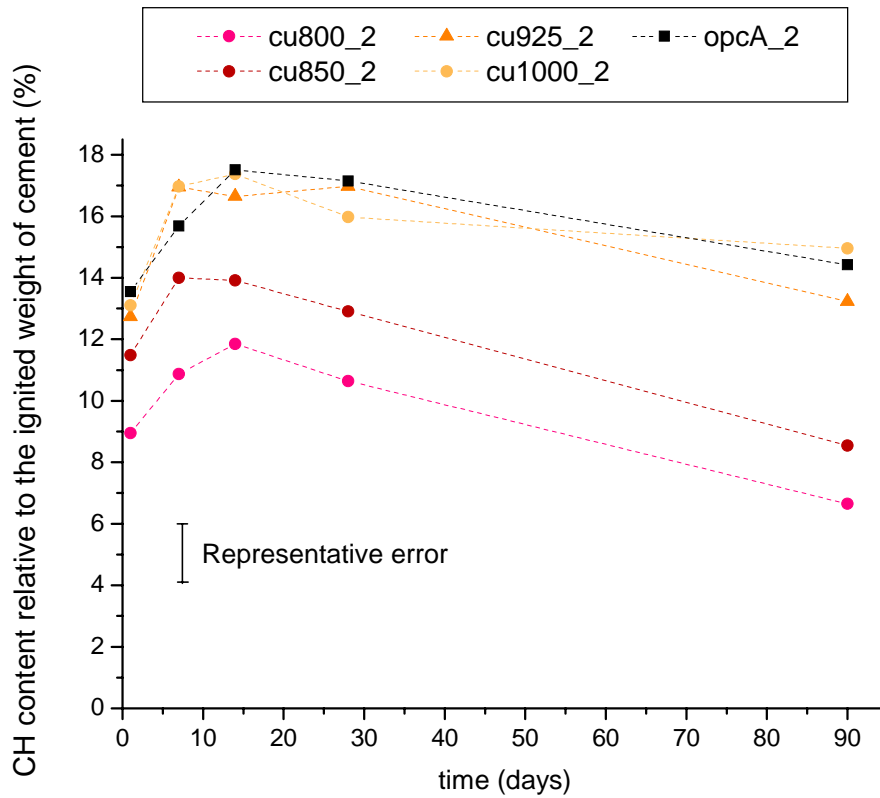


Figure 3-10 : CH content relative to cement, series 2 (20°C)

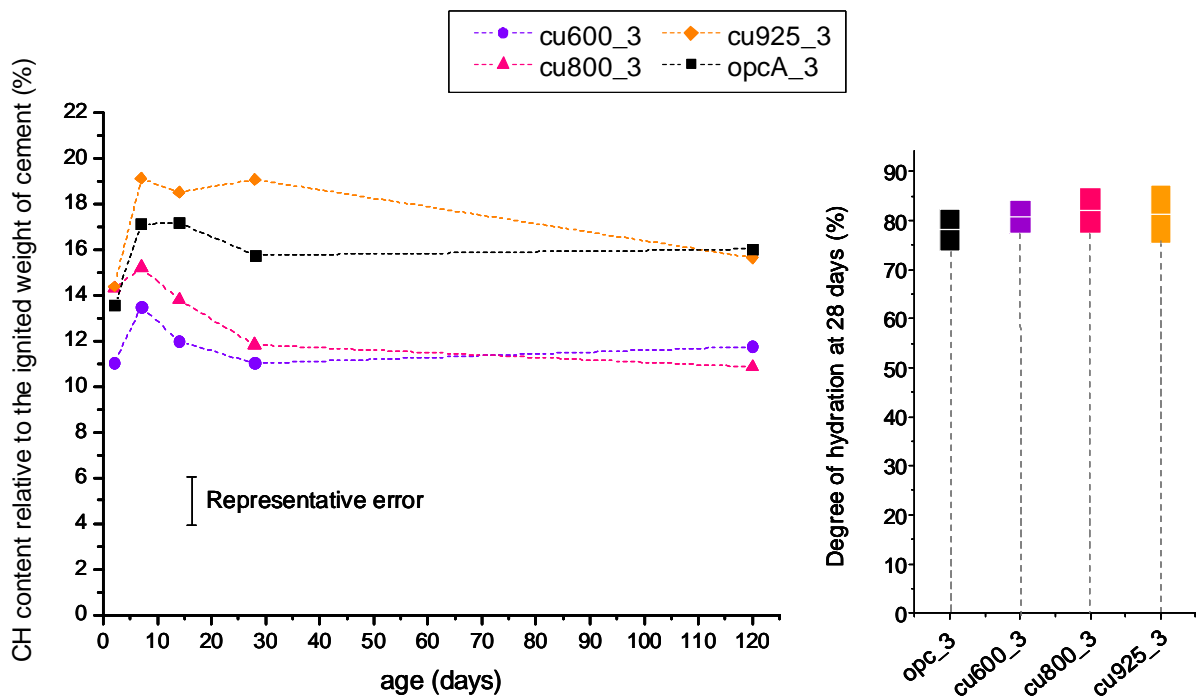


Figure 3-11 : CH content relative to cement vs degree of hydration at 28 days, series 3 (20°C)

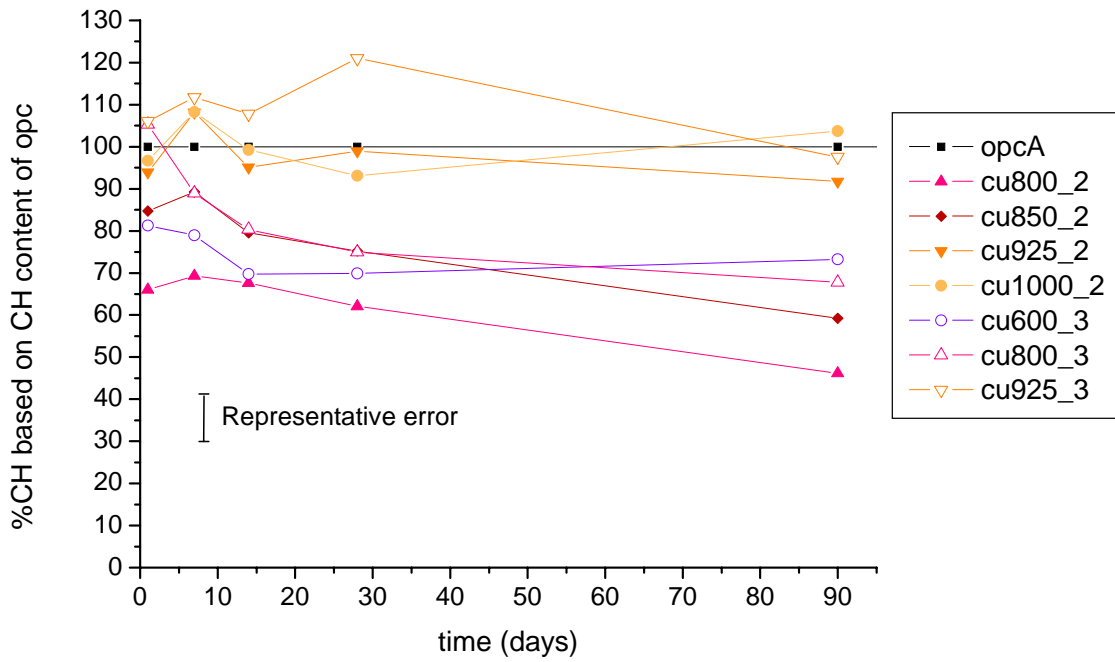


Figure 3-12 : CH content based on CH content of opc, series 2 and 3 (20°C)

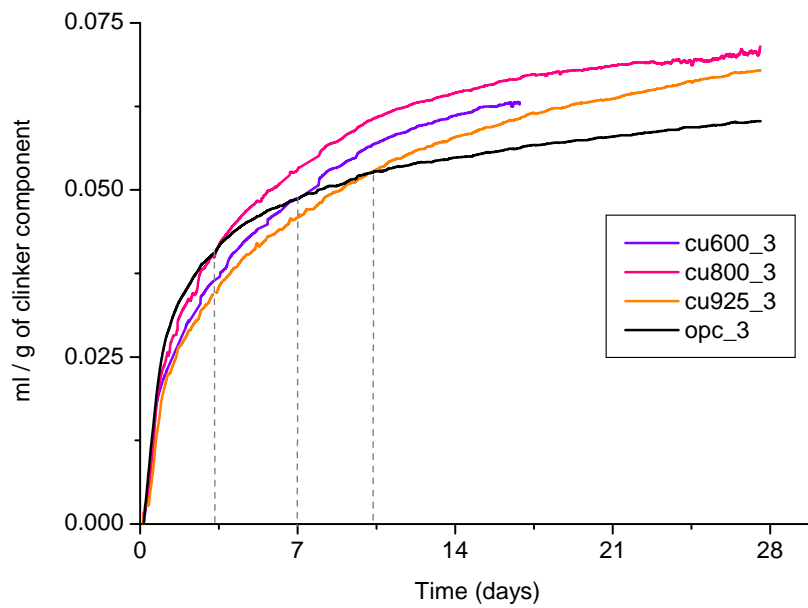


Figure 3-13 : Chemical shrinkage, series 3 (20°C)

Chemical shrinkage measurements are presented in Figure 3-13. As could be expected, the shape of these curves seems to follow that of degree of hydration, which would typically be extracted from cumulative calorimetric values. It is interesting to see that the shape of the curves for the blended systems differs from that of the control. Indeed, while chemical activity seems to be more important for the control in the first 3 days, the activity of the blended systems is more important at later ages and overtakes that of the control. The time at

which the shrinkage becomes greater than the control is different for each blend (approx. 3.5 days for cu800, 7 days for cu600 and 10.5 days for cu925). Assuming that the evolution of the degree of hydration of the cement in the blended pastes is the same, the filler effect could be considered as equal and therefore would not depend on the calcination temperature. In this case the shift in time observed together with the total shrinkage at 28 days could be representative of the reactivity of the pozzolan. 800°C would thus be the optimum activation temperature for the Cuban clay.

<sup>27</sup>Al NMR spectra of cement-Cuban clay blends can be seen in Figure 3-14. Spectrum of cu800\_3 system is not presented as it showed no difference from system cu600\_3. The location and assignment of the peaks can be seen in Table 3-10. They are very similar to those of systems with standard clays presented in the previous section (Figure 3-7).

The peak at 60ppm corresponding to strätlingite is seen in the blends but not in the control paste, showing that it is a phase that developed due to the presence of calcined clays in the system. Also, the ratio AFm/AFt is increased for the blended systems with a preference for systems cu600 and cu800, reinforcing the idea that reactive calcined clays favour the formation of AFm-type phases. The availability of aluminium may also influence the level of substitution for silicon in C-S-H, as the peak at 70ppm is higher for cu600 and cu800 than cu925. Surprisingly, there seems to be more Al<sup>[5]</sup> substituting for Ca in C-S-H in system cu925\_3. This could be due to the contribution of the Al<sup>[5]</sup> peak present in the clay calcined at 925°C. Although this spectrum was not acquired in this study, it was shown by Rocha [34] who studied two different kaolinites that this peak is still present at 900°C and disappears only at 1000°C.

Peak shift [ppm]	Assignment
9	Al <sup>[6]</sup> in AFm-type phase
11	Al <sup>[6]</sup> in AFt-type phase
30	Al <sup>[5]</sup> substituting for Ca in C-S-H interlayer
60	Al <sup>[4]</sup> in the interlayer of strätlingite
70	Al <sup>[4]</sup> in C-S-H

**Table 3-10 : Assignment of <sup>27</sup>Al peaks for pastes of series 3**

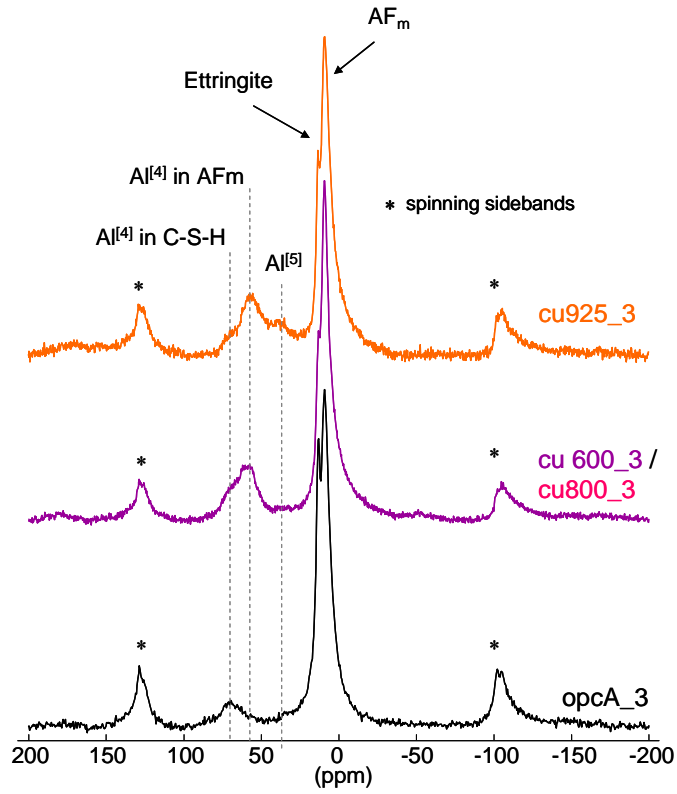


Figure 3-14 :  $^{27}\text{Al}$  NMR spectra of hydrated pastes at 28 days, series 3 (20°C)

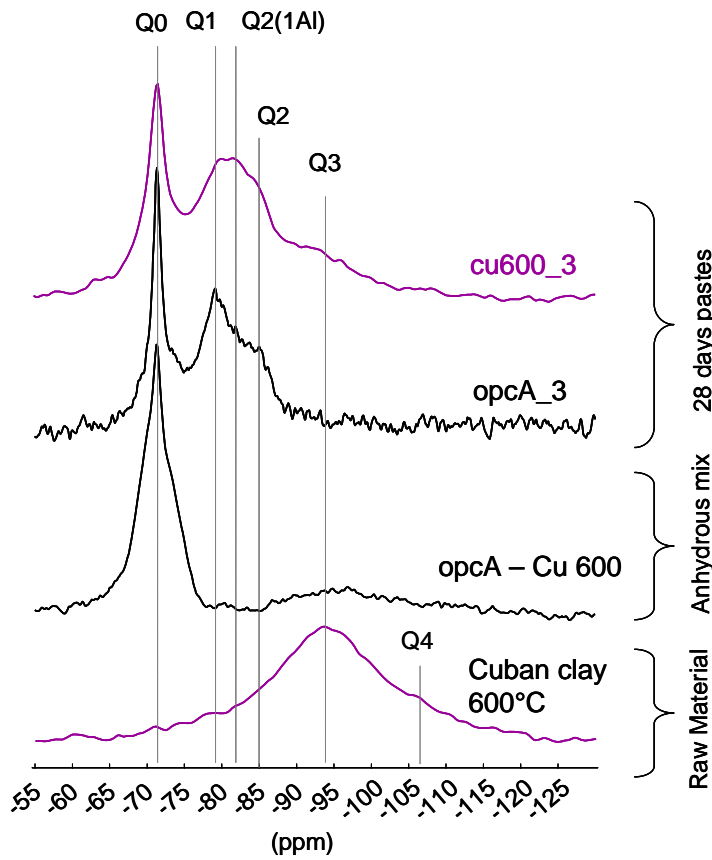


Figure 3-15 :  $^{29}\text{Si}$  NMR spectra of anhydrous and hydrated pastes (opc and cu600), series 3 (20°C)

As for  $^{29}\text{Si}$  NMR results presented in Figure 3-15, peaks were detected around -72 ( $Q^0$ ), -79 ( $Q^1$ ), -82 ( $Q^2(1\text{Al})$ ), -85 ( $Q^2$ ), -94 ( $Q^3$ ) and possibly -107 ( $Q^4$ ). By looking first at the calcined clay alone, the broad peak around -94 ppm is representative of a lack of crystallinity of the silicate sheets, as described in section 2.2.2. The resonance at -107 ppm is characteristic of one  $Q^4$  Si environment in silica polymorphs [34] [81]. In the case of the anhydrous mix, the  $Q^0$  peak is assigned to unreacted cement. It is well documented (e.g. by Love et al. [68]) that belite is the main contributor to the peak intensity, while resonance of Si in alite induces a slightly different chemical shift and overlap the belite peak around -74 ppm. Also, the broad  $Q^3$  signal corresponding to calcined clay could be detected. At 28 days, the pastes do not show the same extent of cement reaction, as a lower intensity of the  $Q^0$  peak was observed in the blended system. This translates into larger peaks for  $Q^2$  and  $Q^2(1\text{Al})$  in the blended paste than the control, indicating the presence of longer chains of C-S-H where Al is substituted for Si. Note that at 28 days the  $Q^3$  signal of the calcined clay is still detectable, suggesting that not all the pozzolan has reacted. The control, with a  $Q^1$  peak larger than  $Q^2$ , indicates that chains are shorter and less Al-substituted. The significant results from this part concerning the reactivity of the Cuban clay are summarised below.

- Activation temperature plays an important role in reactivity. Due to sintering effects and recrystallisations, temperatures above 900°C did not give much sign of pozzolanic activity. The temperature of activation should thus be maintained below 900°C with a preference to 800°C as indicated by TGA and chemical shrinkage techniques.
- Calcined Cuban clay has a double effect when mixed with cement. It first acts as a filler, facilitating the nucleation and growth process of cement hydrates. This was observed by both TGA (by monitoring CH content) and SEM-IA (by measuring the degree of hydration). Calcined Cuban clay also reacts with calcium hydroxide to form additional C-S-H. In general, this pozzolanic reaction seems to become significant between 7 and 14 days and carries on until later ages (90 days in this particular study).
- The formation of strätlingite could be observed in the blended systems thanks to  $^{27}\text{Al}$  NMR. Hence, calcined Cuban clay favours the stabilization of AFm phases. Also, substitution of Al for Si in C-S-H could be observed with the detection of  $\text{Al}^{[5]}$  in  $^{27}\text{Al}$  NMR and  $Q^2(1\text{Al})$  in  $^{29}\text{Si}$  NMR. This last technique also showed that longer C-S-H chains are formed in the blended systems compared to the control.

3.4.3 Comparing reactivity of the Cuban clay with other kaolinite-rich activated clays

With an understanding of the type of clays that could be thermally activated, it was decided to concentrate on kaolinite-rich clays to try and assess the influence of kaolinite content on the pozzolanic activity in pastes. This section also explores further the mechanisms of the interaction between cement and calcined clays. The results of series 4 (including MK) and series 5 are discussed. The results of the standard kaolinites from series 1 including the Cuban clay calcined at 600°C (cu600\_1) were also discussed (for more details see the mix designs on Table 3-7 and Table 3-8, page 67).

A comparison of the characteristics of kaolinite-rich clays used to mix with cement is presented in Table 3-11. For complete chemical analysis refer to Table 3-3 on page 63. Note that the MK was already calcined and used as received.

Type of clay	Kaolinite content (TGA)	Al <sub>2</sub> O <sub>3</sub> content before calcination (XRF)	activation temperature	calcination time	Al <sub>2</sub> O <sub>3</sub> content (XRF)	d <sub>50</sub> [μ]	Specific Surface [m <sup>2</sup> /g] (BET)	density [gr/cm <sup>3</sup> ]
MK	~95%	~40%	~800°C	-	40.4 %	10.30	35.2	2.61
Kaolinite	85%	36.4 %	600°C	60min	-	6.97	24.7	2.55
			800°C			8.28	24.13	2.65
Cuban	40%	24.7 %	600°C	60min	25.7 %	4.40	38	2.68
			800°C		26.6 %	6.07	25.11	2.69

Table 3-11 : Characteristics of kaolinite-rich clays

The heat evolution curves from Isothermal Calorimetry are presented in Figure 3-16. the experiments were run at 20°C and results were normalized by gram of cement in the mix<sup>3</sup>.

<sup>3</sup> Problems of calibration for 20°C were encountered with the new calorimeter device recently installed. The heat signal had to be recalibrated by a scaling factor of 1.6. This factor was determined by comparing the heat evolution curves for the first 24 hours of the reference Portland cement (opc\_5) with those of the same material under the exact same hydration conditions but coming from a well-calibrated device. To double-check on that, degree of reaction of the C<sub>3</sub>S phase for this cement at 7 days was determined by XRD Rietveld analysis assuming all C<sub>3</sub>A had reacted and C<sub>2</sub>S had not reacted. It was found to be 83%. Thus, the total heat generated after 7 days could be determined knowing the phase composition and the reaction enthalpies for C<sub>3</sub>S and C<sub>3</sub>A. The same scaling factor was found when comparing the total heat at 7 days from the experiment with the calculated value.

The sharp peak observed for system MK\_5 and k600\_5 around 5 and 7 hours respectively are due to the reaction of the aluminates and is representative of an under-sulphated system. Due to the additional aluminium ions brought by the mineral admixtures, sulphate ions are rapidly depleted and the formation of AFm phases occurs before the main silicate reaction. The reason why the reaction of MK starts before that of k600 could be explained by its higher specific surface but certainly more by its high alumina content. Peaks corresponding to the silicate reaction are difficult to identify as they are overlapped to the right of the alumina peak and are smaller, but they could possibly be located around 7 hours for MK\_5 paste and around 11 hours for k600\_5 paste. The filler system does not seem to change significantly the time at which this reaction starts nor the rate at which it develops. Similar effects are seen for the Cuban clays systems, except maybe for the cu800\_5 were a slight reduction of the induction period before the main peak could be observed. However, systems incorporating Cuban clays do not seem to alter the normal process of hydration of the cement, that is to say the main reaction of the silicates starting around 5h. It should also be said that as opposed to the under-sulphated systems, the main contribution of the aluminates to the heat development start after that of the silicates for system cu600 and cu800. This can be particularly observed in curve cu600\_5, where a change of slope could be detected around 12h, marking the time at which the reaction of the aluminates starts to be significant. Also, cu600\_5 and cu800\_5 systems show higher heat in the induction period as compared to the control and the filler systems. This is associated with more ettringite formation.

Simulating Cuban conditions, isothermal calorimetry was also run at 30°C. Results in Figure 3-17 show that compared to the curves at 20°C all peaks appear earlier and the rates of reaction of the aluminates and the silicates are considerably increased. Increased curing temperature seems to favour the reaction of the aluminates of the k600\_1 system over those of the MK system. Compared to 20°C, both cu800 and cu600 systems considerably shorten the induction period before the reaction of the silicates, clearly indicating a chemical interaction between the activated clays and the cement. This interaction is not yet fully understood but could possibly be related to a faster dissolution of the cement grains due to the chemical activity of the pozzolans lowering the Ca ions in solution. Calcined clays would therefore act as an accelerator for the cement hydration. This has been previously suggested by Mostafa [58] Note that for the MK\_5 system the overlapping peak of the silicates (around 4h) is more easily identified and seems to be more important than at 20°C. Another peak appeared in that same system around 15h that could not yet be assigned to a particular reaction.



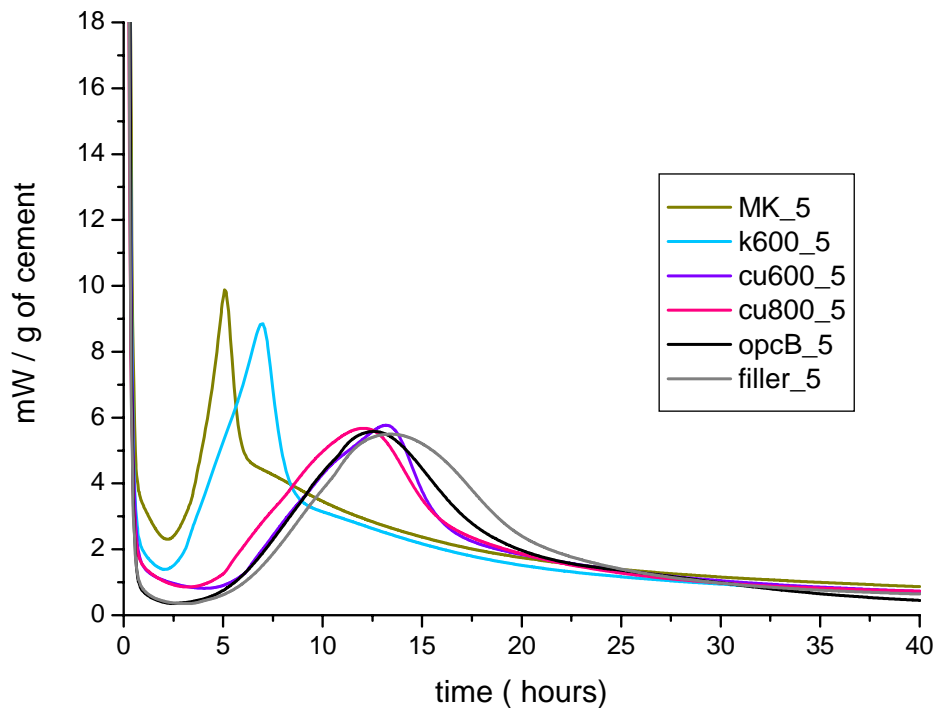


Figure 3-16 : Isothermal calorimetry, series 5 (20°C)

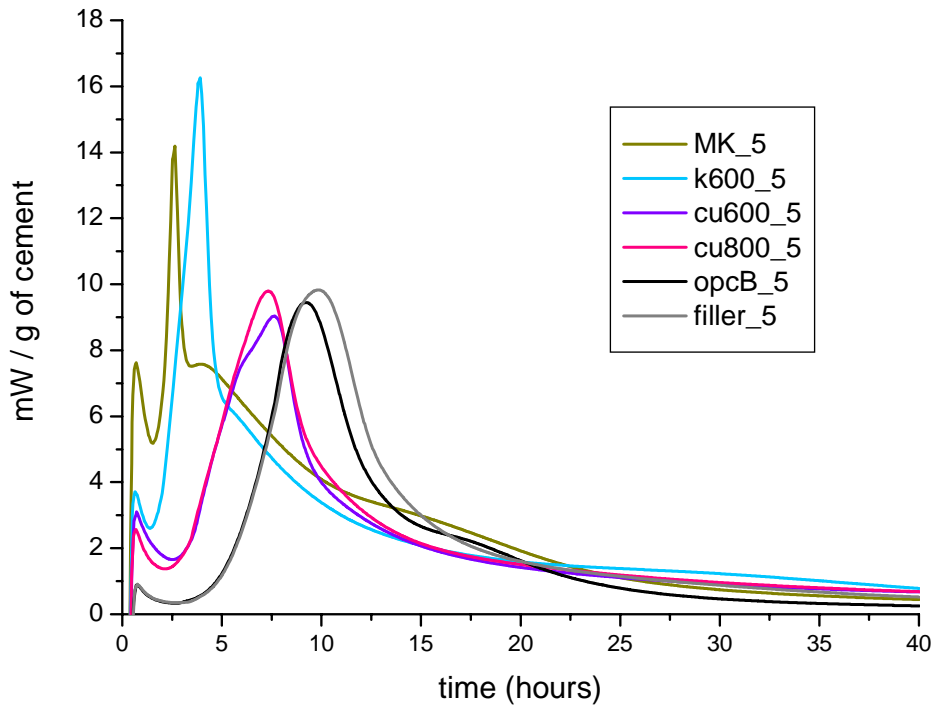


Figure 3-17 : Isothermal calorimetry, series 5 (30°C)

The curves of cumulated heat over a period of 28 days, presented in Figure 3-18, show clear differences between the control and the blended systems. Indeed, the heat developed per gram of cement rapidly surpasses that of the control to end up at 28 days with cumulated heat

values considerably higher than the control paste. Similar results were obtained for the chemical shrinkage test, indicating that chemical activity per gram of cement is more important in the blended systems. This implies that the additional heat (or shrinkage) developed is due to a combination of a filler effect enhancing the hydration of cement and the pozzolanic reaction of the calcined clays.

Going back to the calorimetric results, the curve of the filler system deserves particular attention as it is located in between the control and that of the systems incorporating pozzolans (MK\_5, cu600\_5 and cu800\_5). It is interesting to note that the additional heat generated by the filler effect compared to the control is more important than the additional heat generated by the pozzolanic reaction alone. Assuming that the filler is chemically inert and that the physical effect it induces is the same as that of the reactive pozzolans, the difference in heat between any blended system and the filler system would represent the heat generated by the pozzolanic reaction alone. Thus, as an attempt to extract the contribution to heat brought by the pozzolanic reaction, the cumulative heat curve of the filler system was subtracted to the blended systems. In order to do this, curves had to be normalised by the amount of anhydrous material (cement + pozzolan), as shown in Figure 3-19.

After the subtraction, curves were normalized again by the amount of pozzolan to present values in Joules per gram of pozzolan:

$$\frac{J}{g_{anhydrous}} \cdot \left( \frac{g_{anhydrous}}{g_{pozzolan}} \right) = \frac{J}{g_{anhydrous}} \cdot \left( \frac{1}{0.3} \right) = \frac{J}{g_{pozzolan}}$$

Results of this subtraction are very interesting as they show the profile of reaction of the different calcined clays over time. While the contribution to heat due to the reaction of MK seems to be more important in the first 10 days, Cuban clays reaction seems to increase gradually with time to become more important at later ages. Negative values are due to the fact that the filler and the pozzolans do not have exactly the same filler effect as the filler system develops more heat than cu600 and cu800 systems at early age. This reinforces the idea that this is an approximation of the real phenomena. Nevertheless, the interest of this calculation lies in the indication of the long term contribution of the pozzolans to the total heat generated in the system.

Cumulated heat curves for a curing temperature of 30°C are presented in Figure 3-20 and Figure 3-21. MK reacts more than k600 and the Cuban clays for the first 2 days. Then,

pozzolanic activity of k600 surpasses MK to develop significant heat in the long term. The activity of the calcined Cuban clays seems to start later than the other kaolinite-rich clays. From Figure 3-19 (right) and Figure 3-21 (right) we can conclude that higher temperatures seem to accelerate the pozzolanic reaction the same way it would accelerate the hydration of cement. The figures show that an increase of the temperature from 20°C to 30°C reduced by half the time taken for the pozzolanic activity to be significant ( approx. 2.5 days and 5 days at 20°C and 1.25 days and 2.5 days at 30°C, for cu800 and cu600 respectively). Note also that temperature does not favour the reaction of the different pozzolans to the same extent, as the Cuban clay calcined at 600°C seems to perform better in the long term than the cu800 at 30°C, when the contrary was observed at 20°C. At 30°C, k600 shows the highest heat contributions over 28 days.

Hence, isothermal calorimetry, combined with chemical shrinkage data, showed that the presence of calcined clay can influence the kinetics of reaction of the cement, which seems to be more related to the kaolinite content than the activation temperature of the clay. The subtraction method showed clearly that the time at which pozzolanic reaction seems to be significant seems to be dependant on temperature and on the amount of reactive material of the calcined clay (beginning of the reaction were in the order: MK, k600, cu800 and cu600). It was also shown that some pozzolans tend to react over long periods of time. This was the case of cu600 and cu800 at 20°C, and k600 and cu600 at 30°C, as their heat contribution was constantly increasing over a 28 days period. Alternatively, contribution to heat of the MK system at 20°C and 30°C decreased after approximately 5 days and 2 days respectively, suggesting that the action of this pozzolan is important but restrained in time.

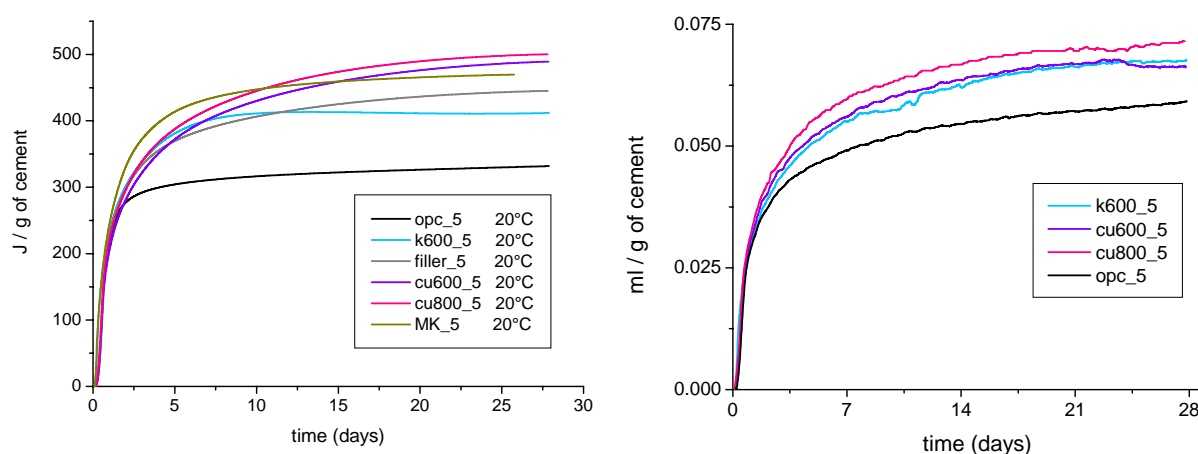
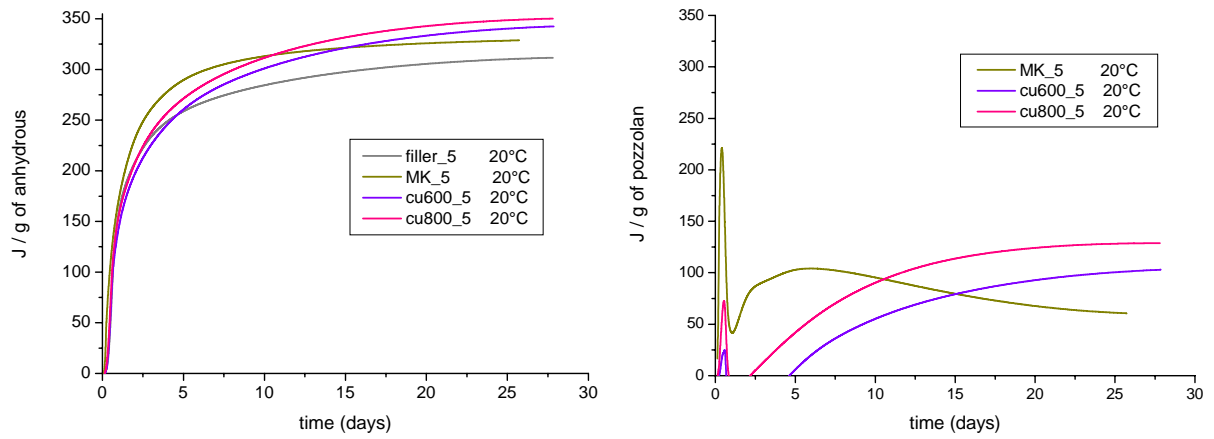
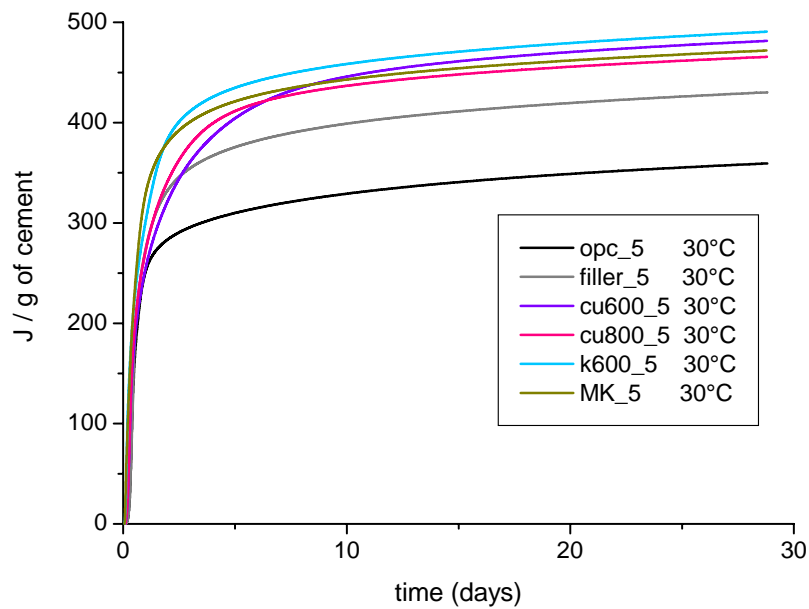


Figure 3-18 : Cumulated heat relative to cement and chemical shrinkage, series 5 (20°C)



**Figure 3-19 : Cumulated heat relative to anhydrous content and filler-substracted curves, series 5 (20°C)**



**Figure 3-20 : Cumulated heat relative to cement, series 5 (30°C)**

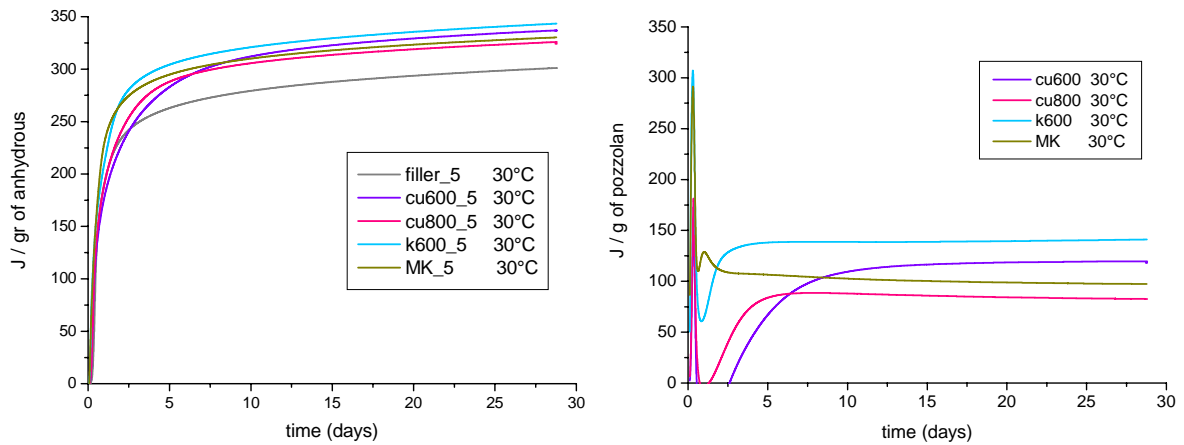


**Figure 3-21 : Cumulated heat relative to anhydrous content and filler-substracted curves, series 5 (30°C)**

Figure 3-22 presents the 28 days XRD pattern for the series 4, allowing qualitative comparison of the pozzolanic behaviour of MK and the Cuban clay at various temperatures. On the one hand, MK seems to have almost completely depleted CH, suggesting a strong pozzolanic behaviour of this system. On the other hand, the intensity of the  $C_3S$  and  $C_2S$  peaks compared with the other systems indicates a lower reaction of the silicates for the MK system. As for the Cuban clay, a decrease of pozzolanic activity could be seen with increasing activation temperature, confirming results of section 3.4.2. Note also that despite the care that was taken to avoid contact with air, carbonation could be detected in most of the systems with the presence of calcite at  $2\theta = 29.5$ .

Diffraction of X-Rays at low angle shown in Figure 3-23 reveals the presence of strätlingite in the MK system from 7 days. Although strätlingite could be detected in the Cuban clay systems by  $^{27}Al$  NMR (see Figure 3-14), it was not detected by XRD due to its low content.

To be more quantitative, CH content measurements by TGA are presented in Figure 3-24 for that same series. Systems with Cuban clays show the same trends as series 2 and 3 at 20°C, except for cu925\_4 that for the first time showed levels of CH below that of the reference. This pozzolanic activity could be explained by the curing temperature that in this case was 30°C. That being said, the most interesting results are those for the MK system, with values of CH way below the usual measurements. The reason for this can be found when looking at the degree of hydration of the paste at 28 days and realizing that with only 50% of the reaction of the cement in the MK system, the amount of portlandite produced is small compared to other systems. Thus, lower values of CH in the MK system are principally due to the low degree of hydration of the cement and to a lesser extent to the pozzolanic reaction. This also explains the absence of CH peak in XRD previously observed. Although series 4 and 5 were not made with the same cement, this corresponds to the isothermal calorimetry curves of the MK system (see Figure 3-16 and Figure 3-17) where the early reaction of the aluminates altered the process of hydration of the cement, resulting in lower degrees of hydration observed in SEM- IA.

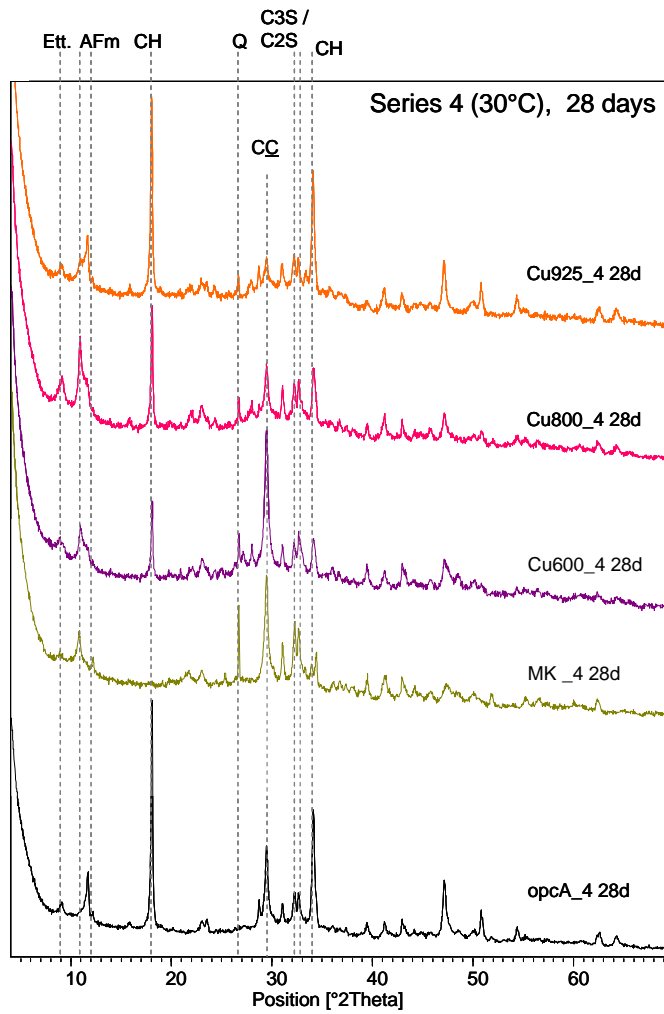


Figure 3-22 : 28 days XRD patterns of cement-calcined clays pastes, series 4 (30°C)

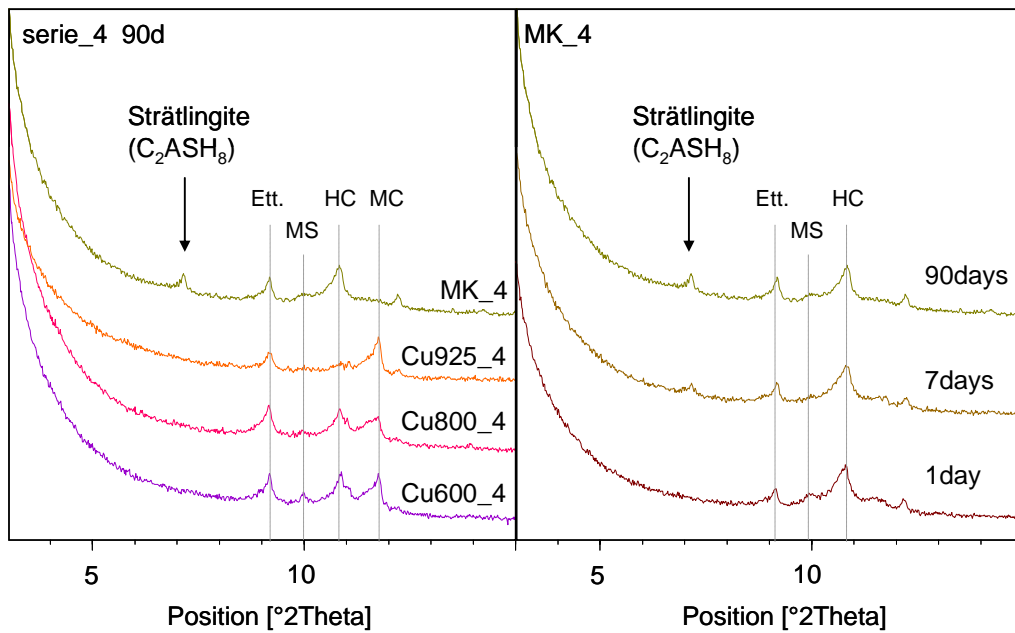


Figure 3-23 : Detection of Strätlingite by low-angle XRD, series 4 (30°C)

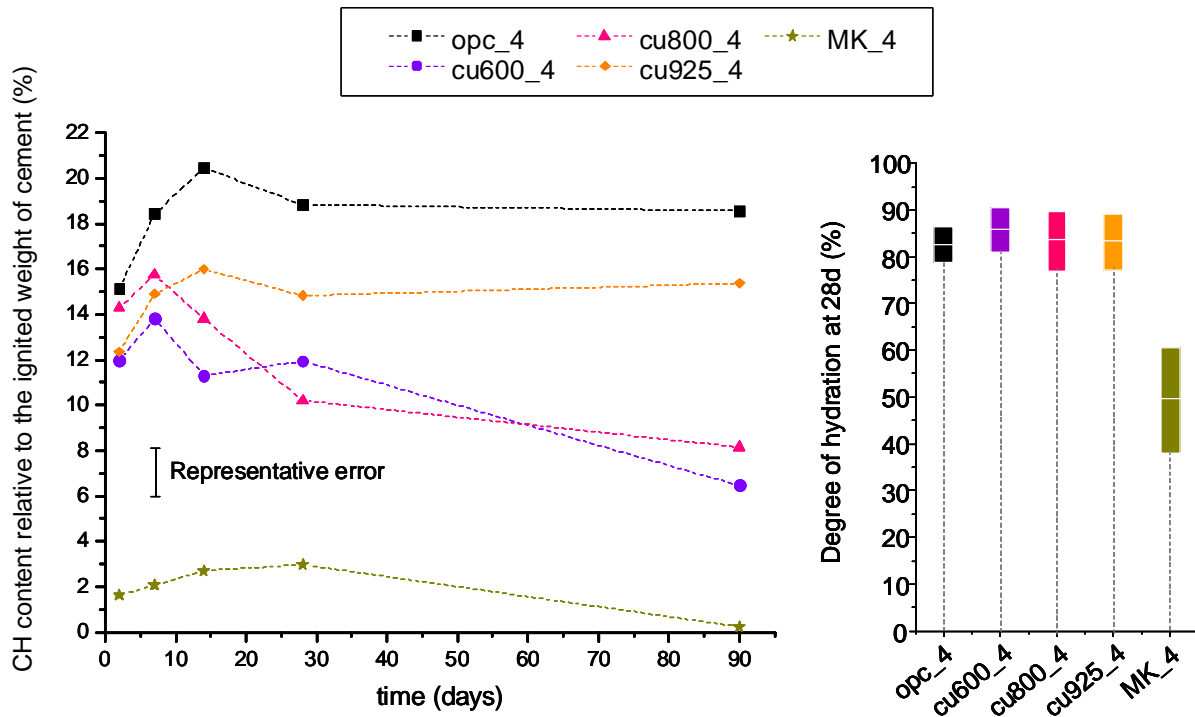


Figure 3-24 : CH content relative to cement, series 4, (30°C)

XRD and TGA results of series 1 incorporating the cu600\_1 paste are presented in Figure 3-25 and Figure 3-26 respectively. Diffraction patterns show clearly that at 28 days the pozzolans reacted with calcium hydroxide. This consumption is quantified in the TGA measurements and seems to be more important for the k600\_1 and k800\_1 pastes. Again, results of degree of hydration confirm that these levels are due to the pozzolanic activity and not to a reduced hydration of cement. However, based on the results of isothermal calorimetry showing the early reaction of the aluminates in system k600\_1, the values of degree of hydration together with CH content presented were expected to be much lower. Surprisingly, although the fast reaction of the aluminates could be observed, it does not seem in this case to have affected the reaction of the silicate. By observing again the heat evolution curve of k600\_1 (Figure 3-16 and Figure 3-17), the peak turned to be much broader than the peak of MK\_1. Assuming that the amount of reactive alumina is lower for clay k600, this suggests that there could be an overlap of the silicate reaction on that of the aluminate. Thus, it is believed that there must be threshold value above which the silica reaction of cement is altered. This value could well be the content of reactive alumina in the calcined material.

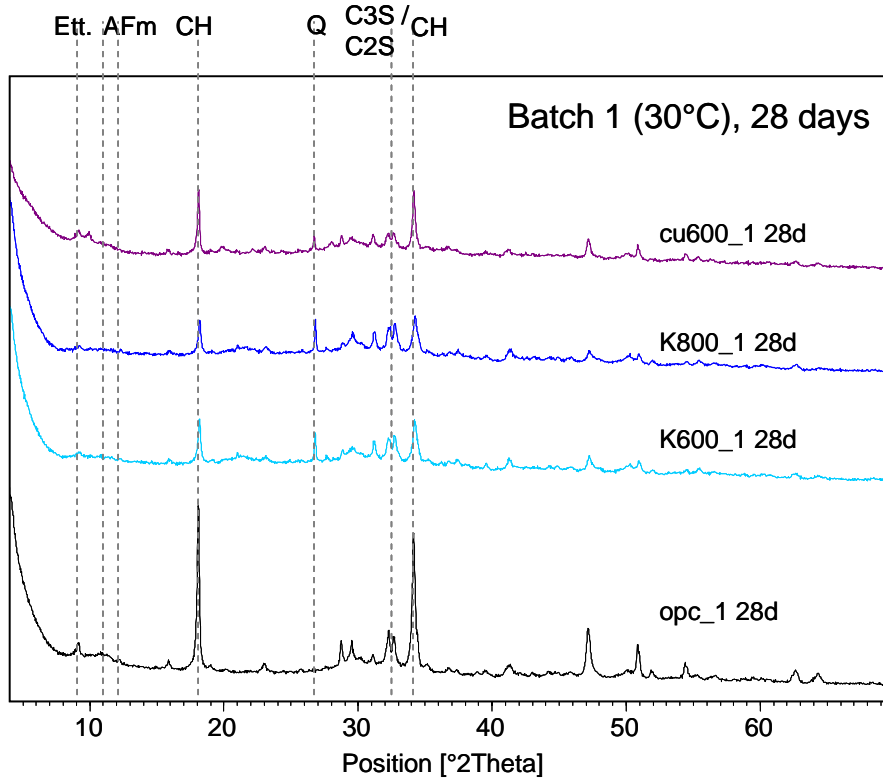


Figure 3-25 : 28 days XRD pattern of cu600, k600 and k800, series 1 (30°C)

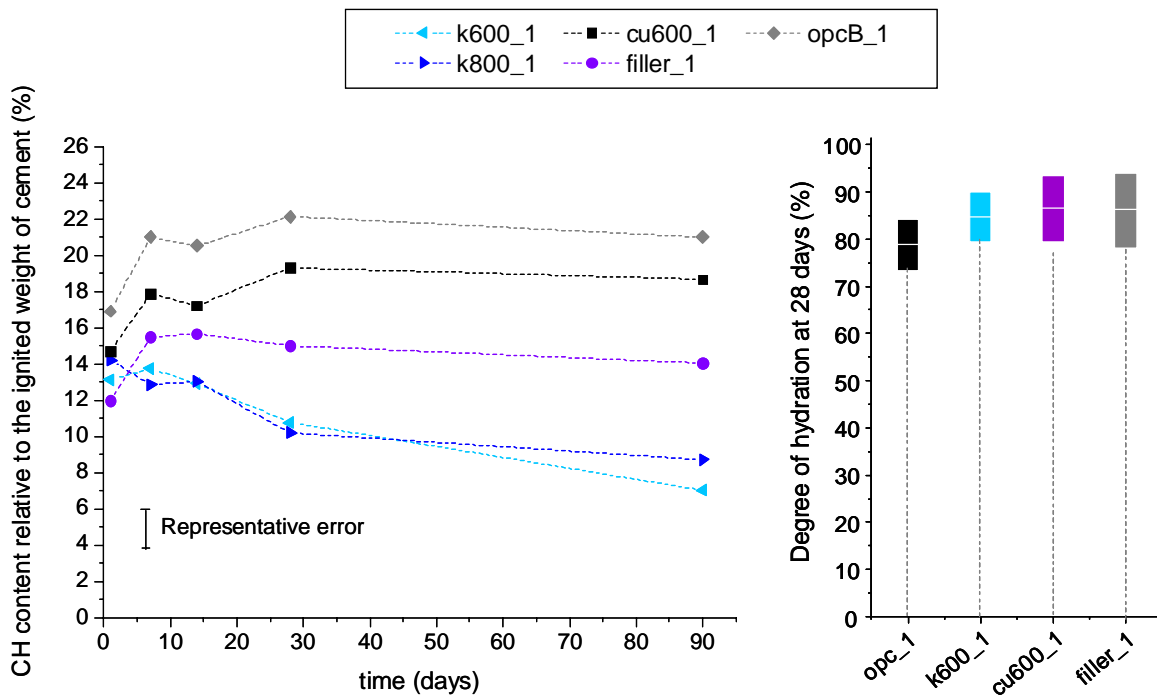


Figure 3-26 : CH content of cu600, k600 and k800 and degree of hydration at 28 days, series1 (30°C)



In order to compare simultaneously the reactivity of all kaolin-rich clays, CH contents of series 1 and 4 were plotted as a percentage of the CH content of the control mix (opc) in Figure 3-27.

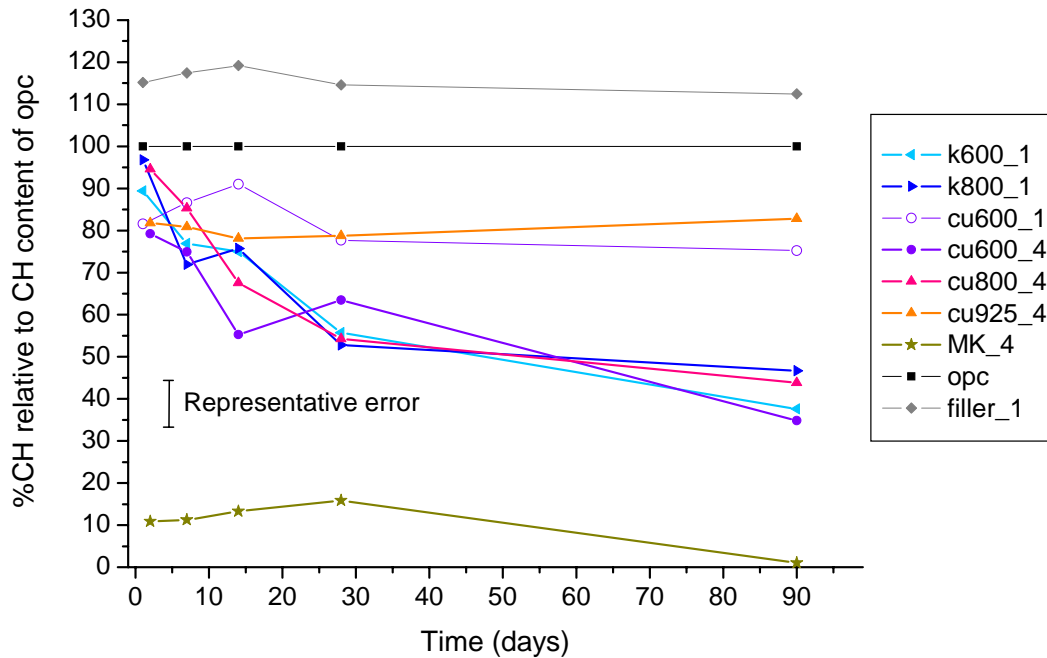


Figure 3-27 : CH content based on CH content of opc, series 1 and 4, (30°C)

What comes out of these results is that to a certain extent, kaolinite content dictates the pozzolanic potential of the clay. Then, the thermal process together with the activation temperature define the reactivity of the calcined product, that is to say the amount of reactive alumina and silica. Hence, standard kaolin, with 85% of the mineral kaolinite before calcination, consumes more CH than the Cuban clay with only 40% kaolinite. It was difficult to assess the reactivity of MK due to the strong disturbances it created in the kinetics of the cement reactions. It should also be said that not much was discussed about the activation process independently of the temperature and how this could affect reactivity, but the influence is surely very strong. This topic is also addressed in more details in section 6.2.4.

#### 3.4.4 Scanning electron microscopy

In order to assess qualitatively the effect of partial substitution of cement by the calcined clays on the microstructure, a series of images was taken. EDX analyses were made on particular points of interest to identify the phases present. A representative microstructure of a 28 days paste is shown in Figure 3-28, showing unreacted phases as well as common hydrates. The calcined clay particle on the top left corner (calcined illite) shows different mineralogical compositions, probably due to the presence of several companion minerals in the raw material such as quartz and chlinochlore (see Figure 2-9). Due to their high calcium content (and iron content in the case of ferrite), anhydrous cement phases appear as the brightest phases.  $C_3S$  grains have partially reacted and their hydration products formed either out of the original boundaries of the grain (outer C-S-H and CH), or in the empty spaces left by the dissolving cement forming a dense layer (inner C-S-H). Note that crystals of portlandite tend to form clusters that are scattered throughout the microstructure, intermixing with C-S-H. AFm phases can often be recognised by their fracture along the cleavage planes due to drying. The differentiation of the different groups of AFm is difficult due to their similar chemical composition and EDX analysis can be useful to try and discriminate on composition from another. In this particular case AFm phases were identified as being of the monosulfo aluminate type.

Pores can remain when insufficient amounts of hydrates are formed, but in this particular case they are mostly due to small cement grains having completely reacted and whose hydration products were deposited out of its original boundaries. These are commonly called Hadley grains. Another external factor that could explain small cavities on the surface of the microstructure is the sample preparation. Indeed, despite the resin impregnation, the polishing process is mechanically aggressive and can pull out loosely bound grains.

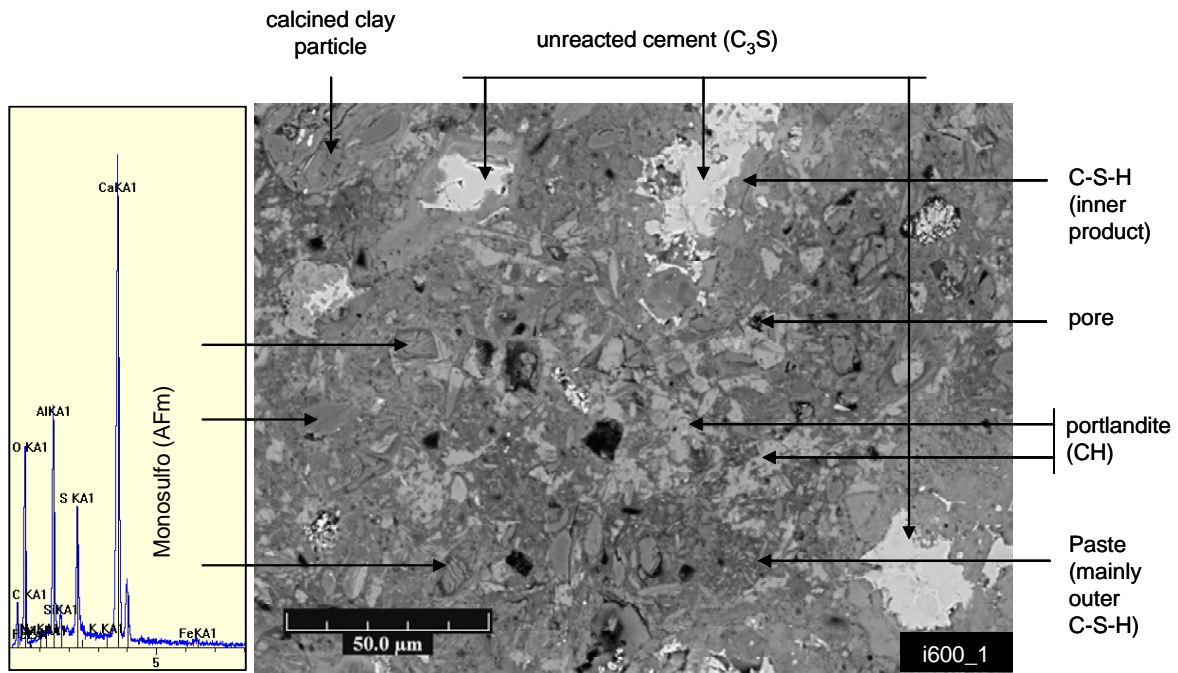


Figure 3-28 : Representative BSE image of a 28 days calcined clay-cement paste

Having these basics aspects of a microstructure in mind, different clay-containing pastes were compared to the reference at 28 days. Microstructures for pastes of series 1 (opcB, 30°C) can be seen from Figure 3-29 to Figure 3-33. The control mortar exhibits similar features to the microstructure described above, with an even distribution of calcium hydroxide crystals over the microstructure. Smaller cement grains have reacted more than big ones and a layer of hydrates can be observed around grains ranging from 10 to 20 microns. Smaller grains of cement are difficult to see due to their advanced state of reaction. Several Hadley grains can be identified on the top left area of the image. Dark zones indicate zones of lower density of hydrates and increased quantity of small pores. This porosity is not observed for sample k600\_1 that shows a very homogeneous and dense microstructure (see Figure 3-30). The layer of hydration products around the anhydrous cement grain is less pronounced, indicating that the development of the microstructure was different from the control. This is probably due to the presence of calcined clays that provided surface for the hydrates to nucleate and grow away from the cement grains. Calcined kaolin particles can be easily recognised by their grey level being lower that that of CH and even C-S-H. This is due to their relatively high alumina content. Although TGA showed that CH was still present in this system at 28 days, note that CH clusters are not visible in this microstructure, suggesting that CH is more finely divided and part of it reacted with the pozzolan to form AFm or C-S-H phases.

Direct evidence of pozzolanic activity is almost impossible to detect in the cement microstructure. First because the most reactive grains are the smaller ones that are difficult to see even at high magnification, and second because the C-S-H they form is finely intermixed with the hydrates of the cement and has similar chemical compositions. However, the detection of appreciable quantities of AFm phases with increased magnification, as seen in Figure 3-31, indicates that there is a contribution of the calcined kaolinite to the chemical activity of the paste that tends to favour the formation of other types of hydrates phases. In the particular case of paste k600\_1, strätlingite could be identified by EDX analysis, confirming the interpretation of the NMR spectra in Figure 3-7. The presence of calcium in the calcined kaolin particles indicate that these particles are permeable to external ions. This is probably due to the fact that clayey particles have kept some of their original interlayer structure after calcination. This may be confirmed by the observation of some calcined kaolinite particles (i.e. bottom left of Figure 3-31) that seem to have kept their characteristic original stacking arrangement, composed of several hundreds of layers.

The microstructure of systems i600\_1 and m600\_1 could be described as very similar to that of OPC, with the difference that calcined clays particles can be observed. Their grey level is similar to that of C-S-H and are therefore more difficult to identify, particularly in the case of calcined illite. Some monosulfoaluminate (AFm) was found in both microstructures, as showed in Figure 3-28. Grain pull-out seems to have been more important during the preparation of these two polished surfaces.

Microstructures for pastes of series 4 (opcA, 30°C) can be seen from Figure 3-34 to Figure 3-40. Systems incorporating calcined Cuban clays (Figure 3-35 to Figure 3-37 and Figure 3-40) tend to develop the same dense microstructure, independently of the calcination temperature. Alternatively to the control opc paste, CH tends to crystallise on the surface of the pozzolans. Apart from particles calcined at 925°C where smaller calcined clayey particles seem to have agglomerated at the surface of bigger particles, it is very difficult from these images to see differences in morphology of the Cuban particles. The MK\_4 system (Figure 3-38 and Figure 3-39) reveals a very different microstructure, resembling that of the k600\_1 system presented earlier. With the same grey level as the matrix of hydrated products, MK particles can be distinguished by their round shape, probably originating from the activation process they went through. The low degree of hydration determined by image analysis (see Figure 3-24) is appreciable on this image as cement appears to have reacted much less than in the other systems. The morphology of the hydrated phases is also very different, with needle-

like hydrates that seem to link grains together. Strätlingite was more difficult to identify than in sample k600\_1, probably due to the fact that it is finely intermixed with C-S-H. The EDX analysis shown in Figure 3-39 does not coincide perfectly with the chemical composition of strätlingite and higher amounts of silicon could well be due to the simultaneous detection of C-S-H.  $^{27}\text{Al}$  NMR was not performed on this sample but could be very useful to confirm the presence of this phase, as shown for the k600\_1 system (see Figure 3-7). Strätlingite could not be seen in samples containing calcined Cuban clays, suggesting that it could be present in minor amounts and too finely divided for an observation under the SEM. However, monosulfoaluminate was easily detected by EDX analysis, as shown in Figure 3-40.

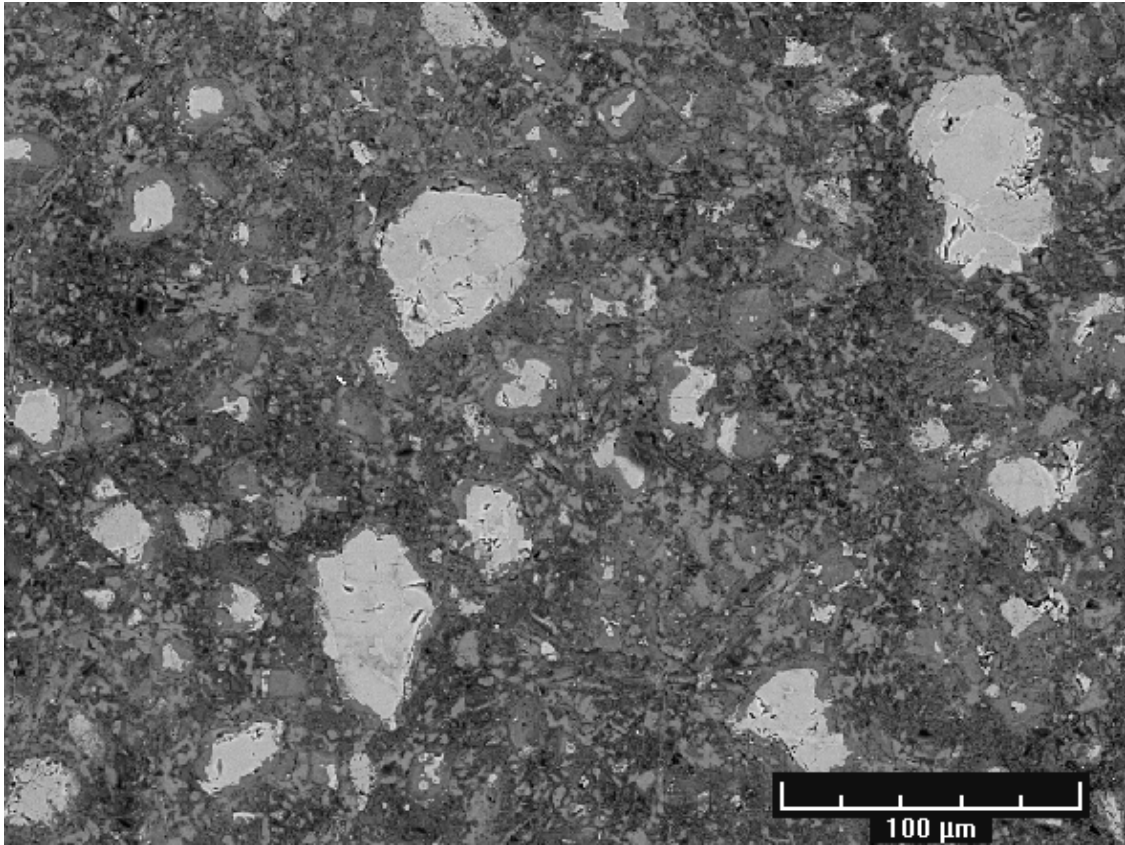


**Figure 3-29 : 28 days microstructure of opcB\_1, series 1 (30°C)**

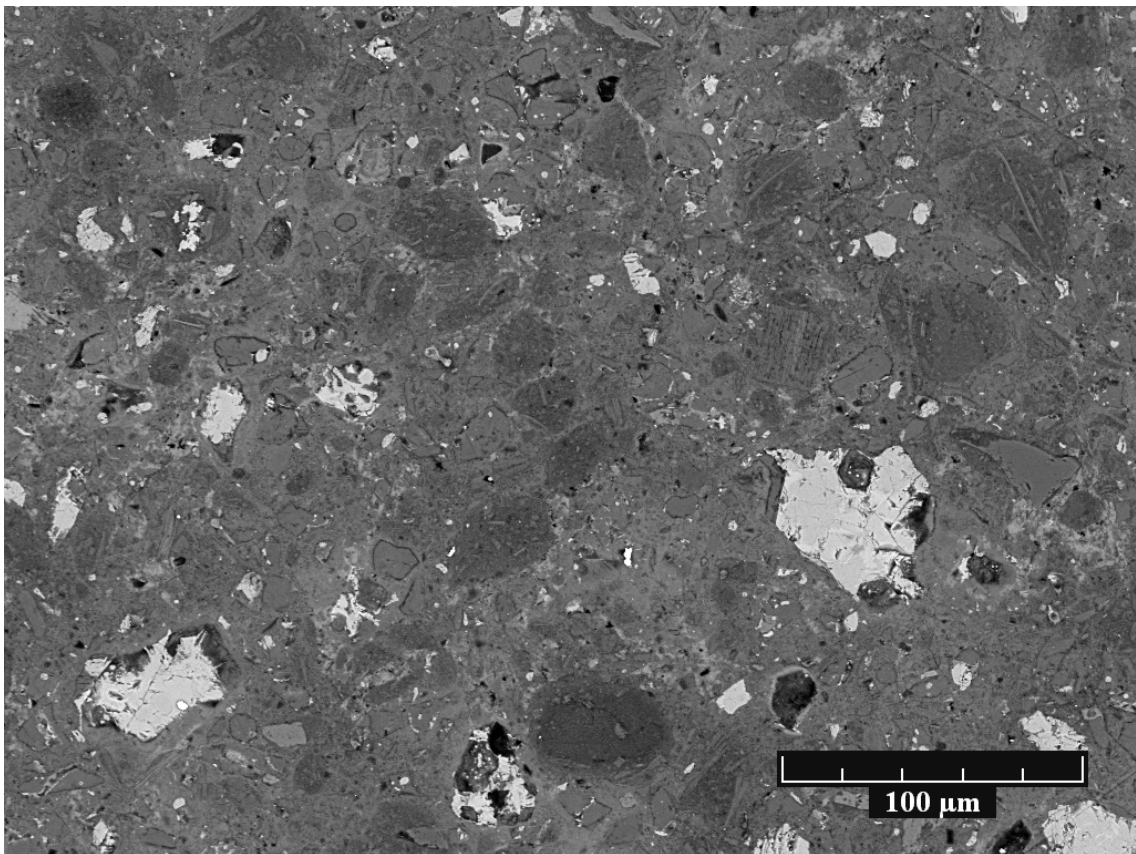


**Figure 3-30 : 28 days microstructure of k600\_1, series 1 (30°C)**

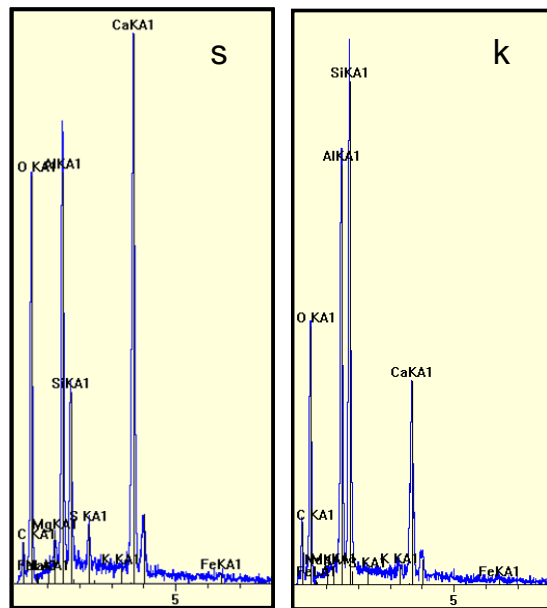
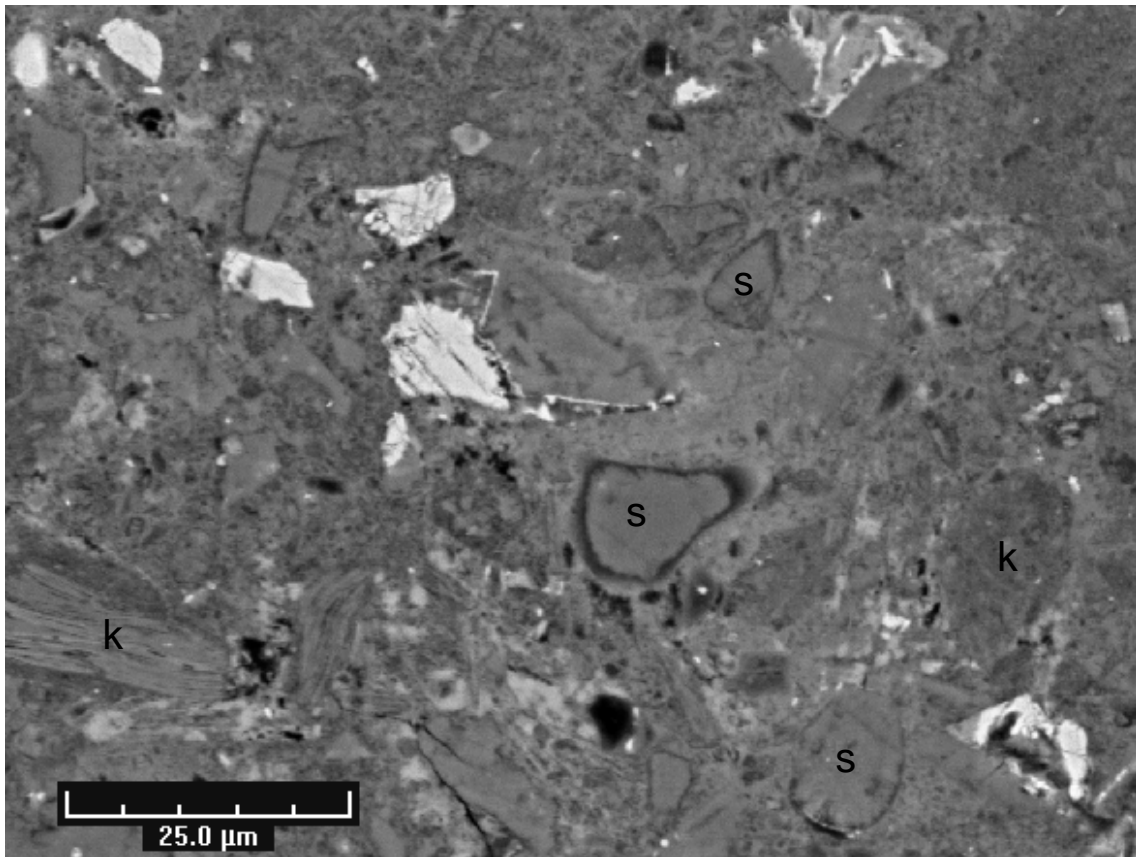


Figure 3-31 : k600\_1 paste at 28 days with EDS spectrum for s: strätlingite, k: calcined kaolinite



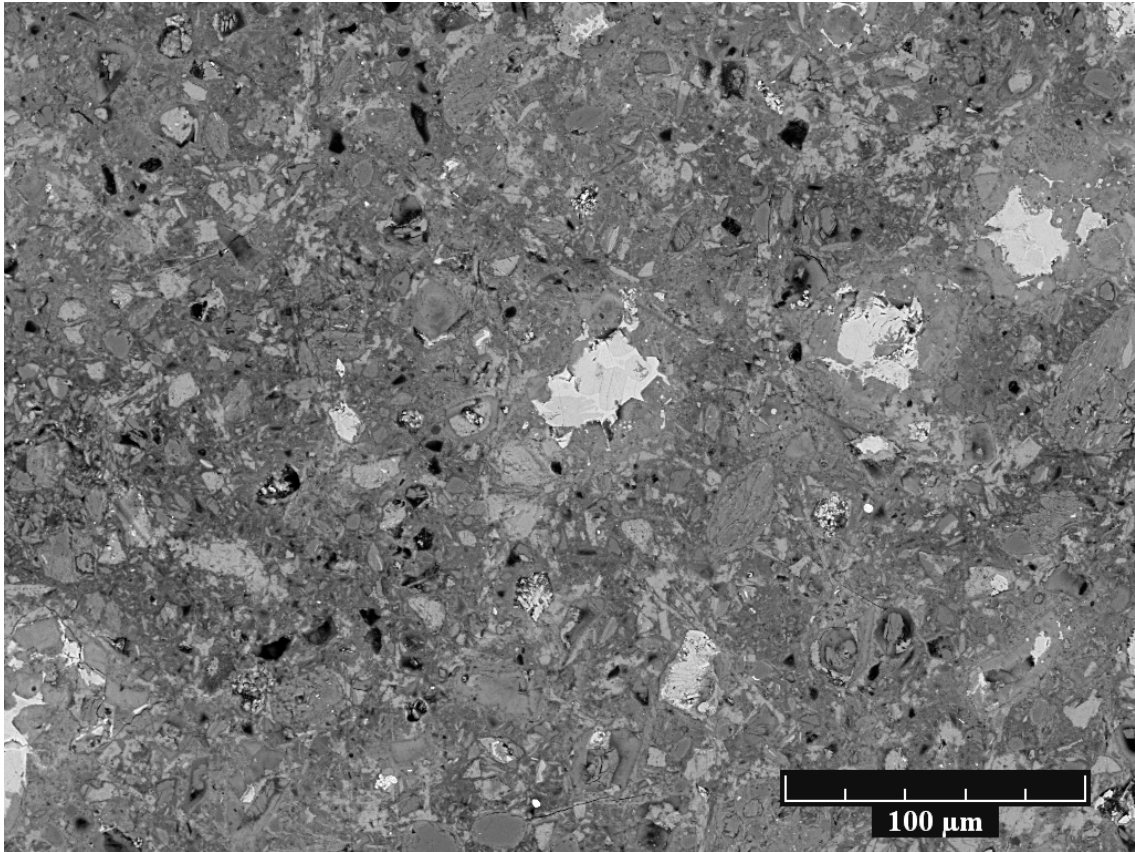


Figure 3-32: 28 days microstructure of i600\_1, series 1 (30°C)

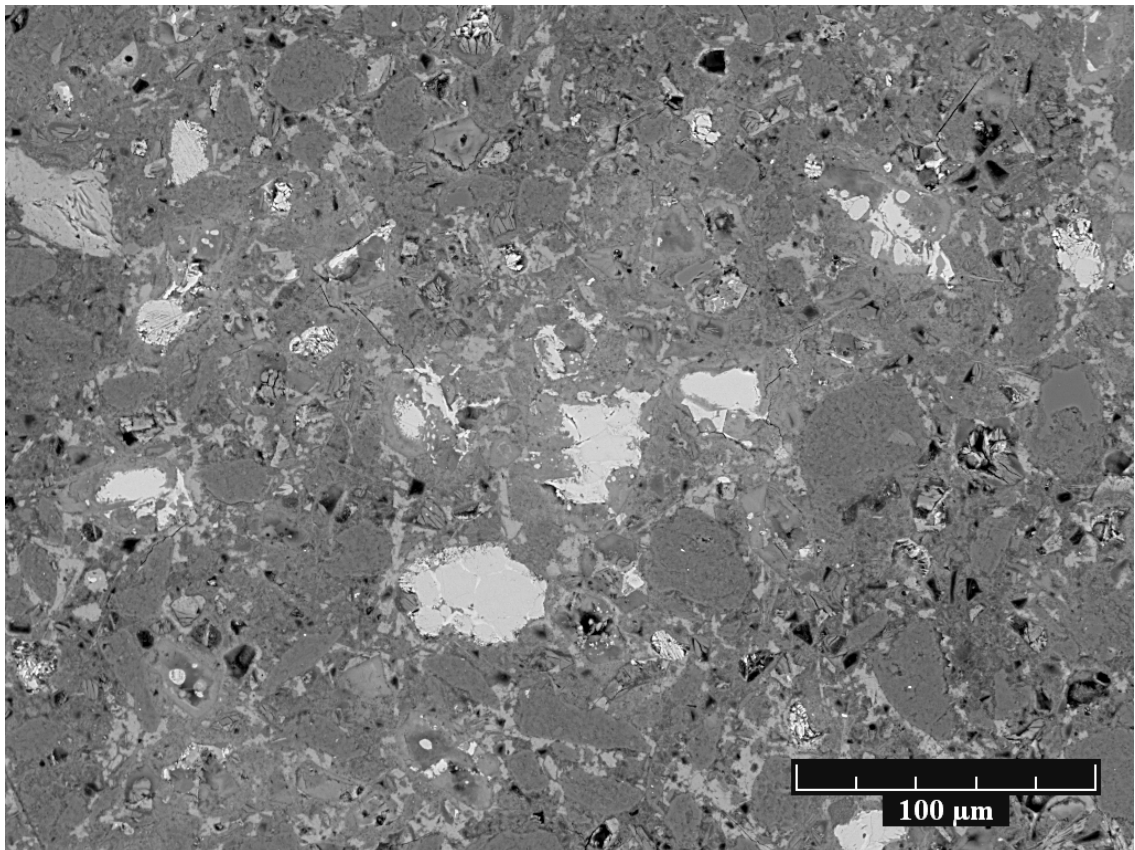


Figure 3-33: 28 days microstructure of m600\_1, series 1 (30°C)



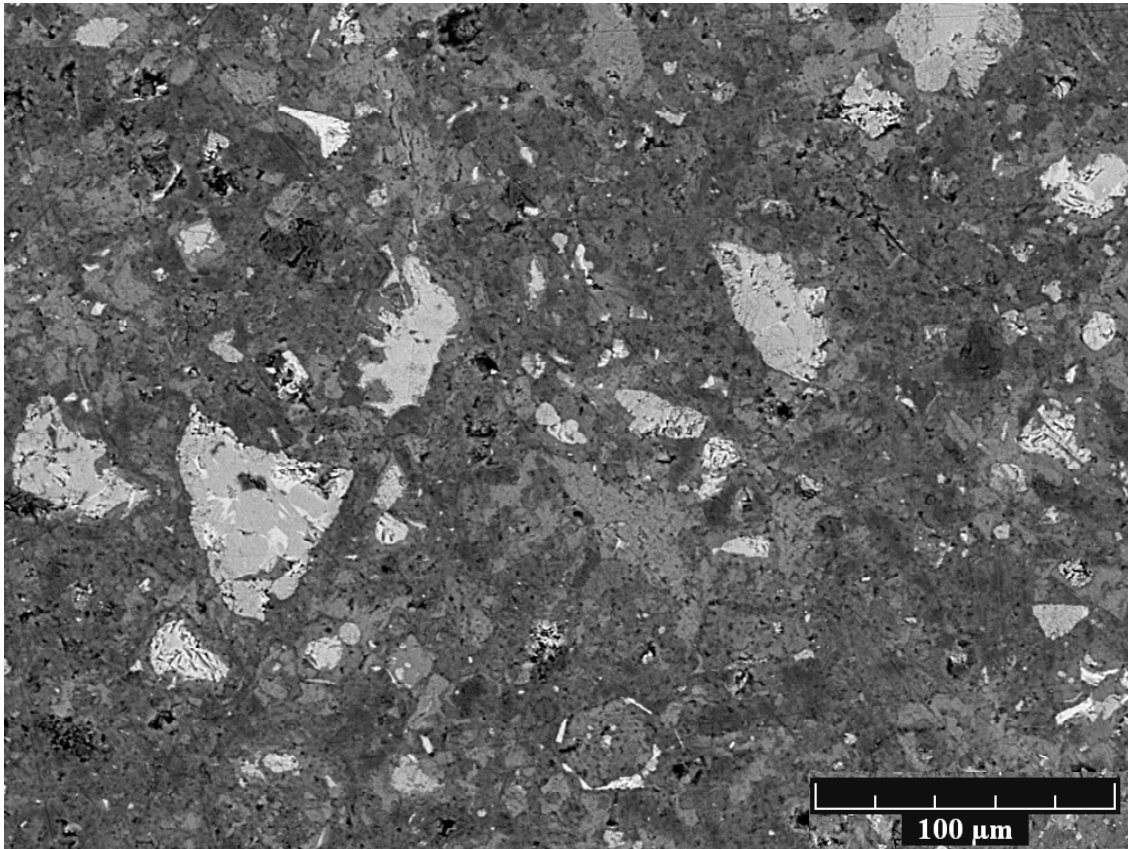


Figure 3-34 : 28 days microstructure of opcA\_4, series 4 (30°C)

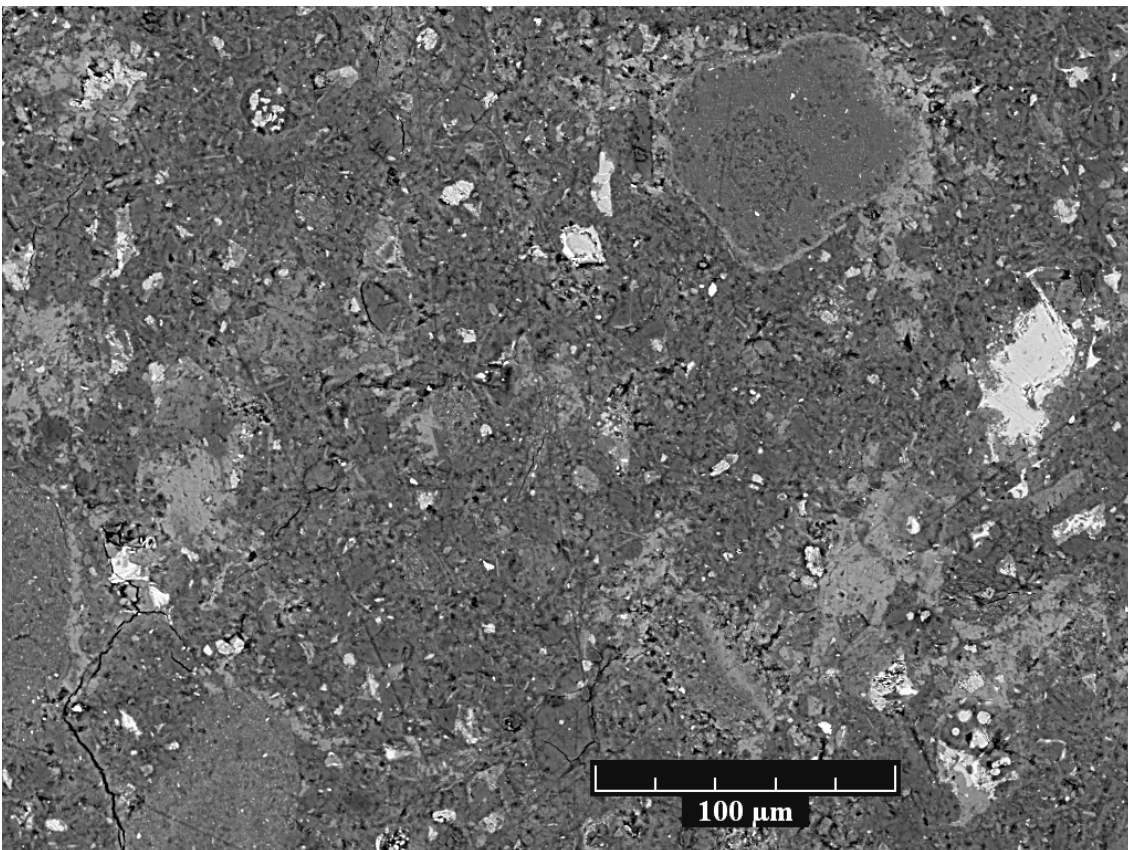


Figure 3-35: 28 days microstructure of cu600\_4, series 4 (30°C)

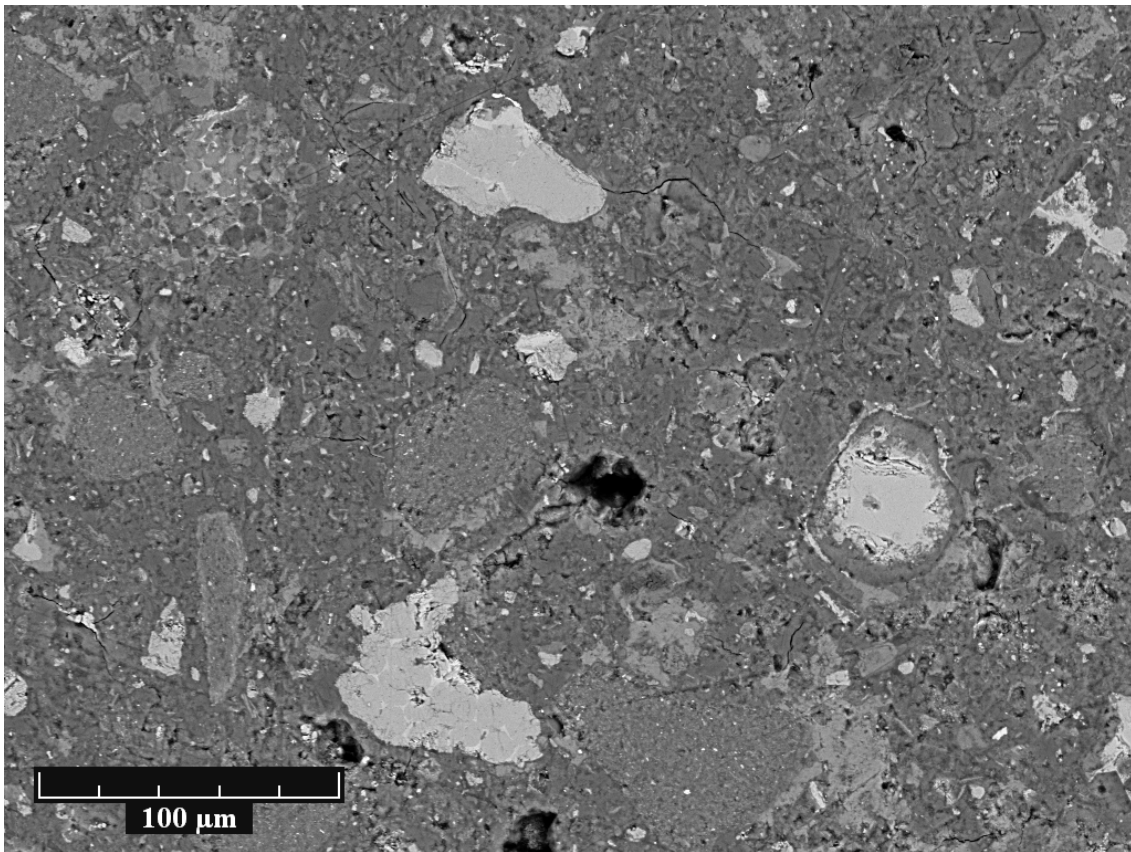


Figure 3-36 : 28 days microstructure of cu800\_4, series 4 (30°C)

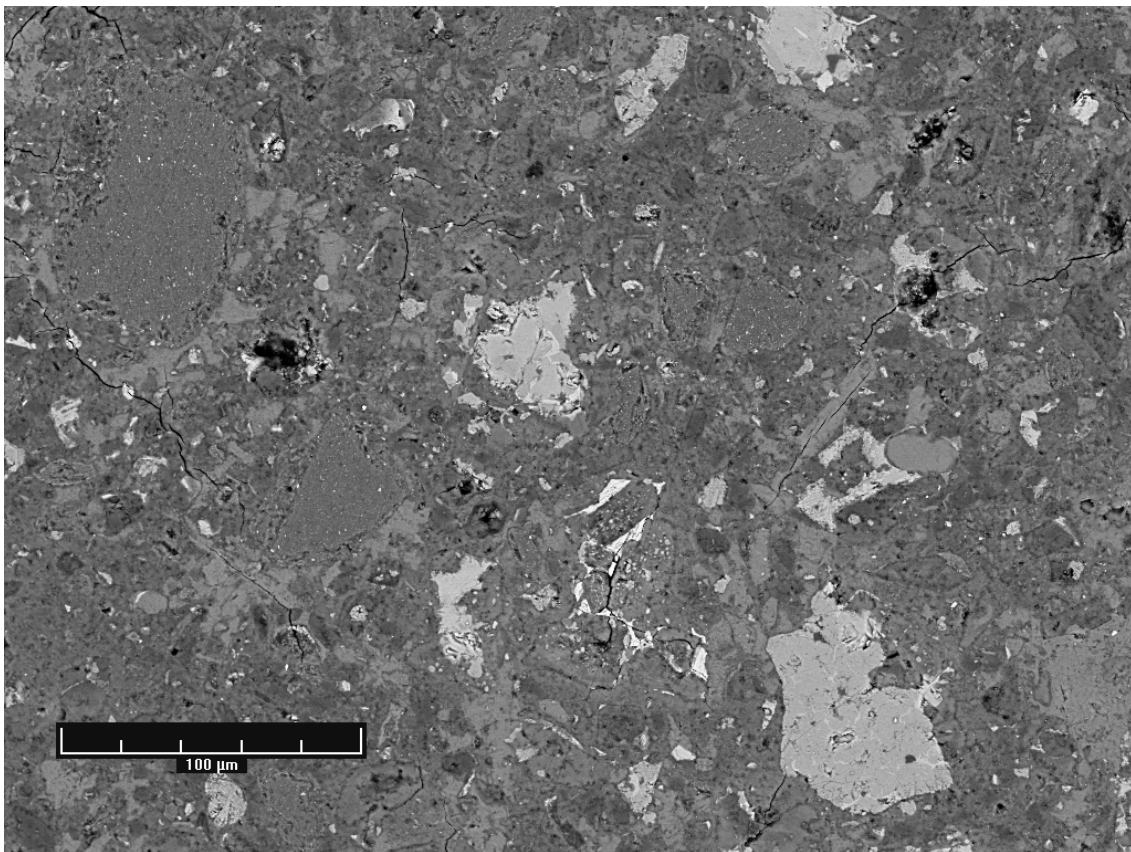


Figure 3-37: 28 days microstructure of cu925\_4, series 4 (30°C)



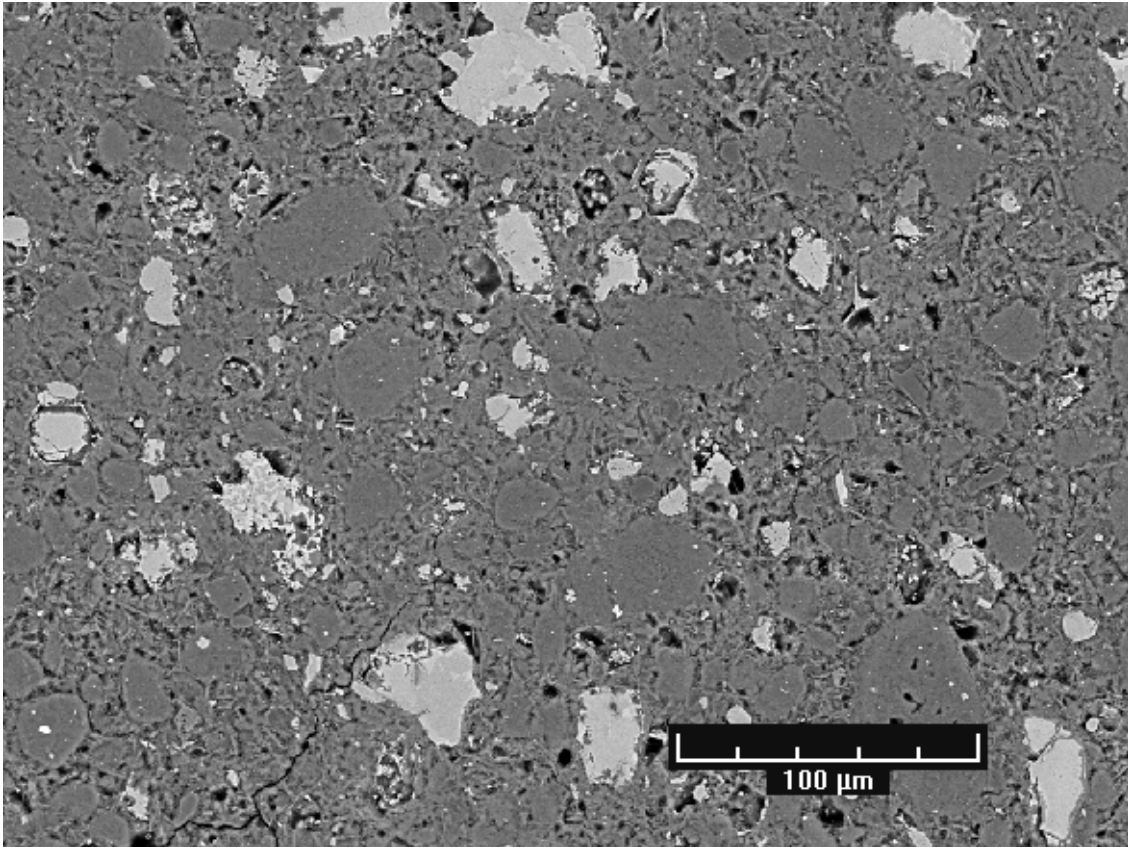


Figure 3-38 : 28 days microstructure of MK\_4, series 4 (30°C)

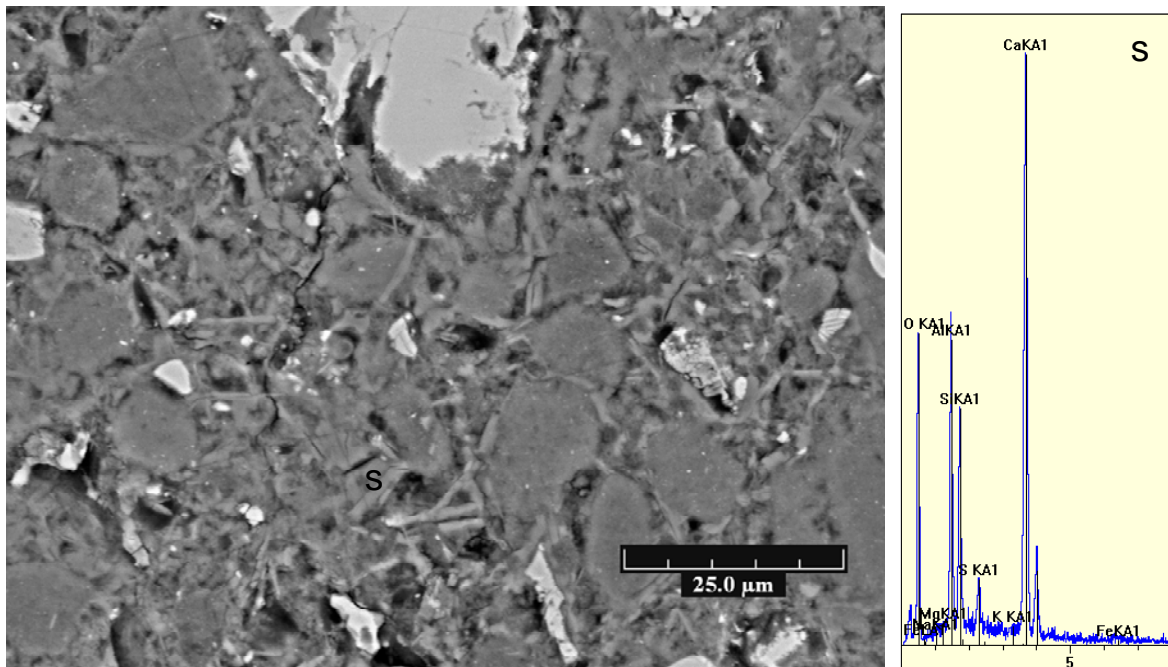
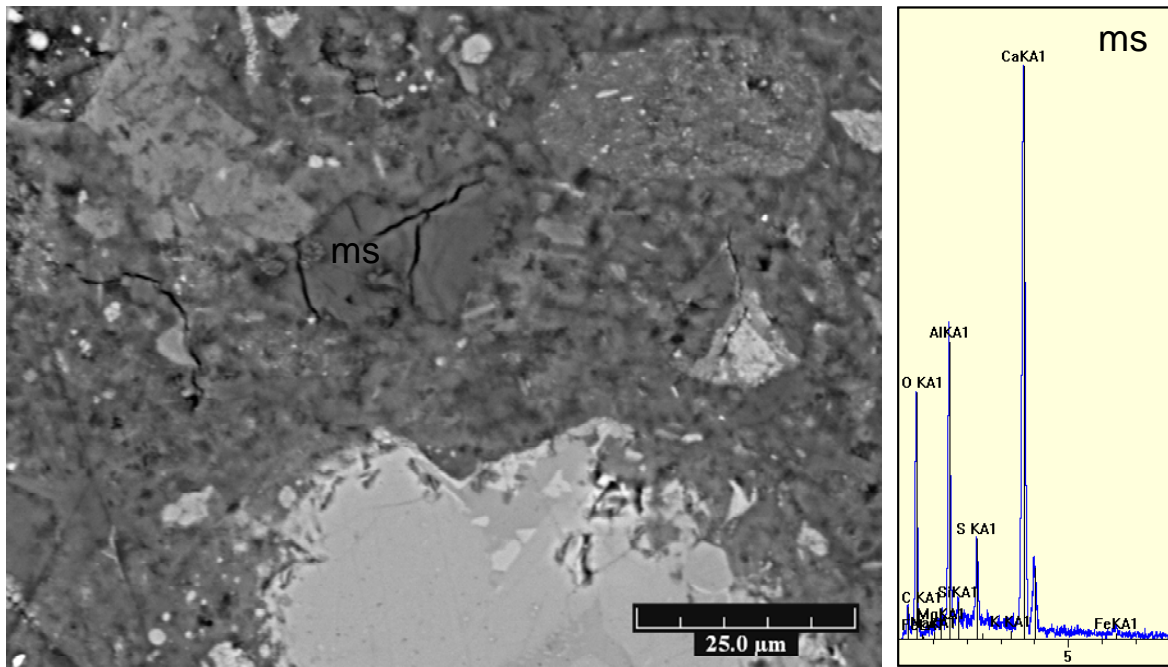


Figure 3-39 : MK\_4 paste at 28 days with EDS spectrum for strätlingite (s)



**Figure 3-40: cu800\_4 paste at 28 days with EDS spectrum for calcium monosulfoaluminate (ms)**

To compare the chemical composition of C-S-H in a pure cement paste with that of a blend of cement and calcined clays, EDX analysis was performed. This analysis focused on series 3 (20°C), comparing the cu600\_3 and cu800\_3 systems with the reference opc\_3 at 14 days. EDX analysis was done systematically on the inner C-S-H (dense layer around cement grains) and on the outer C-S-H (in the matrix away from cement grains). Figure 3-41 and Figure 3-42 show the typical location of the tags where the EDX analysis was done for the inner C-S-H and outer C-S-H respectively. Results are presented in Figure 3-43 to Figure 3-46 for the composition of the inner C-S-H and outer C-S-H systematically. Plots of Al/Ca vs Si/Ca are meant to inform on the variability of composition of the C-S-H, whereas plots of S/Ca vs Al/Ca are more likely to reveal the presence and type of AFt or AFm phases intermixed with the C-S-H.

The first observation is that compositions are much more variable in the outer C-S-H due to the coexistence of various hydrated and anhydrous phases. Each localised EDX analysis gives an averaged composition if the sphere of interaction of the electrons into the sample covers more than one phase. This results in a more scattered distribution of points than on the inner C-S-H.

In blended pastes, C-S-H is richer in aluminium and its Ca/Si ratio is decreased compared to a pure cement paste. The first observation is coherent with  $^{29}\text{Si}$  NMR that indicated a substitution of Al for Si in C-S-H in cu600\_3 (see Figure 3-15). This enrichment in

aluminium is logically more important in the outer C-S-H than in the inner C-S-H, due to the availability of aluminium ions. However, the amount of points located at high Al/Ca and Si/Ca ratios (see Figure 3-44 and Figure 3-46 left) suggest that fine particles of calcined clays were detected that are intermixed with the outer C-S-H. It is also interesting to note that AFm phases were detected in the inner layer of C-S-H for the cu800\_3 system (see Figure 3-45 left). Surprisingly, this was not observed for the cu600\_1 system. Generally speaking, calcined clays favour the formation of AFm phases, as previously reported [61, 62, 74]. AFt was shown to be the main phase intermixed with C-S-H in the pure cement paste at 14 days.

Ca/(Si+Al) and Al/Ca average ratios in C-S-H from EDX analysis are presented in Figure 3-47. They confirm results discussed above by showing how the Ca/(Si+Al) ratios are lowered from around 2 to around 1.5 in blended systems. Important Al/Ca ratios (and error bars) in blended systems indicate that Al content in outer C-S-H is overestimated due to the presence of fine clayey particles simultaneously detected when analysing the cementitious matrix.

Figure 3-48 and Figure 3-49 reports on a phenomenon that was repeatedly observed in the cu600 and cu800 systems but not in the cu925 system, independently of the type of cement used and the curing conditions. It applies for series 2, series 3 and series 4 where calcined Cuban clay was used. An EDX analysis was done on one image at the level of every pixel to see the distribution of the elements in the microstructure. Results on Ca, Si and Al mapping as well as the original picture are presented in Figure 3-48. The distribution of Ca in this microstructure first confirms that portlandite tends to crystallize at the surface of calcined clays (see top and left side of the clayey particle). It also shows that there is a layer within the calcined clay particles that is enriched in Ca, suggesting that these materials are porous and have allowed the ingress of Ca ions in the structure. Al concentrations in this layer are lower than in the centre of the particle, suggesting that it could have dissolved in the cementitious matrix. This phenomenon is certainly not an evidence of the pozzolanic reaction but simply indicates that there is a chemical interaction between the different components of the paste. The morphology of the calcined particle seems to play a major role in the intermixing of Ca ions, as shown in Figure 3-49. It may be possible that the zone where Ca ions could penetrate is actually a layer of small clayey particles that agglomerated to a bigger particle during the calcination process. As they were not seen in non reactive calcined clays, these characteristic features may be associated with reactive particles but more work should be done in this area in order to confirm these assumptions.



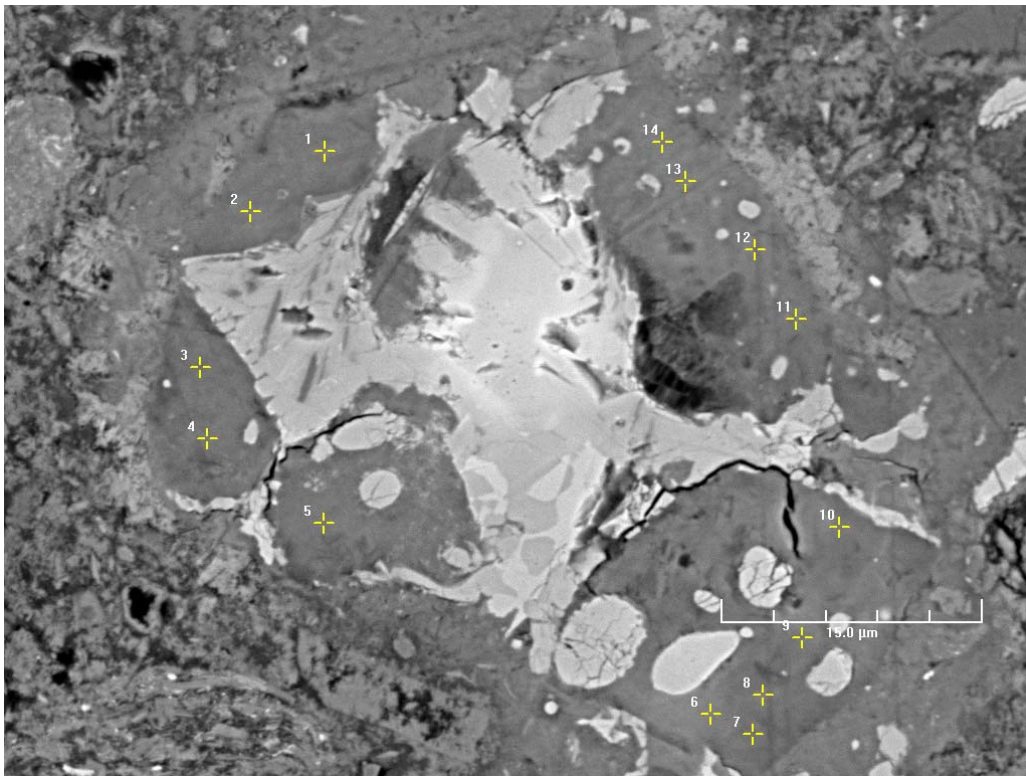


Figure 3-41: Example for the choice of points for EDX analysis on inner C-S-H, (sample cu800\_3, 14 days)

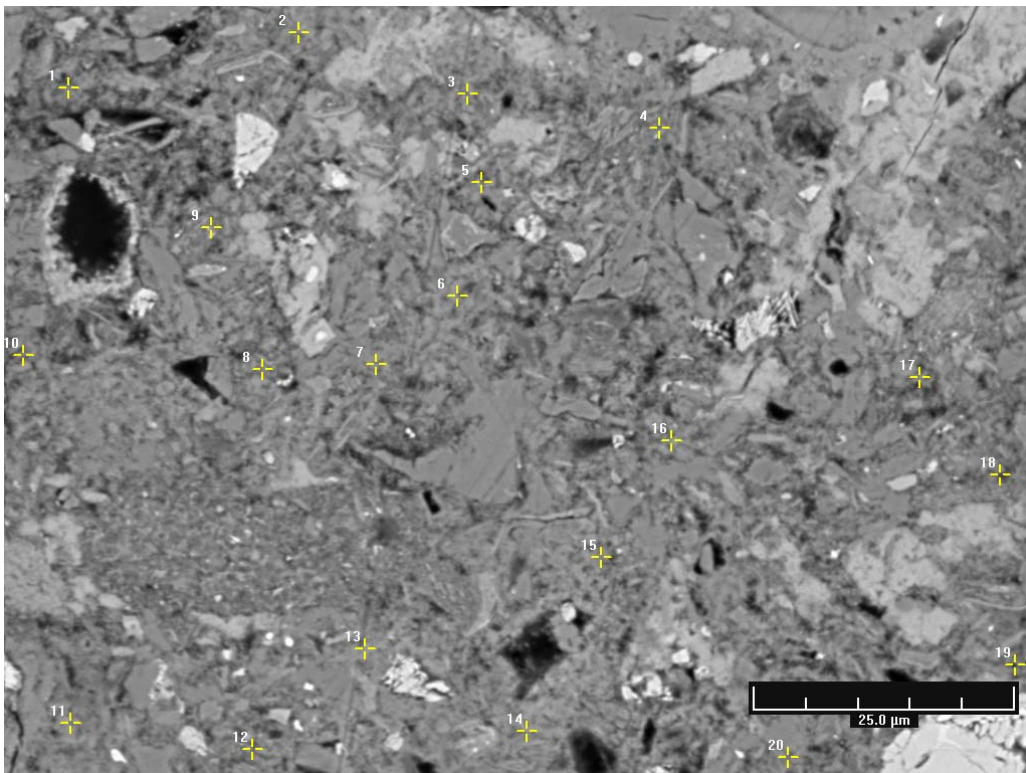


Figure 3-42: Example for the choice of points for EDX analysis on outer C-S-H, (sample cu600\_3, 14 days)

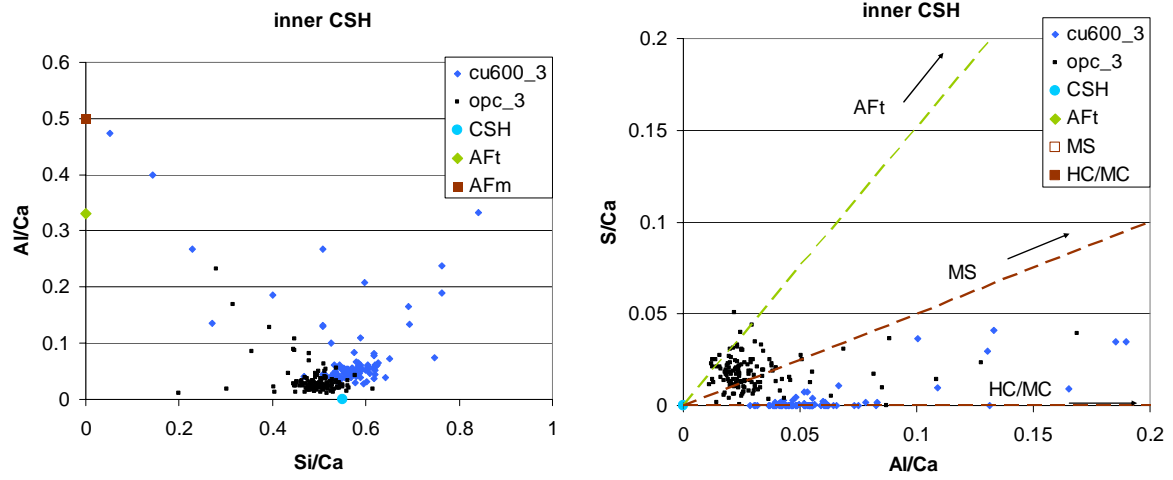


Figure 3-43 : EDS analysis in inner CSH of cu600\_3 and control paste at 14 days (20°C)

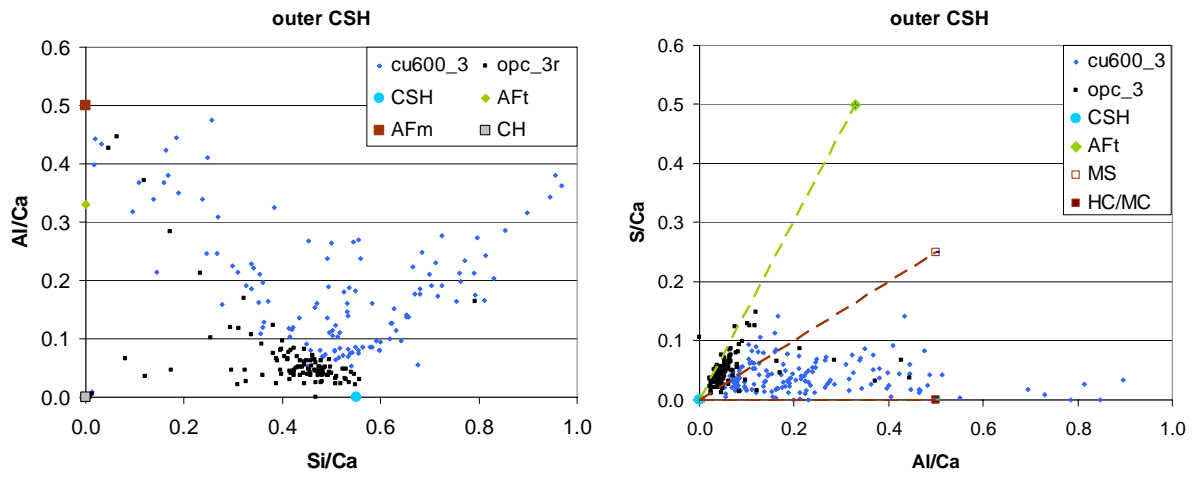


Figure 3-44 : EDS analysis in outer CSH of cu600\_3 and control paste at 14 days (20°C)

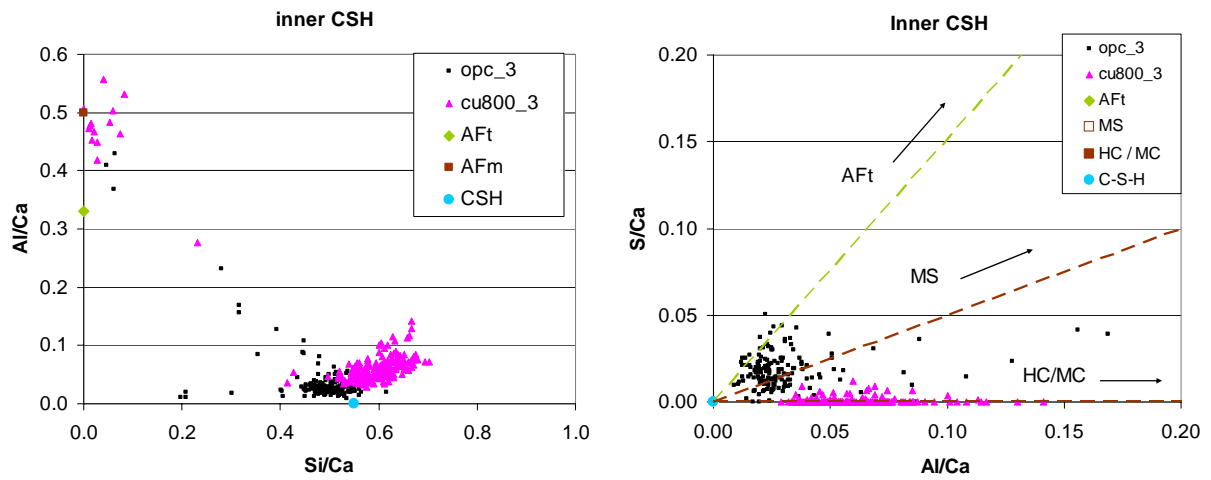


Figure 3-45 : EDS analysis in inner CSH of cu800\_3 and control paste at 14 days (20°C)

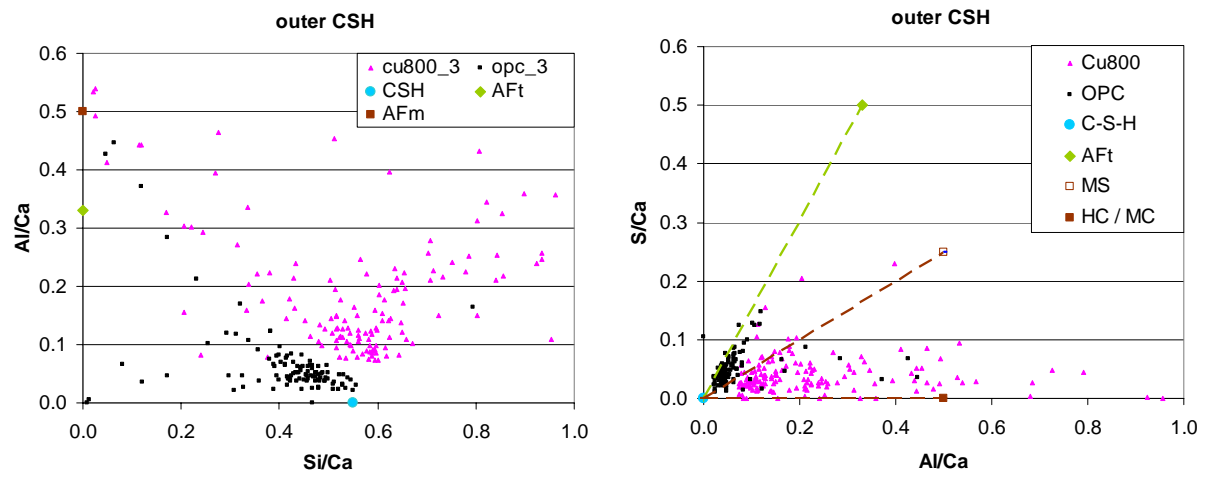


Figure 3-46 : EDS analysis in outer CSH of cu800\_3 and control paste at 14 days (20°C)

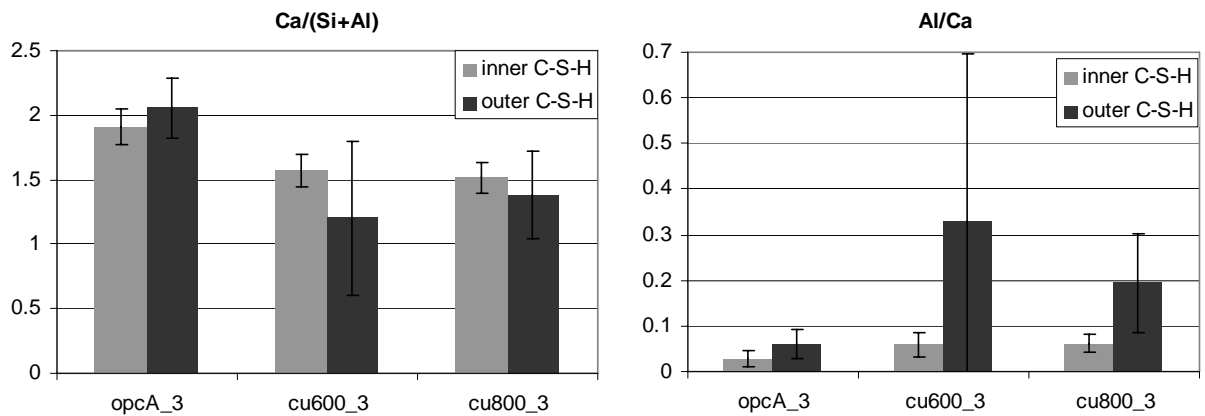


Figure 3-47 : Average Ca/(Si+Al) and Al/Ca ratios for inner and outer C-S-H, series 3, (20°C)



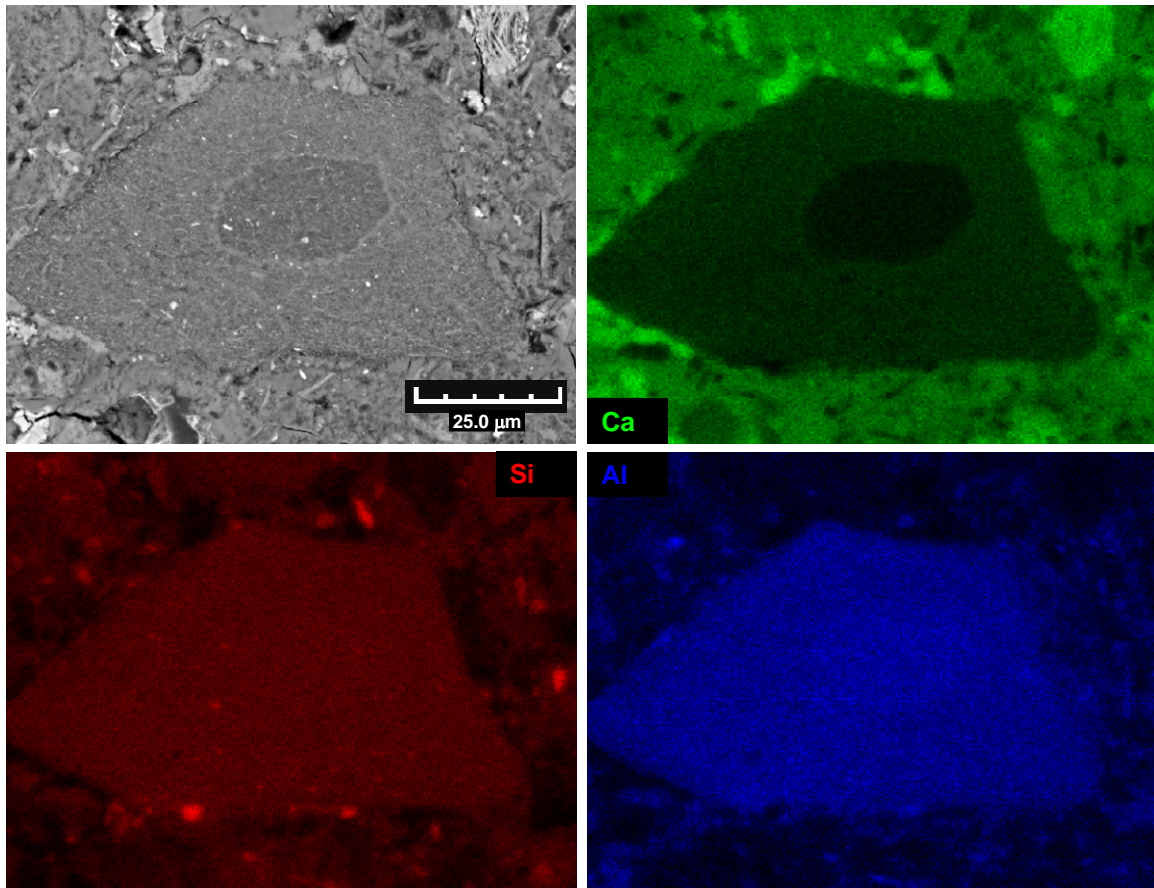


Figure 3-48: Mapping of calcined clay grain in cu800\_3 system at 28 days (20°C)

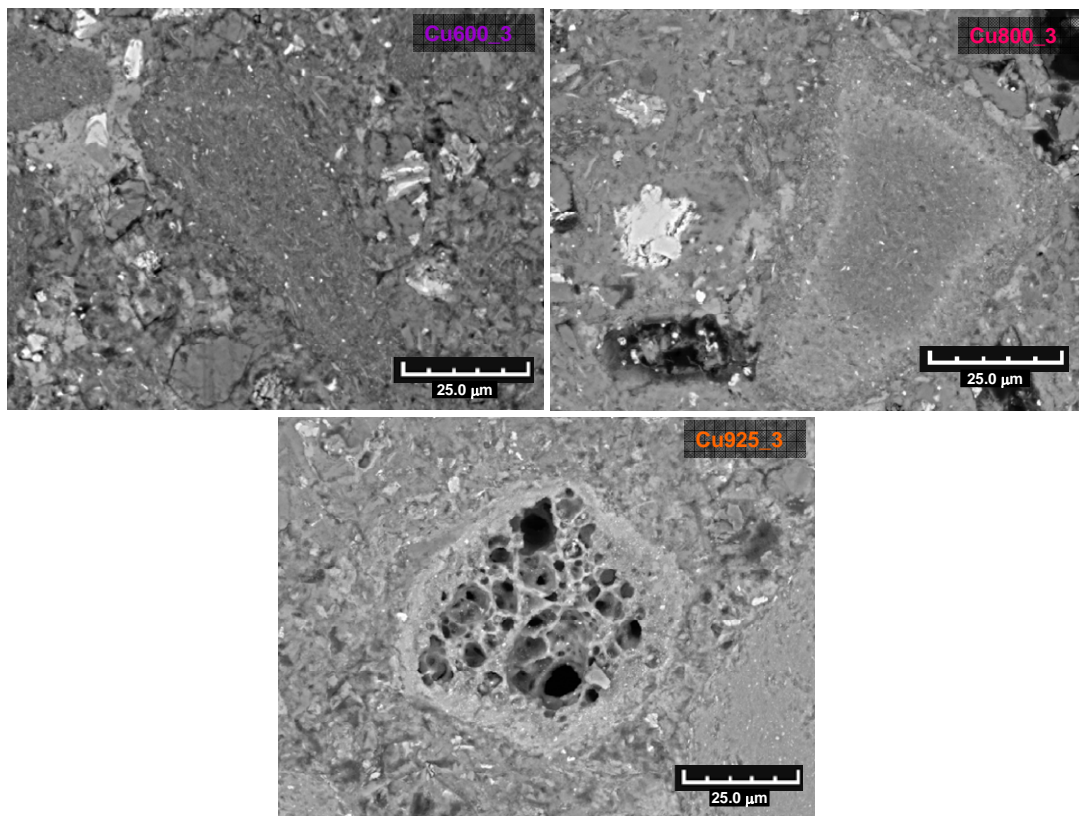


Figure 3-49: Typical calcined clays grains in a 28days microstructure, serie 3 (20°C)



## 4 Mechanical properties and sorptivity of cement-calcined clays mortars

### 4.1 Starting materials and mix designs

The mechanical properties and in particular compressive strength are generally used as a reference for assessing the overall quality of a construction material. This is due to the fact that in the final application they are primarily used for their load-bearing capacities, and also as strength generally correlates well with other properties such as permeability. It was thus important to ensure that the substitution of cement by calcined clays in mortars could still lead to the development of sufficient strength in order to comply with the field requirements. Differences in compressive strengths do not reflect the difference in pozzolanic reactivities alone, as other parameters are known to have a strong influence such as the porosity and the particle size distribution of the constituting materials. The use of microcrystalline quartz as a filler for the substitution of cement in the same proportions as the calcined clays was adopted, as was done in the study of the pastes. This allowed the comparison of samples incorporating the same amount of clinker component. It was assumed that this filler did not interact chemically with cement, and could therefore be considered as an inert material. However, the presence of a filler is associated with various physical phenomena that affect the hydration reaction, as seen in the previous chapter. First, there is an increased space for the hydrated phases to form due to the dilution effect (70% of reactive material in the same volume of 100% reactive material). Second, at early age, the filler provides surface for the hydrates to nucleate and grow. Both phenomena result in an enhancement of the cement hydration compared to a pure cement system without filler. It is assumed that this physical effect is similar for the filler and the calcined clay so the comparison of both systems gives an indication of the chemical role of the calcined clays and thus the pozzolanic reaction.

The formulation of mortars as well as mixing protocol followed Swiss standards SIA 215.001, which is equivalent to the European norm EN 196\_1. Two series of mortars were prepared, as described in Table 4-1. Each batch consisted of 1350 g of standardised sand and 450 of binder and allowed the casting of 3 40 x 40 x 160mm mortar bars. The w/b ratio was set to 0.5. It is meant to reproduce the same workability and hydration conditions as a paste with a w/b ratio of 0.4 due to the fact that in mortars a certain amount of water will be adsorbed at the surface of the aggregates and not be available for hydration. The moulds were kept at 90% relative humidity for 24 hours. Then, the mortar prisms were demoulded and submerged in a water

bath at 30°C until the day of testing. As already mentioned for the study on pastes, this temperature was chosen to better simulate the field conditions in Cuba.

150 x 150 x 150 mm mortar cubes were cast for the capillary sorption test following the same mixing protocol, except that the size of one batch was three times that for the mechanical tests. Cubes were demoulded at 24h and kept in a humidity chamber at 90% relative humidity and 20°C. Due to their size, they could not be placed in a 30°C water bath to replicate the curing conditions of the 40 x 40 x 160 mm mortar bars. A 50 mm-diameter core was drilled in the cubes at each tested curing time. It was cut in three cylinders of equivalent height (45mm) and submerged in isopropanol for a minimum of 30 days. Then, samples were dried in a desiccator for a minimum of 30 days before testing.

serie n°	type of clay	calcination temperature	calcination time	cement used	substitution level	w/b	mortar curing temperature	label
1	kaolinite	600°C	60min	Cem B	30%	0.5	30°C	K600_1
	illite	600°C						I600_1
	montmorillonite	600°C						M600_1
	cuban	600°C						Cu600_1
	cuban	800°C						Cu800_1
	filler				Filler_1			
	opc (reference mortar)				0%			OPC_B
2	cuban	600°C	60min	Cem A	30%	0.5	30°C	Cu600_2
		800°C						Cu800_2
		925°C						Cu925_2
	MK	-	-					MK_2
	filler							Filler_2
	opc (reference mortar)				0%			OPC_A

**Table 4-1 : Formulation of cement-calcined clays mortars**

	Properties assessed			
	Compressive Strength	Degree of Hydration at 28days	Capillary porosity	Sorptivity
technique / protocol	SIA 215.001 (EN 196-1)	SEM-IA	SIA 262/1	SIA 262/1
serie 1	x	x	x	x
serie 2	x	x	-	-

**Table 4-2 : Assessed mortar properties**

The properties assessed for the mortars are shown in Table 4-2. The determination of the degree of hydration was done by image analysis and followed the sequence of operation described in section 3.3.1 for pastes, with the difference that grey level segmentation also

discriminated the quartz aggregates from the rest of the phases. The degree of hydration of the clinker component could thus be measured relative to the volume of paste and not by volume of sample, allowing the comparison of the degree of hydration in a cement paste and its corresponding mortar.

The capillary porosity was obtained by the difference of weights between the water saturated samples and the dry sample divided by the volume of solids. More details on this method can be found in the appendix VI. For the determination of sorptivity, the dry mortar cylinders were weighed and then submerged in 3mm of water to observe their water absorption properties. The samples were weighed every 10min for the first hour, every 20min for the second hour, every 30min for the third and fourth hour and then every hour until 8h with one last measurement at 24h. Up to saturation, it has been found that there is a linear relationship between the water absorption and the square root of time [71]. Considering that all tested samples had the same volume and the same area exposed to water, the slope of this linear fit is a direct measurement of the sorptivity of the samples. Details for the determination of capillary porosity as well as sorptivity can be found in the Swiss norm SIA 262/1.

#### **4.2 Assessment of mechanical performances and degree of hydration**

The compressive strength as well as degree of hydration for mortars incorporating standard calcined clays is presented in Figure 4-1. Cuban clay systems are compared to the standard kaolinite in Figure 4-2 and the reactive metakaolin in Figure 4-3 . Comparing the blended systems with the curve of the filler gives a better indication when it comes to assess the contribution to strength brought by the chemical activity of the pozzolan, similarly to the methodology used for isothermal calorimetry on pastes (see section 3.4.3).

The lower strength observed for systems I600 M600 and Filler in Figure 4-1 was partly compensated by the higher degree of hydration of the clinker component. This result is coherent with that of TGA and XRD on pastes presented in section 3.4.1 indicating that illite behaves like an inert filler and montmorillonite exhibits little pozzolanic activity. Note that the late reaction of calcined montmorillonite seen by TGA in pastes does not seem to play much role in the development of the compressive strength between 28 and 90 days, although still noticeable. On the contrary, substitution of cement by calcined kaolinite resulted in a considerable increase in strength from 7 days compared to the control mortar. This increase is explained by the pozzolanic character of the calcined clay that combines CH to form additional C-S-H, filling more space and thus increasing the mechanical properties. In

addition there is an enhanced hydration of Portland cement due to the filler effect. That being said, the increase in degree of hydration by the presence of an inert filler does not induce an amount of hydration products equivalent to that of the 30% of the cement that was substituted, as illustrated in Figure 4-1 when comparing the filler curve with the control.

In Figure 4-2 the influence of the reactivity of a pozzolan on compressive strength can be observed while comparing two systems with Cuban calcined clays with that of the standard calcined kaolin. With half of the kaolinite content of the latter (39% against 76%), the Cuban clays contribute substantially to the strength development of the mortars. Values of strength for the Cu800 system are comparable to the control, whereas those of the Cu600 system are slightly lower. It is interesting to see that from 7 days the evolution of strength is very similar in the Cu600 and Cu800 system, showing the importance of early age reactions in defining the ultimate strength of the material. The increase in strength between 1 and 7 days, also detected for the K600 mortar, must be related to the amount of reactive material that was generated by thermal activation. Indeed, it can not be explained by the specific surface nor by the distribution of particles of the calcined clays, as these properties should favour the reaction of the Cuban clay calcined at 600°C (see properties of calcined clays on Table 3-11).

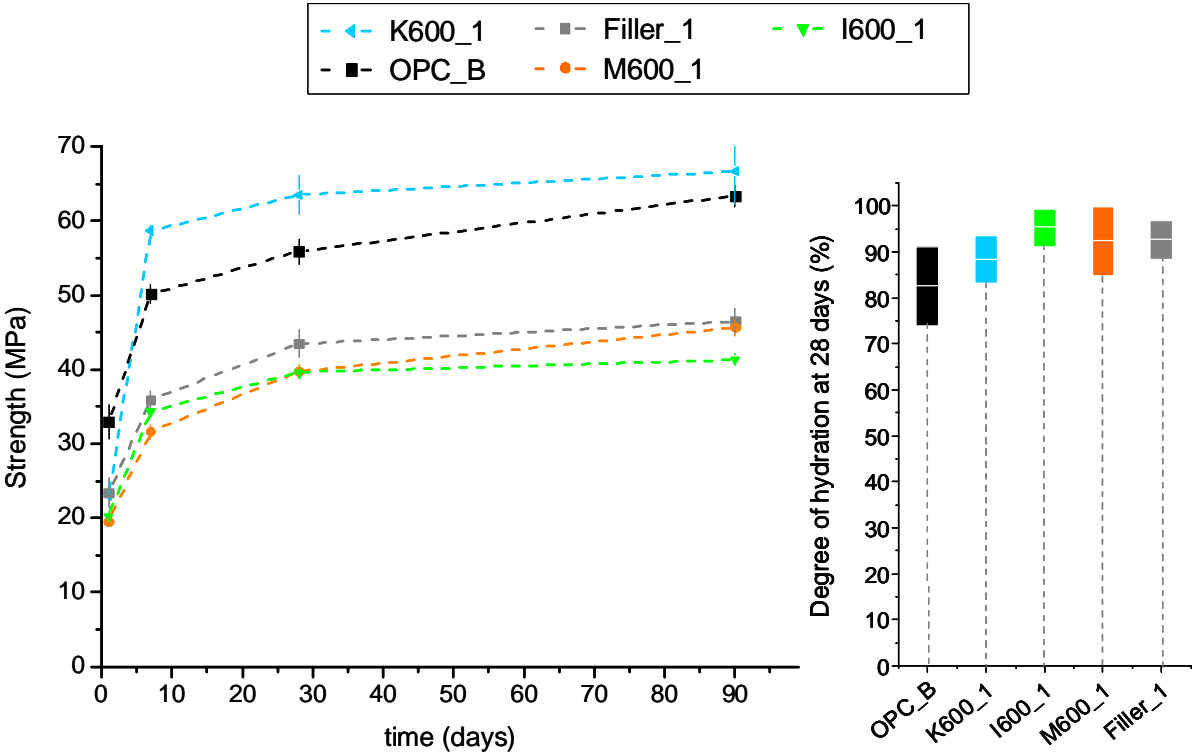


Figure 4-1 : Compressive strength and degree of hydration for standard calcined clays, series 1 (30°C)

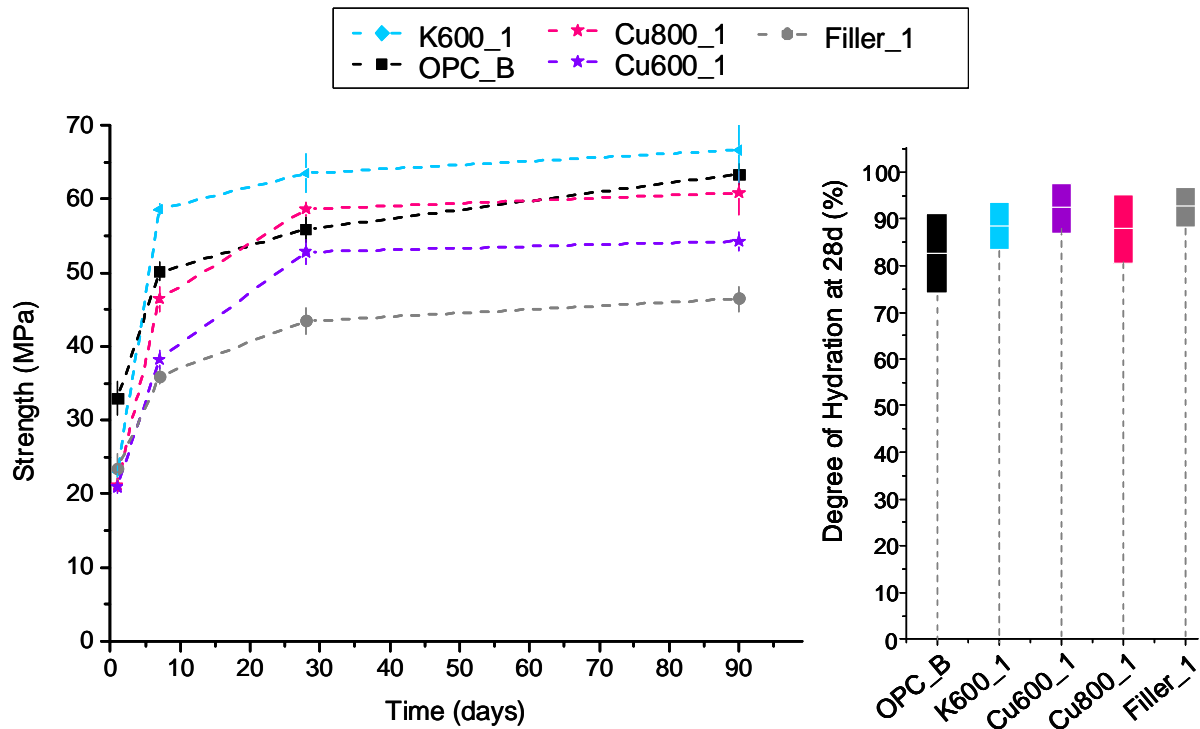


Figure 4-2 : Compressive strength and degree of hydration for kaolin-based calcined clays, series 1 (30°C)

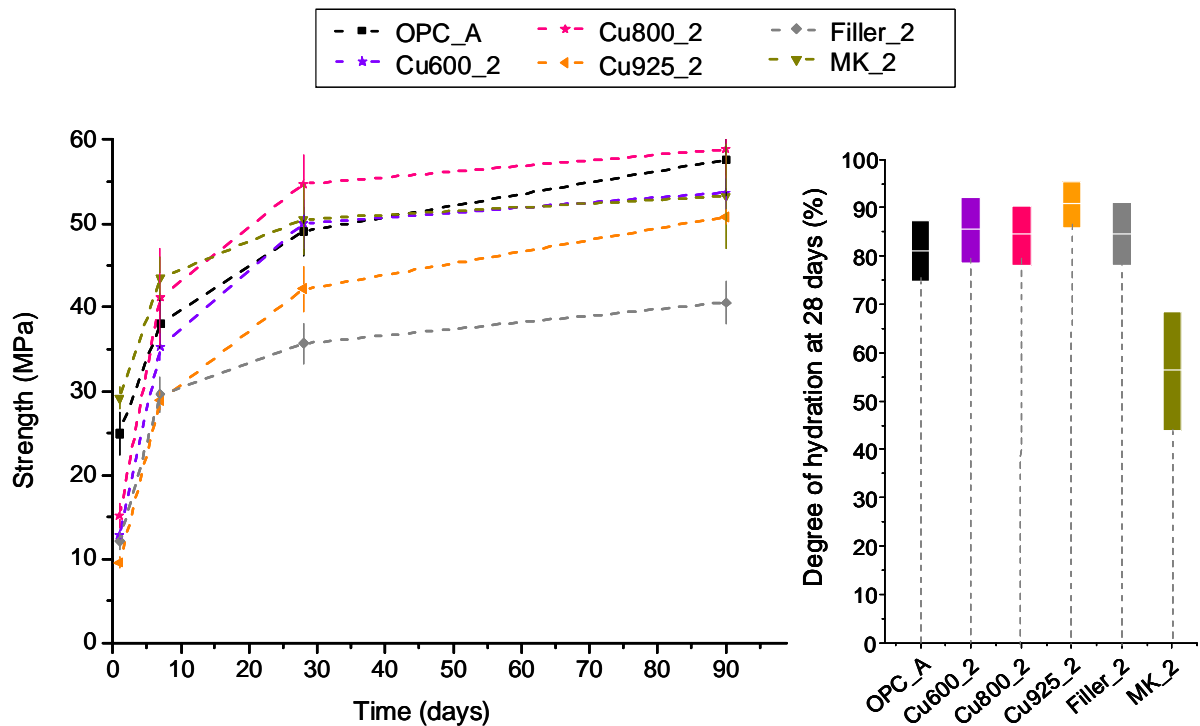


Figure 4-3 : Compressive strength and degree of hydration for series 2 (30°C)

Figure 4-3 shows that The MK system has a different strength evolution than the Cuban clays systems, with values at 1 day exceeding that of the control. This result can be explained by the rapid and substantial reaction of the aluminates to form AFm phases due to the

undersulfation that was observed with isothermal calorimetry on pastes. The SEM image presented in Figure 3-39 confirmed the presence of such platelet-like hydrates that seemed to be evenly distributed throughout the microstructure linking particles together. However, from 7 days, the increase in strength is not as significant as the other pozzolans and values at 90 days are below that of the control and the Cu800\_1 system. The very low degree of hydration of cement for the MK\_1 system presented in the same figure explains this slow rate of strength development at later ages. The low degree of reaction of the cement was also observed in isothermal calorimetry when comparing the peak corresponding to the reaction of the silicates in the MK system with that of the systems where sulphate content was properly adjusted (see Figure 3-16 and Figure 3-17). Nevertheless, with only around 55 % of degree of hydration compared to 85 % for the other blended systems, the pozzolanic activity of the MK must have been very significant to give to the mortar the observed strength.

The effect of calcination temperature of the Cuban clay on the mechanical properties of mortars was also studied as shown in Figure 4-3. In agreement with the reactivity assessment on pastes and compressive strength for series 1 in Figure 4-2, the Cuban clay calcined at 800°C contributes significantly to the strength increase to exceed values of the control from 7 days. As already observed above, the evolution of strength between Cu800\_2 and Cu600\_2 is very similar from 7 days, suggesting that it is the quantity of reactive material rather than the mechanisms of reaction that induces the early differences in strength. The same interpretation could apply for the Cu925\_2 system, which showed to have the least amounts of reactive products.

Another important point to retain from all mechanical results except the MK system is that strength at 1 day for all blended systems is considerably lower than the control, representing a major limitation when considering field applications. This is due to the fact that the amount of hydration products formed through pozzolanic reaction did not yet compensate for the dilution effect. Hence, as the strength values are similar to the filler system, it can be concluded that not much pozzolanic activity is found in the first 24 hours. This correlates well with the results of chemical activity on pastes assessed by isothermal calorimetry and chemical shrinkage on Figure 3-13, Figure 3-18 and Figure 3-20, showing that the moment when the pozzolanic activity was becoming significant was systematically between 1 and 7 days.



To compare the different mortar series where different OPC's were used, the results are summarised in Figure 4-4 and Figure 4-5 in the form of columns representing strength. On the first graph, the strength values of the series are normalised by that of their respective control mortar, OPC A and OPC B. It allows a direct comparison of the strength brought by the addition of pozzolan for mortars that were prepared with different cements. Only kaolinite-rich systems reached similar value to the 100% OPC, emphasising the importance of the nature of the clay for obtaining a reactive pozzolan through firing. The use of reactive calcined clays seems to be more effective in enhancing mechanical properties of mortars based on the CEM A (series 2) as opposed to the CEM B (series 1). This is simply due to the fact that CEM B has considerably higher amounts of alite and is also finer than CEM A (see section 3.3.2 on the characteristics of starting materials). As a consequence the contribution to strength brought by the pozzolanic reaction relative to that of CEM B is smaller than the contribution relative to that of CEM A. Note that this comment does not apply for the strength at one day (except for MK that has been shown to behave differently than the other pozzolans), simply because in the first 24 hours this value is dominated by the reaction of hydration due to the fact that pozzolanic activity becomes significant only after one day.

The second figure is more indicative of the strength that was generated in addition to the 70% of the cement included in the filler system. All values above 100% can be interpreted as the contribution to strength brought about by the pozzolanic reaction. It is interesting to note that the strength evolution of the reactive systems above 100% seems to follow the estimated heat developed by the pozzolanic reaction by isothermal calorimetry, as shown in Figure 4-6, suggesting that influence of pozzolans on mechanical properties could be related the total heat released by the pozzolanic reaction.

As an attempt to correlate the strength results due to the pozzolanic reaction with the CH content monitored by TGA, the strength values (relative to the filler) were plotted against the CH consumed (% CH in the blended systems relative to the % CH in the opc pastes). By looking at Figure 4-7, there seems to be a relationship between the pozzolanic activity and its contribution to compressive strength of the mortars for the first 28 days. Values at 90 days suggest that the calcined clays would still be reacting but without having much influence on the compressive strength. It should be mentioned that systems based on different cements were compared in this graph that could partly explain the deviations observed.

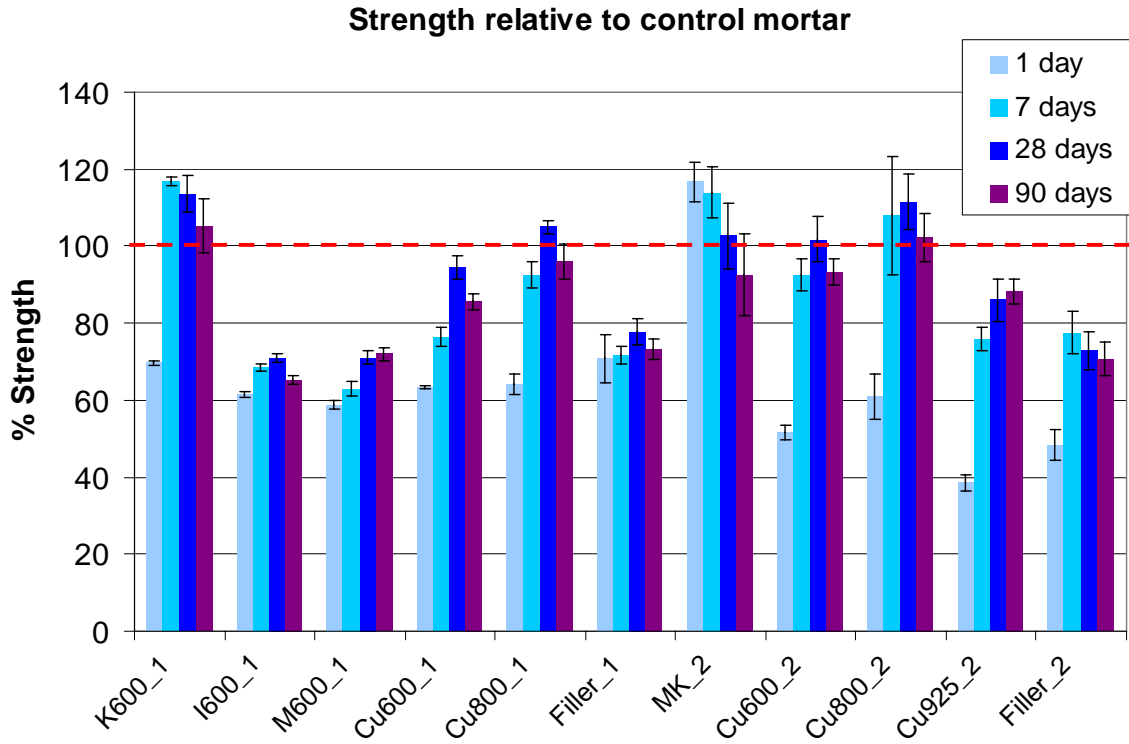


Figure 4-4 : Strength relative to control mortar for series 1 and 2

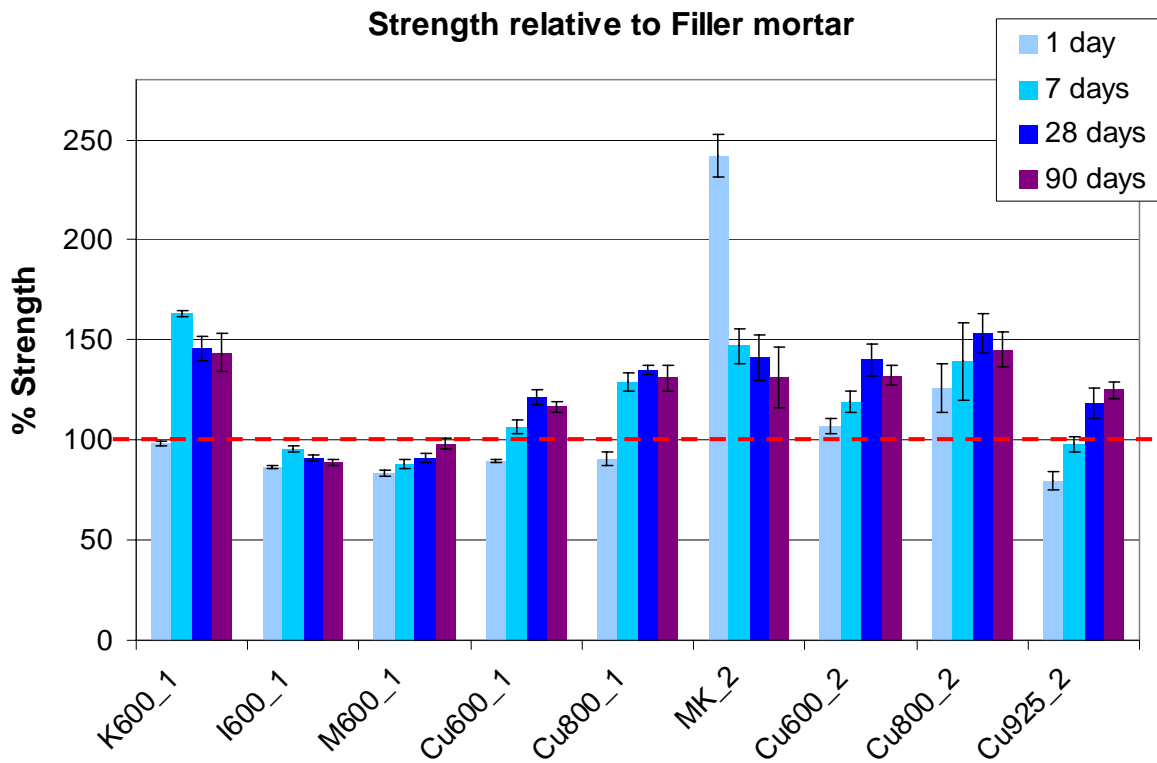


Figure 4-5 : Strength relative to filler system for series 1 and 2

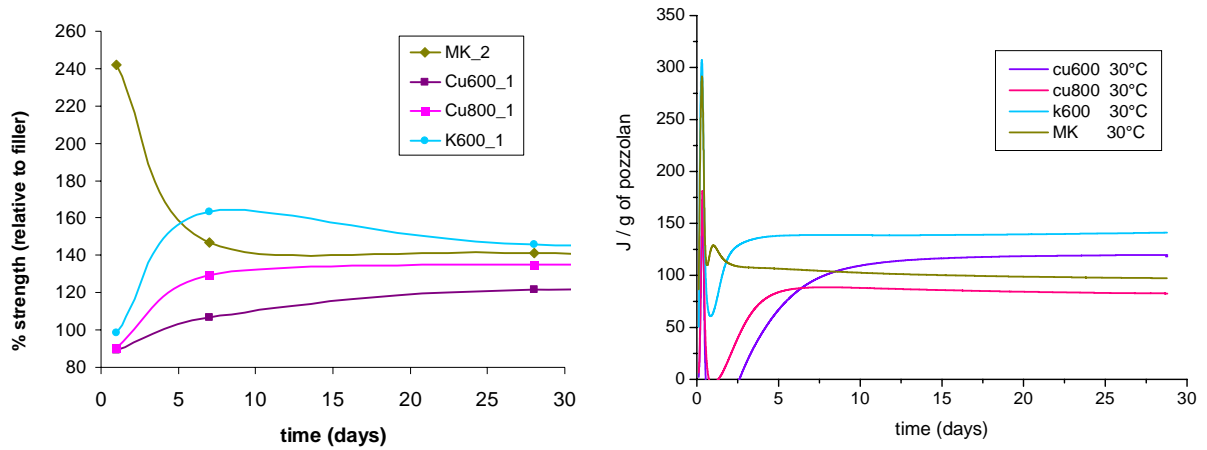


Figure 4-6: Comparison of strength profiles with heat of pozzolanic reaction by isothermal calorimetry

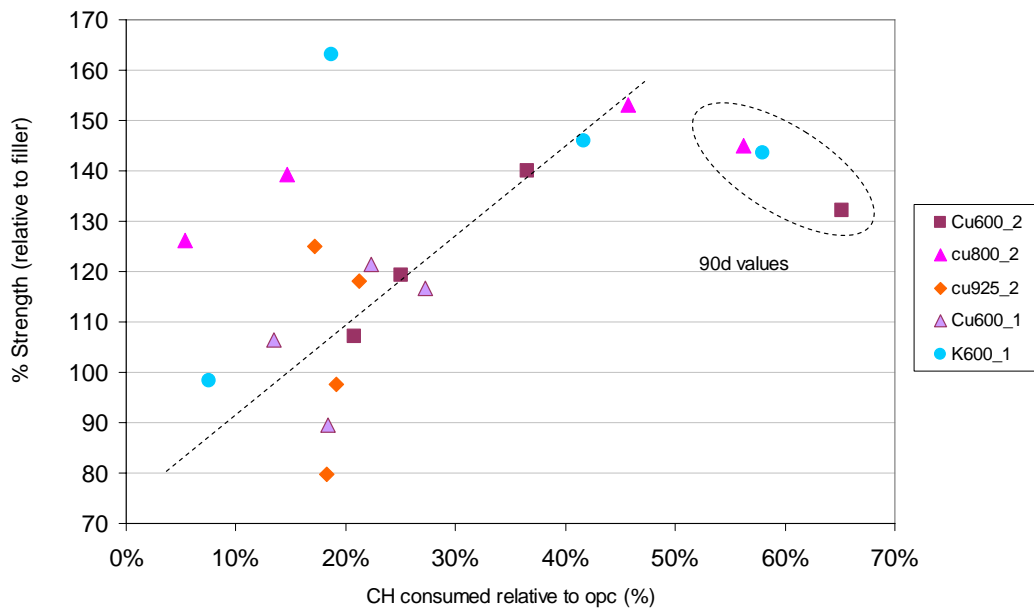


Figure 4-7: Correlation between strength increase and CH consumed in the pozzolanic systems

To conclude on this section, it is reasonable to say that the reactivity assessment on pastes could to a good extent predict the results of compressive strength, with the exception of systems that alter the cement hydration process such as MK. From 7 days, the amount of hydrates formed through the pozzolanic reaction compensate for the dilution effect brought by the substitution of cement. This was clearly observed in K600\_1, Cu800\_1, Cu600\_2 and Cu800\_2 systems, and to a lesser extent in Cu600\_1. As for calcined illite and montmorillonite, no clear sign of pozzolanic activity was observed, apart from a slight increase in strength for the M600\_1 system between 28 and 90 days.

### 4.3 Capillary sorption

Results of capillary porosity are presented in Figure 4-8. It is first interesting to see that compared to the OPC mortar, non reactive clays and the inert filler increase the capillary porosity. On the contrary, kaolin-rich clays are effective in reducing the capillary porosity even from early ages. The generally accepted idea that compressive strength is highly dependent on porosity is here confirmed as the evolution of porosity is inversely proportional to the strength in Figure 4-1 and Figure 4-2. However, this correlation does not apply at one day, suggesting that at early ages other parameters dominate over the porosity to define strength.

Sorptivity results are presented in two graphs, one showing the water absorption in the first 8 hours of testing for all samples at several curing times (Figure 4-9), and the other showing the evolution of sorptivity with age of the specimen (Figure 4-10). Results shown in these figures represent an average of 3 measurements of water absorption performed on 3 mortar replicas.

The curves in the first figure show logically a decrease of the water absorption for all specimens with ageing, indicating a densification of the microstructure due to the formation of hydrates. Values of sorptivity in Figure 4-10 graph allow the comparison of the different samples and the influence of ageing simultaneously. Non-reactive pozzolans show a very low performance in this test with values above those of the inert filler. System incorporating calcined montmorillonite shows however a considerable decrease of the sorptivity between 28 and 90 days that is very consistent with values of compressive strength. The system Cu600\_1 has a very similar behaviour to the reference OPC mortar, whereas systems Cu800 and K600 reduce considerably the values of sorptivity from early ages, suggesting that additional hydration products were formed through the pozzolanic reaction.

An increase in the values of sorptivity from 3 to 7 days could be observed in most of the samples. This was rather unexpected but could be attributed to the refinement of the porosity due to the important chemical activity in this time interval. At very early ages the size of pores would be too large to allow capillary rise, whereas at 7 days the increase in volume of hydrated phases could facilitate the water absorption. After 7 days, further refinement probably leads to the decrease of the connectivity and the general resulting trend is a decrease of the sorptivity.

In the point of view of durability, the results indicate that reactive pozzolans in substitution for cement in concrete could perform very well due to the reduction of the capillary porosity and consequently the sorptivity of the samples. The resistance to aggressive environments such as chlorides or sulphates has not been studied here to confirm the above assumptions but these tests should definitely be considered in some future work.

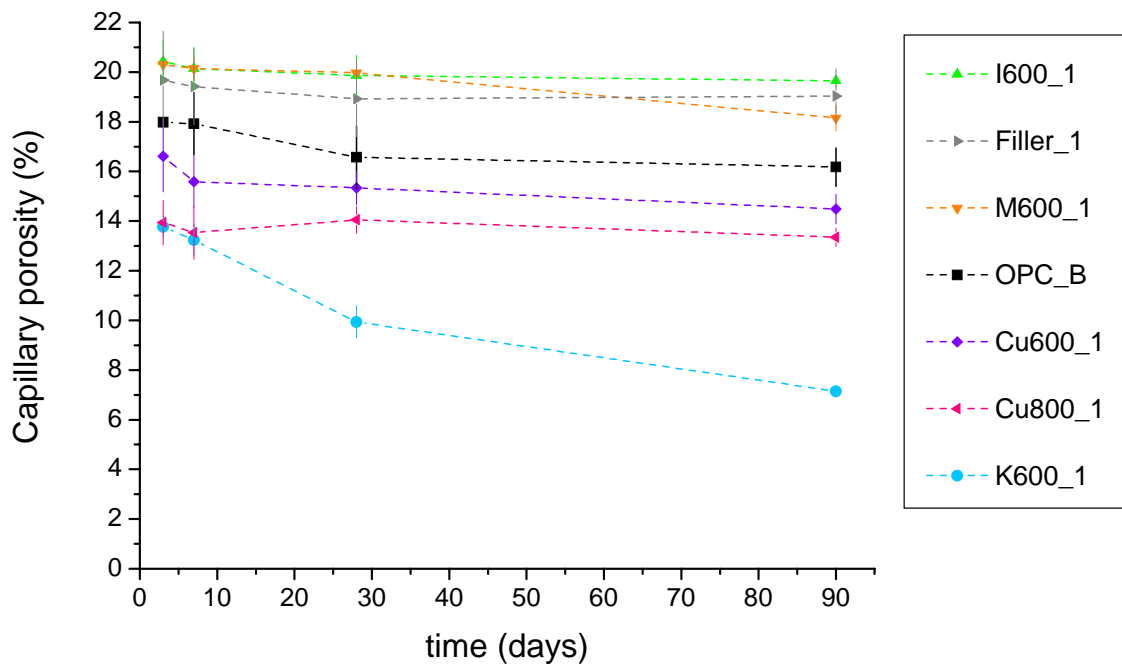


Figure 4-8 : Capillary porosity for series 1 (30°C)

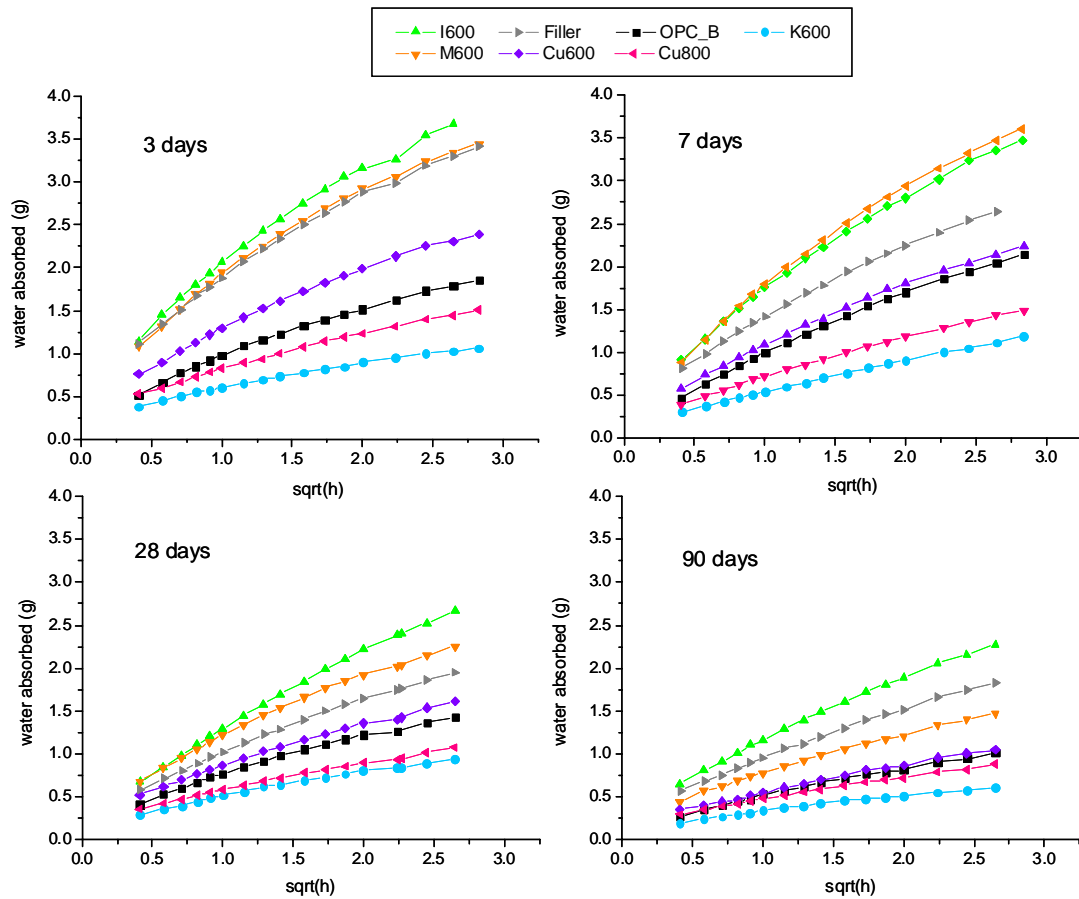


Figure 4-9 : Water absorption for the first 8 hours, series 1 (30°C)

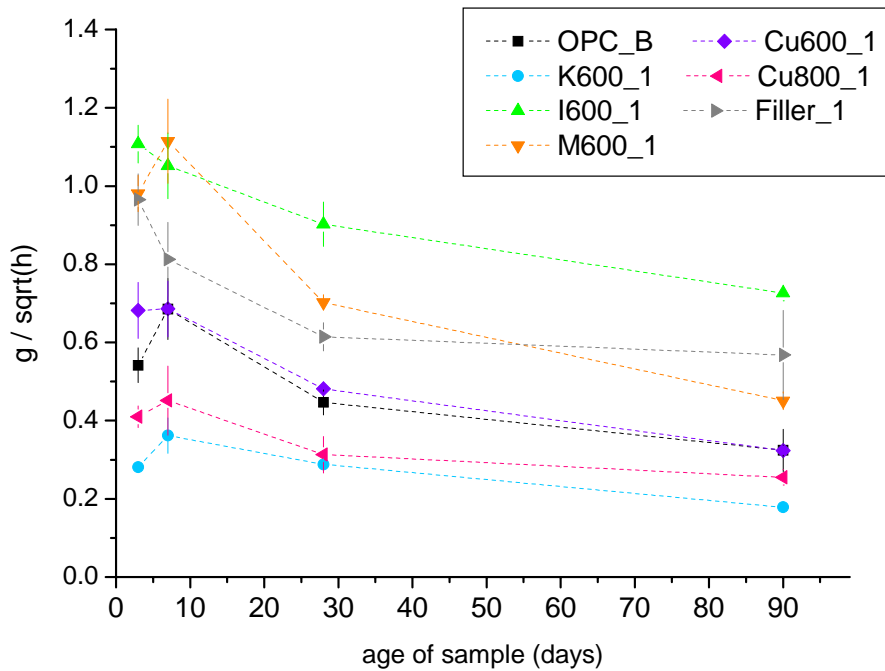
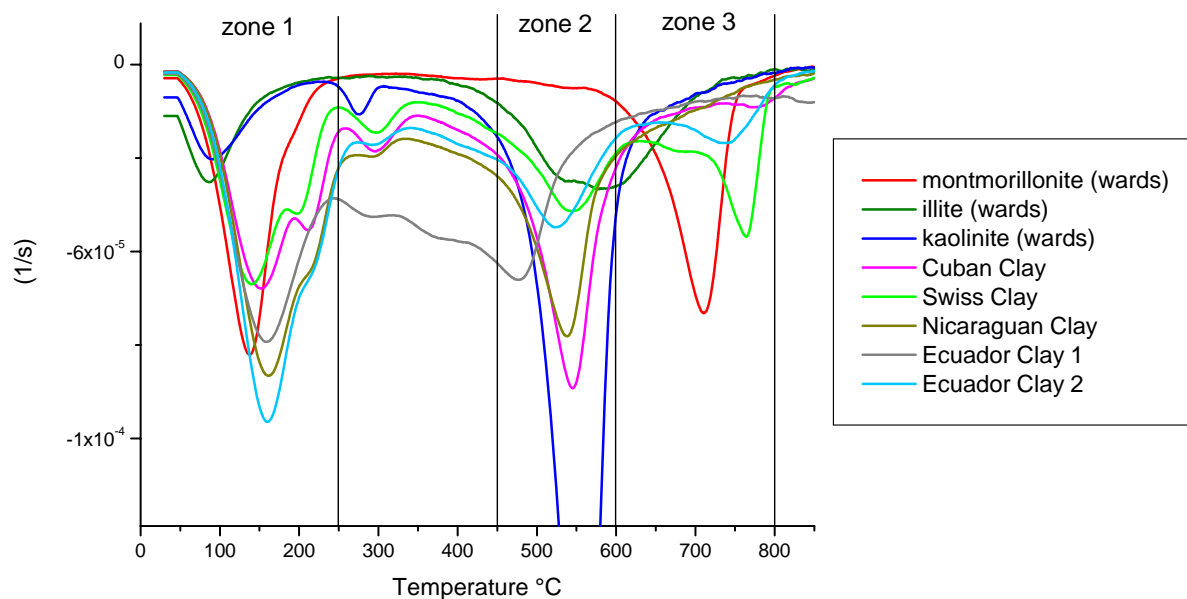


Figure 4-10: Sorptivity of cement-calcined clays mortars, serie 1 (30°C)

## 5 Towards practical use of activated clays

This study aimed at investigating on the potential use of clayey soils for the small scale development of low-cost housing materials in developing countries. Therefore, it would be necessary to simplify the characterization techniques for the identification of potential soils by the local communities. The necessity of formulating a sort of “tool kit” or basic guideline based on the fundamental research that was undertaken during this project arose naturally. This guideline should be based on very simple experiments requiring simple tools and little time for the evaluation of the activation potential of a clay. It was therefore decided to base the study on thermogravimetric analysis for the identification of kaolinite in soils. Due to the relatively precise location of the dehydroxylation peak of this type of clay, a method that could assess the mass loss in this range of temperature could be envisaged. Figure 5-1 shows the DTG curves of a set of clays, including the standard clays for comparison. The clayey fraction of the soils was extracted by sedimentation using sodium hexametaphosphate and dried at 60°C until constant mass. The presence of kaolinite in the clay from Nicaragua could be easily detected as the main dehydroxylation peak resembles that of the Cuban clay. The two other clays that might contain kaolinite could be the clay from Switzerland and the Ecuador 2. However, the important mass losses observed at lower temperature suggest that montmorillonite could also be present. The clay from Ecuador, number 1, could not be associated with any of the studied types of standard structure. Typical zones were mass losses are generally observed were delimited by 4 key temperatures ( 250°C, 450°C, 600°C and 800°C) as can be seen in Figure 5-1. The determination of the kaolinite content and eventually of the montmorillonite content could be done by comparing the mass losses obtained in each temperature range (or zone) with that of the standard materials from Ward’s natural science. To make sure that this experiment could be made without the need of a TGA instrument, around 6 grams of each clay were put in crucibles and heated to the 4 key temperatures with a ramp of 5°C/min. The furnace was maintained for one hour at each key temperature to allow the removal and weighing of the crucibles. Percentage mass losses from this experiment are presented in Table 5-1, together with typical values of mass losses for the standard clay structures. The mass losses in each zones were also reported as a percentage of the total losses observed in the 3 zones.



**Figure 5-1: DTG curves of a set of clays**

mass losses %		references						tested materials							
		Montm. (Wards)	% of 3 zones	illite (Wards)	% of 3 zones	kaolin. (Wards)	% of 3 zones	Cuban clay	% of 3 zones	Swiss clay	% of 3 zones	Nicara. clay	% of 3 zones	Ecuad. clay 2	% of 3 zones
zone 1	0-250°C	4.8	51%	2.5	35%	2.1	15%	5.33	48%	5.2	45%	7.9	66%	4.2	63%
zone 2	450-600°C	0.6	7%	2.7	39%	10.7	75%	4.57	41%	3.0	26%	3.2	27%	1.4	21%
zone 3	600-800°C	3.9	42%	1.8	26%	1.4	10%	1.15	10%	3.3	29%	0.9	8%	1.0	16%

**Table 5-1: % mass losses of the set of clays for each temperature zone, determined experimentally with a laboratory furnace and a balance**

These results seem to reproduce fairly well the mass losses observed by TGA. The Cuban clay revealed important mass losses in zone 1 and 2, typical of montmorillonites and kaolinites. The mass losses as percentage of the 3 zones for the Swiss clay were fairly well equilibrated, suggesting that this material could be made of illite. Nicaraguan clay showed a sequence of mass losses very similar to the Cuban clay. Ecuadorian clay 2 showed important mass losses in zone 1, indicating that montmorillonite could be present.

XRD analysis was used to check results of this theory of dehydration zones. The diffraction patterns are presented in Figure 5-2.



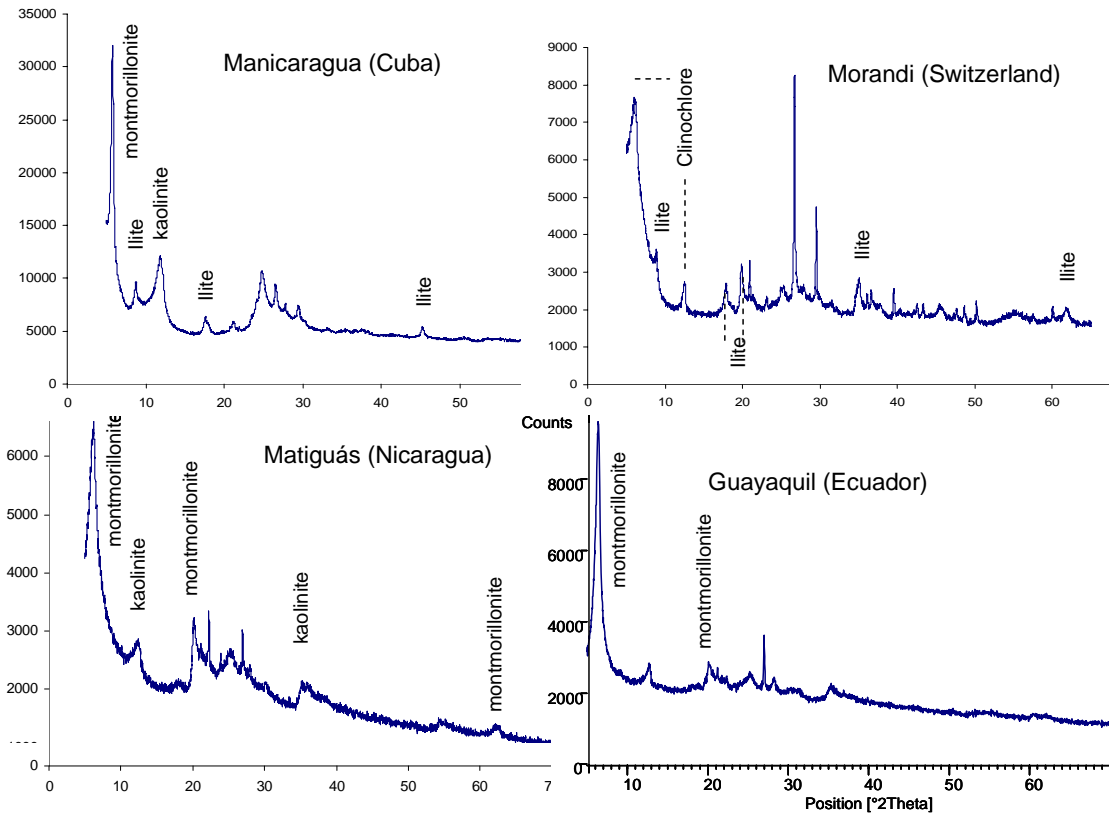


Figure 5-2 : XRD pattern of 3 south american clays and one swiss clay

Apart from the clay of Ecuador that actually had some kaolinite, most of the clay types could be detected based on a simple method that would actually only require a furnace and a balance. Hence, Reactivity of clays could be somehow predicted based on their mass losses between 400 and 650°C curves only. This represents an interesting approach for the simple identification of clayey material in remote areas where no access to characterization techniques is expected.



## 6 Conclusions and perspectives

### 6.1 Conclusions

#### 6.1.1 Activation of standard and locally available clays

- Kaolinite was shown to have the highest potential for activation. Kaolinite content plays a major role in the pozzolanic activity of the calcined clays.
- Calcined illite behaved like an inert filler and cannot be considered as a pozzolanic material. Calcined montmorillonite showed a little reactivity at later ages.
- The activation of kaolinite in the Cuban clay is not affected by the presence of other minerals, although some interaction during the calcination stage should not be excluded.
- The kaolin component in the Cuban clay appeared to have a lower crystallinity by XRD and DSC than the standard kaolinite.
- The recrystallisation of the phases in the Cuban clay occurred at a lower temperature (~900°C) than the standard kaolinite probably due to the presence of iron oxide acting as flux.
- The values of specific surface and particle size distribution for the reactive calcined clays (k600, MK, cu600, cu800) were in the same order of magnitude. Therefore, the differences in reactivity observed are mainly chemical.

#### 6.1.2 The calcined clay-cement interaction

- TGA was found to be the most accurate and reliable technique to assess pozzolanic reaction over time. The monitoring of calcium hydroxide content gives a good indication of the pozzolanic character of a system when compared to the reference cement paste. For temperatures of calcination between 600 and 850°C, the calcined Cuban clay showed a good pozzolanic activity, comparable to the standard kaolinite.
- Long term (28 days) calorimetry is another method that proved to be very efficient in isolating the contribution of the pozzolans from the hydration reaction of the cement, providing an inert material having a similar filler effect than the calcined clays is simultaneously studied.

- Calcined kaolinites in substitution for cement favour the formation of AFm phases. This was shown by XRD, EDX analysis as well as DTG.  $^{27}\text{Al}$  NMR also indicated the presence of strätlingite, which was more difficult to see with other techniques.
- The contribution of pozzolanic activity starts to be significant between 1 and 7 days. This is confirmed by the results of chemical shrinkage, long-term isothermal calorimetry on pastes and compressive strength of mortars.
- It was shown that mechanical properties could be maintained and even increased from 7 days by substituting 30% of the cement in mortars by calcined clays with low-kaolinite content (40% for the Cuban clay). There is a good correlation between the pozzolanic activity observed in pastes and the results of compressive strength of mortars.
- In the long term (90 days), strength development was the highest for the calcined standard kaolinite system, followed by the system incorporating Cuban Clays calcined at 800°C, then MK and then Cuban calcined clays at 600°C.
- The calcination temperature of the Cuban clay has a strong influence on the compressive strength. This reinforced the importance of understanding the mineralogy and thermal behaviour of the mixed clays for defining their optimal calcination temperatures. The pozzolanic activity of the Cuban clay calcined at 800°C contributed the most to the compressive strength of mortars. The decrease in strength for higher calcination temperatures of the Cuban clay (925°C) is possibly due to recrystallisations.
- Results of the sorptivity test indicated that the durability properties of concrete where cement has been partly substituted by reactive calcined clays could be enhanced.
- Low compressive strength at one day for the blended systems is probably the major drawback in the use of these mineral admixtures from an engineering point of view and efforts should be invested to improve the early age properties. Nevertheless, considering low-cost housing applications such as hollow concrete blocks, low-early strength may not be such a problem.

## 6.2 Perspectives

### 6.2.1 *Minimum kaolinite content of a clay*

It has been shown that 40% of kaolinite in clays can be sufficient to give good pozzolanic activity after calcination. It could be interesting to test a material with lower amounts of kaolinite to determine the minimum kaolinite content required to produce a good pozzolan. Assuming the reactivity of these materials could be enhanced by an optimized calcination process, as discussed above, this limit may be lower than 40%, opening the scope of application to a wider variety of mixed clays types. The study of the Cuban soil (before the sedimentation with deflocculating agent that was used in this study) with only 17% of kaolinite, could be an interesting starting point. If sedimentation could not be applied for several reasons such as lack of water, difficulties in separating clayey particles or time constraints, the soil could be calcined without any treatment and the grinding after calcination could help increasing the specific surface and lowering the particle size distribution. This study was undertaken by the sub-project 3 of this joint research programme and showed promising results.

### 6.2.2 *Moving to concrete applications and addressing the workability issues*

It was not possible to test concrete applications during this study due to insufficient amounts of calcined clays produced per batch of calcination (~200gr). However, the reactivity of calcined clays should be tested in concrete in order to validate results obtained for mortars and get closer to the application. A calcination process allowing the activation of more important quantities of clay should be considered, as explained in the following section.

Due to use of a fixed water to binder ratio for all blends, the mortars prepared for this study exhibited different workability in the fresh state. It varied from fluid behaviours (OPC and Filler systems) to plastic behaviours (K600 and MK systems). Surprisingly the mortars incorporating Cuban clay had only a slight reduction in workability compared to the control mortar. Workability parameters will have to be taken into account when moving to the production of concretes, as they become critical parameters for the production good quality products. Moreover, the implementation of this type of concrete in low-cost housing applications in developing countries will have to consider the working conditions of the field. It is probable that not all facilities will be available to ensure the best practice in the production of the concretes (water dosage, time of mixing, curing conditions). Simple protocols should therefore be formulated to ensure that the calcined clays will perform well.

Jeknavorian et al [82] reported on the interaction of with clay-bearing aggregates and found that the effectiveness of the superplasticizer was reduced due to their absorption by expansive clays of the smectite group. This has become a serious issue for concrete manufacturers in the United States. Bringing these considerations to the context of this study, it was shown that the calcination process of the clays induced a collapse of the interlayer space of the clayey structures and this phenomenon is believed to be irreversible. Thus, the absorption properties of expandable clays should be suppressed. However, simple experiments should be considered in order to confirm these assumptions.

### *6.2.3 Durability*

Sustainable development in the construction industry will not be achieved through the replacement of cement by more ecologically friendly materials only. It will also require durability of concrete structures. Hence, more tests should be performed to assess the long term performance of concrete incorporating large amounts of calcined clays, such as resistance to chlorides and sulphates ingress or freeze-thaw resistance. It has been widely reported that the use of supplementary cementitious materials in concrete could enhance durability properties (see section 3.2.5). Nevertheless, more practical approaches than laboratory testing should be envisaged to take into account the field conditions and the different concrete practices that could be found in developing countries. This topic was addressed in sub-project 4 of the joint research programme.

### *6.2.4 Moving towards a more efficient calcination process*

It may also be possible to further improve the reactivity of the activated materials by reducing the calcination time from 1 hour to a few seconds. Figure 6-1 shows the change in specific surface of Cuban clay particles with reduced times of calcination.

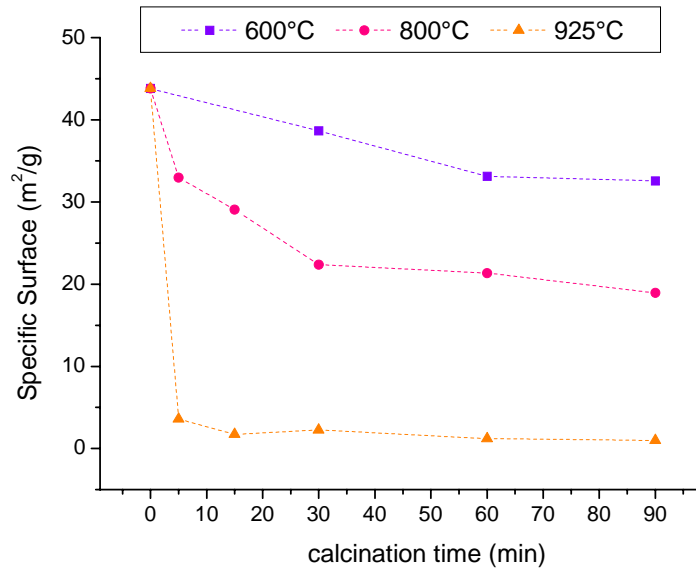


**Figure 6-1: Influence of calcination time on specific surface of Cuban clays**

This simple experiment suggests that the reactivity of the clay calcined at 800°C, considered as the optimum activation temperature for the Cuban clay, could still be improved if calcination times were shorter. The reactivity observed for MK (a product with very short calcination times) and its contribution to the early age strength of mortars supports this idea. St-Gobain© have patented a complex process along these lines [83]. Such an approach could perhaps be adapted to be suitable for the development of low-cost building materials.

Although such perspective processing routes might appear over complex for developing countries, potential sources of waste heat could be exploited. In the Cuban context, fluidised bed boilers used in the sugar cane industry could represent a potential target for implementing the clay activation process. The temperature of the fluidized bed reaches generally 900°C, considered as the upper limit of the calcination window for obtaining a reactive pozzolan from calcining kaolin-rich clays. However, the clay does not necessarily have to be injected in the combustion chamber together with the fuel (in this case shredded sugar cane bagasse and sugar cane straw) and a separate activation chamber using the hot air flow coming out of the combustion chamber could be envisaged. This may decrease the efficiency regarding the production process of the sugar but the volume of agricultural wastes generated is much more than what it actually needed to operate these boilers at present time.





## Bibliography

- [1] G. Landaeta, Strategies for low-income housing : a comparative study on Nicaragua, Mexico, Guatemala, Cuba, Panama, Costa Rica and El Salvador in "Lund : Lund Univ., Division of Architecture and Development Studies, 1994" (Lund University, Sweden, 1994).
- [2] U. N. C. f. H. S. (UNHabitat), The Use of selected indigenous building materials with potential for wide application in developing countries, (Nairobi, 1985).
- [3] F. Martirena, B. Middendorf, R. L. Day, M. Gehrke, P. Roque, L. Martinez and S. Betancourt, Rudimentary, low tech incinerators as a means to produce reactive pozzolan out of sugar cane straw, *Cement and Concrete Research* 36 (2006) 1056.
- [4] J. F. Martirena Hernandez, B. Middendorf, M. Gehrke and H. Budelmann, Use of wastes of the sugar industry as pozzolana in lime-pozzolana binders: study of the reaction, *Cement and Concrete Research* 28 (1998) 1525.
- [5] H. G. H. Houben, *Earth Construction* (ITDG Publishing, London, 1994).
- [6] R. G. Burns, *Marine Minerals* (Mineralogical society of america, 1979).
- [7] R. Grim, *Applied clay mineralogy* (McGraw-Hill, 1962).
- [8] J.K. Mitchell, *Fundamentals of soil behaviour*, 3rd edition (John Wiley & Sons, Inc., 2005).
- [9] G. Baudet, V. Perrotel, A. Seron and M. Stelletti, Two dimensions comminution of kaolinite clay particles, *Powder Technology* 105 (1999) 125.
- [10] H. H. Murray, Major kaolin processing developments, *International Journal of Mineral Processing* 7 (1980) 263.
- [11] A. Vanerek, B. Alince and T. G. M. van de Ven, Delamination and flocculation efficiency of sodium-activated kaolin and montmorillonite, *Colloids and Surfaces A: Physicochemical and Engineering Aspects* 273 (2006) 193.
- [12] T. Jiang, G. Li, G. Qiu, X. Fan and Z. Huang, Thermal activation and alkali dissolution of silicon from illite, *Applied Clay Science* 40 (2008) 81.
- [13] S. Alonso and A. Palomo, Calorimetric study of alkaline activation of calcium hydroxide-metakaolin solid mixtures, *Cement and Concrete Research* 31 (2001) 25.
- [14] K. Elert, E. Sebastián, I. Valverde and C. Rodriguez-Navarro, Alkaline treatment of clay minerals from the Alhambra Formation: Implications for the conservation of earthen architecture, *Applied Clay Science* 39 (2008) 122.
- [15] L. Heller-Kallai, *Hanbook of clay science*, chapter 7.2: Thermally modified clay minerals (Elsevier Ltd., 2006).
- [16] G. Z. J.P. Mercier, W. Kurz, *Introduction à la science des matériaux* (PPUR, 1999).
- [17] C. He, B. Osbaeck and E. Makovicky, Pozzolanic reactions of six principal clay minerals: Activation, reactivity assessments and technological effects, *Cement and Concrete Research* 25 (1995) 1691.
- [18] M. Kaloumenou, effect of the kaolin particle size on the pozzolanic behaviour of the metakaolinite, *Journal of Thermal Analysis and Calorimetry* 56 (1999) 901.
- [19] C. He, E. Makovicky and B. Osbaeck, Thermal treatment and pozzolanic activity of Na- and Ca-montmorillonite, *Applied Clay Science* 10 (1996) 351.
- [20] C. He, E. Makovicky and B. Osbaeck, Thermal stability and pozzolanic activity of calcined illite, *Applied Clay Science* 9 (1995) 337.
- [21] C. He, E. Makovicky and B. Osbaeck, Thermal stability and pozzolanic activity of raw and calcined mixed-layer mica/smectite, *Applied Clay Science* 17 (2000) 141.

- [22] C. He, E. Makovicky and B. Osbaeck, Thermal treatment and pozzolanic activity of sepiolite, *Applied Clay Science* 10 (1996) 337.
- [23] C. He, E. Makovicky and B. Osbaeck, Thermal stability and pozzolanic activity of calcined kaolin, *Applied Clay Science* 9 (1994) 165.
- [24] A.M.Neville, *Properties of Concrete*, Pearson Education Limited 1995).
- [25] J. Ambroise, Elaboration de liants pouzzolaniques a moyenne température et étude de leurs propriétés physico-chimiques et mécaniques (Thesis), in "Laboratoire matériaux Minéraux, INSA, Lyon" (1984).
- [26] J. Ambroise, M. Murat and J. Pera, Hydration reaction and hardening of calcined clays and related minerals V. Extension of the research and general conclusions, *Cement and Concrete Research* 15 (1985) 261.
- [27] M. Murat and C. Comel, Hydration reaction and hardening of calcined clays and related minerals III. Influence of calcination process of kaolinite on mechanical strengths of hardened metakaolinite, *Cement and Concrete Research* 13 (1983) 631.
- [28] A. Chakchouk, B. Samet and T. Mnif, Study on the potential use of Tunisian clays as pozzolanic material, *Applied Clay Science* 33 (2006) 79.
- [29] B. B. Sabir, S. Wild and J. Bai, Metakaolin and calcined clays as pozzolans for concrete: a review, *Cement and Concrete Composites* 23 (2001) 441.
- [30] G. W. Brindley and M. Nakahira, The Kaolinite-Mullite Reaction Series: I, A Survey of Outstanding Problems, *Journal of the american ceramics society* 42 (1959) 311.
- [31] G. W. Brindley and M. Nakahira, The Kaolinite-Mullite Reaction Series: II, Metakaolin, *Journal of the american ceramics society* 42 (1959) 314.
- [32] G. W. Brindley and M. Nakahira, The Kaolinite-Mullite Reaction Series: III, The High-Temperature Phases, *Journal of the american ceramics society* 42 (1959) 319.
- [33] I. B. Mackenzie KJD, Outstanding problems in the kaolinite-mullite reaction sequence investigated by Si and Al solid state NMR: I Metakaolinite, *Journal of the american ceramics society* 68 (1985) 293.
- [34] J. Rocha and J. Klinowski,  $^{29}\text{Si}$  and  $^{27}\text{Al}$  magic-angle-spinning NMR studies of the thermal transformation of kaolinite, *Physics and Chemistry of Minerals* 17 (1990) 179.
- [35] E. Lippmaa, A. Samoson and M. Magi, High-resolution aluminum-27 NMR of aluminosilicates, *Journal of the american chemical society* 108 (1986) 1730.
- [36] Gilson, penta-coordinated aluminium in zeolites and aluminosilicates, *Journal of the Chemical Society, Chemical Communications* 2 (1987) 91.
- [37] J. D. Macedo, C. J. A. Mota, S. M. C. de Menezes and V. Camorim, NMR and acidity studies of dealuminated metakaolin and their correlation with cumene cracking, *Applied Clay Science* 8 (1994) 321.
- [38] D. Massiot, P. Dion, J. F. Alcover and F. Bergaya,  $^{27}\text{Al}$  and  $^{29}\text{Si}$  MAS NMR Study of Kaolinite Thermal Decomposition by Controlled Rate Thermal Analysis 1995).
- [39] Q. Liu, D. A. Spears and Q. Liu, MAS NMR study of surface-modified calcined kaolin, *Applied Clay Science* 19 (2001) 89.
- [40] D. L. Carroll, T. F. Kemp, T. J. Bastow and M. E. Smith, Solid-state NMR characterisation of the thermal transformation of a Hungarian white illite, *Solid State Nuclear Magnetic Resonance* 28 (2005) 31.
- [41] I. W. M. Brown, K. J. D. MacKenzie and R. H. Meinhold, The thermal reactions of montmorillonite studied by high-resolution solid-state  $^{29}\text{Si}$  and  $^{27}\text{Al}$  NMR, *Journal of Materials Science* 22 (1987) 3265.
- [42] Martin-Calle, Pouzzolanicité d'argiles thermiquement activées: Influence de la minéralogie et des conditions de calcination (Thesis), in "Laboratoire matériaux Minéraux, INSA, Lyon" (1989).

- [43] S. Salvador, Pozzolanic properties of flash-calcined kaolinite: A comparative study with soak-calcined products, *Cement and Concrete Research* 25 (1995) 102.
- [44] A. Shvarzman, K. Kovler, G. S. Grader and G. E. Shter, The effect of dehydroxylation/amorphization degree on pozzolanic activity of kaolinite, *Cement and Concrete Research* 33 (2003) 405.
- [45] E. Badogiannis, G. Kakali and S. Tsivilis, Metakaolin as supplementary cementitious material, *Journal of Thermal Analysis and Calorimetry* 81 (2005) 457.
- [46] S. Cara, G. Carcangiu, L. Massidda, P. Meloni, U. Sanna and M. Tamanini, Assessment of pozzolanic potential in lime-water systems of raw and calcined kaolinic clays from the Donnigazza Mine (Sardinia-Italy), *Applied Clay Science* 33 (2006) 66.
- [47] F. W. Ph.larque, Techniques de préparation des minéraux argileux en vue de l'analyse para diffraction des rayons X, *Laboratoire de Géologie et de Paléontologie, CNRS, Strasbourg* (1978).
- [48] N. Todor, *Thermal Analysis of Minerals* (Abacus Press, 1976).
- [49] J.Barshad, Differential thermal analysis of vermiculite, *American mineralogist* 33 (1948) 655.
- [50] C. W. Parmelee, Catalytic mullitization of kaolinite, *Journal of the american ceramics society* 25 (1942).
- [51] R. M. German, *Liquid Phase Sintering* 1985).
- [52] G.C.Bye, *Portland Cement*, 2nd edition 1999).
- [53] H.F.W.Taylor, *Cement Chemistry*, 2nd edition (Thomas Telford, 2004).
- [54] J. Ambroise, M. Murat and J. Pera, Hydration reaction and hardening of calcined clays and related minerals. IV. Experimental conditions for strength improvement on metakaolinite minicylinders, *Cement and Concrete Research* 15 (1985) 83.
- [55] M. Frías, M. I. S. de Rojas and J. Cabrera, The effect that the pozzolanic reaction of metakaolin has on the heat evolution in metakaolin-cement mortars, *Cement and Concrete Research* 30 (2000) 209.
- [56] J. Cabrera and M. F. Rojas, Mechanism of hydration of the metakaolin-lime-water system, *Cement and Concrete Research* 31 (2001) 177.
- [57] M. F. Rojas and J. Cabrera, The effect of temperature on the hydration rate and stability of the hydration phases of metakaolin-lime-water systems, *Cement and Concrete Research* 32 (2002) 133.
- [58] N. Y. Mostafa and P. W. Brown, Heat of hydration of high reactive pozzolans in blended cements: Isothermal conduction calorimetry, *Thermochemica Acta* 435 (2005) 162.
- [59] S. Wild and J. M. Khatib, Portlandite consumption in metakaolin cement pastes and mortars, *Cement and Concrete Research* 27 (1997) 137.
- [60] B. K. Marsh and R. L. Day, Pozzolanic and cementitious reactions of fly ash in blended cement pastes, *Cement and Concrete Research* 18 (1988) 301.
- [61] M. S. Morsy, S. A. A. El-Enein and G. B. Hanna, Microstructure and hydration characteristics of artificial pozzolana-cement pastes containing burnt kaolinite clay, *Cement and Concrete Research* 27 (1997) 1307.
- [62] M. Singh and M. Garg, Reactive pozzolana from Indian clays--their use in cement mortars, *Cement and Concrete Research* 36 (2006) 1903.
- [63] M. I. Sanchez de Rojas, F. Marin, J. Rivera and M. Frias, Morphology and Properties in Blended Cements with Ceramic Wastes as a Pozzolanic Material, *Journal of the american ceramics society* 89 (2006) 3701.
- [64] I. G. Richardson, The nature of C-S-H in hardened cements, *Cement and Concrete Research* 29 (1999) 1131.

- [65] P. Faucon, A. Delagrave, J. C. Petit, C. Richet, J. M. Marchand and H. Zanni, Aluminum Incorporation in Calcium Silicate Hydrates (C-S-H) Depending on Their Ca/Si Ratio, *J. Phys. Chem. B* 103 (1999) 7796.
- [66] M. D. Andersen, H. J. Jakobsen and J. Skibsted, Incorporation of Aluminum in the Calcium Silicate Hydrate (C-S-H) of Hydrated Portland Cements: A High-Field  $^{27}\text{Al}$  and  $^{29}\text{Si}$  MAS NMR Investigation, *Inorganic Chemistry* 42 (2003) 2280.
- [67] M. D. Andersen, H. J. Jakobsen and J. Skibsted, Characterization of white Portland cement hydration and the C-S-H structure in the presence of sodium aluminate by  $^{27}\text{Al}$  and  $^{29}\text{Si}$  MAS NMR spectroscopy, *Cement and Concrete Research* 34 (2004) 857.
- [68] C. A. Love, I. G. Richardson and A. R. Brough, Composition and structure of C-S-H in white Portland cement-20% metakaolin pastes hydrated at 25°C, *Cement and Concrete Research* 37 (2007) 109.
- [69] S.Kwan,  $^{29}\text{Si}$  and  $^{27}\text{Al}$  MAS NMR Study of Stratlingite, *Journal of the American Ceramics Society* 78 (1995).
- [70] M. R. Jones, D. E. Macphee, J. A. Chudek, G. Hunter, R. Lannegrand, R. Talero and S. N. Scrimgeour, Studies using  $^{27}\text{Al}$  MAS NMR of AFm and AFt phases and the formation of Friedel's salt, *Cement and Concrete Research* 33 (2003) 177.
- [71] S.Kelham, A water absorption test for concrete, *Magazine of Concrete Research* 40 (1988) 5.
- [72] M. H. Zhang and V. M. Malhotra, Characteristics of a thermally activated aluminosilicate pozzolanic material and its use in concrete, *Cement and Concrete Research* 25 (1995) 1713.
- [73] J. Ambroise, S. Maximilien and J. Pera, Properties of Metakaolin blended cements, *Advanced Cement Based Materials* 1 (1994) 161.
- [74] P. S. de Silva and F. P. Glasser, Phase relations in the system  $\text{CaO}---\text{Al}_2\text{O}_3---\text{SiO}_2---\text{H}_2\text{O}$  relevant to metakaolin - calcium hydroxide hydration, *Cement and Concrete Research* 23 (1993) 627.
- [75] N. Y. Mostafa, S. A. S. El-Hemaly, E. I. Al-Wakeel, S. A. El-Korashy and P. W. Brown, Characterization and evaluation of the pozzolanic activity of Egyptian industrial by-products: I: Silica fume and dealuminated kaolin, *Cement and Concrete Research* 31 (2001) 467.
- [76] M. Frías and J. Cabrera, Influence of MK on the reaction kinetics in MK/lime and MK-blended cement systems at 20°C, *Cement and Concrete Research* 31 (2001) 519.
- [77] I. Papayianni and M. Stefanidou, Strength-porosity relationships in lime-pozzolan mortars, *Construction and Building Materials* 20 (2006) 700.
- [78] M. Kaloumenou, E. Badogiannis, S. Tsvivilis and G. Kakali, Effect of the Kaolin Particle Size on the Pozzolan Behaviour of the Metakaolinite Produced, *Journal of Thermal Analysis and Calorimetry* 56 (1999) 901.
- [79] D. R. L. Martirena J.F., Middendorf B., Scrivener K, Mixtures of Lime and Pozzolan for High Volume Portland Cement Replacement in Concrete, *Proceedings of the XVI International Conference IBAUSIL, Weimar, Germany* (2006).
- [80] K. L. Scrivener, T. Füllmann, E. Gallucci, G. Walenta and E. Bermejo, Quantitative study of Portland cement hydration by X-ray diffraction/Rietveld analysis and independent methods, *Cement and Concrete Research* 34 (2004) 1541.
- [81] J. V. Smith and C. S. Blackwell, Nuclear magnetic resonance of silica polymorphs, *Nature* 303 (1983) 223.
- [82] A. A. Jeknavorian, Jardine, L., Ou, C.C., Koyata, H. and Folliard, K.J., Interaction of Superplasticizers with Clay-Bearing Aggregates, in "Fourth International ACI/CANMET Conference on Concrete Durability" (Special Publication (SP-217), Sydney, Australia, 2003).

[83] G. Cadoret, Dehydroxilated aluminium silicate based material, process and installation for the manufacture thereof, in "US Patent Application publications US 2005/0039637 A1", edited by U. P. A. publications (Saint-Gobain Matériaux de Construction S.A.S., United States, 2005).



## Appendices

### Appendix I Technical data for standard clays (<http://wardsci.com>)

#### KAOLINITE - $\text{Al}_2\text{Si}_2\text{O}_5(\text{OH})_4$

- **Crystallography:** Triclinic; 1. In very minute, thin, rhombic or hexagonal plates. More commonly in clay-like masses.
- **Physical Properties:** *Cleavage:* {001} perfect; flexible, inelastic. Usually unctuous and plastic. *H.* 2.0. *G.* 2.6. *Luster:* Usually dull, earthy; crystal plates pearly. *Color:* White, often stained brown or gray by impurities. Translucent to opaque. *Streak:* White.
- **Composition/Features:** One of a group of substances known as the *clay minerals* (essentially hydrous aluminum silicates). Kaolinite shows little compositional variation, and is nearly impossible to distinguish from other clay minerals without X-ray tests. Infusible and insoluble.
- **Occurrence/Use:** A common mineral, kaolinite always forms secondarily by weathering or hydrothermal alteration of aluminum silicates, particularly feldspar. It is the chief constituent of *kaolin* or *clay*—one of the most important of the natural industrial substances. Used in making bricks, pottery, china, ceramics, and as filler in paper.
- **Ward's Catalog Reference #:** 46E4330, 46E0995.

**WARD'S** NATURAL SCIENCE ESTABLISHMENT, INC.

#### MONTMORILLONITE - $(\text{Na,Ca})_{0.5}(\text{Al,Mg})_2\text{Si}_4\text{O}_{10}(\text{OH})_2 \cdot n\text{H}_2\text{O}$

- **Crystallography:** Monoclinic. Always in earthy masses; crystals not distinguishable.
- **Physical Properties:** *Cleavage:* None apparent; usually unctuous and plastic. *H.* 1-1.5. *G.* 2-2.5. *Luster:* Greasy or dull, earthy. *Color:* Usually gray or greenish-gray, but may be white, yellow, greenish, pink or brown. Opaque. *Streak:* White.
- **Composition/Features:** An aluminum-rich clay mineral known for its clay-like character, soapy feel, and the property of swelling to form a gel-like mass in water. Similar in composition to other clay minerals, and best distinguished by X-ray tests.
- **Occurrence/Use:** Montmorillonite is the dominant clay mineral in *bentonite*, an altered volcanic ash. Generally forms as an alteration product of aluminum-rich minerals. Useful in industry for its physical properties of cation exchange and expanding in water.
- **Ward's Catalog Reference #:** 46E0435.

**WARD'S** NATURAL SCIENCE ESTABLISHMENT, INC.

#### ILLITE - $(\text{K,H}_3\text{O})(\text{Al,Mg,Fe})_2(\text{Si,Al})_4\text{O}_{10}[(\text{OH})_2\text{H}_2\text{O}]$

- **Crystallography:** Monoclinic. Crystals not distinguishable; usually in clay-like masses, either compact or friable.
- **Physical Properties:** *Cleavage:* {001} perfect, but not observable to the unaided eye. Usually unctuous and plastic. *H.* 2.0 (+/-). *G.* about 2.6. *Luster:* Dull, earthy. *Color:* Earthy gray, green, white. Translucent to opaque. *Streak:* White.
- **Composition/Features:** Illite is a general term for a group of mica-like clay minerals. Essentially hydrous aluminum silicates, the illites differ from micas in having less substitution for Al or Si, in containing more water, and in having K partly replaced by Ca and Mg. Recognized by its clay-like character, but usually requires X-ray tests to distinguish it from other clay minerals.
- **Occurrence/Use:** Illite is the primary constituent of many shales, and forms chiefly by the weathering or hydrothermal alteration of aluminum silicates.
- **Ward's Catalog Reference #:** 46E0315, 46E4100.

**WARD'S** NATURAL SCIENCE ESTABLISHMENT, INC.

## Appendix II Extraction of Clayey phases (from Larque [47])

A clayey suspension is considered stable if the sedimentation of the particles is not total after 12 hours or after centrifugation at 2500 rpm for 10min.

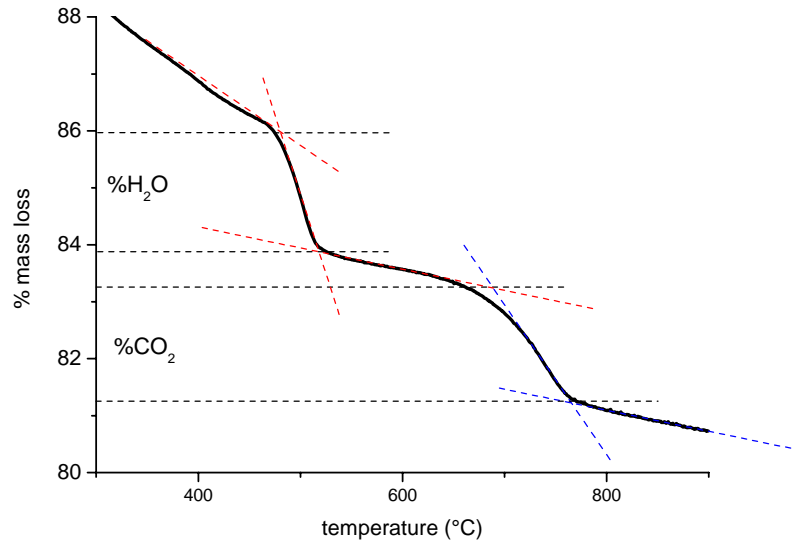
1. Put 15 to 30 g of the crushed clay sample in 50ml of distilled water in a 250ml flask and mix thoroughly until all particles dissolved
2. Decantation by centrifugation : Put the solution in centrifugation tubes and centrifuge at 2000rpm for 5min
3. Mixing with distilled water: Pour gently the water from the tubes avoiding the loss of the decanted material. Refill half of the tubes with distilled water and put the clayey particles in suspension again by mixing thoroughly by hand for 1min. then, fill the tubes up to the top.
4. Repeat step 2 and 3 until the suspension is stable. If you do repeat step 2, do it at 2500rpm for 10min.
5. Once the suspension is stable, centrifuge at 3000rpm for approx. 40min and remove the water.

### Extraction of the clayey phase

1. Suspension: Put the clayey particles in suspension again using 30-40ml of distilled water and mixing with a high shear blender.
2. Wait for 1-3min and pass the solution into a 100ml flask including the bottom particles.
3. Fill the 100ml flask with distilled water..
4. If you experience flocculation, bring the pH back to 7 by using a few drops of  $\text{NH}_4\text{OH}$ , but always keep an acid value.
5. Separation of the  $< 2\mu\text{m}$  particles: Mix thoroughly the 100ml flask to homogenise the suspension
6. Leave it to sediment for 1h40min on the table.
7. Extract the first 20mm of suspension (starting at the surface of the liquid) by using a siphon. During this operation, take care to follow the liquid level to avoid fluid turbulences.
8. The siphoned suspension is put in the tubes and centrifuged at 3500rpm for 35-45min to obtain a clayey paste ready for characterization.



### Appendix III Calculation of CH content



Calculation of CH content (%CH) takes into account the dehydroxilation that could be present in the raw materials.

The corrected CH content (%CH<sub>corrected</sub>) takes also into account the carbonation that could have occurred during the lifetime of the paste as well as the decarbonation that could be present in the raw materials.

$$\%CH = \frac{74}{18} \cdot \left( \%H_2O_{(1d)} - \left( \%H_2O_{(opc)} \cdot \%OPC_{(1d)} + \%H_2O_{(pozz.)} \cdot \%POZZ_{(1d)} \right) \right)$$

$$\%CH_{corrected} = \%CH + \frac{74}{44} \cdot \left( \%CO_{2(1d)} - \left( \%CO_{2(opc)} \cdot \%OPC_{(1d)} + \%CO_{2(poizz.)} \cdot \%POZZ_{(1d)} \right) \right)$$

Where :

74 : MM of CH / 18 : MM of H<sub>2</sub>O / 44 : MM of CO<sub>2</sub>

%H<sub>2</sub>O(1d) : mass loss from dehydroxilation of the paste at 1d (%H<sub>2</sub>O in the graph above)

%H<sub>2</sub>O(OPC) : mass loss from dehydroxilation of the raw material opc (if any)

%oOPC : percentage opc in the mix at 1 day (determined from the mass loss of the TG curve at 1 day knowing the original formulation)

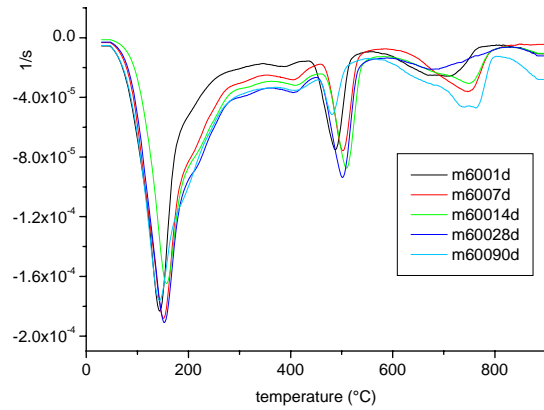
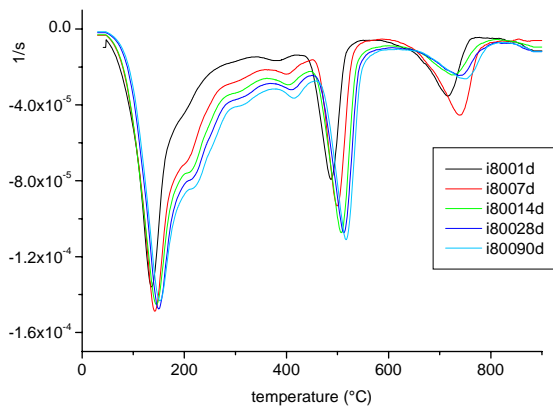
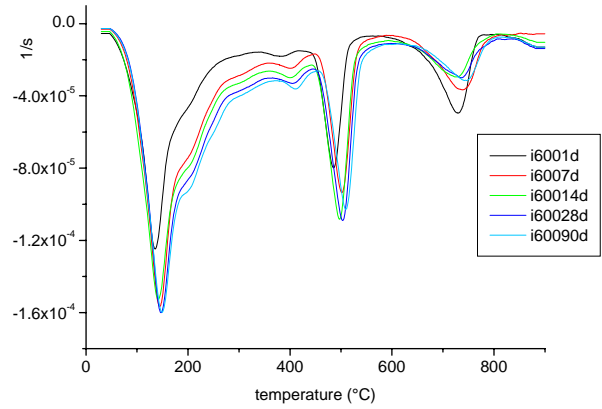
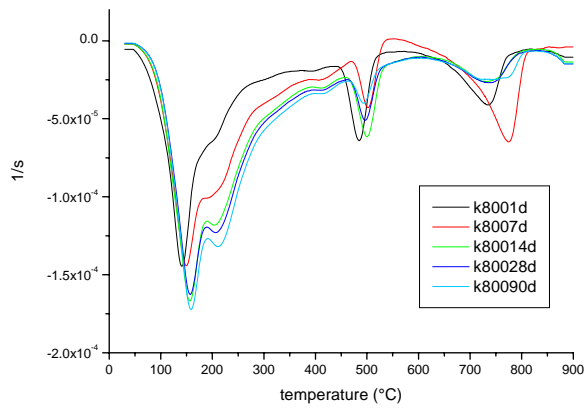
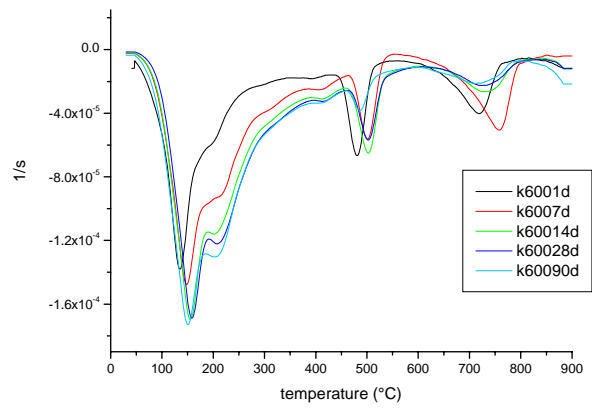
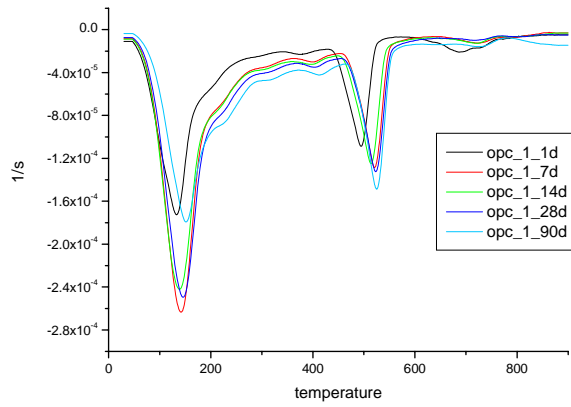
%H<sub>2</sub>O(Pozz) : mass loss from dehydroxilation of the raw material pozz (if any)

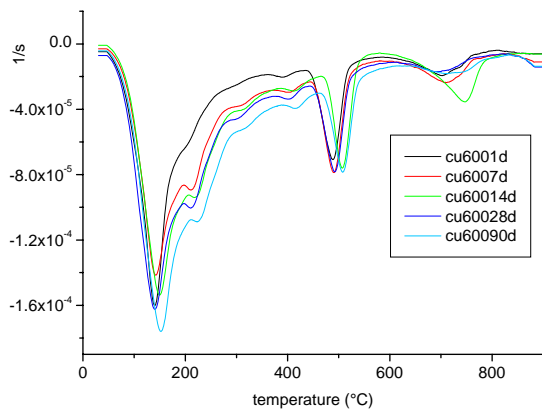
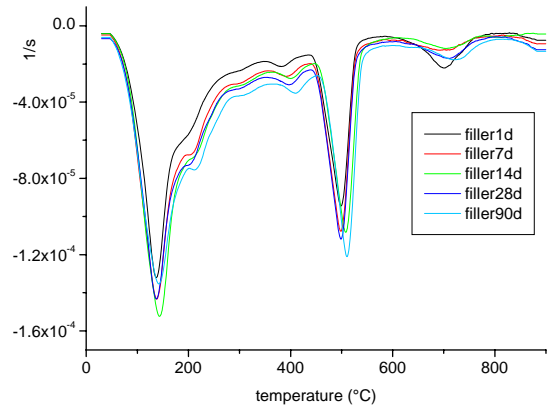
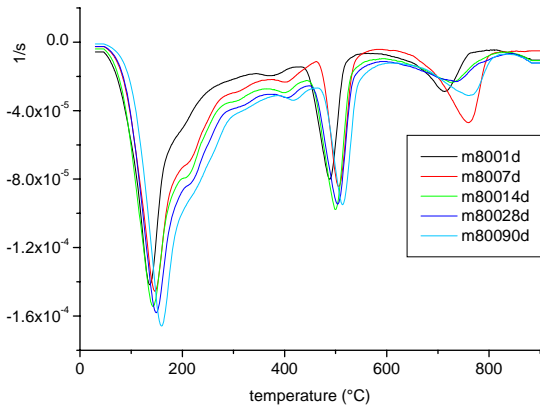
%oPozz : Percentage pozz in the mix at 1 day (determined from the mass loss of the TG curve at 1day knowing the original formulation)

(The second part of the formula is exactly the same as first part but related to the mass losses of CO<sub>2</sub>)

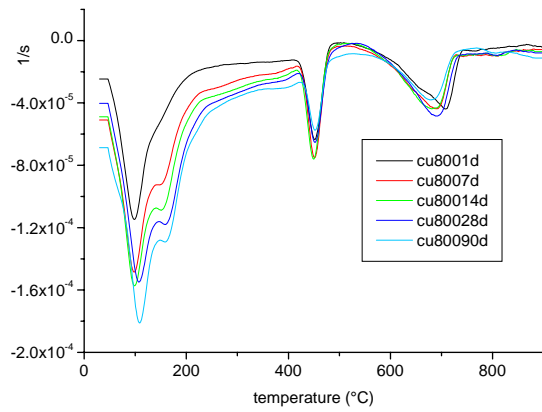
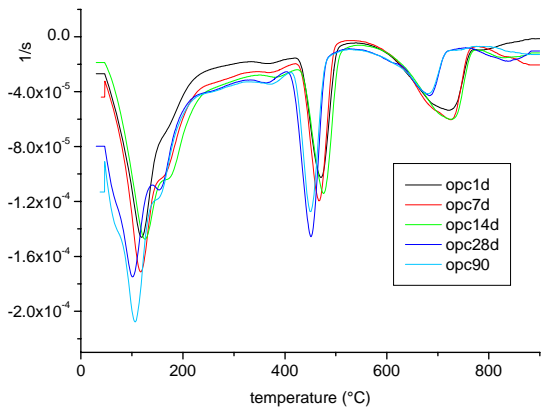
## Appendix IV TGA curves

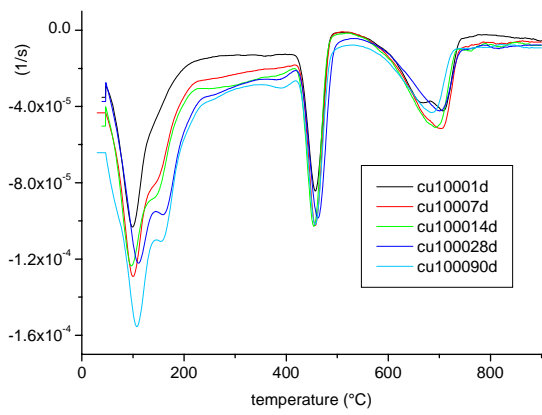
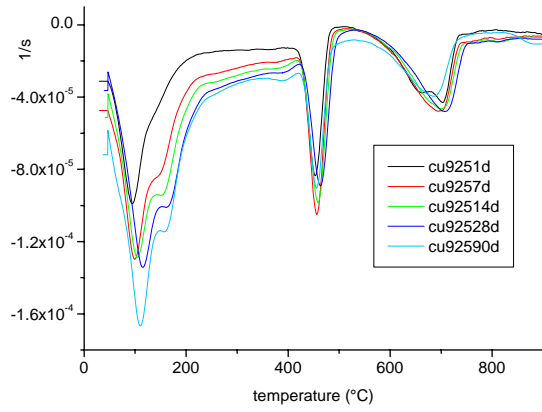
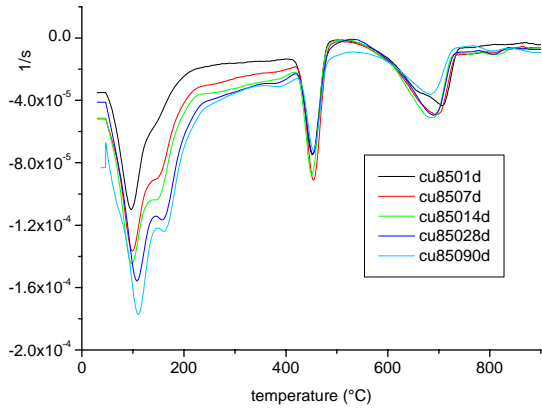
### Series 1



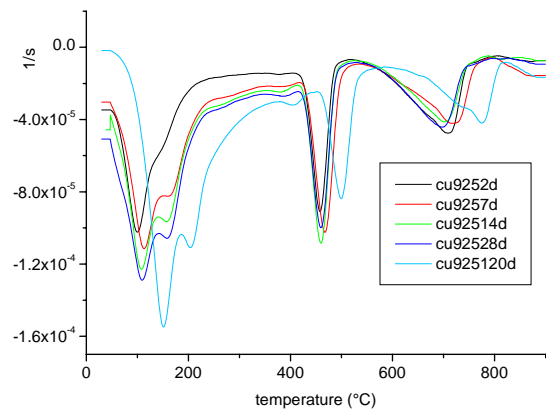
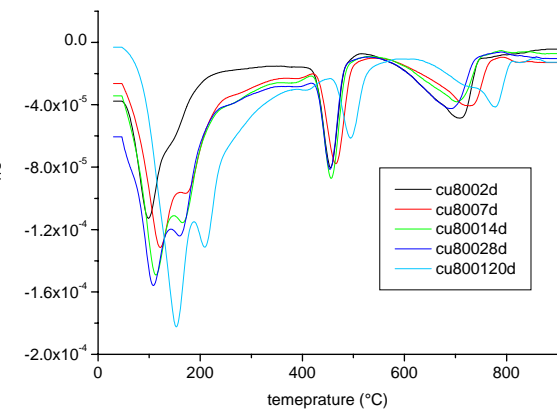
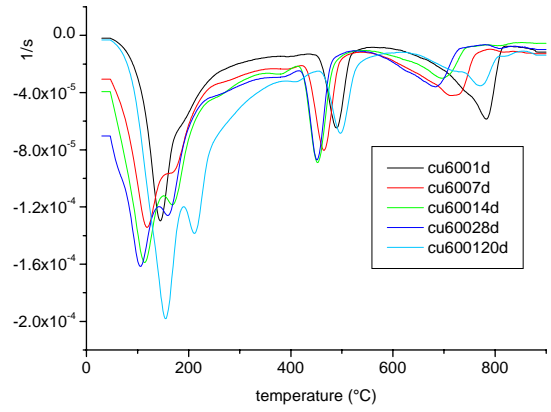
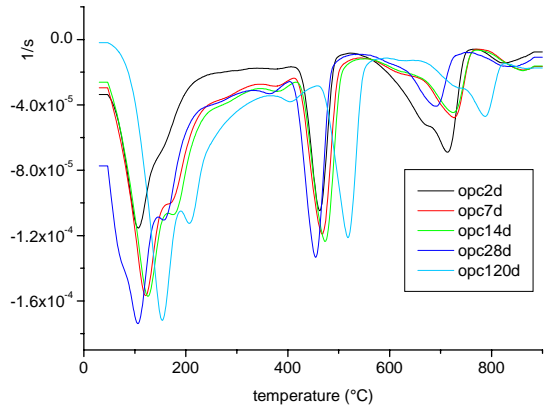


Series 2

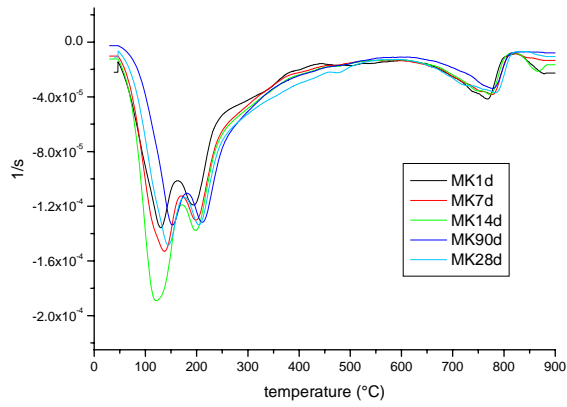
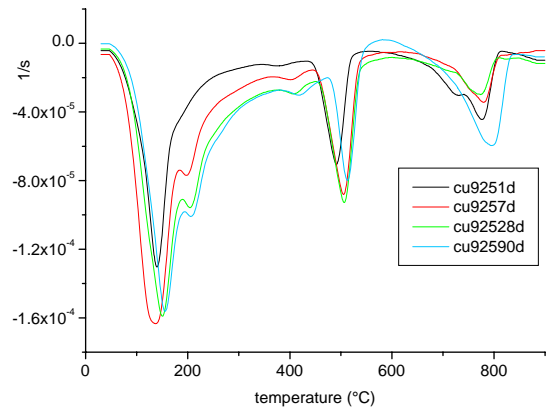
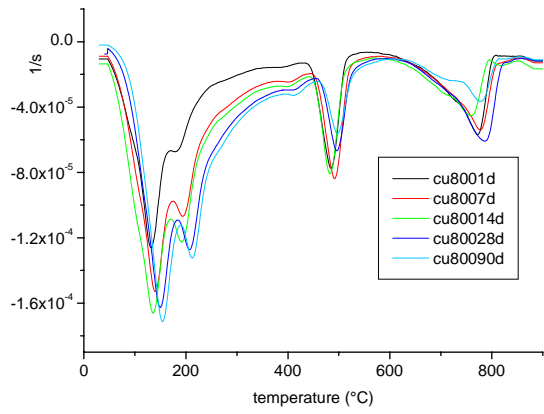
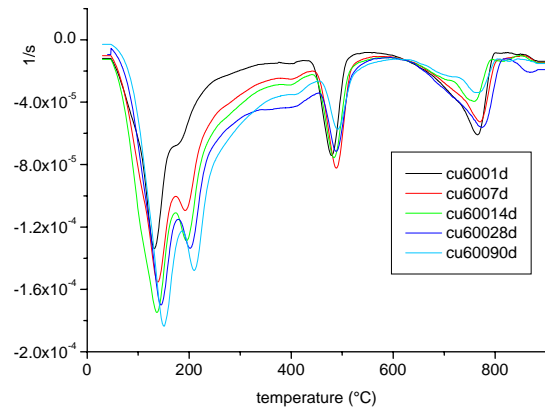
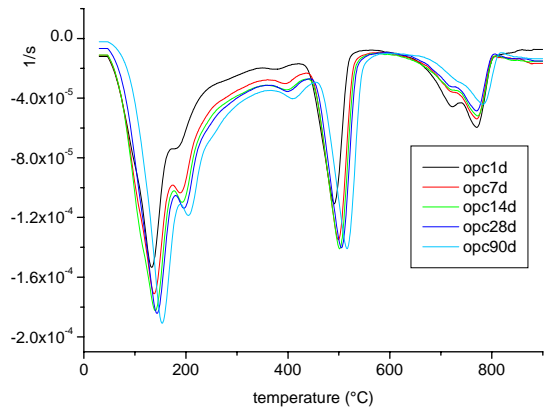




Series 3

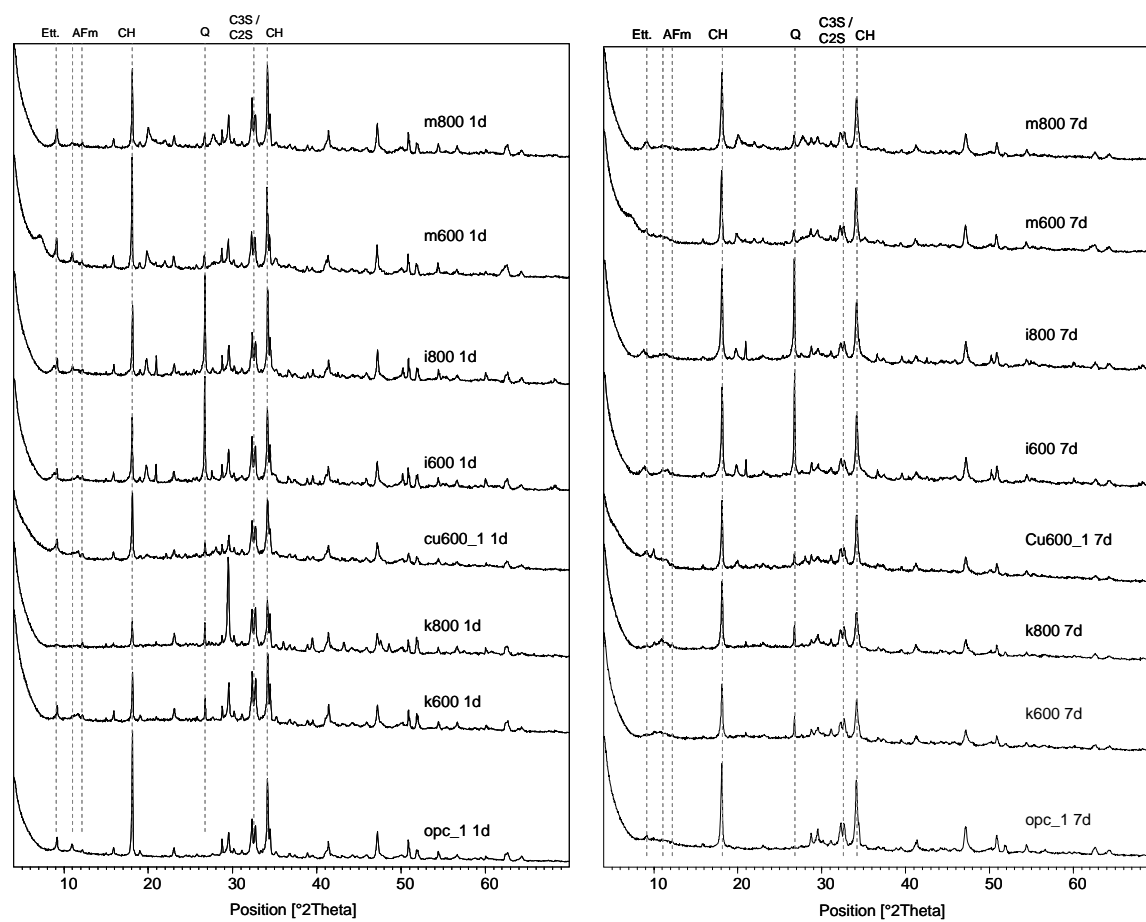


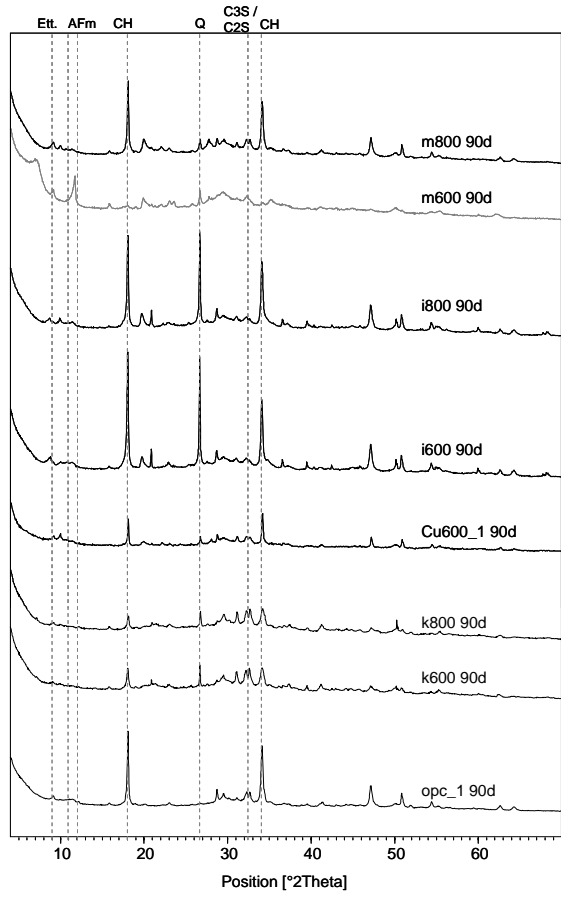
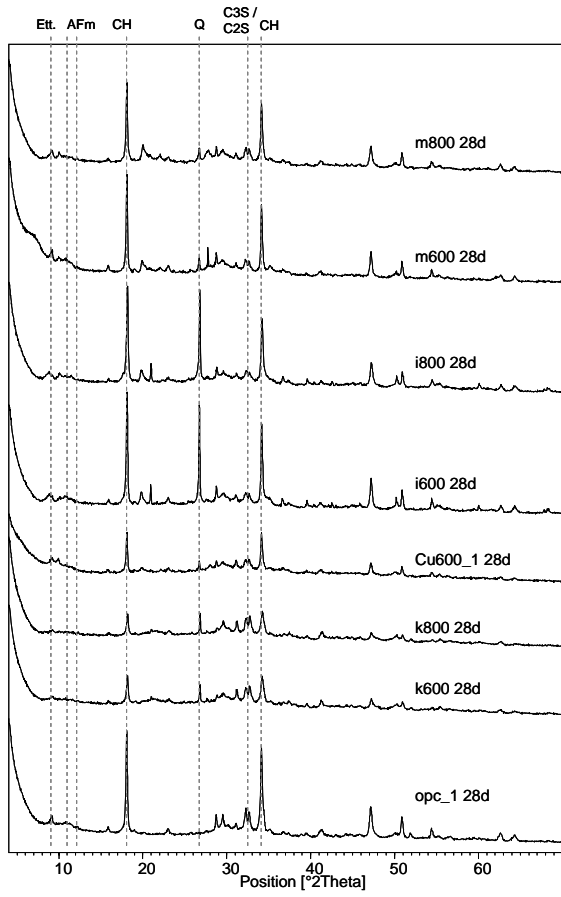
## Series 4



## Appendix V XRD patterns for all series

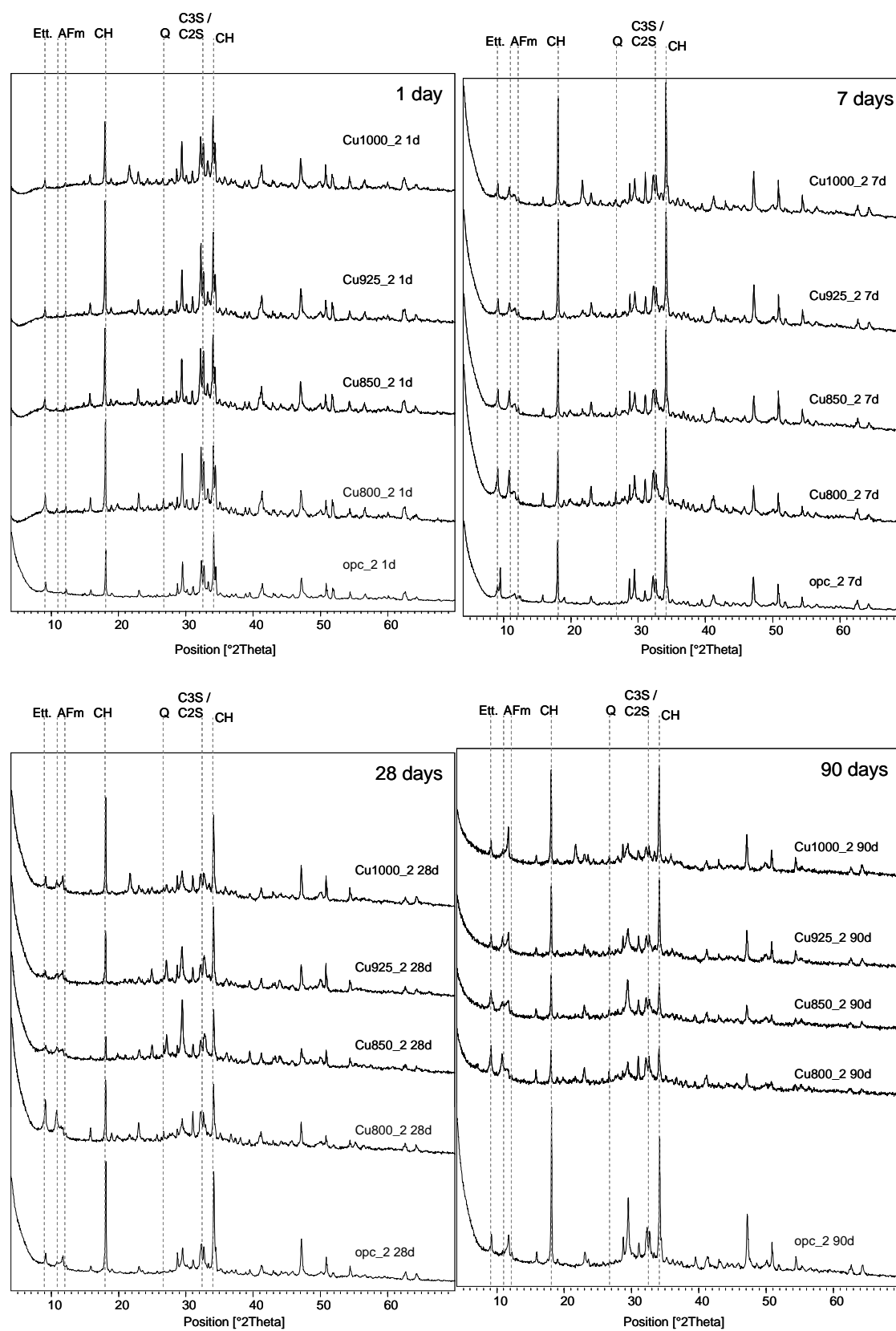
XRD pattern of series 1, 30°C



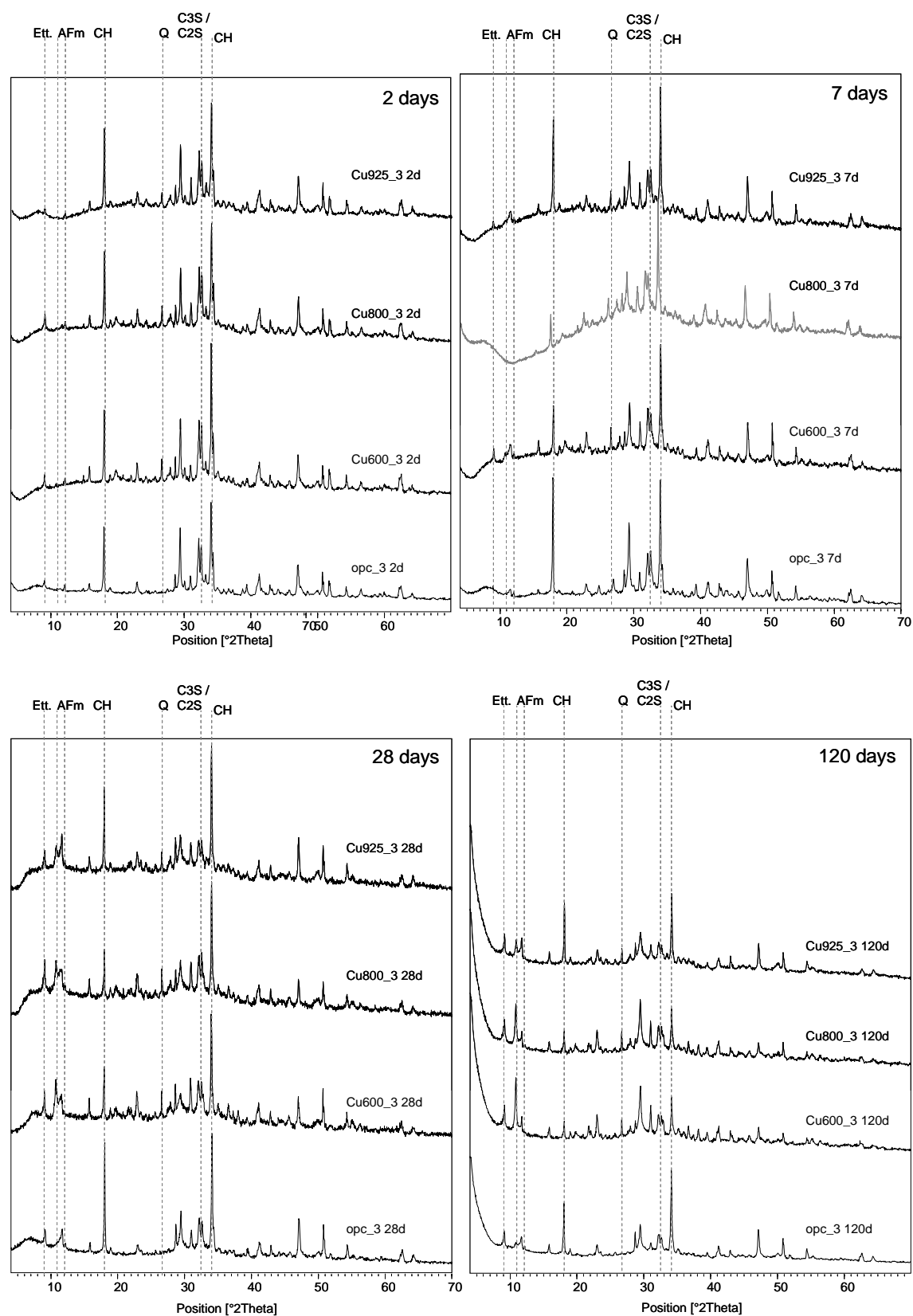




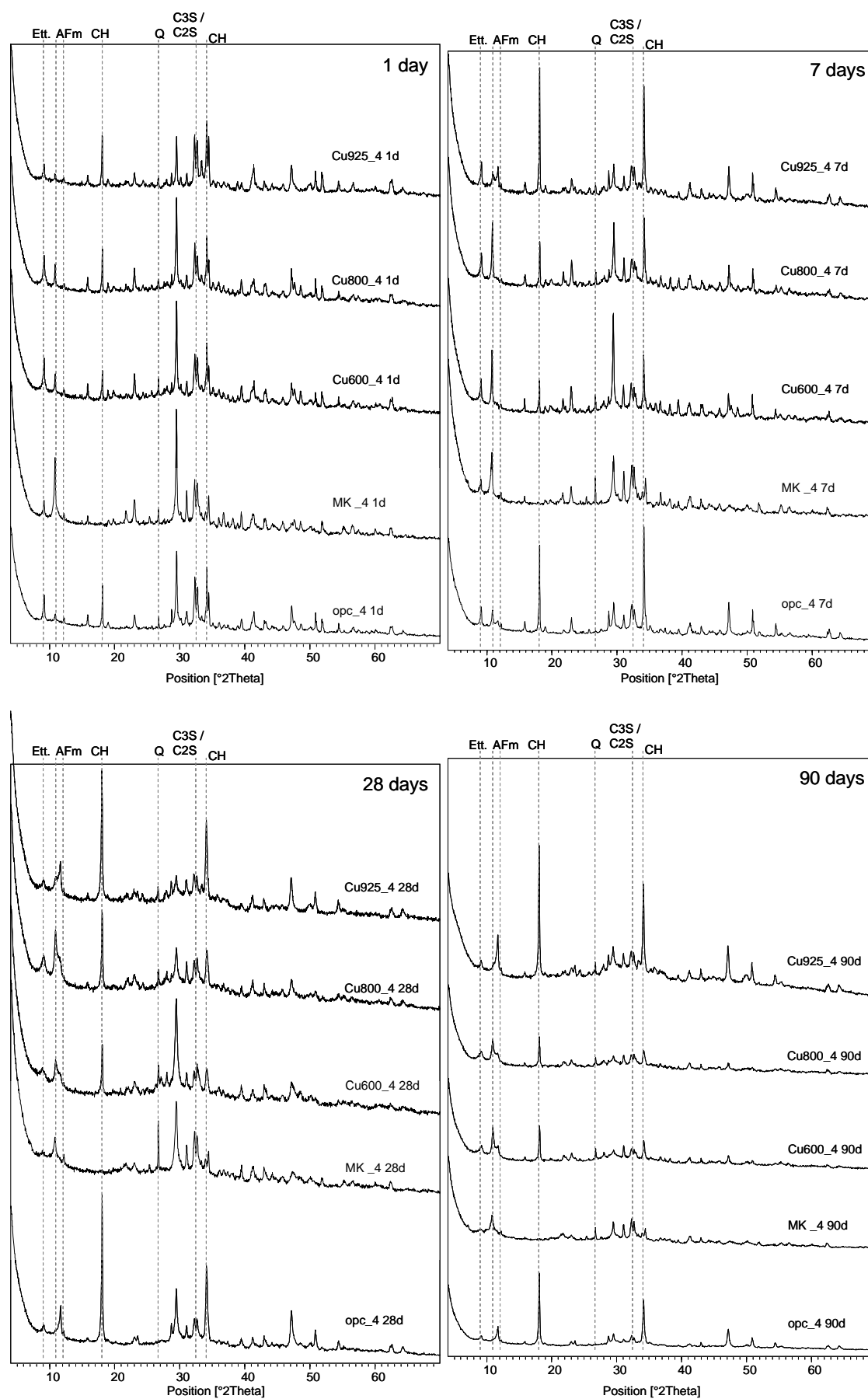
# XRD pattern of series 2, 20°C



# XRD pattern of series 3, 20°C



# XRD pattern of series 4, 30°C



## Appendix VI Capillary porosity (from the Swiss norm SIA 262/1)

Capillary porosity:  $n = \frac{m_{SAT} - m_{110}}{V_E}$  (% vol) (with  $V_E = \frac{4(m_{E0} - m_{Eu})}{\rho_w}$ )

$m_{SAT}$ : mass of the water-saturated sample (under vacuum for 24h) (g)

$m_{110}$ : mass of the sample dried at 110°C for 48h (g)

$m_{E0}$ : mass of the water-saturated sample (in water for 4 days) (g)

$m_{Eu}$ : mass of the water-saturated sample under water (g)

$\rho_w$ : density of water (g/m<sup>3</sup>)

## Curriculum Vitae

### Rodrigo Fernandez Lopez

Address: 24 Rue Ernest-Pictet, 1204  
Geneva, Switzerland

Birth Date : 11.10.1979

Tel: +41 22 340 64 22

Marital Status : single

Cel: +41 76 378 87 02

Nationality : Uruguayan / Swiss

E-mail: fernandezrod@gmail.com

---

### Education

- Lausanne Federal Institute of Technology (EPFL)  
Ph.D. student in the Laboratory of Construction Materials. Sep2005 – Jan2009
  - Lausanne Federal Institute of Technology (EPFL)  
Masters Degree in Material Science Engineering Oct. 1999 – Mar. 2004
  - St-Andrews University, Scotland  
English litterature and English language studies 1998 – 1999
  - Collège Calvin, Geneva, Swiss scientific baccalaureate 1994 – 1998
- 

### Job Experiences

- Flybaboo SA (Geneva based regional airline)  
Sales and Marketing Assistant Jun. - Dec 2004
  - Engineer Internship at the Academy of Science  
of Vienna, Austria Jul. – Sep. 2002
  - International Motor Show, Geneva,  
Customer relationship for Mazda Motor Company Mar. 2002, 03, 04
- 

### Languages

- Spanish mother tongue
  - French mother tongue
  - English speaking and writing fluently
  - German good knowledge in writing and speaking
- 

### Non-profitable activities

- Organization of the International Football Tournament  
of the US Meinier, Geneva (annual budget CHF 60,000.-) Jun. 1999 – Jun. 2005
  - Class spokesman at EPFL Oct. 2003 – Jan. 2004
- 

### Special Interests

- Football, Tennis, Trekking, Fishing

